UNIVERSIDADE DE LISBOA
FACULDADE DE CIÊNCIAS
DEPARTAMENTO DE BIOLOGIA VEGETAL

Comparative Systems Biology analyses of *Lactococcus lactis* subsp. *lactis* strain LMG 19460

Diogo de Lucena Antunes

Mestrado em Microbiologia Aplicada

Dissertação orientada por:
Professora Doutora Leonilde Fátima Morais Moreira
Professor Doutor Rogério Paulo de Andrade Tenreiro

2020

This Dissertation was fully performed at the Institute for Bioengineering and Biosciences, at Instituto Superior Técnico (IST), Universidade de Lisboa (UL), under the direct supervision of Professor Leonilde Moreira, Ph. D.

Professor Rogério Tenreiro, Ph. D., was the internal supervisor designated in the scope of the Master in Applied Microbiology of the Faculty of Sciences of the University of Lisbon

2020

Acknowledgments

This work was supported by the FCT — Portuguese Foundation for Science and Technology — under the project grant PTDC/BTM-SAL/28624/2017.

I would like to express my sincere gratitude towards Professor Leonilde Moreira and Professor Gabriel Monteiro for accepting me into this project. Moreover, I would like to thank them kindly for their patience and always present motivating words, both in the best and in the most challenging of times. Furthermore, I must sincerely thank them for granting me the chance of discovering the brilliantly interesting field of genome-scale metabolic models. In that same thread, I would also like to sincerely thank Doctor Paulo Dias for introducing and so patiently mentoring me through a field of knowledge completely new to me.

I must also sincerely thank Master José Santos, who so kindly and thoroughly taught me the details of working *in vitro* with *Lactococcus lactis*, and all while finishing his own Master's project and thesis. Finally, I would like to thank every remaining member of Professor Gabriel Monteiro's research group for so kindly welcoming me into their environment and for always being available to share their help and valuable advice.

Doctor Petri-Jaan Lahtvee, from the University of Tartu (Estonia), is also here kindly regarded, for so promptly sharing the unpublished exometabolomics data obtained by his group for *L. lactis* IL1403, which would then be of great use for this work.

In Faculdade de Ciências da Universidade de Lisboa, I would like to sincerely thank Professor Ana Reis, Professor Lélia Chambel, and Professor Mónica Cunha, for their wise advice and the ever-available support shown to their students. In the same institution, I would also like to thank Professor Rogério Tenreiro on his support leading to the accomplishment of this thesis.

Last, but not least, I here demonstrate the utmost gratitude and love towards my parents, for their crucial support and for being the fundamental reason why I could even partake in such an interesting project and experience.

Abstract

Lactic acid bacteria (LAB) have long had a prominent role in human society, where many of its individuals are used to produce various fermented food products and a few others are clinically-relevant pathogens. Since the late twenty-first century, many of these bacteria have also demonstrated their potential as biotechnological organisms, thanks to their proven safety for human health. *Lactococcus lactis* is one of such LAB, with a long history in the production of dairy products and a recently well established role in biotechnology. There, *L. lactis* strains have been used as microbial cell factories for the production of recombinant protein, as vectors for mucosal vaccination, and more. *L. lactis* subsp. *lactis* LMG 19460 is a strain whose genome was recently sequenced and whose lack of intrinsic plasmids makes it an ideal candidate for biotechnological applications. For the better understanding and use of such biotechnological organisms, genome-scale metabolic models, or genome-scale models (GEMs), can be a great tool. However, developing robust GEMs for organisms which have no available experimental data can be a difficult task, since they cannot be validated through comparison with published phenotypes. As such, strategies different from traditional methodologies are necessary.

Here, two GEMs were developed, one for the well characterised, reference strain *L. lactis* subsp. *lactis* IL1403 and another for *L. lactis* LMG 19460. The GEM for *L. lactis* IL1403 accounts for 575 genes, 921 reactions and 639 metabolites. It was reconstructed through comparative genomic approaches, where metabolic functions in strain IL1403 were inferred from high-quality published GEMs. The assembled model was then refined and validated through comparison with the comprehensive published data available for the organism. The model demonstrates good capabilities in predicting experimentally determined phenotypes of strain IL1403. Using this validated and working model, a GEM was then developed for the lesser-known strain LMG 19460. The metabolic model for *L. lactis* LMG 19460 accounts for 570 genes, 916 reactions and 638 metabolites. It is a functional model, capable of performing *in silico* predictions using data available for other *L. lactis* strains. However, it still requires true validation through comparison with experimentally determined, strain-specific phenotypes. As a first step in the experimental characterisation of *L. lactis* LMG 19460, a chemically defined medium was here developed and optimised, supporting clear growth and considerable biomass production when compared with published media (final OD_{600} = 2.02). The GEM for *L. lactis* LMG 19460 is capable of simulating unconstrained growth in this medium.

In future applications, both metabolic reconstructions here assembled should be further refined and validated, in order to fully develop them into high-quality GEMs. Then, these models will be of significant use for further studying the metabolism of their respective strains, where they can be used to map high-throughput data and drive experimental design. Furthermore, by testing synthetic biology hypothesis and predicting the effects of metabolic engineering, these models will be invaluable tools for the applications of their respective strains in biotechnology.

Keywords: Lactic acid bacteria; *Lactococcus lactis*; genome-scale metabolic models; flux balance analysis; chemically defined media.

Resumo

As bactérias do ácido láctico (BAL), correspondentes à ordem taxonómica Lactobacillales, são um grupo de bactérias Gram-positivas com baixo conteúdo G+C, caracterizadas por produzirem ácido láctico como principal produto do metabolismo. São um grupo altamente diversificado, quer nas suas características fisionómicas, quer no leque de habitats que ocupam, os quais vão desde numerosos produtos alimentares fermentados, a ambientes vegetais, superfícies animais e vias gastrointestinais. Embora alguns membros desta ordem sejam agentes patogénicos, a maioria destas espécies é reconhecida como segura para a saúde humana. Estes microrganismos estão tradicionalmente associados à indústria alimentar, onde servem para a produção de variados produtos fermentados. Mais ainda, desde o final do século vinte, têm vindo a adquirir um papel cada vez mais relevante na área da biotecnologia.

Uma das espécies mais bem caracterizadas no grupo de BAL é *Lactococcus lactis.* Esta bactéria partilha já uma longa história com o ser humano, em grande parte devido ao seu uso na produção de inúmeros lacticínios. Recentemente, adquiriu também um papel distinto na biotecnologia, onde a sua segurança para a saúde humana lhe confere inúmeras vantagens sobre os organismos tradicionalmente utilizados nesta área. Um exemplo destas aplicações é a sua utilização como fábrica celular microbiana para a produção de inúmeros compostos e enzimas de relevância industrial. Outro exemplo, é a sua aplicação nas áreas da terapêutica e imunologia, onde *L. lactis* tem sido utilizada para a produção e administração *in vivo* de compostos terapêuticos e para a vacinação através de mucosas. A estirpe *L. lactis* spp. *lactis* LMG 19460, cujo genoma foi recentemente sequenciado, é uma boa candidata para estas várias aplicações biotecnológicas. Isto deve-se, em particular, ao facto de não ter plasmídeos intrínsecos, o que reduz os seus custos metabólicos e permite, em princípio, maior rendimento na produção de proteína recombinante.

Qualquer aplicação biotecnológica de um organismo beneficia de um conhecimento integral e abrangente das suas funções celulares, nomeadamente do seu metabolismo. Para alcançar essa compreensão holística, existem na área da biologia de sistemas inúmeras ferramentas, dais quais se destacam os modelos metabólicos à escala genómica (MMEG). Estes modelos são representações matemáticas e, consequentemente, computacionais de todas funções metabólicas de um dado organismo, permitindo, assim, simular estados fisiológicos e prever fenótipos em variadas condições ambientais. Surgiram no final dos anos 1990, logo após a sequenciação dos primeiros genomas, e têm desde então sido desenvolvidos para cada vez mais organismos, cobrindo agora todos os domínios da vida celular. Quando estes modelos são gerados de um modo cuidado e compreensivo, resultam em MMEG de alta qualidade, que podem, então, ser aplicados para inúmeros fins. Destes, destacam-se particularmente o mapeamento de dados ómicos, permitindo, assim, a melhor interpretação dos mesmos, e, reciprocamente, a melhoria e o refinamento do modelo. Destacam-se, também, as aplicações na área da biotecnologia, designadamente na biologia sintética e engenharia metabólica. Aí, MMEG simulam, entre outras coisas, a inserção de plasmídeos e manipulações genéticas, permitindo, assim, testar hipóteses antes da sua aplicação experimental.

A construção de um MMEG é um processo trabalhoso e minucioso que, de modo geral, segue quatro passos essenciais. No primeiro, é gerada uma reconstrução esboço da rede metabólica do organismo em questão. No segundo passo, o esboço obtido é revisto e refinado, de modo a conceder maior qualidade e realismo à reconstrução metabólica, mas também para lhe dar a estrutura necessária aos passos seguintes. O terceiro passo é a conversão da rede metabólica para um formato matemático e, consequentemente, computacional. A lista das reações metabólicas de uma reconstrução pode ser representada numa matriz, denominada matriz estequiométrica (ou matriz S), onde as colunas correspondem a cada reação, as linhas a metabolitos e as entradas aos seus respetivos coeficientes

estequiométricos. É esta abstração da rede metabólica numa matriz matemática que permite a computação de estados fisiológicos e previsão de fenótipos. O último passo para o desenvolvimento de um MMEG é a sua avaliação e validação. Em primeiro, são analisados e corrigidos possíveis erros na rede metabólica, e, de seguida, as capacidades do modelo são validadas pela comparação com dados experimentais. Como tal, para desenvolver o modelo de um dado organismo, é essencial que exista boa e variada literatura experimental para o mesmo. Alternativamente, estes dados experimentais podem ser obtidos em paralelo ao desenvolvimento do modelo. Para organismos cuja literatura metabólica é bastante limitada ou inexistente, são, então, necessárias estratégias alternativas para a construção e validação do seu MMEG.

Neste trabalho foram desenvolvidos dois MMEG, um para a estirpe de referência *L. lactis* spp. *lactis* IL1403 e outro para a estirpe *L. lactis* LMG 19460. O MMEG para a estirpe IL1403 contabiliza 575 genes, 921 reações e 639 metabolitos. Para a sua construção, foram aplicadas abordagens de genómica comparativa que permitiram inferir as funções metabólicas de *L. lactis* IL1403. Nomeadamente, foram detetadas homologias bidirecionais entre a estripe e uma série de organismos-alvo para os quais estão publicados MMEG de alta qualidade. De seguida, foram corrigidos erros na rede metabólica e o modelo foi validado pela comparação das suas capacidades com dados disponíveis na extensa literatura de *L. lactis* IL1403. O MMEG resultante demonstra boas capacidades de simular fenótipos determinados experimentalmente, tais como, requisitos nutritivos, capacidade de utilizar diferentes fontes de carbono, crescimento em meios quimicamente definidos e crescimento respeitante de taxas específicas de consumo de nutrientes e produção de metabolitos.

Após a construção de um MMEG para *L. lactis* IL1403 validado e funcional, o mesmo foi utilizado como base para inferir as funções metabólicas da estirpe LMG 19460, ainda não caracterizada ao nível do seu metabolismo. O MMEG aqui desenvolvido para *L. lactis* LMG 19460 contabiliza 570 genes, 916 reações e 638 metabolitos. É funcional e capaz de simular crescimento e diferentes fenótipos quando utilizados dados publicados para outras estirpes de *L. lactis*. De qualquer forma, para a sua correta validação e melhoria da especificidade, as capacidades deste modelo precisam de ser comparadas com dados experimentais específicos à estirpe, ainda a obter.

De modo a iniciar o processo da caracterização metabólica de *L. lactis* LMG 19460, foi aqui desenvolvido um meio quimicamente definido capaz de suster crescimento da estirpe. Este meio é constituído por uma fonte de carbono, todos os aminoácidos e uma série de vitaminas, minerais e outros micronutrientes. Pela sua otimização, nomeadamente no que diz respeito à concentração da fonte de carbono e tampão, foi possível obter um meio capaz de suster uma produção considerável de biomassa de *L. lactis* LMG 19460 (densidade ótica final de 2,02, a 600 nm). De modo a iniciar, também, o processo de validação do MMEG desenvolvido para este organismo, o meio aqui construído foi aplicado como condições ambientais *in silico*. Depois, o modelo foi avaliado quanto à sua capacidade de reproduzir a ocorrência de crescimento verificada *in vitro*; teste para o qual foi positivo. De qualquer forma, são ainda necessários muitos mais dados experimentais para corretamente validar o modelo para *L. lactis* LMG 19460.

No futuro serão necessários ainda mais esforços de refinamento e validação dos dois modelos aqui construídos, de modo a eventualmente torná-los em MMEG de alta qualidade. Para o modelo de *L. lactis* IL1403, isto significa continuar o trabalho de revisão de todas as reações incluídas, quer pela continuação da pesquisa de funções metabólicas na respetiva literatura publicada, quer pela investigação mais detalhada das homologias aqui detetadas entre a estirpe e os organismos-alvo utilizados. Mais ainda, o processo de validação pode ser melhorado e continuado pela obtenção de dados experimentais de maior qualidade e dados ainda não disponíveis para a estirpe, tais como a determinação dos seus genes letais. Quanto ao modelo de *L. lactis* LMG 19460, tudo o que foi referido para o anterior modelo aplica-se também a este, com o acréscimo de ser necessária a obtenção de

ainda mais dados experimentais específicos à estirpe. Estes dados serão, tais como, a determinação das suas auxotrofias e requisitos nutritivos, a sua capacidade de utilizar diferentes fontes de carbono e as suas taxas de consumo de nutrientes e produção de metabolitos. Só quando determinados estes fenótipos da estirpe é que será possível a devida validação do MMEG. Para muitos destes fins, pode ser aplicado o meio sintético aqui desenvolvido. Este deve também continuar a ser desenvolvido e otimizado para o crescimento de *L. lactis* LMG 19460.

Quando atingido o ponto da alta qualidade, os MMEG aqui desenvolvidos para as duas estirpes de *L. lactis* poderão então ser utilizados para fins mais aplicados, tais como o estudo detalhado dos seus processos metabólicos, a previsão realística de fenótipos resultantes de manipulações genéticas e a participação no desenho e otimização destas estirpes como fábricas celulares microbianas.

Palavras-chave: bactérias do ácido láctico; *Lactococcus lactis*; modelos metabólicos à escala genómica; análise de balanço de fluxos; meios quimicamente definidos.

Table of Contents

Acknowledgments....III
Abstract....IV
Resumo....V
Index of Tables....IX
Index of Figures....X
Table of Abbreviations....XI
1. Introduction....1
1.1. Lactic acid bacteria....1
1.1.1. *Lactococcus lactis*....2
1.2. Genome-scale metabolic models....3
1.2.1. General metabolic reconstruction process and its first stage....4
1.2.2. Manual curation of the draft reconstruction....5
1.2.3. Conversion into a mathematical form and its theoretical foundations....6
1.2.4. Network evaluation and model validation....9
1.2.5. Applications and future prospects of genome-scale models....11
1.3. Currently-available *L. lactis* genome-scale models....14
1.4. Objectives of this work....15
2. Materials and methods....16
2.1. Metabolic reconstruction for *L. lactis* IL1403....16
2.2. Biomass reaction and energy requirements of *L. lactis* IL1403....19
2.3. Conversion to a mathematical form and network evaluation....19
2.4. Model validation: nutritional requirements....21
2.5. Model validation: simulations in published chemically defined media....21
2.6. Model validation: carbon source utilization....22
2.7. Metabolic reconstruction for *L. lactis* LMG 19460 and respective evaluation....22
2.8. Organism and media....22
2.9. Growth conditions and analytical methods....24
2.10. *L. lactis* LMG 19460 partial model validation....24
3. Results and discussion....26
3.1. Genome-scale model for *L. lactis* IL1403 and general properties....26
3.2. Biomass reaction....29
3.3. Network evaluation....33
3.4. Model validation: nutritional requirements....35
3.5. Model validation: simulations in published chemically defined media....41
3.6. Model validation: exometabolomics data....44
3.7. Model validation: carbon source utilization....45
3.8. *L. lactis* LMG 19460 metabolic reconstruction and evaluation....48
3.9. Performance of the model for *L. lactis* LMG 19460....50
3.10. *L. lactis* LMG 19460 growth assays in chemically defined media....52
3.11. Application of CDM1 in the GEM for *L. lactis* LMG 19460....57
4. Conclusions and future prospects....59
References....62
Supplementary Materials....68

Index of Tables

Table 2.1: Organisms selected for iterative sequence homology analysis with *L. lactis* IL1403.....18
Table 2.2: Constitution of the first assembled chemically defined medium, CDM1.....23
Table 3.1: Summary of characteristics of the metabolic model here developed for *L. lactis* IL1403.…26
Table 3.2: Comparison of the number of reactions in major subsystem groups between the GEM by Oliveira *et al.* (71) and the metabolic model here developed.....28
Table 3.3: Partial chemical composition of *L. lactis* IL1403 cells.....30
Table 3.4: Summarized development of the constructed BOF.....32
Table 3.5: Summary of the network evaluation performed.....33
Table 3.6: Mass-imbalanced reactions for which no solution was found and respective metabolites…33
Table 3.7: Reactions participating in SBCs determined to have an incorrect directionality.....35
Table 3.8: Nutrient requirements of *L. lactis* IL1403 agreed on by the published literature.....36
Table 3.9: Nutrients on *L. lactis* IL1403 essentiality assays for which conflicting evidence was found.....37
Table 3.10: Erroneous *in silico* results from the first tests on expected *L. lactis* IL1403 nutritional requirements.....38
Table 3.11: Confusion matrix for the predictions on nutritional requirements by the model for *L. lactis* IL1403.....40
Table 3.12: I*n silico* tests using published chemically defined media for *L. lactis* IL1403.....42
Table 3.13: L-histidine consumption rates kindly provided by Dr. Petri-Jaan Lahtvee.....44
Table 3.14: *L. lactis* IL1403 growth simulations under exometabolomics constraints.....45
Table 3.15: Final *in silico* results on carbon source utilization.....47
Table 3.16: Confusion matrix for the GEM's capability of predicting *L. lactis* IL1403 carbon source utilization.....48
Table 3.17: Reactions in the metabolic reconstruction for *L. lactis* IL1403 for which no homology was found with *L. lactis* LMG 19460.....49
Table 3.18: Protein sequence alignment results between *L. lactis* IL1403 and the genes coding for reactions PKETF, PKETX, and ALDD2y, in their respective original GEMs.....50
Table 3.19: Growth comparison between the two GEMs in the collected published synthetic media...51
Table 3.20: Growth comparison between the two GEMs using the consumption and production rates determined by Flahaut e*t al.* (73).....52
Table 3.21: Comparison between average growth kinetics in the synthetic media developed for *L. lactis* LMG 19460 and published values for *L. lactis*.....57
Supplementary Table S1: Tabular representation of the two GEMs developed in this work, for better convenience and visualisation.....68
Supplementary Table S2: List of metabolites present in the GEM here developed for L. lactis IL1403.....111
Supplementary Table S3: Metabolite composition of the assembled BOF, contained in both GEMs.....124
Supplementary Table S4: Dead-end metabolites present in the final version of the GEM for *L. lactis* IL1403.....125
Supplementary Table S5: Reactions leading to dead-end metabolites, present in the final version of the GEM for *L. lactis* IL4103.....126
Supplementary Table S6: Blocked reactions (reactions unable to carry flux) present in the final version of the model for *L. lactis* IL1403.....127
Supplementary Table S7: Identified stoichiometric balanced cycles involving ATP and their respective reactions.....128

Index of Figures

Figure 1.1: Unrooted phylogenetic tree of Lactobacillales at the genera level.....1

Figure 1.2: Scanning electron micrographs of *L. lactis* mutant cells.....2

Figure 1.3: The four stages of genome-scale metabolic network reconstruction, as outlined by Thiele and Palsson (40).....4

Figure 1.4: Conversion of an assembled metabolic reconstruction into a mathematical, and thus computable, form.....7

Figure 1.5: Schematic representation of dead-end metabolites in a metabolic reconstruction.....10

Figure 1.6: A phylogenetic-like representation of the many currently available *in silico* tools for genome-scale modelling of metabolism.....13

Figure 3.1: Retrospective quantification of the target models from which metabolic reactions in the reconstruction for *L. lactis* IL1403 were inferred from.....27

Figure 3.2: Stoichiometrically balanced cycles involving ATP detected in the network evaluation step.....35

Figure 3.3: Growth curves for *L. lactis* LMG 19460 cultivated in CDM1 and in M17.....53

Figure 3.4: Growth and pH curves for *L. lactis* LMG 19460 cultivated in CDM2 and in M17.....54

Figure 3.5: Growth and pH curves for *L. lactis* LMG 19460 cultivated in CDM3 and in M17.....56

Table of Abbreviations

BOF — Biomass objective function

CDM — Chemically defined medium

COBRA — Constraint-based reconstruction and analysis

FBA — Flux balance analysis

GAM — Growth-associated maintenance

GEM — Genome-scale model

GPR — Gene-protein-reaction

LAB — Lactic acid bacteria

NGAM — Non-growth-associated maintenance

SBC — Stoichiometrically balanced cycle

SBML — Systems biology markup language

YNB — Yeast nitrogen base

1. Introduction

1.1. Lactic acid bacteria

The taxonomic order Lactobacillales, also known as lactic acid bacteria (LAB), represents a group of Gram-positive bacteria sharing a long history with humankind. Traditionally known for their fermentative capabilities, they have long been used in food processes, where lactic acid, their major metabolic end-product, acts as a preservative. This association with the food industry has mostly painted LAB as safe and harmless organisms. Throughout the twentieth and twenty-first century this idea would be somewhat lessened, however, with the progressive discovery of pathogenic groups in this order (1). Nowadays, LAB are known be a highly diverse order (Figure 1.1), covering numerous ecological niches (2). Despite the diversity observed within the order, the defining characteristics of LAB remain, generally, a cocci or rod shape, low G+C content, no production of endospores, no metabolic respiration—but some tolerance of oxygen—, and lactic acid as at least one of the major products of fermentation (3). The metabolism of carbohydrates serves not only to define the order, but also to distinguish its genera. Substrate level phosphorylation can take the form of homolactic fermentation, where only lactic acid is produced, or of heterolactic fermentation, which additionally produces CO_2 and ethanol or acetate. While the majority of LAB have a main homofermentative phenotype that can facultatively change to heterofermentative, some genera are obligatory heterofermentative, such as *Leuconostoc* and *Oenococcus*, while some *Lactobacillus* species are obligatory homofermentative (1, 3).

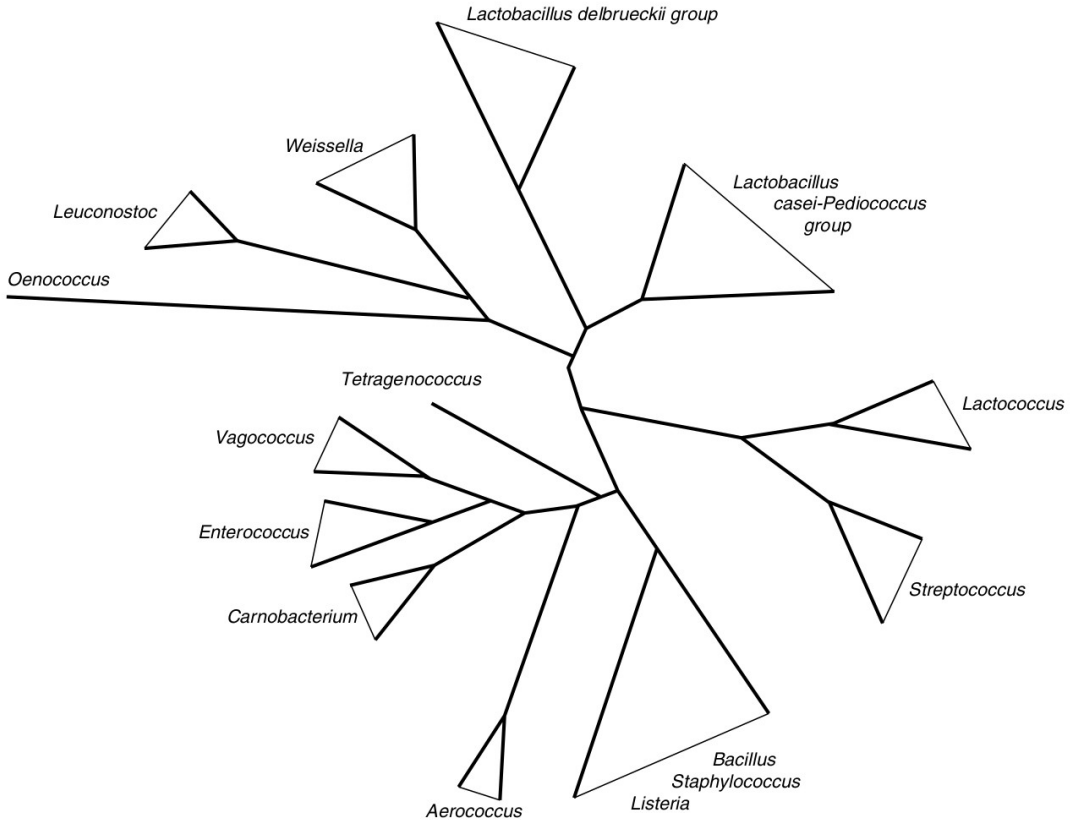

Figure 1.1: Unrooted phylogenetic tree of Lactobacillales at the genera level. Though not part of this order, the genera *Bacillus*, *Staphylococcus* and *Listeria* are also represented. Adapted from (10).

While traditionally associated with the food industry, the applications of LAB in the past decades have expanded into new fields, such as those of probiotics, biotechnology, and medicine. As probiotics, species of LAB have been shown to have a number of health benefits, from stimulating the host's immune system, to protecting the gastrointestinal tract from pathogenic colonization, assisting digestive processes, and more (4). As biotechnological organisms, LAB have been subject to the development of many molecular tools, such as expression systems, genome editing tools, protein secretion and presenting mechanisms, and more (5, 6). These molecular tools have led to increasingly varied biotechnological applications of these organisms. For instance, LAB species are now used as cell factories for the production of recombinant protein, where they offer a cheaper and safer alternative to traditional expression systems such as *Escherichia coli* (7). Furthermore, LAB have increasingly been the subject of therapeutical research, where several species can act as vehicles for mucosal vaccination, production of cytokines and antibodies, treatment of gastrointestinal track disorders, and more (5, 8).

1.1.1. *Lactococcus lactis*

Lactococcus lactis is one of such LAB and arguably the most well studied and characterised member of this order. It is a Gram-positive, low G+C content, coccoid bacterium, typically characterised by its homolactic fermentation of carbohydrates (1). Cells are sphere or ovoid shaped and usually under 1.5 µm in diameter, while colonies tend to exhibit groups of single, paired or chained cells (Figure 1.2). It is non-motile, due to the lack of flagella, and it does not produce endospores. The bacterium is distinctly mesophilic, generally capable of growing at ranges from 10 to 40 °C. Strains also display a slightly halophilic phenotype, the majority of which are capable of growing in media containing up to 4% (w/v) NaCl (2). *L. lactis* is capable of growing in aerobiosis, most likely due to the presence of enzymes such as superoxide dismutase and NADH oxidases (1, 2). Furthermore, it has an incomplete respiratory chain which allows it to preform respiration when cultivated in a medium supplemented with haem under aerobiosis (9).

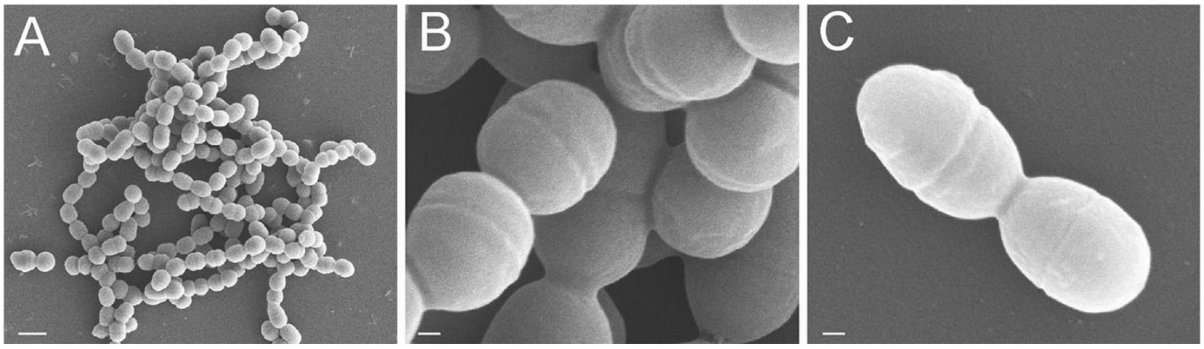

Figure 1.2: Scanning electron micrographs of *L. lactis* mutant cells. These cells were described by the original authors as similar in size and morphology to wild-type cells (11). A: X6,000 magnification with a 1µm bar. B and C: X45,000 magnification, with a 100 nm bar. Adapted from (11).

The carbohydrate metabolism is one of the defining characteristics of *L. lactis*. There, hexose sugars are converted to pyruvate via the glycolytic pathway, generating energy, lactic acid, and resulting in the distinctive homofermentative phenotype (3, 12). Homolactic metabolism has, however, been shown to shift to heterolactic fermentation depending on the flux through glycolysis, as a consequence of specific sugar consumption rates and the intracellular ratio of $NADH/NAD^+$ (13).

In nature, *L. lactis* inhabits various ecosystems and is most typically found in plant surfaces, animal surfaces, some gastrointestinal tracts, and raw milk (14, 3, 15). Furthermore, it has been isolated from unexpected places, such as drain water and human vaginal samples (15). Outside these environments, *L. lactis* is most traditionally found in dairy products. Curiously, however, the majority

of dairy isolates are believed to have descended from ancestral plant strains, possibly consequence of plant contact with milk or cattle (16). Nevertheless, it is in the dairy industry where most strain diversity has been observed and where *L. lactis* serves the greatest use for mankind. It is one of the most commonly used starters for the production of cheeses and fermented milk products, important not only for its fermentative capabilities, but also the production of flavour forming compounds (17, 18).

The mentioned habitat range results in high strain phenotypic variety, most noticeable in nutritional requirements and the ability to use certain carbon sources (19, 20). Furthermore, it also leads to high plasmid diversity, from the classic plasmid-coded functions linked to dairy strains, to others such as: primary lactose and casein utilization; citrate transport and metabolism; environmental stress responses; bacteriophage resistance; complex carbohydrate utilization associated to plant habitats; and more (1, 21).

Technological developments in the fields of genome sequencing and genetic engineering have extended *L. lactis* from its traditional role in the food industry firmly into the field of biotechnology. There, multiple species-specific molecular tools have been developed, covering expression systems in the form of constitutive and inducible promoters, strategies for secretion and membrane display of heterologous proteins, and more (22, 23). These tools have turned *L. lactis* into a successful cell factory, currently used in the production of industry relevant metabolites and enzymes, such as lactic acid, varied food additives, antimicrobial compounds, vitamins, biofuels, and more (23). Furthermore, when combined with its ability to survive the gastrointestinal tract (24), the molecular libraries of *L. lactis* present it as a promising immunological and therapeutical instrument. In this role, it is particularly relevant as a live vector for the production and delivery of mucosal antigenic or DNA vaccines (25, 23). The species' non-pathogenicity grants it even more potential in these clinical uses, where *L. lactis* is presented as a safer alternative to the attenuated live pathogens generally used as vectors.

The first description and classification of an *L. lactis* strain was performed by Lister, when describing *Bacterium lactis* (26). Ever since then, numerous *L. lactis* strains have been isolated, many of which have also had their genome sequenced (27). The genome database of the National Center for Biotechnology Information (https://www.ncbi.nlm.nih.gov/) currently lists 242 genome assembly and annotation reports. The first of these strains to have had its full genome sequenced was *L. lactis* IL1403 (14), arguably the most studied and well characterised strain in this species. This strain has been used in numerous studies and applications and it is generally acknowledged as the reference strain for *L. lactis* (2).

1.2. Genome-scale metabolic models

For the better biotechnological application of industry relevant organisms such as *L. lactis*, a holistic understanding of their biology is fundamental. In the field of systems biology, genome-scale metabolic models, or, simply, genome-scale models (GEMs), have emerged as a versatile tool in achieving such comprehensive knowledge (28). These are computational representations of an organism's reconstructed metabolic network, and they allow for the prediction of cell-wide metabolic phenotypes under varied environmental conditions (29).

Initial metabolic network reconstructions relied on direct enzymatic characterization and biochemical literature data. Consequently, they were often limited to model organisms and well-studied pathways, such as the central carbon metabolism (30, 31). However, with the advent of whole genome sequencing and annotation in the late 1990s, it became possible to generate metabolic models at a genome scale, even for lesser-known organisms. The first genome-scale metabolic model was that of the opportunistic pathogen *Haemophilus influenzae* (32), also the first free-living organism to have

its full genome sequenced (33). Soon after, and as the publishing of full genomes grew drastically, so did the development of GEMs. A recent review by Gu *et al*. (34) counted, as of February 2019, 183 organisms for which manually curated metabolic models had been developed, and a further 6056 for which models were generated using automated tools. These models now cover all three domains of life, although bacteria account for at least 94.51% of the covered organisms (34).

1.2.1. General metabolic reconstruction process and its first stage

The reconstruction of high-quality genome-scale metabolic networks is an intensive and time-consuming process. Throughout the years, many generic workflows have been published with the aim of guiding and assisting the reconstruction process (35, 36, 37, 38, 39). However, it would be the protocol developed by Thiele and Palsson (40) the one to become, arguably, the fundamental standard operating procedure for the development of GEMs. There, the authors outline the reconstruction process in detail and define the four fundamental stages in developing metabolic models (Figure 1.3).

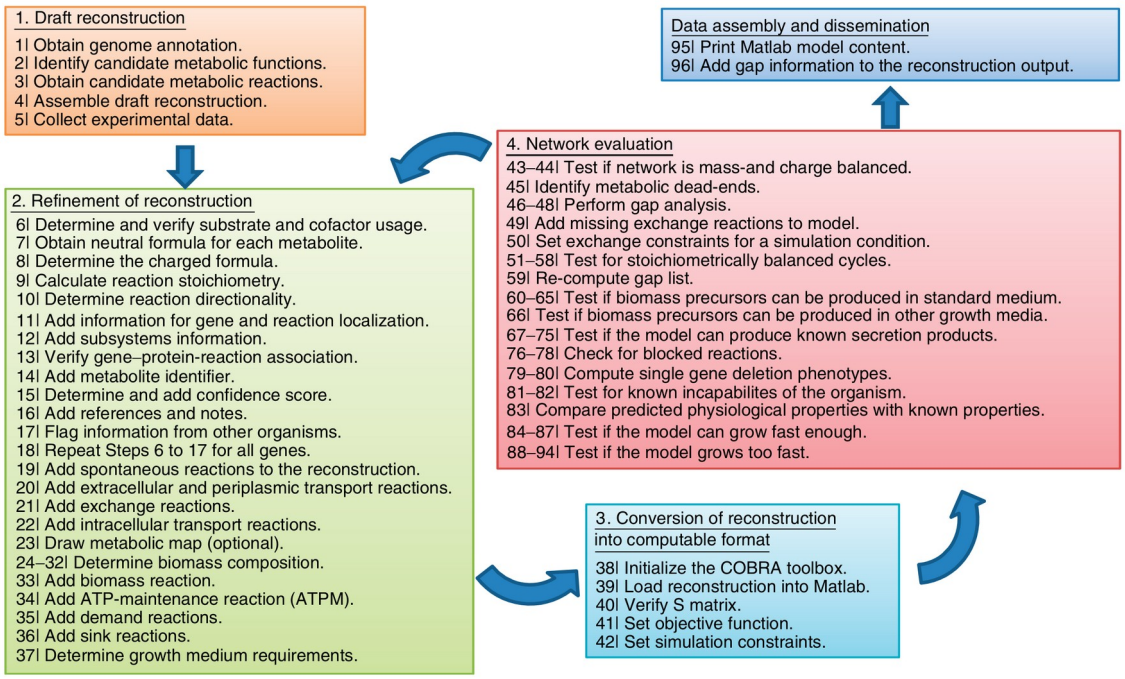

Figure 1.3: The four stages of genome-scale metabolic network reconstruction, as outlined by Thiele and Palsson (40). Figure adapted from (40).

The first step in developing a GEM for a target organism is the assembly of a draft reconstruction. It refers to collecting candidate metabolic reactions and the genes encoding enzymes responsible for said reactions. This is done by scanning the organism's annotated genome sequence for metabolic functions, through comparative genomics, or through the use of automated reconstruction tools.

When assembling a draft reconstruction, one must choose the identifiers in which the reactions and metabolites will be written. This choice typically lies between the sets used by each of the most common metabolic databases, such as KEGG (81), ModelSEED (83), and MetaCyc (82), in which each reaction and metabolite is given a unique identifier. This has the purpose of abbreviating extensive compound and enzymatic names, but also of standardizing the form of GEMs and, thus, facilitate their analysis and comparison. Another such metabolic database is the BiGG database, an online repository for published high-quality, manually curated GEMs (74). In this database, all models share the same standardized BiGG identifiers, which have a simple, unique, and human-readable form,

unlike the typical alphanumeric keys used by most databases. These characteristics typically make BiGG identifiers much easier to memorize and, in turn, facilitate the quick analysis of GEMs written in such nomenclature.

1.2.2. Manual curation of the draft reconstruction

Regardless of the method chosen in the first step, the assembled draft must then be reviewed and analysed in detail. This refers to the second step in network reconstruction, that of manual curation. This stage is possibly the most time-consuming one, as it involves many thorough steps of manual analysis and comparison with published data and chemical, enzymatic, and genetic databases. Generally, if little published data is available for the target organism, one can use phylogenetically close organisms.

In this second step, collected reactions must be evaluated on the confidence of their inclusion, as false-positives are likely to be present. Furthermore, their biochemical properties must also be reviewed and completed, from substrate and co-factor usage, to stoichiometry and directionality. Genetic information for each enzyme must also be curated and gene-protein-reaction (GPR) associations must be determined. GPR associations detail which genes code the enzymes catalysing each metabolic reaction. Furthermore, they also detail the complexity and versatility of those enzymes, by specifying cases of protein complexes (that is, heteromeric enzymes) and cases of isozymes (that is, different enzymes catalysing the same reaction).

The stage of manual curation also refers to the assignment of reactions into subsystems (that is, groups of known metabolic pathways) and the inclusion of their respective EC numbers. As previously mentioned, reconstructions are typically written in nomenclatures specific to one of the many metabolic databases (81, 82, 83, 84). This inevitably hinders inter-database GEM comparisons. As such, each assembled reaction and metabolite should also be attributed an identifier corresponding to their respective entries in different databases.

When combined, the categorization of reactions into subsystems, identification of their EC numbers, and attribution of database identifiers greatly facilitates comparing different metabolic models. This applies to cases of different nomenclatures, but also to models using the same identifiers, as even those can suffer from duplicated database entries and nomenclature updates making older models outdated. As steps are taken in trying to automate the comparison and mapping of different GEMs (42), an even greater value is placed on reaction and metabolite identifiers.

It is possible to accelerate the manual curation step by using a published, high-quality GEM from a closely related organism as the starting base. Furthermore, one can generate a draft reconstruction with one of the many available automated tools (43). Nonetheless, some manual curation will always be necessary in order to develop a high-quality model, as either method of acceleration might result in missing reactions or excessive inclusions.

Finally, in the second step, a series of non-metabolic or non-biological functions must be abstracted as pseudo-reactions, in order to prepare for future computations.

The consumption of metabolites required for cellular division is abstracted in the biomass reaction, also known as the biomass objective function (BOF). This is a pseudo-reaction which accounts for all metabolites making up the cell’s chemical composition and the energy requirements associated with biomass production, also known as growth-associated maintenance (GAM) (44). These parameters should be determined experimentally, thus leading to a reaction that represents the metabolic constituents necessary for biomass production. Maintenance energy requirements, specifically, must be determined in carbon-limited, continuous culture experiments, in order to ensure all energy obtained from the carbon source is used for the production of ATP and not cellular carbon (45). At a simple level, the BOF may account only for the macromolecular biomass composition,

where macro-components are represented directly by the metabolites from which they are made (such as amino acids, nucleotides, *etc*.). At more complex levels, it can also cover growth-associated energy requirements and essential cofactors, vitamins, and ions.

Not all cellular energy expenditures are associated with growth, as cellular functions such as maintenance of osmotic pressure, motility, cell signalling, *etc*., also require energy. This is known as non-growth-associated maintenance (NGAM) and these consumptions must also be abstracted. For this purpose, GEMs usually contain a single pseudo-reaction representing ATP hydrolysis (known as the ATP maintenance reaction) which represents the mentioned energy costs (Equation 1.1). These costs should also be determined experimentally in continuous culture assays under carbon-limited conditions, for the reasons outlined above.

$$1\,ATP + 1\,H_2O \rightarrow 1\,ADP + 1\,P_i + 1\,H^+ \tag{1.1}$$

Further necessary abstractions take the form of: exchange reactions, which represent the system's boundaries with the extracellular space; demand reactions, representing the flow of compounds into non-metabolic cellular functions; and sink reactions, which account for compounds produced in non-metabolic processes.

1.2.3. Conversion into a mathematical form and its theoretical foundations

Following the manual curation stage, the reconstruction can now be considered a database of metabolic information specific to an organism (Figure 1.4B). It lists the chemical reactions involved in the target's metabolism and the genes responsible for the enzymatic portion of those reactions. Both these datasets can be described in a mathematical form. GPR associations can be represented as Boolean algebraic operations, where conjunctions (denoted "and") represent monomers of a protein complex and disjunctions (denoted "or") represent isozymes (Figure 1.4A). Reactions composing the metabolic network can be represented as a matrix, where columns denote each reaction, rows list all unique metabolites, and matrix elements correspond to the stoichiometric coefficients (Figure 1.4C). These coefficients confer directionality to the matrix by being negative values, when referring to substrate compounds, and positive values, when referring to product compounds. On account of its composition, this matrix is often named the stoichiometric matrix, or S matrix.

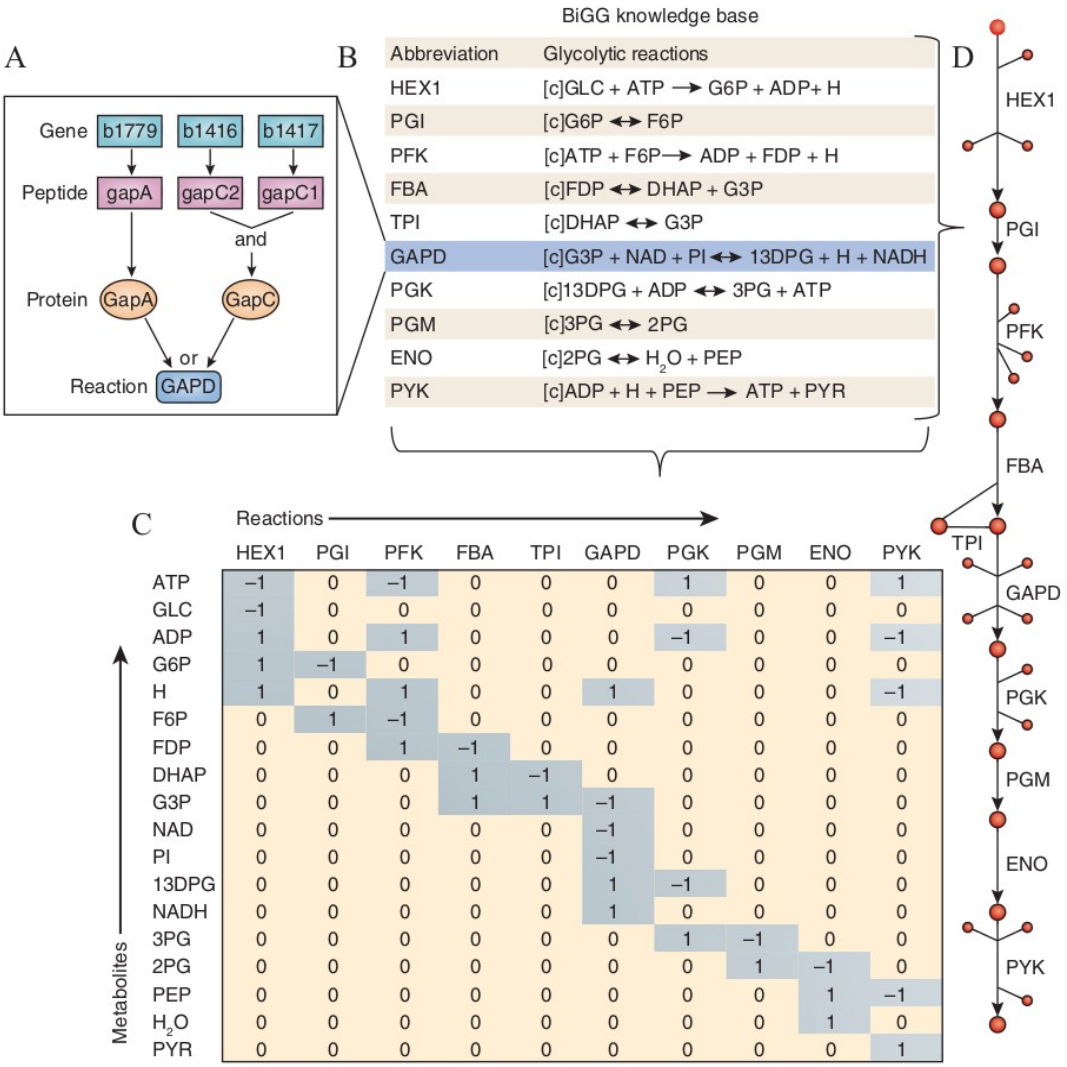

Figure 1.4: Conversion of an assembled metabolic reconstruction into a mathematical, and thus computable, form. A: genes are associated to their respective reaction through the assignment of GPR rules; these GPR associations also permit distinguishing protein complexes from isozymes. B: at its core, a reconstruction is a database of available metabolic knowledge for a target organism; it is an abstraction of biological functions and pathways (D). C: a reconstruction can be mathematically represented in a matrix by listing its reactions as the columns, metabolites as the rows, and stoichiometric coefficients as matrix elements; this refers to the stoichiometric (S) matrix. Adapted from (46).

The stoichiometric matrix is the fundamental aspect behind *in silico* simulations of cellular metabolism. In order to do such simulations, however, a number of laws and assumptions must be considered. All reactions in a reconstruction must respect the law of mass conservation, something covered in the step of manual curation. This then allows to determine mass balances for each metabolite in the stoichiometric matrix as a set of differential equations, represented in Equation 1.2:

$$\frac{dx}{dt} = S \cdot v(t) \tag{1.2}$$

where x is the concentration of a given metabolite, S is the stoichiometric matrix and $v(t)$ is a vector of reaction fluxes (47).

The intracellular concentration of metabolites and enzyme activity rates can vary over time, as consequence of metabolic and regulatory factors. Determining any of these variable parameters is challenging, as quantifying compound concentrations and enzymatic rates at a cell-wide scale is still a difficult undertaking. However, metabolic functions generally take place at much faster rates than regulatory changes or cell modification events (such as cell division). As such, it is possible to assume cells reach a steady state when growing in continuous culture or a pseudo steady state during exponential growth in non-continuous cultures (47, 48). This assumption allows to surpass the difficulty in measuring cell-wide metabolite concentrations and enzyme kinetics. In homeostasis, consumption of metabolites takes place at the same rate as their production and, therefore, concentrations do not change. This steady state assumption can be imposed on the system of material balance equations (Equation 1.2), as represented in Equation 1.3:

$$S \cdot v = 0 \tag{1.3}$$

Metabolic reconstructions at a genome scale typically contain a larger number of reactions than metabolites. This results in more variables than equations and, thus, an under-determined system of linear equations, for which no unique solution can be found. Nevertheless, it is possible to analyse biologically-relevant points in the solution space through the use of different mathematical methods. Flux balance analysis (FBA) is one of such methods and arguably the most widely used one. It is the application of linear programming to determine the optimal value of an objective function in a system of linear equations (49). The formal representation of FBA is as follows:

$$\begin{array}{ll} \text{maximize} & c^T v \\ \text{subject to} & S \cdot v = 0 \\ \text{and} & l \leq v \leq u \end{array} \tag{1.4}$$

where $c^T v$ is the objective function, that is, the expression to be maximized (or minimized), and l and u are the minimum and maximum reaction rates allowed on the unknown vector of reaction fluxes, v.

The presented formalization shows that FBA lies on two fundamental sets of constraints. The first one is the previously discussed imposition of mass balance, which guarantees a steady state of null accumulation. The second one is the imposition of maximum and minimum reaction rates, which define a solution space of possible reaction fluxes and, thus, allow for more realistic predictions. In a GEM, lower and upper boundaries on each reaction define the rate constraints, at the units of mmol g_{DW}^{-1} h^{-1}. When defined in the set of exchange reactions, these boundaries allow determining environmental constrains. There, a negative value indicates the rate of nutrient uptake (that is, flux from outside the system into the extracellular space) and a positive value indicates the rate of product secretion (that is, flux from the extracellular space to outside the system). Reaction rates are determined experimentally, by measuring the consumption and secretion of metabolites in continuous culture, ideally, or during exponential growth in non-continuous cultures.

Through the experimental determination of enzymatic capacities, it is also possible to thermodynamically constrain intracellular reactions and, thus, grant further realism to *in silico* predictions. By ranging from positive to negative values, boundaries can also represent reaction directionality. A non-zero negative lower boundary and a non-zero positive upper boundary determine a reversible reaction (Equation 1.5). A single null lower boundary determines an irreversible reaction (Equation 1.6). For any reaction whose flux rate remains unknown, its boundaries assume an infinite value, typically named unconstrained or unbounded flux.

$$l_i \leq v_i \leq u_i$$
$$\text{where} \quad l_i \in]-\infty, 0[\quad \text{and} \quad u_i \in]0, \infty] \tag{1.5}$$

$$0 \leq v_i \leq u_i$$
$$\text{where} \quad u_i \in]0, \infty] \tag{1.6}$$

While FBA can theoretically assume any network reaction as the objective function, in practice, only biologically relevant objectives are typically chosen. These can vary from maximization of ATP production, to minimizing redox metabolism, maximizing a by-product's secretion and many more (50). However, the fundamental and most commonly used objective is the BOF. As mentioned above, this reaction mathematically represents all metabolites making up cellular biomass and the energy required for its synthesis. Given the BOF's scaling (where metabolites have units of mmol g_{DW}^{-1} and flux through the reaction units of mmol g_{DW}^{-1} h^{-1}), any flux calculated through this reaction will consequently be equal to the organism's specific growth rate (μ_{max}), at units of h^{-1}. Fundamentally, it is the abstraction of cellular composition by the BOF that allows simulating organic growth *in silico*.

In its mathematical representation, the metabolic reconstruction can thus be converted to a computational format, the third major step of developing GEMs. This conversion is typically performed automatically by appropriate software tools, specific to the field of metabolic modelling (51, 52). In its computational form, the metabolic reconstruction can then be subject to a plethora of tools for network evaluation and refinement.

1.2.4. Network evaluation and model validation

The fourth step in GEM development is network evaluation and validation, where, in its computational form, the metabolic reconstruction is subject to a series of tests. Errors are searched for, network properties are evaluated and its capabilities are validated. Network errors can be such as: mass imbalanced reactions; metabolites only produced or consumed; reactions unable to carry flux; loops leading to the production or consumption of ATP without any nutrient uptake; and more (40).

Save for pseudo-reactions, all metabolic reactions in a reconstructed network should respect the principle of mass conservation. As described above, this is a fundamental rule behind the steady-state assumption, which, in turn, will allow future computations using FBA.

Compounds only produced or only consumed are known as dead-end metabolites (Figure 1.5). They result from network gaps where reactions are missing and, with some minor exceptions, they should not be present in a reconstruction. These missing reactions can be classified as: knowledge gaps, when genetic and biochemical data specific to the organism is missing or when the metabolic function is still unknown; scope gaps, when the subsequent pathway leads to non-metabolic cellular functions; or biological gaps, when there's experimental evidence against the expression or activity of the missing enzyme(s).

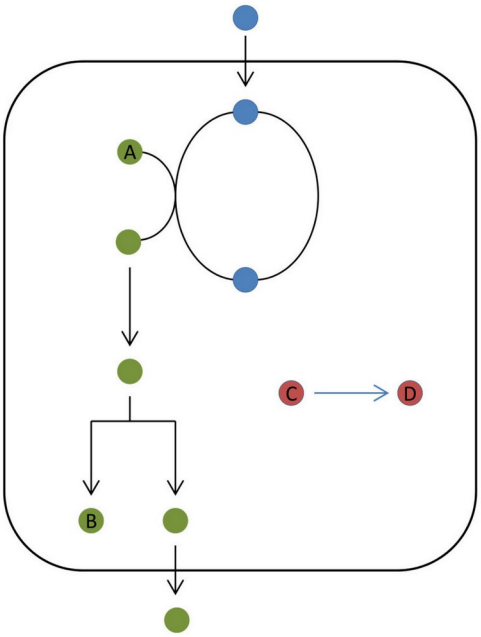

Figure 1.5: Schematic representation of dead-end metabolites in a metabolic reconstruction. A metabolite is considered a dead-end when it is only consumed (A, C) or only produced (B, D). Adapted from (53).

Reactions unable to carry flux, regardless of the set environmental conditions, are known as blocked reactions. They typically result from dead-end metabolites, but not strictly, as, depending on the set objective function, certain segments of the metabolic network might not participate in the linear optimization of said objective. Thus, despite the absence of gaps, these reactions will have zero flux.

When all exchange reactions in a model are closed, no flux should exist in the metabolic network. However, if flux does exist, it indicates the presence of stoichiometrically balanced cycles (SBCs) (40). These are thermodynamically infeasible internal loops, where reactions are active and carry flux, despite the system being in a closed state (54). They are unrealistic and should not exist in a GEM, for if they involve the consumption or production of ATP, *in silico* predictions related to energetic metabolism risk being inaccurate.

After applying all possible corrections on identified network errors, the step of model validation follows. The first step in this process is assessing whether the model can generate all biomass precursor metabolites, a requirement for future growth simulations. Afterwards, further validation tests are performed, such as: evaluating the ability to produce known secretion products; simulating experimentally determined nutritional requirements; supporting growth on experimentally determined carbon sources; displaying consistency with experimentally determined gene-deletion phenotypes; and more (40). All validation tests require extensive experimental data, and this should be obtained either from primary literature or experimental work performed in parallel to the model's development.

Throughout the fourth stage, resolution of identified inconsistencies will always require the revaluation of involved pathways. This evaluation might lead to solutions such as correcting reaction reversibility, removal of false-positive reactions or, more often, filling network gaps with missing functions. Gap filling can be performed manually, by searching the literature and metabolic databases for missing information, or algorithmically, for which there are now many software tools available

(55). Nevertheless, paramount care should be taken when adding new reactions, in order to guarantee the reconstructed model does not gain phenotypic traits different from those of the target organism.

The development of GEMs following the four steps outlined above should be an iterative process, where any change introduced to the reconstruction must lead to the repetition of network testing and validation. Likewise, the process of updating a model with new available information should also be iterative, leading to the same network revision and assuring that no previous functions are disturbed.

When the development of a GEM is finished, it can then be shared with the community, either through publication or its inclusion in specific databases. This sharing can be done through multiple different ways. At the simplest level, a metabolic reconstruction can be shared as the list of reactions that compose it. This, however, is discouraged, as it greatly hinder the use and testing of the GEM by different individuals, or groups, not directly connected to its development. As such, nowadays metabolic reconstructions are most commonly shared in their computational form, ideally with the validating constraints already pre-loaded. Sharing in this form is done using many different computer file formats, such as '.mat' (specific to the MATLAB environment), '.json' or, most frequently, '.sbml'. SBML, standing for Systems Biology Markup Language, is an open-source, XML-based format, specifically developed for describing and sharing mathematical models representing biological networks (56). This model format has the added advantage of being readable by the large majority of software tools related to biological modelling.

1.2.5. Applications and future prospects of genome-scale models

One could argue the development of a GEM is not finished for as long as metabolic functions remain unknown. The fact that many organisms continue to receive updated models years or decades after the publication of their first GEM is a testament to that statement. Organisms such as *Escherichia coli*, *Bacillus subtilis*, and even the human being, have received numerous updates to their GEMs and will likely be subject to many more (34). Nevertheless, the reconstruction of a metabolic network ends when all relevant knowledge available at the time has been incorporated. After this point, the GEM is ready to be used for prospective applications.

Since the emergence of metabolic modelling at a genomic scale in the 1990s, a wide range of methods and applications have been developed for these models. Traditionally, GEMs are used to predict cellular growth under varying environmental and genetic conditions and to interpret the resulting metabolic behaviours (57, 46). Moreover, growth predictions can be a fundamental tool in analysing general network properties and for studying the more complex metabolic mechanisms (28, 57, 46). Regarding genetic questions, these models can be of use in answering how single or double gene knockouts affect metabolic functions and what phenotypes result from such manipulations (58, 59). All these applications demonstrate the central link between GEMs and wet lab work, where they often serve to interpret experimental data. Beyond that, however, metabolic models can also guide experimental design and discoveries, by, for instance, modelling reactions that fill knowledge gaps in a network and, therefore, suggest where investigative assays should head (60, 61).

The applications that have arguably garnered the most interest in GEMs are those of mapping omics data and metabolic engineering. These models can be used to map and analyse a wide range of high-throughput data, such as transcriptomics, proteomics and metabolomics, which can detail the up- and downregulation of various pathways, help realistically constrain reaction fluxes and enable the creation of highly accurate, context-specific models (57, 59, 60, 61). GEMs can also be used to compute manipulations such as gene or reaction knockouts and insertion of novel functions (28, 57). These applications are particularly relevant for metabolic engineering, where these models have come to participate in the design and optimization of microbial strains as cell factories by, for instance,

testing synthetic biology hypothesis before they are applied (58, 59). Furthermore, in the context of synthetic biology, GEMs can also be used to model the production of inserted plasmids, by accounting for all the metabolic requirements and costs associated with plasmid synthesis (62).

Emerging applications of metabolic models have also progressively been under greater focus. They have now been used to uncover potential novel drug targets against pathogens and some cancers, thanks to, on one hand, the development of models specific to these organisms and cell forms and, on the other, the ability to compute the metabolic effects of gene knockouts and reaction blockage (34, 61). Furthermore, they have been used to study multi-cellular interactions, an application possible in part due to the ever-growing taxonomic and morphological coverage by GEMs. These interactions can be between different organisms at a community level, where ecologically realistic behaviours can be modelled, between a host and a pathogen, where the metabolic consequences of infections can be studied, or even between different human cell types, where, for instance, the interaction between different organs or tissues can be modelled (34, 60).

Finally, a growing use for GEMs is the study of pan-genomes, where, through comparative genomics, a base high-quality, manually curated reconstruction is used to generate many strain-specific separate models (63). These genome scale models can then be applied to study, for instance, strain-specific nutritional requirements, how different habitats and ecological niches lead to specific metabolic adaptations, and more (64).

For all the possible applications described above, and more, different modelling tools have been developed and utilized throughout the years. Briefly, these now range from numerous variations on FBA, where different optimization strategies can be employed, to multiple methods of perturbing genes and reactions—particularly important in metabolic engineering—, to different tools for applying high-throughput data and thermodynamically constrain models, and many more (65). Together, these *in silico* tools form what is known as constraint-based reconstruction and analysis methods, also known as COBRA methods (Figure 1.6).

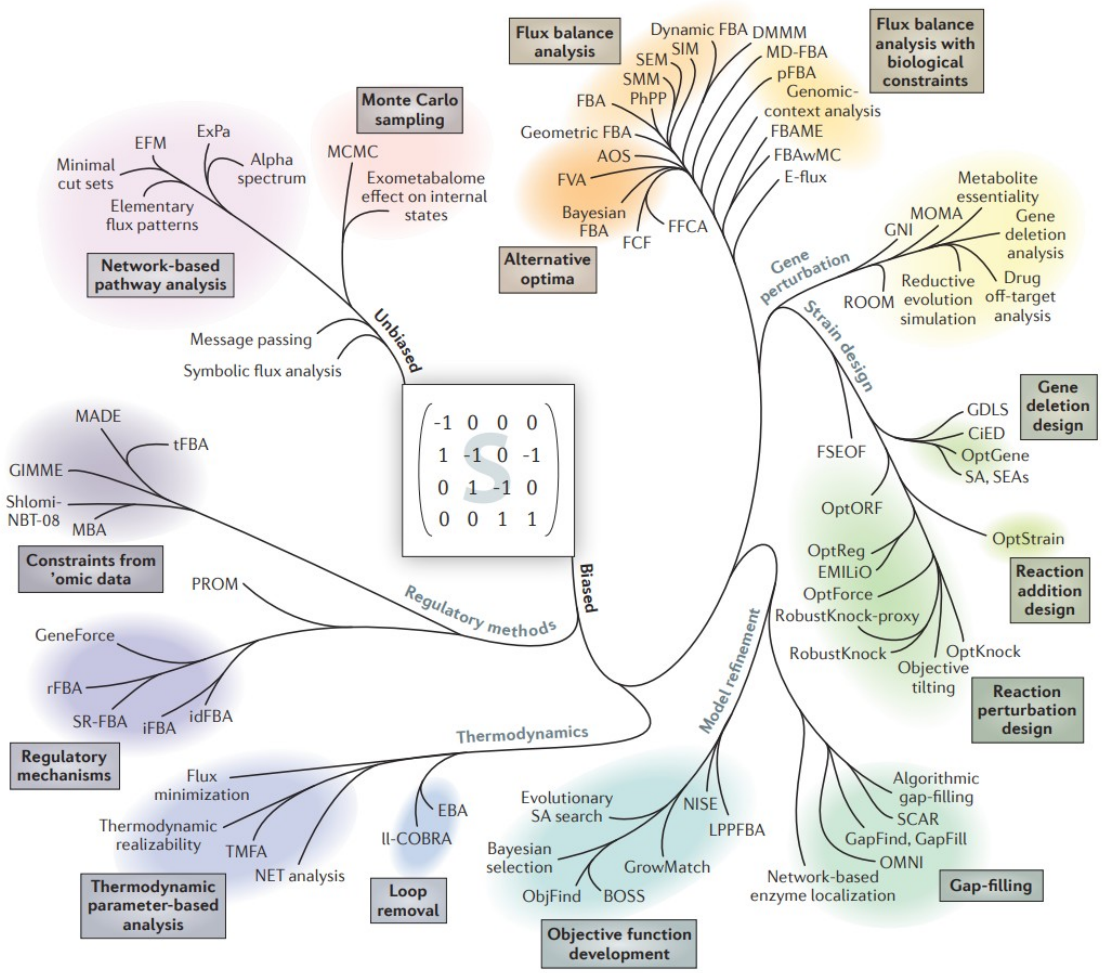

Figure 1.6: A phylogenetic-like representation of the many currently available *in silico* tools for genome-scale modelling of metabolism. Together these methods form what is known as constraint-based reconstruction and analysis (COBRA) methods. Adapted from (65).

Parallel to the expansion of modelling methods, new types of GEMs have also been developed, now beyond the original scope of simulating only metabolic fluxes. In conjunction with metabolism, these models generally cover gene expression, 3D protein structures, probabilistic transcriptional regulation or even an organism's entire cellular functions (66). The first three model variations are briefly discussed, given the increasing attention they have gathered.

By representing transcriptional and translational processes, metabolism and expression models (also known as ME-Models) account for of the metabolic cost behind macromolecular synthesis and pathway operation (67). This enables the simulation of enzyme synthesis costs and their maximum availability, which, in turn, allows computing realistic growth rates without the need for nutrient consumption measurements. Furthermore, they permit greater realism in mapping gene expression data and modelling genetic manipulations. Models of metabolism and protein structures (also known as GEM-PROs) offer greater information on the target organism. Furthermore, they enable studying the effects of protein structures on metabolism, particularly relevant in environmental conditions known to affect protein structures (68). Finally, probabilistic transcriptional regulation models of metabolism (also known as PROM models) are GEMs which integrate regulatory networks by probabilistically representing genetic states and the effects of transcription factors (69). The inclusion

of these cellular functions, alongside with metabolism, enables integrating high-throughput data in a more comprehensive way and, thus, perform more realistic simulations on the effects of environmental and genetic changes.

It is worth noting, however, that these advanced GEMs are still very rare when compared to the number of available metabolic models. This can be due a number of reasons. These new models are still relatively recent developments, with the first metabolism and expression model having been published in 2013 (70), fifteen years after the first GEM (32). However, it might also be due to the fact that many of these advancements have led to an exponential increase in the number of reactions and metabolites, which in turn greatly increase computer processing times.

1.3. Currently-available *L. lactis* genome-scale models

Two high-quality, manually curated GEMs have been published for *L. lactis* so far.

The first one, developed by Oliveira *et al*. (71), was published in 2005 and accounts for 358 genes, 649 reactions (when also accounting for psuedo reactions) and 509 metabolites. This model was used to compute growth requirements, predict single gene and single reaction deletion phenotypes and model the experimentally observed shift from homo- to heterolactic fermentation in *L. lactis* (13). Additionally, and as a theoretical example of the application of GEMs in metabolic engineering, the authors employed single gene deletions to build *in silico* mutants capable of producing greater yields of 2-acetolactate. This is a compound which, through spontaneous oxidative decarboxylation, is converted to diacetyl, a known by-product of fermentation in *L. lactis* and an industry-relevant flavour compound.

This model presents some issues, however, regarding modern standards for GEMs. While the network reconstruction was based on the genome annotation of *L. lactis* subsp. *lactis* IL1403, many functions incorporated by the authors come from experimental data on different strains. Furthermore, the BOF was also based on experimental data from multiple different *L. lactis* strains, none of which IL1403. This is in agreement with the authors' goal of developing a metabolic model for *L. lactis*, not necessarily specific to any strain. Nevertheless, this generality can be problematic, for instance, in computing nutritional requirements and carbon source utilization, both of which have been experimentally shown to vary greatly between *L. lactis* strains (19, 20, 72). Furthermore, the development of generic species-level metabolic models has fallen out of use, in favour of strain-specific reconstructions. Finally, it is worth noting no official version of this model is available in a computable format and only its reaction list is shared as a supplementary material.

The second GEM available for this species was developed by Flahaut *et al*. (73). Published in 2013, this model accounts for 518 genes, 754 reactions, and 650 metabolites. It is now available in the BiGG database (74), where it was given the identification *i*NF517. This is a metabolic model specific to *L. lactis* subsp. *cremoris* MG1363 and it was used in analysing amino acid and flavour-forming pathways, studying how gene manipulations in the latter pathway affect growth, and in estimating cellular energetic parameters, both associated and not associated with biomass formation. The model was validated using rates of nutrient consumption and metabolic by-product formation, experimentally determined by the authors in carbon-limited continuous culture. Furthermore, it was validated by the comparison of amino acid requirements predicted *in silico* with the ones experimentally determined by the authors for *L. lactis* MG1363.

1.4. Objectives of this work

The plasmid-free strain *L. lactis* subsp. *lactis* LMG 19460 recently had its genome sequenced (75). Its lack of intrinsic plasmids makes it an ideal candidate for the insertion of exogenous, genetically engineered plasmids. When combined with the general safety status associated with LAB, in particular *L. lactis*, this characteristic presents the strain as a viable option for various biotechnological applications, from the production of recombinant protein and mucosal vaccination, to many more (22).

In these biotechnological applications, a GEM can be a fundamental tool for better understanding and better using the organism of interest. However, reconstructing the metabolic network of organisms for which there is no published, metabolically-relevant data can be a difficult, if not ineffectual, undertaking, without carrying out parallel experimental work. As mentioned above, many crucial steps in the development of a GEM require the use of quality, strain-specific experimental data. As such, for less studied organisms, alternative strategies are necessary for the reconstruction of their metabolism. One of those strategies is to first develop a high-quality model for a closely related, well characterised organism, and then, through sequence homology, use that model to infer metabolic functions for the organism of interest (76, 77, 78).

With these considerations in mind, this work aimed to develop a GEM for *L. lactis* LMG 19460, on top of which future developments can be made. However, seeing as no published metabolic data exists for this strain, an alternative approach to traditional reconstruction methods had to be applied. Therefore, an additional goal for this work was to develop a GEM for the well characterised *L. lactis* reference strain, IL1403, and validate it through comparison with its extensive published experimental data. Then, through sequence homology, this model would be used to infer metabolic functions in strain LMG 19460. Furthermore, this study also had the purpose of starting the experimental metabolic characterization of *L. lactis* LMG 19460. For this end, and parallel to the work developed *in silico*, it was established the objective of developing a chemically defined medium capable of sustain clear and robust growth of strain LMG 19460. Then, finally, the results obtained on the synthetic medium were to be used as a beginning validation of the GEM developed for *L. lactis* LMG 19460.

2. Materials and methods

2.1. Metabolic reconstruction for *L. lactis* IL1403

The protocol developed by Thiele and Palsson (40) was generally followed for reconstructing the metabolic network of *L. lactis* IL1403. This comprehensive standard operating procedure covers all necessary steps for the development of a GEM. It starts with the assembly of a draft reconstruction and its manual curation, followed by its conversion into a computable form, the execution of qualitative tests and, finally, its practical applications (40). However, to accelerate the first stages of manually generating and refining a draft reconstruction, an alternative semi-automated approach was followed. Here, it was conducted an analysis of amino acid sequence homology between *L. lactis* IL1403 and target prokaryote organisms for which there are manually curated published GEMs. This comparative biology approach also serves to identify candidate metabolic functions not yet experimentally determined in the target organism, a common occurrence in non-model organisms such as *L. lactis*.

The software Proteinortho (79), with the algorithm BLASTp+ (80) as the search option and remaining settings as default, was used to identify reciprocal best hits between *L. lactis* IL1403 and a series of target organisms. The results for metabolic genes covered by the target's model were analysed and positive matches were considered of equivalent function in *L. lactis* IL1403. Reactions were selected as candidate additions to the reconstruction only when homology was observed with all associated genes, in case of protein complexes, or at least one of multiple genes, in case of isozymes. After the first iteration of this process, the list was subsequently filtered for reactions already present in the reconstruction. For any duplicate found, the GPR association was reviewed by comparing it with KEGG (81) and MetaCyc (82) database entries for *L. lactis* IL1403, or any found published experimental data. For reactions identified as new, the target's genes were replaced by their orthologous in *L. lactis* IL1403 and the GPR rule was maintained as determined by the authors. An identification representing a known metabolic pathway, referred to as a subsystem, was attributed to each reaction. This categorisation was based either on the respective model from which the reaction was inferred or from information found in the KEGG (81) and MetaCyc (82) databases. Finally, EC numbers and reaction identifiers in the databases KEGG (81), ModelSEED (83), and MetaCyc (82) were also attributed to each reaction introduced in the reconstruction. This was done whenever the original model from which the reaction was inferred did not account for such identifiers or when its information was incomplete. Not all metabolic reactions have an identifier in all these databases. This is particularly noticeable for more peripheral pathways.

The first target organism for sequence homology was *L. lactis* MG1363, chosen for being the closest strain to *L. lactis* IL1403 for which there is a recent, manually curated, published GEM (73). Reactions with GPR associations were processed as described above. However, exclusive to this step and in order to generate a working first draft reconstruction, every other reaction in *i*NF517 was also added, including reactions without an associated gene (known as orphan reactions) and exchange reactions.

To infer further metabolic functions, the literature was scanned for published GEMs of organisms in the same taxonomic class as *L. lactis* IL1403, *i.e.*, Bacilli. However, as too many candidates were found (at least 24 published models), the criterium was further narrowed. Only GEMs published in the year of or years after *i*NF517 and only the ones using the same metabolic nomenclature as *i*NF517, BiGG identifiers (84), were selected. The list was thus reduced to a manageable 6 target organisms, which are listed in Table 2.1, along with their taxonomy and a series of relevant model and genome assembly characteristics. Despite falling outside the set criteria, *E. coli*

K12 MG1655 was chosen as an extra 7th target, for having arguably the highest quality and most comprehensive prokaryote GEM available, *i*ML1515. Metabolic models for *E. coli* are generally at the forefront of prokaryote modelling and may account for reactions that, while present in other organisms, may not have yet been described experimentally or inferred via comparative genomics approaches.

Table 2.1: Organisms selected for iterative sequence homology analysis with *L. lactis* IL1403. Entries for the genome assemblies of *L. lactis* IL1403 and *L. lactis* LMG 19460 are included as to allow comparing the number of protein-coding genes with the remaining organisms. All genome assemblies were downloaded from the Reference Sequence database of the National Center for Biotechnology Information (https://www.ncbi.nlm.nih.gov/). The GEMs from references 68, 73, and 85 were downloaded from the BiGG database (74). For some models, the authors did not attribute a model identification (N/A). a: this number of model genes is reported in the BiGG database (74), from where the latest model version was obtained from.

Phylum	**Class**	**Order**	**Family**	**Organism**	**Model ID**	**Protein-coding genes**	**Model genes**	**Model reactions**	**Model metabolites**	**Genome assembly**	**Model reference**
Firmicutes	Bacilli	Lactobacillales	Streptococcaceae	*Lactococcus lactis* spp. *lactis* IL1403	—	2219	—	—	—	ASM686v1	—
Firmicutes	Bacilli	Lactobacillales	Streptococcaceae	*Lactococcus lactis* spp. *lactis* LMG 19460	—	2131	—	—	—	ASM198478v1	—
Firmicutes	Bacilli	Lactobacillales	Streptococcaceae	*Lactococcus lactis* spp. *cremoris* MG1363	*i*NF517	2319	516[a]	754	650	ASM942v1	73
Firmicutes	Bacilli	Lactobacillales	Streptococcaceae	*Streptococcus oralis* spp. *oralis* SK141	*i*CJ415	1758	415	604	504	ASM72267v1	86
Firmicutes	Bacilli	Lactobacillales	Streptococcaceae	*Streptococcus pyogenes* NZ131 serotype M49	N/A	1608	480	576	558	ASM1812v1	87
Firmicutes	Bacilli	Lactobacillales	Leuconostocaceae	*Leuconostoc mesenteroides* spp. *mesenteroides* ATCC-8923	*i*LME620	1975	620	763	754	ASM1444v1	88
Firmicutes	Bacilli	Lactobacillales	Enterococcaceae	*Enterococcus faecalis* V583	N/A	3172	668	706	642	ASM778v1	89
Firmicutes	Bacilli	Bacillales	Staphylococcaceae	*Staphylococcus aureus* spp. *aureus* USA300_TCH1516	*i*YS854	2800	866	1455	1335	ASM1708v1	68
Proteobacteria	Gamma-proteobacteria	Enterobacteriales	Enterobacteriaceae	*Escherichia coli* str. K-12 substr. MG1655	*i*ML1515	4242	1516	2712	1877	ASM584v2	85

As a final step in the search for candidate metabolic reactions, an automated reconstruction was generated by applying the software CarveMe (90) to the genome of *L. lactis* IL1403, with Gram-positive as the universal template option and remaining settings as default. The resulting model was then processed and evaluated as described above for the published GEMs. CarveMe (90) is a tool for the automatic reconstruction of metabolic models, in which manually curated generic models, assembled by the authors, are adapted to specific input genomes via sequence homology. These homologies, however, are mono-directional and performed with an algorithm less sensitive than classical BLAST+, the algorithm DIAMOND (91). Therefore, the manual curation of new reactions was performed with particular care. The tool was chosen for its use of BiGG metabolic identifiers (84), thus allowing an easier and direct comparison with the reconstruction under development for *L. lactis* IL1403.

The model generated by CarveMe was also used as a kickstart for the search of candidate transport reactions. Though the automated tool inevitably predicts excessive transport reactions, due to the mentioned lower sensitive of its homology-prediction algorithm (91), this list can serve as a starting point for evaluating possible additions to the global reconstruction. In order to evaluate their inclusion, the transport reactions predicted by CarveMe were reviewed and compared to a series of databases. These were the TransportDB (92) entry for *L. lactis* IL1403, the reciprocal best hits determined by BLASTp between *L. lactis* IL1403 and the entire sequence data available at the Transport Classification Database (93), as well as the mentioned KEGG (81) and MetaCyc (82) entries for the strain.

2.2. Biomass reaction and energy requirements of *L. lactis* IL1403

The BOF is a reaction accounting for all metabolites which make up cellular biomass and the energy required for its synthesis. This biomass reaction can then serve as an objective function for the linear programming problem formalized by FBA, where the maximization of said objective, combined with the application of experimentally determined constraints, enables the prediction of specific growth rates (44).

For the development of a BOF, the standard operating procedure by Thiele and Palsson (40) continued to be followed. Taking the base cellular composition values assembled by Oliveira *et al*. (71), values specific to *L. lactis* IL1403 were then searched for in the literature, in order to create an updated and strain-specific biomass reaction. A single lumped reaction was created, where all biomass constituents are directly present. Lipid and cell wall constituents inferred by Oliveira *et al*. (71) were converted to the BiGG (84) identifier nomenclature, using the work done by Flahaut *et al*. (73), also based on data assembled by the previous authors. The literature was searched for data determining vitamins, cofactors, ions, and other micronutrients essential for *L. lactis* IL1403 growth. Any such compounds were then added to the BOF. Finally, the literature was also searched for *L. lactis* IL1403 growth in carbon-limited, continuous culture experiments in order to determine the GAM and NGAM parameters.

2.3. Conversion to a mathematical form and network evaluation

Having assembled the candidate reactions for the metabolic network of *L. lactis* IL1403, the reconstruction was then converted to a mathematical, and thus computable, form. For this and future computational purposes, the COBRA Toolbox v3 (94) was used. This is a MATLAB suite that enables the reconstruction and analysis of GEMs, as well as their application to a multitude of goals related to metabolic modelling, such as phenotype prediction, strain design and optimization, integration of multiomics data, and more (94).

In its mathematical form, the network was then evaluated for errors and missing metabolic functions. More specifically, COBRA Toolbox functions were applied to detect mass-imbalanced reactions, dead-end metabolites, network gaps, blocked reactions and stoichiometrically balanced cycles. These errors were processed in an iterative manner, meaning that, whenever solutions led to changes in the network, tests were repeated in order to assure the previous error was solved and no new ones were created.

Mass imbalanced reactions were searched for using the COBRA Toolbox function 'checkMassChargeBalance'. Positive results were solved through the application of appropriate chemical and stoichiometric corrections. These corrections were inferred by comparing the reactions with the previously mentioned metabolic databases, as well the ModelSEED database (83) and the enzymatic database BRENDA (104).

In order to identify dead-end metabolites and network gaps, the COBRA Toolbox functions 'detectDeadEnds' and 'gapFind' were respectively applied on the model. For the solution of these errors, pathways leading to and from the participating metabolites were evaluated. This evaluation was performed by comparing pathways with the previously mentioned databases and by searching for relevant literature. Gaps identified as biological by experimental evidence were not filled, scope gaps were solved by adding pseudo-reactions representing the metabolite drainage into other cellular functions, and knowledge gaps were solved by completing the respective pathway with information found in the analysis step. In case of a conservative reconstruction process, where, initially, only reactions with high confidence levels are accounted for, knowledge gaps are typically solved by adding missing reactions. The confidence level for these reactions might be lower, but they are necessary to match experimentally observed phenotypes. However, in case of accelerated reconstruction processes, such as the one here applied, false-positive reactions might be present. Therefore, a further possible solution for knowledge gaps was the removal of poorly supported reactions, wrongfully added in the initial reconstruction step.

For the analysis of blocked reactions, all exchange reactions were opened by respectively setting their lower and upper boundaries to -1000 and 1000 mmol g_{DW}^{-1} h^{-1}. These are purposefully high values in order to represent unconstrained flux. Although unrealistic, these exchange settings enable maximum activation of the metabolic network when optimizing the BOF and, thus, leave out false-positive results of, for instance, inactive pathways due to absence of nutrients. Afterwards, the COBRA Toolbox function 'findBlockedReaction' was used to identify reactions unable to carry flux. For their solution, the same procedure as described for dead-end metabolites and network gaps was followed, where: participating pathways were reviewed; missing functions were added; and false-positive inclusions were removed.

In the work by Heirendt *et al*. (94), a mathematical method named sparse FBA is defined and presented as a tool for identifying reactions involved in SBCs leading to ATP production or consumption. This was the chosen method to identify such cycles in the reconstructed metabolic network. For their resolution, the identified reactions were re-evaluated on the confidence of their inclusion and, again, false-positive reactions were removed. As for strongly supported reactions, their directionality was re-evaluated by comparing with the previously mentioned metabolic and enzymatic databases, as well as by analysing the calculated Gibbs free energy variation, at pH 7 and a standard concentration of reactants of 1 mM; the appropriate conditions for estimating metabolic reactions in living cells. To obtain these values, the web interface eQuilibrator (105) was used, where the component contribution method outlined by Noor *et al*. (106) is automatically used to estimate the standard Gibbs energy of chemical reactions.

2.4. Model validation: nutritional requirements

Model validation is the application of experimentally determined constraints on a metabolic network and subsequent testing for expected phenotypes. These constraints can represent media composition, experimentally determined reaction fluxes, metabolic by-product secretion, gene expression profiles and more (107). These phenotypes can be specific growth rates in continuous culture, carbon source utilization, nutritional requirements, production of known secretions, and more (40). Unless stated otherwise, all henceforth growth tests were performed by FBA, while maximizing the BOF, and under boundary constraints specified in each chapter or test description.

The validation step was first performed by testing for expected phenotypes regarding nutritional requirements. To do so, the literature was scanned for experimental determination of essential nutrients specific to *L. lactis* IL1403 and a list of compounds to be tested was assembled. From the evidence found, a generic medium was composed *in silico*, accounting for all components present in the media of each collected work. Whenever experimental evidence was performed in batch cultures or microtiter plates, application of the assembled medium as *in silico* constraints took the form of unbounded nutrient uptake (that is, lower boundaries set to -1000 mmol g_{DW}^{-1} h^{-1}).

Testing for the essentiality of medium components was performed by omitting each compound individually and subsequently maximizing for growth (also known *in vitro* as the single omission technique). Therefore, the subject of evaluation was the phenotypical effect of removing each medium component, where a positive result refers to achieving simulated growth and a negative result refers to achieving none.

2.5. Model validation: simulations in published chemically defined media

The following step in model validation was to ascertain growth in published chemically defined media for *L. lactis* IL1403. Furthermore, the model's capability to simulate expected specific growth rates under experimentally determined nutrient uptake and product secretion rates was also evaluated.

Any media reported in the previously collected studies were used, as well as further relevant experimental data found in the literature. Special emphasis was put on data determining metabolite consumption and production rates, as this is the only data type which allows simulating realistic growth rates.

When no flux rate was determined or reported in the literature, media composition was represented as unbounded uptake of each present compound. When flux data was available, the reported values for compound consumption and production were respectively applied as the lower and upper boundaries on their exchange reactions (at units mmol g_{DW}^{-1} h^{-1}). All tests were performed with the additional constraints determined by Oliveira *et al*. (71) based on experimental evidence. Namely, these constraints were, in anaerobiosis, inactivating the pyruvate dehydrogenase reaction (PDH in the model), while, in aerobiosis, inactivating pyruvate-formate lyase (PFL in the model) instead and setting oxygen consumption as -3.61 mmol g_{DW}^{-1} h^{-1} on its respective exchange reaction.

Any data regarding growth in chemically defined media without the full measurement of carbon source and amino acid consumption rates was regarded as Boolean data. More specifically, media composition and any possible incomplete flux rates were applied as exchange constraints, but the model was only tested for positive or negative growth, and not the ability to match specific growth rates. For validation tests using the mentioned full rate data, the model was evaluated on its capacity to meet expected Boolean growth, but also expected specific growth rates.

2.6. Model validation: carbon source utilization

A further step in model validation is the assessment of growth on substrates experimentally determined as possible single carbon sources. To do so, the literature was scanned for such data specific to *L. lactis* IL1403 and the model was evaluated for growth on each individual, experimentally tested carbon source. A chemically defined medium was defined based on found literature and applied as *in silico* exchange constraints. Carbon sources were evaluated iteratively by their addition one at a time, followed by the simulation of growth. As a cut-off point, compounds were considered possible carbon sources when simulated growth rates were higher than the value obtained for growth in the same medium without a carbon source. A result was considered negative when the simulated growth rate was equal or lower than the mentioned threshold or when no respective transport reaction was found in the model.

2.7. Metabolic reconstruction for *L. lactis* LMG 19460 and respective evaluation

The metabolic network of *L. lactis* LMG 19460 was reconstructed using the previously developed GEM for *L. lactis* IL1403. A similar workflow to the one described above was followed for the identification of amino acid sequence homologies between the two organisms. Namely, reciprocal best hits were identified using the software Proteinortho (79) on the genome assemblies of *L. lactis* IL1403 (ASM686v1) and *L. lactis* LMG 19460 (ASM198478v1). The software tool was applied with the algorithm BLASTp+ (80) as the search option and remaining settings as default. Afterwards, it was followed the same procedure as when generating the first working draft reconstruction for *L. lactis* IL1403 from sequence homology with the model *i*NF517. More specifically, genes covered in the GEM developed for strain IL1403 were replaced by their respective orthologous in *L. lactis* LMG 19460, thus, maintaining the previously established GPR associations. Genes for which no homology was detected with strain LMG 19460 were removed from the model. Consequently, their respective reactions were either also removed or had their GPR associations corrected, in case of available isozymes. Every other function in the model was inherited to the reconstruction for strain LMG 19460, namely the remaining orphan reactions, pseudo-reactions (including the previously developed BOF), and corresponding metabolite list.

Conversion of the reconstructed network to a computable form was again done using the MATLAB suit COBRA Toolbox v3 (94). The process of network evaluation was performed as described above for the metabolic network of *L. lactis* IL1403.

2.8. Organism and media

A series of growth experiments using different rich chemically defined media and varying culture conditions were performed for *L. lactis* LMG 19460 cells, obtained from the Belgian Coordinated Collections of Microorganisms (Brussels, Belgium). The cells were stored in frozen stocks at -80 °C, in M17 medium supplemented with 40% glycerol.

The first chemically defined medium (CDM1) was designed on the basis of previous works by Cocaign-Bousquet *et al*. (95), Zhang *et al*. (96) and Aller *et al*. (97). A particular difference from those works, however, was the use of yeast nitrogen base without amino acids and ammonium sulphate (YNB) as replacement for various of vitamins, minerals and other micronutrients typically present in rich chemically defined media. Despite being a pre-made base medium, YNB is itself chemically defined and composed of specific compounds with detailed concentrations, thus not affecting the classification of CDM1 as a chemically defined medium. The composition of CDM1 is presented in Table 2.2. The second chemically defined medium used, CDM2, is a modification of the previous one, where the concentration of D-glucose is increased from 3.5 to 10 g L^{-1} and ascorbic acid is added at

0.5 g L^{-1}. Ascorbic acid is a reducing agent, many of which have been used in *Lactococcus* cultures as a way to overcome the slight growth inhibition observed under aerobic conditions (95, 98, 99). Finally, the third chemically defined medium (CDM3) is itself a variation on CDM2, with the concentration of the buffer MOPS being altered from 7.5 to 26.16 g L^{-1}, and pH adjusted to 7.0.

Individual, concentrated stock solutions were prepared for each amino acid (Table 2.2), choline chloride, coenzyme B12, (±)-α-Lipoic acid and the chemically defined nutrient solution YNB. Furthermore, a concentrated group stock solution was also prepared, containing the inorganic compounds cobalt(II) sulphate, iron(II) sulphate, and ammonium heptamolybdate. All stock solutions were stored at -4 °C.

Table 2.2: Constitution of the first assembled chemically defined medium, CDM1. Yeast nitrogen base (without amino acids and ammonium sulphate) was used as the source of most vitamins, minerals and micronutrients.

Medium component	**Concentration (g L^{-1})**
D-glucose monohydrate	3.5
Ammonium sulphate	1.0
Dipotassium phosphate	0.9
MOPS	7.5
Potassium acetate	0.9
L-Alanine	0.078
L-Arginine	0.185
L-Asparagine	0.074
L-Aspartic acid	0.072
L-Cysteine hydrochloride	0.064
L-Glutamic acid	0.07
L-Glutamine	0.132
Glycine	0.058
L-Histidine	0.06
L-Isoleucine	0.102
L-Leucine	0.207
L-Lysine monohydrochloride	0.158
L-Methionine	0.041
L-Phenylalanine	0.086
L-Proline	0.092
L-Serine	0.163
L-Threonine	0.076
L-Tryptophan	0.016
L-Tyrosine	0.029
L-Valine	0.107
Ammonium heptamolybdate tetrahydrate	0.003
Cobalt(II) sulphate heptahydrate	0.003
Iron(II) sulphate heptahydrate	0.0014
Choline chloride	0.0098
Coenzyme B_{12}	0.00098
(±)-α-Lipoic acid	0.001
Yeast Nitrogen Base without amino acids and ammonium sulphate	6.8

For preparing the mentioned chemically defined media, a base solution consisting of all non-stock components was first composed. These non-stock compounds were D-glucose and the remaining

buffers, but also ascorbic acid in media where it is present. Afterwards, each stock solution was supplemented to the desired final concentration, following the order of amino acids, minerals, vitamins and, finally, YNB. In the case of CDM3, the assembled medium solution then had its pH adjusted to 7.0 by the drop-by-drop addition of potassium hydroxide (10 M). At last, the media were sterilized by vacuum filtration (0.2 μm pore size) into sterile recipients (autoclave, at 121 °C for 20 min) and stored at room temperature and away from light.

Parallel growth experiments were also performed in the complex medium M17, supplemented with glucose at 20 g L^{-1} (henceforth referred to as M17) and sterilized by autoclave, at 121 °C for 20 min.

2.9. Growth conditions and analytical methods

In total, six sets of *L. lactis* LMG 19460 growth experiments were performed, two for each of the chemically defined media described above. Some of these sets also contained a parallel growth assay in M17 broth. The general procedure is first described, followed by the varying characteristics and conditions of each experiment.

A pre-inoculum was prepared by growing cells overnight in M17 broth. Afterwards, cells were washed three times by centrifuging cultures for 3 min, at 6000 G and 20 °C, and resuspending the cell pellet in a saline solution (NaCl at 9 g L^{-1}). Test tubes containing a chemically defined medium were inoculated with the calculated volume necessary for a starting optical density at 600 nm (OD_{600}) of 0.1. All growth experiments were negative controlled and performed at least in triplicate, unless stated otherwise. All cell cultures, including those for pre-inoculum production, were incubated at a temperature of 30 °C and an agitation speed of 100 RPM. Cell growth was followed by measuring the OD of culture samples at a wavelength of 600 nm against a calibrating white measurement of the same media, not inoculated, sterile and kept in the same growth conditions as the culture vessels. The OD_{600} measurements were performed every hour, ideally until cultures reached stationary phase. Stationary phases were confirmed by resuming measurements around 24 h after the start of incubation. Measurements of pH, when applying, were also performed every hour, at the same time as OD_{600} measurements. Final pH values were confirmed in parallel to the 24 h OD measurements.

In the set of two experiments in CDM1, cells were inoculated in a volume of 10 mL. In the second of these two assays, cells were also inoculated in M17 and grown in parallel to the CDM1 cultures. In the set of experiments in CDM2, the first one was carried in a culture volume of 10 mL, while the second one was carried in an upscaled volume of 40 mL. Parallel to the second assay, cells were also inoculated in a set of M17 cultures. In the same second assay, the pH of cultures in both media was also followed. In the set of two experiments in CDM3, the first one was carried in culture volumes of 35 mL and cells were also inoculated in a single, non-replicated M17 vessel. In this first experiment, culture pH was also followed. The second of the two experiments in CDM3 was carried only in duplicate, in culture volumes of 20 mL and with cells, again, also inoculated in a single parallel M17 test tube.

2.10. *L. lactis* LMG 19460 partial model validation

For the partial validation of the GEM developed for *L. lactis* LMG 19460, the chemically defined media previously constructed were applied as *in silico* constraints and simulated growth was tested for. However, given the steady-state assumption inherent to FBA, only composition variations, and not varying concentrations, can be accounted for. As such, only media CDM1 and CDM2 were used when performing these tests. Furthermore, given that no metabolite consumption or production rates were measured, the media could only be applied as unconstrained fluxes on the exchange reactions

corresponding to each of its constituents. Consequently, the model was only evaluated for positive or negative growth.

3. Results and discussion

3.1. Genome-scale model for *L. lactis* IL1403 and general properties

The reconstructed metabolic network for *L. lactis* IL1403 accounts for 575 unique genes, 921 reactions and 639 metabolites. It contains two distinct compartments, cytosol and the extracellular space, and covers 60 unique metabolic subsystems. It is presented in a tabular form in Supplementary Table S1, where every reaction is listed along with each respective part: GPR association; flux boundaries; network subsystem; EC number(s); and reaction identifiers for the metabolic databases KEGG (81), ModelSEED (83), and MetaCyc (82). Furthermore, a column is also included indicating the current objective function. Finally, the model is also presented with a set of external constraints pre-loaded. This has the aim of demonstrating how experimentally determined rates of nutrient consumption and product formation are applied as exchange reaction constraints. The chosen *in silico* medium refers to flux rate data by Lahtvee *et al*. (100) for chemostat cultures of *L. lactis* IL1403 at a dilution rate of 0.45 h^{-1}, with a correction applied to the histidine measurement, acknowledged by the authors as erroneous (further discussed in Chapters 2.5 and 3.5). Supplementary Table S2 lists the GEM's metabolites, along with their respective chemical name, formula, charge and compartment.

Out of the total reactions present in the reconstruction, 789 are metabolic, while 132 are pseudo-reactions necessary for *in silico* simulations. Of the total metabolic reactions, 718 are associated to a GPR rule, 18 are non-enzymatic spontaneous reactions and 53 have no known gene. Furthermore, the reconstruction identifies 145 chemical reactions connected to the extracellular space, of which 144 are transport reactions and 1 fully takes place outside the cell. This fully external reaction (BG_CELLB, in the model) is catalysed by a β-glucosidase enzyme specific to cellobiose (EC 3.2.1.21), whose hydrolysis results in the production of two glucose molecules. These results are summarised in Table 3.1.

Table 3.1: Summary of characteristics of the metabolic model here developed for *L. lactis* IL1403. a: The genome assembly for *L. lactis* IL1403 (ASM686v1) accounts for 2219 protein coding genes. b: c, cytosol; e, extracellular space.

Category	Number of	Relevant percentages (%)
1. Genes (unique)	575	25.91[a]
2. Metabolites	639	–
2.1. Unique	526	82.32
2.2. Cytosolic	517	80.91
2.3. Extracellular	122	19.09
3. Reactions	921	–
3.1. Pseudo-reactions	132	14.33
3.1.1. Exchange reactions	122	92.42
3.2. Metabolic	789	85.67
3.2.1. Known gene	718	91
3.2.2. Spontaneous	18	2.28
3.2.3. Unknown gene	53	6.72
4. Compartments	2 (c, e)[b]	–
4.1. Cytosolic reactions	654	71
4.2. Extracellular reactions	267	28.99

Every reaction has been attributed a subsystem and these cover the various pathways associated with energetic metabolism, such as glycolysis and pentose phosphate pathways, as well as the metabolism of carbohydrates alternative to glucose, such as galactose, fructose, various complex sugars, and more. Furthermore, the subsystem categorization distinguishes the various amino acid, nucleotide, and lipid metabolic pathways, as well as a series of biosynthetic pathways related to cofactor groups and cell wall constituents. When available, each chemical reaction included in the reconstruction has been annotated with its respective EC number, as well as an identifier corresponding to the same reaction in different metabolic databases. The chosen databases were KEGG (81), ModelSEED (83), and MetaCyc (82) databases.

Given the semi-automated nature of the reconstruction process (described in Chapter 2.1), a retrospective analysis was performed on the origin of each metabolic reaction, regarding the organism and GEM from which they were inferred. The number of models each reaction was found in, when having determined an orthologous with *L. lactis* IL1403, was accounted for, in order to partially evaluate the confidence of their inclusion. For this purpose only, the automated reconstruction generated with CarveMe was considered as an 8th target model. This analysis is partial in nature, because not every reaction is present in every model and reactions present in few models can still have high confidence. This is the case, for instance, when an enzyme is supported by strong bidirectional homologies or by experimental evidence.

Figure 3.1 shows the result of this review, where it is observed that 51.71% of reactions are supported by at least 4 models and 74.27% by at least 2 models. Individual values show that most reactions are, however, only supported by 1 model (17.24%). Finally, it is observed the presence of 67 orphan reactions, which were not supported by direct homology with any of the target organisms. These are reactions either included from the base model *i*NF517, in which they originally lacked a coding gene, reactions inferred from the transporter revision, or reactions added as gap filling in the network revision step (whose results are discussed further ahead).

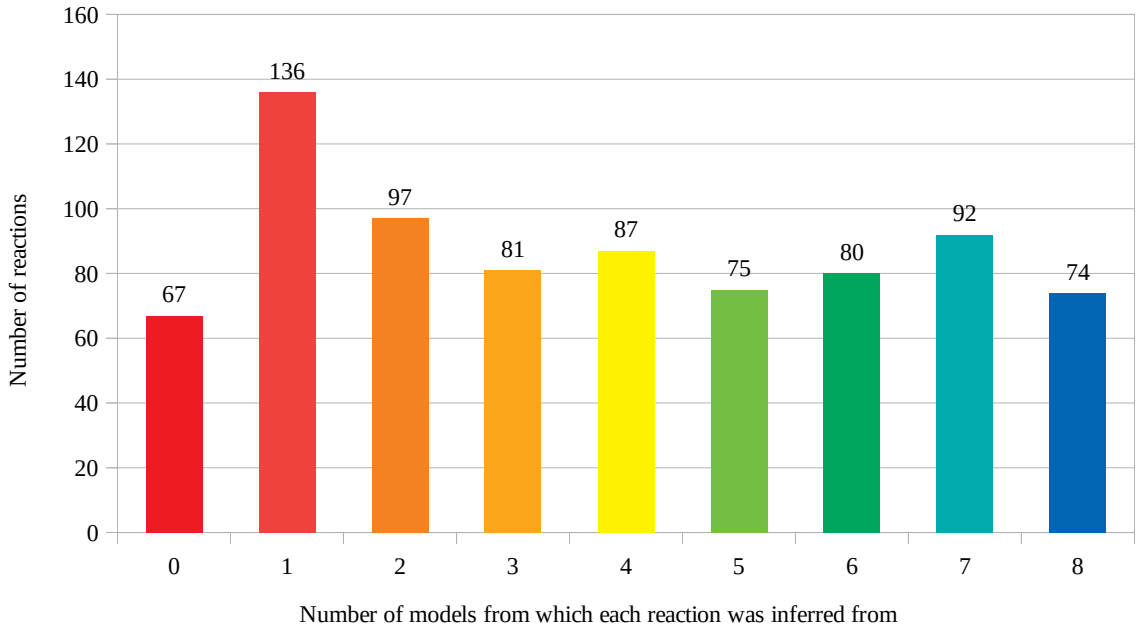

Figure 3.1: Retrospective quantification of the target models from which metabolic reactions in the reconstruction for *L. lactis* IL1403 were inferred from. Although exceptions exist, reactions product of homology with a higher number of organisms usually mean greater confidence on the inclusion.

These results show how it was possible to assemble a list of well supported metabolic functions for *L. lactis* IL1403 through the determination of sequence homology with organisms having high-quality GEMs available. As it is shown (Figure 3.1), the majority of reactions result from gene homology with a considerable number of organisms, which confers good confidence to most of the reconstructed network. Nonetheless, a significant number of the assembled reactions is also only supported by 1 model. This group of reactions is of the highest priority for further manual revision in future works, as it may still contain false-positive inclusions which could lead to erroneous *in silico* predictions. Finally, it is noted that, despite the use of 7 target organisms and an automated reconstruction for the identification of metabolic functions in *L. lactis* IL1403, some orphan reactions are still present. This is a common occurrence in non-model organisms and shows the limitations of the methodology here applied. The process of inferring gene functions through sequence homology is inherently limited to knowledge available in other organisms. However, some metabolic processes are genera-, species- or even strain-specific. This demonstrates the importance of conducting experimental work parallel to the development of high-quality GEMs, but also how these models can be used to drive that same experimentation, by suggesting, for instance, cellular processes in need of greater scrutiny.

While the GEM developed by Oliveira *et al*. (71) is not presented as specific to *L. lactis* IL1403, the authors used its genome annotation as the starting point for the reconstruction process and also for inferring metabolic functions from sequence homology. As such, some comparisons can be drawn between the mentioned metabolic model and the one developed in this work.

When compared with the GEM developed by Oliveira *et al*. (71), the metabolic reconstruction here presented for *L. lactis* IL1403 accounts for an additional 272 reactions, 130 metabolites and 217 metabolic genes. Curiously, however, it defines only 4 more subsystems, in quantitative terms. This shows how differences between the two reconstructions take place mostly inside each of these pathways. In terms of pathways at a greater scale, the largest number of reactions added by the present reconstruction is observed in cofactor and prosthetic group metabolism, followed by lipid metabolism, central metabolism, nucleotide metabolism and membrane transport reactions (Table 3.2).

Table 3.2: Comparison of the number of reactions in major subsystem groups between the GEM by Oliveira *et al.* (71) and the metabolic model here developed. The identification chosen for each major group is based on the one defined by Oliveira *et al.* (71) and adapted for the presented model.

	Number of reactions	
Major subsystem groups	**Oliveira *et al*. (71)**	**Present work**
Carbohydrate metabolism	57	53
Amino acid metabolism	137	135
Cell Envelope Biosynthesis	23	29
Central metabolism	47	89
Lipid metabolism	39	98
Membrane transport	105	142
Nucleotide metabolism	94	133
Cofactor and prosthetic group metabolism	46	106
Others	3	4
Pseudo-reactions	98	132

The greater detailing of cofactor and vitamin metabolism is in line with the work here developed, where a particular effort was made in reviewing vitamin metabolism in order to meet published nutrient requirements of *L. lactis* IL1403 (further discussed ahead). The greater number of reactions in lipid metabolism is also expected, as the original model by Oliveira *et al*. (71) abstracted the majority of this pathway with unrealistic reactions. This was in line with other GEMs published at the time (103), but has since fallen out of use with a progressive greater detailing of the reactions composing these pathways. Thanks to the determination of orthologous genes between *L. lactis* IL1403 and organisms for which high-quality, recent GEMs are available, it was possible to offer new insights and greater detail into the strain's lipid metabolism. In fatty acid metabolism in particular, the unrealistic, abstracted reactions used by Oliveira *et al*. (71) have been replaced with true chemical reactions, such as, for instance, the ones catalysed by acyl-carrier-protein dehydratases (EC 4.2.1.59), reductases (EC 1.1.1.100), synthases (EC 2.3.1.179) and more (Supplementary Table S1).

While many transport reactions were reviewed in order to match the expected published phenotypes of *L. lactis* IL1403 (further discussed ahead), others did not suffer this manual curation. The inclusion of transport reactions solely based on sequence similarity might lead to false inclusions, as this class of proteins is still far less known than cytosolic enzymes. As such, unknown structures or substrate specificities consequence of nuanced sequence variation might be lost in an approach solely based on sequence homology.

The nucleotide metabolism pathways did not suffer extensive manual curation either and, as such, might account for false-positive inclusions. Upon inspecting the reconstruction, it is noted that a significant part the reactions inferred from homology with a single organism or inherited from the model *i*NF517 (73) are present in this group. While not necessarily an indicative of wrongful inclusions, this at least suggests future works should aim to thoroughly review these pathways in order to distinguish new additions to the metabolic knowledge of *L. lactis* IL1403. Finally, the greater number of reactions included in central metabolism pathways present the most worrisome result of this comparison. While new metabolic functions are expected to be uncovered in lesser known peripheral pathways, the same cannot safely be said for central metabolism. Excessive additions in energetic metabolism risk leading to unrealistic *in silico* predictions of growth rate, energy requirements, by-product formation and more. As such, future works aiming to further curate the metabolic network here reconstructed should place the greatest priority in reviewing these pathways.

3.2. Biomass reaction

Following the initial step of assembling the candidate metabolic network for *L. lactis* IL1403, and in agreement with the mentioned standard operating procedure (40), a biomass reaction was constructed for the strain.

The values for *L. lactis* cellular composition collected and determined by Oliveira *et al*. (71) were used as a starting point for the development of a BOF. In a first step, the multiple biomass reactions developed by the authors (where the synthesis of each macro-component is individualized in its own separate reaction) were lumped in a single one, with all stoichiometric coefficients recalculated to be in the same units (mmol g_{DW}^{-1}). This is a commonly observed form for BOFs, and such conversion permits better comparability with other GEMs.

In the following steps, knowledge regarding the cellular composition of *L. lactis* IL1403 was searched for in the literature. Lahtvee *et al*. (100) determine the macromolecular composition of *L. lactis* IL1403 cells grown in accelerostat, at each of multiple dilution rates. While Oliveira *et al*. (71) used the average biomass composition values determined for multiple strains of *Lactococcus*, none were the strain IL1403. Therefore, the average values determined by Lahtvee *et al*. (100) were used to update the BOF when possible, namely for the protein, RNA, DNA, peptidoglycan sugars and lipid

fractions. For the remaining fractions accounted by the BOF, namely the lipoteichoic acids and polysaccharides fractions, the values calculated by Oliveira *et al*. (71) were maintained. Table 3.3 summarizes the cellular composition values used for constructing the biomass reaction.

Table 3.3: Partial chemical composition of *L. lactis* IL1403 cells. The values of each macromolecular fraction used for constructing the biomass reaction are shown, as well as their respective references.

Macromolecular fraction	**% (w/w)**	**Reference**
Protein	45.43	100
DNA	1.00	100
RNA	5.32	100
Lipids	5.93	100
Peptidoglycan sugars	22.01	100
Lipoteichoic acids	8.00	71
Polysaccharides	12.00	71

For GEMs written in the nomenclature established by BiGG identifiers (84), it is noted that metabolites related to the cell wall and lipid fractions are often written as species or strain specific (as observed in 5 out of the 7 target models previously mentioned). With that in mind, the identifiers created by Flahaut *et al*. (73) for model *i*NF517 were used for the constituents of these fractions, given that they're presented as *L*. *lactis* specific. The mentioned model's BOF was also based on the composition determined by Oliveira *et al*. (71), which further supports the use of the identifiers created by Flahaut *et al*. (73) in BiGG nomenclature. According to the methodology applied by Oliveira *et al*. (71), the stoichiometric values for cell wall and lipid components were calculated from the elemental composition determined by Flahaut *et al.* (73).

By analysing the BOFs of 71 published prokaryote GEMs and datasets for gene essentiality and enzyme-cofactor association, Xavier *et al*. (101) determine a list of universally essential and conditionally essential organic cofactors, which should generally be present in metabolic models for these organisms. This knowledge was taken into consideration when updating the BOF for *L*. *lactis* IL1403 and the literature was scanned for information on cellular quantification of these components, either for the strain, preferentially, or the species. However, as no study was found under these criteria, only the universally essential cofactors were introduced, and their stoichiometric values were inferred from the biomass reaction present in the automated reconstruction generated by CarveMe.

Thiele and Palsson (40) suggest the BOF should also account for the ion content of the cell. However, as no literature was found on its cellular quantification in *L*. *lactis* IL1403 either, no ions were included other than magnesium. Reviewing the literature for nutrient essentiality studies in *L*. *lactis* IL1403 (further discussed in chapter 3.4) revealed magnesium to be essential for growth (95, 96, 97). As such, the compound was included in the BOF. Again, the stoichiometric values generated by CarveMe were used, due to no data being found on cellular quantifications specific to the strain or species.

Regarding the energy requirements associated with growth, no data on the estimation of cellular energetics for *L*. *lactis* IL1403 grown in carbon-limited continuous culture was found in the literature. While Lahtvee *et al*. (100) utilize the strain in continuous culture growth assays, the conditions used were not carbon-limiting. This leads to the dissipation of metabolised energy into cellular function other than the production of ATP (45). As such, GAM and NGAM values could not trustingly be calculated from the results by the mentioned authors (100). Instead, the estimations by

Flahaut *et al*. (73), of 39.5 mmol g_{DW}^{-1} for GAM and 0.92 mmol g_{DW}^{-1} for NGAM, were used in place of the one by Oliveira *et al*. (71), acknowledged by the latter authors as carrying high uncertainty.

This choice behind GAM and NGAM parameters lied on two further factors. Firstly, the data from which Oliveira *et al*. (71) made their estimation, the work by Novák and Loubiere (102), was not obtained in carbon-limited conditions. On the other hand, the calculated values by Flahaut *et al*. (73) are based on carbon-limited continuous culture experiments, performed by the authors in the same work. Secondly, in their growth experiments, Novák and Loubiere (102) used the strain *L. lactis* subsp. *lactis* NCDO 2118, which has a metabolic plasticity significantly different from that of *L. lactis* IL1403 (95), most likely due to being a plasmid-carrying, vegetal strain. Meanwhile, much like *L. lactis* IL1403, the strain used by Flahaut *et al*. (73), *L. lactis* MG1363, is a plasmid-free, dairy strain which, despite belonging to a different subspecies from that of the prior strain, is characterised by a *lactis* phenotype (27).

The resulting BOF contains 51 cell constituents and accounts for protein, DNA, RNA, lipids, lipoteichoic acids, peptidoglycan and polysaccharides fractions of the average composition of *L. lactis* cells. Furthermore, it accounts for universally essential organic cofactors and published estimated values for growth-associated energy requirements at a species level. It offers some specificity to the *L. lactis* strain IL1403 and the greatest detailing of essential compounds in BOFs currently available for the species (71, 73). Table 3.4 presents the reaction equations of the original branched BOF composed by Oliveira *et al*. (71), followed by the single reaction here composed merging all the branched equations and, lastly, the final version of the biomass reaction included in the metabolic model here developed for *L. lactis* IL1403. The full detailed composition of the BOF can be found in Supplementary Table S3.

Table 3.4: Summarized development of the constructed BOF. a: original branched biomass reactions by Oliveira *et al.* (71). b: the first iteration of the BOF; it consisted in the branched biomass equations by Oliveira *et al.* (71) lumped into a single reaction, updated to BiGG nomenclature, and using the identifiers developed by Flahaut *et al.* (73) for the lipid and cell wall fractions.

Reaction name	**Reaction equation**	**Reference**
Protein assembly[a]	8.6 L-alanine + 4.1 L-arginine + 3.1 L-aspartate + 5.9 L-asparagine + 3.4 L-cysteine + 3.6 L-glutamate + 6.4 L-glutamine + 9.2 glycine + 1.5 L-histidine + 6.1 L-isoleucine + 8.7 L-leucine + 7.2 L-lysine + 2.5 L-methionine + 3.8 L-phenylalanine + 3.5 L-proline + 5.1 L-serine + 5.6 L-threonine + 1.7 L-tryptophan + 2.7 L-tyrosine + 7.2 L-valine + 430.6 ATP → 100 PROT + 430.6 ADP + 430.6 phosphate	71
DNA assembly[a]	32.3 dAMP + 17.7 dCMP + 17.7 dGMP + 32.3 dTMP + 337.2 ATP → 100 DNA + 337.2 ADP + 337.2 phosphate	71
RNA assembly[a]	26.2 AMP + 20 CMP + 32.2 GMP + 21.6 UMP + 240 ATP → 100 RNA + 240 ADP + 240 phosphate	71
Lipid assembly[a]	18.9 phosphatidylglycerol + 42.5 cardiolipin + 4.3 lysophosphatidylglycerol + 30.3 diglucosyl diacylglycerol + 4 monoglucosyl diacylglycerol → 100 LIP	71
Biomass assembly[a]	4.201 PROT + 0.074 DNA + 0.329 RNA + 0.015 LTA + 0.032 LIP + 0.119 PG + 0.064 POLYS + 18.15 ATP → BIOMASS + 18.15 ADP + 18.15 phosphate	71
Lumped biomass reaction[b]	0.361 ala__L[c] + 0.172 arg__L[c] + 0.130 asp__L[c] + 0.248 asn__L[c] + 0.143 cys__L[c] + 0.151 glu__L[c] + 0.269 gln__L[c] + 0.386 gly[c] + 0.063 his__L[c] + 0.256 ile__L[c] + 0.365 leu__L[c] + 0.302 lys__L[c] + 0.105 met__L[c] + 0.160 phe__L[c] + 0.147 pro__L[c] + 0.214 ser__L[c] + 0.235 thr__L[c] + 0.0714 trp__L[c] + 0.113 tyr__L[c] + 0.302 val__L[c] + 0.015 datp[c] + 0.015 dttp[c] + 0.008 dctp[c] + 0.008 dgtp[c] + 31.284 atp[c] + 0.046 utp[c] + 0.043 ctp[c] + 0.069 gtp[c] + 0.006 pg_LLA[c] + 0.013 clpn_LLA[c] + 0.001 lyspg_LLA[c] + 0.010 d12dg_LLA[c] + 0.001 m12dg_LLA[c] + 0.0145 LTAAlaGal_LLA[c] + 0.119 PG[c] + 0.064 CPS_LLA[c] → 31.228 adp[c] + 31.228 pi[c] + 31.228 h[c]	This work
Final biomass reaction	0.54366 ala__L[c] + 0.19632 arg__L[c] + 0.19665 asp__L[c] + 0.19665 asn__L[c] + 0.01452 cys__L[c] + 0.16616 glu__L[c] + 0.16616 gln__L[c] + 0.39012 gly[c] + 0.06834 his__L[c] + 0.21804 ile__L[c] + 0.33684 leu__L[c] + 0.3693 lys__L[c] + 0.09006 met__L[c] + 0.15408 phe__L[c] + 0.14898 pro__L[c] + 0.23322 ser__L[c] + 0.24636 thr__L[c] + 0.06 trp__L[c] + 0.1173 tyr__L[c] + 0.2934 val__L[c] + 0.00663 datp[c] + 0.00663 dttp[c] + 0.00364 dctp[c] + 0.00364 dgtp[c] + 39.52774 atp[c] + 0.02287 utp[c] + 0.02117 ctp[c] + 0.03409 gtp[c] + 0.0001 pg_LLA[c] + 0.00023 clpn_LLA[c] + 0.00002 lyspg_LLA[c] + 0.00017 d12dg_LLA[c] + 0.00002 m12dg_LLA[c] + 0.00015 LTAAlaGal_LLA[c] + 0.23197 PG[c] + 0.15334 CPS_LLA[c] + 0.00178 nad[c] + 0.00043 nadp[c] + 0.00022 amet[c] + 0.00022 fad[c] + 0.00022 ribflv[c] + 0.00022 pydx5p[c] + 0.00056 coa[c] + 0.00022 10fthf[c] + 0.00022 thf[c] + 0.00022 mlthf[c] + 0.00022 thmpp[c] + 0.00842 mg2[c] + 39.5 h2o[c] → 39.5 adp[c] + 39.5 pi[c] + 39.5 h[c]	This work

3.3. Network evaluation

The assembled metabolic reconstruction was converted to a mathematical form and then iteratively evaluated for errors. The results of this analysis on the initial version, the immediate product of the homology analysis, and on the final version of the model, after all error corrections, are presented in Table 3.5.

Table 3.5: Summary of the network evaluation performed. Results are shown for before and after the application of all possible corrections.

Reconstruction version	**After homology analysis with target models**	**After iterative correction of network errors**
1. Mass-imbalanced reactions	12	2
2. Dead-end metabolites	168	35
2.1. Reactions leading to dead ends	132	32
3. Metabolites leading to gaps	120	29
4. Blocked reactions	252	52
5. SBCs involving ATP	2	0
5.1. Reaction involved in SBCs	13	0

By comparing the identified mass-imbalanced reactions with the previously mentioned metabolic databases, all but 2 reactions were solved by the addition or subtraction of a single product or reactant proton. The remaining 2 reactions, presented in Table 3.6, originate from the homology analysis with model *i*NF517 and were written as mass-imbalanced by the authors themselves (73). They belong to pathways postulated as responsible for the formation of flavour compounds experimentally identified in the same work. No further database or experimental information was found for their correction.

Table 3.6: Mass-imbalanced reactions for which no solution was found and respective metabolites.

Abbreviation	**Description**	**Equation/Formula**	**Imbalance**
ACKLEU	Isovaleryl p acyl kinase	adp[c] + ppap[c] → 3mb[c] + atp[c]	4 H, 2 C in excess
adp[c]	Adenosine 5'-diphosphate	C10H12N5O10P2	—
ppap[c]	Propanoyl phosphate	C3H5O5P	—
3mb[c]	3-Methylbutanoic acid	C5H9O2	—
atp[c]	Adenosine 5'-triphosphate	C10H12N5O13P3	—
PTALEU	Isovaleryl coa phosphotransacetylation	pi[c] + ivcoa[c] → coa[c] + ppap[c]	4 H, 2 C missing
pi[c]	Orthophosphate	HO4P	—
ivcoa[c]	Isovaleryl-CoA	C26H40N7O17P3S	—
coa[c]	Coenzyme A	C21H32N7O16P3S	—
ppap[c]	Propanoyl phosphate	C3H5O5P	—

All chemical reactions in a metabolic network should respect the principle of mass conservation, in order to comply with the assumption of mass balance required by FBA (49).

Otherwise, any application of this algorithm for the prediction of biologically relevant phenotypes risks being inaccurate. However, the above mentioned reactions were left in the metabolic reconstruction and in their original state, on the basis of their respective mass imbalances cancelling each other out and due to being published reactions for the still poorly understood flavour forming pathways. Nevertheless, future works should aim to further clarify these pathways and introduce realistic reactions. Moreover, further experimental work should be carried on the actual identification of enzymes responsible for the formation of flavour compounds in *L. lactis*, thus, elucidating the actual reactions taking place.

Most dead-end metabolites leading to network gaps and blocked reactions were solved by the removal of low confidence reactions, wrongfully added in the first step of the reconstruction process. These were reactions inferred via homology with very few organisms and often at stakes with data found in the KEGG and MetaCyc entries for *L. lactis* IL1403. For some few pathways, however, the review step identified possible gap filling reactions and, therefore, these were added to the reconstruction. For metabolites produced but not consumed, but for which their reactions had strong homology support, demand reactions (that is, pseudo-reactions simulating compound drainage into non-metabolic functions) were added according to the workflow established by Thiele and Palsson (40). Lastly, some dead-end metabolites were determined to be a consequence of biological gaps and were therefore kept in the network, leading to 35 remaining present in the reconstruction. Most of these were part of reactions supported by strong and ubiquitous homologies, but for which no homology was found with genes coding for gap filling reactions. Supplementary Table S4 lists the remaining dead-end metabolites in the model's final version, while Supplementary Table S5 lists their respective reactions.

Curiously, while this metabolic model accounts for 272 more reactions than the first GEM for *L. lactis*, it only contains 7 more dead-end metabolites than the one developed by Oliveira *et al*. (71). This highlights the effort here made in expanding the metabolic knowledge on *L. lactis* without introducing network errors.

While 51 out of the total 52 remaining blocked reactions were directly or indirectly consequence of dead-end metabolites, 1 was not. This was undecaprenyl diphosphate synthase (UDCPDPS, in the model) and no solution was found for its inability to carry flux, despite its remaining pathway (isoprenoid biosynthesis) not being blocked. Future works should further evaluate this and neighbouring pathways, in varied sets of environmental conditions, in order to determine the cause of this blockage. The total blocked reactions present in the final version of the model are listed in Supplementary Table S6.

The search for SBCs involving ATP hydrolysis led to the identification of 2 such cycles. One of these involved reactions in amino acid metabolism pathways (Figure 3.2A), while the second one involved transport reactions (Figure 3.2B). For their solution, each reaction was evaluated on the confidence of their inclusion and on its reversibility, as detailed in Chapter 2.3. Reactions HSDA, AHSERL, SHSL3, CITt3 and FORt were determined to be false-positive inclusions and were removed from the reconstruction. This solution immediately led to the resolution of both SBCs. Nevertheless, the analysis of reaction directionality based on Gibbs free energy estimation also determined reactions SHSL4r and AHSERL should not be reversible (Table 3.7). The foremost reaction was thereby corrected to occur only in the anabolic direction. The complete list of reactions involved in SBCs is presented in Supplementary Table S7, along with their respective equation, subsystem, estimated Gibbs free energy variation and calculated flux in the analysis.

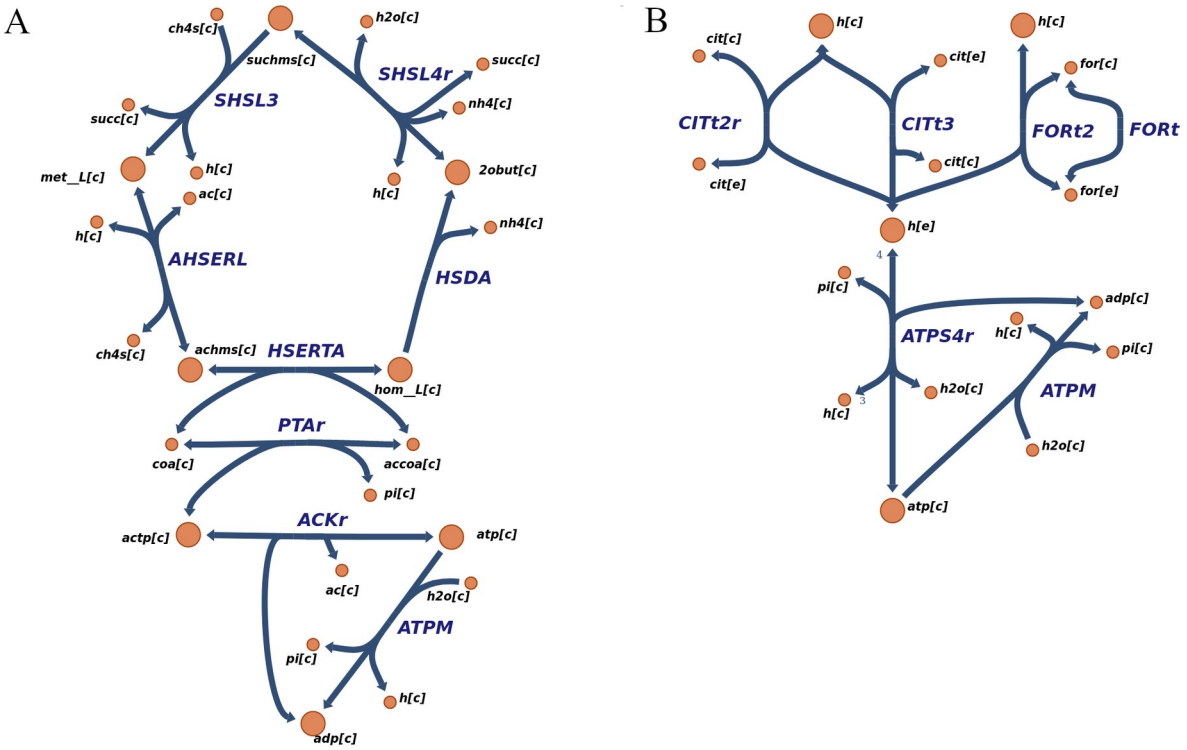

Figure 3.2: Stoichiometrically balanced cycles involving ATP detected in the network evaluation step. A: The cycle involving amino acid metabolism reactions, solved by the removal of the false positive-reactions HSDA, AHSERL and SHSL3. B: The cycle involving the transport reactions, solved by the removal of false-positives CITt3 and FORt.

Table 3.7: Reactions participating in SBCs determined to have an incorrect directionality. $\Delta rG'^{m}$ values were calculated using the online tool eQuilibrator (105), estimated via the component contribution method (106) and with standard reactant concentrations of 1 mM and at pH 7.

Reaction abbreviation	**Reaction name**	**Original reaction formula**	**Estimated $\Delta_r G'^{m}$ (kJ/mol)**
SHSL4r	O-Succinyl-L-homoserine succinate-lyase	h2o[c] + suchms[c] ⇄ 2obut[c] + h[c] + nh4[c] + succ[c]	-92.3 (± 9.2)
AHSERL	O-acetylhomoserine (thiol)-lyase	achms[c] + ch4s[c] ⇄ ac[c] + h[c] + met__L[c]	-57.0 (± 8.7)

After the process of network evaluation, the metabolic reconstruction was thus cleared of most of its errors and of all for which a solution was found. As stated, the results here presented are for the initial and final versions of the reconstructed network in its computational form. However, it is worth noting this was an iterative process carried out throughout the entire development of the metabolic model. Whenever any change was introduced to the reconstructed network, all evaluation steps were repeated in order to ensure no other metabolic function was perturbed.

3.4. Model validation: nutritional requirements

Following network debugging, the step of model validation was performed based on expected phenotypes reported in experimental literature for *L. lactis* IL1403. From such data, appropriate constraints were ascertained and applied to the reconstruction, in order to simulate the conditions reported *in vivo*, and to test whether the model can achieve expected results.

The first goal was to evaluate the model's capability to simulate expected nutrient and environmental requirements. As such, the literature was scanned for studies experimentally determining those requirements in *L. lactis* IL1403. Three distinct studies were found specific to the strain, those of Cocaign-Bousquet *et al*. (95), Zhang *et al*. (96) and Aller *et al*. (97). In order to assemble the list of essential conditions and compounds, a criterium was applied where nutrients were considered essential only when no other study contradicted the finding (that is, the remaining studies either were in agreement or did not evaluate the compound). Table 3.8 lists the concordant growth requirements of *L. lactis* IL1403.

Table 3.8: Nutrient requirements of *L. lactis* IL1403 agreed on by the published literature.

Group	**Compound**	**Supporting reference**
Amino acid	L-Arginine	95, 96, 97
Amino acid	L-Histidine	95, 96, 97
Amino acid	L-Isoleucine	95, 96, 97
Amino acid	L-Leucine	95, 96, 97
Amino acid	L-Methionine	95, 96, 97
Amino acid	L-Valine	95, 96, 97
Mineral group	Magnesium	95, 96, 97

Starting with the gas environment, all mentioned studies collectively show *L. lactis* IL1403 to be capable of growing in the presence and absence of molecular oxygen. Zhang *et al*. (96) report growth in both anaerobiosis, at the microtiter plate scale, and aerobiosis, at the test-tube scale, while Aller *et al*. (97) did not control the gas environment. However, only Cocaign-Bousquet *et al*. (95) evaluated this variable. The authors determined that *L. lactis* IL1403 is slightly inhibited by the presence of either CO_2 or O_2 and, instead, achieves the best growth under a N_2 atmosphere; thus, displaying a facultative anaerobe phenotype.

Moving on to amino acid requirements, all studies agreed on the same 6 essential ones, as well as threonine having a stimulating effect on growth. On the other hand, aspartate, glutamate, phenylalanine and tryptophan are reported to have no effect on cellular growth. For the remaining amino acids, at least one study always reached disagreeing conclusions (further discussed ahead).

Regarding nucleotide bases, both Cocaign-Bousquet *et al*. (95) and Zhang *et al*. (96) found these compounds to have a stimulatory effect on growth, yet none to be essential. Aller *et al*. (97) did not evaluate the effect of nucleotide bases on cellular growth.

As for vitamins and micronutrients, no clear conclusion could be drawn for essential compounds, as a disagreement between at least two studies was always found. Nevertheless, some of these nutrients could be classified as at least growth stimulating. Riboflavin was determined as essential by Cocaign-Bousquet *et al*. (95) and Aller *et al*. (97), while Zhang *et al.* (96) only identified it as having an important effect on growth. It is, therefore, assessed that the vitamin has, at least, a clear stimulatory effect on the growth of *L. lactis* IL1403. Similar contradictory information was found for pantothenate and vitamin B_6. Both are determined as important for growth by Zhang *et al*. (96), while Aller *et al*. (97) ascertain them as essential, but only in conditions of reduced amino acid concentrations. Furthermore, Cocaign-Bousquet *et al*. (95) determine the first as essential and the latter as essential only in the absence of nucleotide bases. Finally, the most contradictory evidence is found for vitamin B_3 and biotin, where all three studies reach different conclusions.

Finally, in respect to mineral groups, all studies agreed on the essentiality of magnesium. The strong evidence for this requirement led to the compound's inclusion in the BOF. This, in turn, allowed for the proper evaluation and simulation of said essentiality. As for the remaining mineral groups, no other compound was determined to be required for growth and, as such, none were included in the biomass reaction. Furthermore, no metabolic functions involving the remaining ions could be inferred from homology, other than transport reactions. As such, these compounds were not included in this model validation step, as their evaluation would lead to meaningless positive results.

Concerning the essentiality of mineral groups, a conclusion drawn by Cocaign-Bousquet *et al*. (95) on results not shown by the authors regarding the subject is here paraphrased: trace metals are often transported into media by being present in other components and, as such, their essentiality might not be as easy to assert. Furthermore, it is highly unlikely no other mineral group is essential for growth of *L. lactis* IL1403, given the wide range of crucial roles these ions and trace metals have in cellular functions and their long history in the evolution of life (108). As such, it is suggested that magnesium most likely is not the only essential mineral group for the strain's growth and, instead, might merely be required in greater concentrations than other ions.

Table 3.9 lists the conflicting cases of nutrient requirements determined by the mentioned works, from which no conclusion could be drawn.

Table 3.9: Nutrients on *L. lactis* IL1403 essentiality assays for which conflicting evidence was found. a: The effect of each compound reported by the authors was normalized as either essential, conditionally essential (with the respective justification in footnote), stimulating or non-essential for growth. b: the authors report essentiality only in experiments with reduced amino acid concentrations. c: aggregated results for vitamin B6, as each referenced study used a different form of this vitamin. d: the authors use the vitamin B6 form pyridoxamine. Essentiality is only reported in the absence of nucleotide bases. e: the authors use the vitamin B6 form pyridoxal. f: the authors use the vitamin B6 form pyridoxine. g: aggregated results for vitamin B3, as some studies used different forms of this vitamin. h: the authors use the vitamin B3 form nicotinate. i: the authors use the vitamin B3 form nicotinamide. j: all vitamins reported as essential by the authors had to be complemented with biotin. k: the authors report essentiality only in re-inoculation experiments.

		Effect on growth reported by each reference[a]		
Group	**Compound**	**Cocaign-Bousquet *et al*. (95)**	**Zhang *et al*. (96)**	**Aller *et al*. (97)**
Amino acid	L-Asparagine	Stimulating	Stimulating	Essential
Amino acid	L-Glutamine	Essential	Non-essential	Stimulating
Amino acid	L-Serine	Stimulating	Stimulating	Essential
Vitamin	Riboflavin	Essential	Stimulating	Essential
Vitamin	Pantothenate	Essential	Stimulating	Conditionally essential[b]
Vitamin	Vitamin B_6[c]	Conditionally essential[d]	Stimulating[e]	Conditionally essential[b, f]
Vitamin	Vitamin B_3[g]	Essential[h]	Stimulating[h]	Non-essential[i]
Vitamin	Biotin	Conditionally essential[j]	Stimulating	Non-essential
Vitamin	Thiamine	Non-essential	Stimulating	Conditionally essential[b]
Micronutrient	Lipoate	Non-essential	Stimulating	Conditionally essential[k]

In order to test the metabolic model for growth requirements previously inferred, a medium was composed *in silico* based on all compounds covered by the mentioned experimental evidence. This medium was applied as exchange constrains to the model and the essentiality of each component

was evaluated by repeatedly omitting each metabolite and testing for growth (further detailed in Chapter 2.4).

The total nutritional conditions amounted to 46 individual tests, covering gas environment, amino acids, nucleotide bases, vitamins and micronutrients. At the first round of testing, the metabolic model correctly predicted 32 of those phenotypes. However, it returned 7 incorrect predictions and it was unable to perform the remaining 7 tests due to the respective pathways being incomplete.

The following step was then to evaluate the pathways leading to erroneous results. These were evaluated for low confidence reactions, which were subsequently removed, and for missing functions, which were solved by gap filling when possible or appropriate. Gaps were filled by determining the orthologous genes between *L. lactis* IL1403 and the ones coding for gap-filling reactions in any of the target models, previously used in the reconstruction step. Moreover, when a reaction was necessary to match expected phenotypes, it was added even if no homology could be detected. Finally, pathways leading to correct predictions were also reviewed for false-positive reactions and missing functions, in order to further polish the metabolic reconstruction. Table 3.10 summarizes the initial incorrect results and the possible solutions found for their correction.

Table 3.10: Erroneous *in silico* results from the first tests on expected *L. lactis* IL1403 nutritional requirements. Some compounds could not be evaluated due to their pathways being incomplete (N/A).

		Effect of single omission from medium		
Compound	**Metabolite ID**	**Expected result**	**Model result**	**Solution found**
L-Arginine	arg__L	No growth	Growth	None
L-Methionine	met__L	No growth	Growth	
Cobalamin	cbl1	Growth	N/A	
L-Histidine	his__L	No growth	Growth	Removal of mutated genes in histidine operon (109)
L-Isoleucine	ile__L	No growth	Growth	Application of published constraints on *bcaT*-coded enzymes (71)
L-Valine	val__L	No growth	Growth	
Biotin	btn	Growth	N/A	Manual pathway gap filling
Pantothenate	pnto__R	Growth	No growth	
Pyridoxal	pydx	Growth	N/A	
Pyridoxamine	pydam	Growth	N/A	
Thiamine	thm	Growth	No growth	
Lipoate	lipoate	Growth	N/A	
myo-Inositol	inost	Growth	N/A	
Choline	chol	Growth	N/A	

The metabolic model correctly predicts both aerobic and anaerobic growth, which is in line with the previously mentioned literature. However, it is unable to match the behaviour observed in *L. lactis* IL1403 of inhibited growth in the presence of O_2 or CO_2 (95). The methods outlined above were applied to attempt solving this disagreement. Some reactions involving oxygen were found to be false-

positive inclusions and were removed. However, these corrections were not enough to achieve a solution. In future works, the mechanisms behind growth inhibition by an aerated environment must be further investigated and incorporated in the metabolic reconstruction here developed. Also, a more thorough comparison should be done with the GEM by Oliveira *et al*. (71), as the model was able to correctly simulate the mentioned phenotype, despite not being strain-specific.

The prediction of prototrophy for arginine and methionine is incorrect, as all mentioned works report these amino acids as essential for growth (Table 3.7). When inspecting their pathways, it was observed that all biosynthetic reactions were included with high homology support. More specifically, each reaction had a direct orthologous gene with at least 3 or more target organisms and the majority with 4 or more. All biosynthetic genes are, therefore, likely present in *L. lactis* IL1403 and the observed auxotrophies must instead be consequence of different cell mechanisms, such as regulation or limited enzymatic rates. However, as no strain-specific literature on arginine biosynthesis was found, no further conclusions could be drawn, and no constraints could be applied to the *in silico* pathway. As for methionine, a study by Sperandio *et al*. (110) determines the strain's metabolic pathways for cysteine and methionine, along with their partial control. However, this partial control (by the regulator protein FhuR) does not cover methionine synthesis reactions. Furthermore, while the authors acknowledge the amino acid as essential for growth in *L. lactis*, no further work was done on determining the mechanism behind the auxotrophy (110).

As such, no changes or constrains could be applied to the arginine and methionine pathways either and the incorrect *in silico* predictions were retained. On the ambiguous results regarding these amino acids and on the subject of distinguishing absence of growth from very low growth rates, a paper by Chopin (111) is briefly mentioned. In his review on the organization and regulation of LAB amino acid biosynthetic pathways (111), the author cites in-house unpublished results where the omission of either arginine or methionine led to very low growth rates of 36 strains of *L. lactis* subsp. *lactis*. This further suggests more nuanced mechanisms might be behind the previously quoted auxotrophy phenotypes. It also highlights the need for more experimental work on these pathways and in greater detail, most likely beyond leave-one-out growth experiments and well into an investigation on the presence and activity of the enzymes composing said pathways.

The model was unable to predict auxotrophy for histidine. Inspecting the respective anabolic pathway showed all biosynthetic reactions to be present and with strong homology support. It was, again, drawn the conclusion that *L. lactis* IL1403 most likely contains in its genome all the necessary genes for histidine biosynthesis. Searching the literature, however, returned a study by Delorme *et al*. (109) where a series of mutations were identified on the strain's histidine operon, both in biosynthetic genes and the promoter region, effectively leading to the auxotrophic phenotype. While these mutations cause to the inactivation of multiple genes, they are generally small and result in a small percentage of base differences (109). This explains the high homology observed with biosynthetic genes in other organisms, both in this and the mentioned author's works (109). The mutated genes, *hisC*, *hisG*, *hisD*, *hisB*, *hisH* and *hisA*, along with their respectively associated reactions, were thus removed from the metabolic reconstruction, solving the incorrect phenotypic prediction.

All branch-chained amino acids are reported as essential by the mentioned nutrient essentiality works (Table 3.8). However, only leucine was correctly predicted as such by the model. Reviewing published literature further identified mutations in its biosynthetic pathway (112), which led to the removal of the mutated genes from the reconstruction, along with their respective reactions. As for the incorrect predictions for isoleucine and valine, these were corrected by applying the reversibility constraints determined by Oliveira *et al*. (71) on the reactions codified by *bcaT* (L_RS06750, in Supplementary Table S1). These were reactions ILETA, LEUTA and VALTA, respectively isoleucine,

leucine and valine transaminases, which were constrained to the forward direction (Supplementary Table S1).

Pantothenate and thiamine were incorrectly predicted as auxotrophies. To correct this inconsistency, their pathways were reviewed, and missing reactions were identified. As the non-essentiality phenotype is experimentally confirmed, the mentioned pathways were gap filled as necessary to meet the expected behaviour. As such, some gap filling reactions were added without an associated gene and done so solely on the necessity to match the non-essentiality phenotype. Following this gap filling step, the model now correctly predicts prototrophy for these vitamins.

Initially, the transport of metabolites biotin, choline, *myo*-inositol, lipoate, pyridoxamine and pyridoxal was not accounted for in the metabolic reconstruction and, as such, the single omission technique could not be applied to test their essentiality. Respective transport reactions were searched for by using the previously mentioned metabolic databases, as well as homology results originally excluded (based on the inclusion criteria set in Chapter 2.1). When possible, transport reactions were added with a gene association, but, otherwise, they were added without one as gap filling. Repeating the tests after applying the assembled corrections led to none of these metabolites being determined as essential for *in silico* growth.

Regarding the previously mentioned compounds, it is important to note, however, that, through the method here applied of inferring reactions via homology, no biosynthetic pathways were found for metabolites biotin, choline and lipoate. Furthermore, and as previously mentioned, no information was found regarding their contribution to cell composition and, as such, they were not included in the BOF either. This leads to the correct non-essentiality results, but with no guarantee of being for the correct biological reasons. No complete biosynthetic pathways could be inferred from homology and none of the currently available Streptococcaceae models account for such pathways either (the published models for *Streptococcus pneumonia* strain R6 [113] and *S. thermophilus* strain LMG18311 [114] were also analysed). As such, it is possible that this Family's biosynthetic pathways are distinct from other bacteria. Nonetheless, further experimental studies should be conducted to determine how or whether the mentioned metabolites are biosynthesized.

Finally, regarding the compound cobalamin, no pathway or reactions could be inferred for *L. lactis* IL1403 and, as such, no essentiality test was performed. However, it is worth noting that, other than *i*ML1515 (85), none of the GEMs here analysed account for this metabolite either. This suggests further experimental work is necessary to determine the essentiality of this compound in Gram-positive bacteria, as well as their biosynthetic capabilities.

After all possible solutions were applied to the metabolic network, the model was once again evaluated for nutritional requirements. The number of correct predictions increased to 43 out of 46 tested phenotypes, while the number of erroneous results lowered to 2, and non-applicable tests to 1 (an incorrect result, in practical terms). According to the mentioned literature revision, 39 growth phenotypes were expected, yet the model returns 40, and 7 non-growths were expected, yet only 6 are returned. Table 3.11 summarizes these results in a confusion matrix, from which it can be inferred that, regarding growth requirement simulations, the model displays a sensitivity of 95%, a specificity of 83.33% and an accuracy of 93.45%.

Table 3.11: Confusion matrix for the predictions on nutritional requirements by the model for *L. lactis* IL1403. A failure to test a nutrient was considered as a false result.

		Experimentally determined effects of single nutrient omission (95, 96, 97)	
		Growth	No growth
Model predicted effects of single nutrient omission	Growth	38	2
	No growth	1	5

Considering the reported number of *in silico* incorrect predictions, it is clear further metabolic studies should be conducted on *L. lactis* IL1403. Vitamin and micronutrient pathways for which incomplete or no information was found need to be clarified. As mentioned in Chapter 3.2, the significance of studies on cell cofactor and ion pools for *L. lactis* is connected not only to the construction of an accurate biomass reaction, but also to proper model testing of reported nutrient requirements. Finally, more detailed studies are also necessary on the mechanisms behind amino acid auxotrophies in this strain, many of which are possibly not consequence of gene deletions or mutations, but rather regulatory processes or other mechanisms.

3.5. Model validation: simulations in published chemically defined media

The following step in validating the model developed for *L. lactis* IL1403 was to test its growth capabilities in published synthetic media. As such, the literature was searched for records of the strain growing in such media, their respective compositions were applied as *in silico* unbounded uptake constraints, and growth was simulated. Any reported compound consumption or production rates were also applied as specific flux constraints. In cases where those rates were determined for most macronutrients and metabolic by-products, the model was also tested for the ability to match specific growth rates.

Regarding batch data, a study by Jensen and Hammer (115) reports *L. lactis* IL1403 growth on SA, a chemically defined medium developed by the authors. Additionally, the published media from works mentioned in Chapter 3.4 were also used for these tests. Specifically, these were: MCD, MS10R and MS15, by Cocaign-Bousquet *et al*. (95); ZBM in aerobiosis and anaerobiosis, by Zhang *et al*. (96); and BS1 and BS7, by Aller *et al*. (97). For the case of BS7, the authors also measured amino acid consumption profiles which were thus applied as specific flux constraints (97). As for continuous culture data, Even *et al*. (116) report *L. lactis* IL1403 growth in media developed by Cocaign-Bousquet *et al*. (95), both in the original composition and using an alternative carbon source (galactose). The carbon source consumption and product formation rates there determined (116) were also applied as stricter flux constraints. Moreover, the authors determine the specific activities of enzymes involved in glycolysis and galactose metabolism, which were converted to units of mmol g_{DW}^{-1} h^{-1} and applied as internal constraints. Finally, Dressaire *et al*. (117) report the strain's growth in anaerobic chemostat cultures using an adapted chemically defined medium, along with measured rates of glucose consumption and lactate production. To test these conditions, the model was constrained with the medium composition and measured flux rates, at each of the dilution rates used by the authors.

The metabolic model here developed achieves growth on all referenced media, under all environmental conditions. These results are presented in Table 3.12, where they show how the reconstructed network can adapt to different nutrient combinations and different environmental conditions. It is, again, stressed that none of these simulations were under full specific rate constraints

and, as such, the predicted growth rates are unrealistically high, as expected. In Table 3.12 it is also presented the results of simulating growth both when allowing full nutrient uptake (unconstrained model) and no nutrient uptake whatsoever (closed system). These results serve to aid in better visualising how each tested medium composition affects simulated growth and how the different media compare to each other.

Table 3.12: I*n silico* tests using published chemically defined media for *L. lactis* IL1403. In the first column ("Medium"), parenthesis include varying conditions used by the authors. In the second column ("Expected result"), parenthesis indicate the specific growth rate (μ_{max}) of *L. lactis* IL1403, whenever reported by the authors. a: all exchange reactions had their lower and upper boundaries set to -1000 and 1000 mmol g_{DW}^{-1} h^{-1}, respectively. b: all exchange reactions had their lower boundary set to 0 mmol g_{DW}^{-1} h^{-1}. c: amino acid consumption rates reported by the authors were set as the specific flux value for their respective exchange reactions. d: test results under specific constraints for carbon source consumption, by-product formation and some enzyme specific activities measured by the authors. e: tests under specific constraints for glucose consumption and lactate production.

Medium	**Expected result (reported μ_{max} at h^{-1})**	**Model result (h^{-1})**	**Reference**
Unconstrained[a]	Growth	137.7528	—
Closed system[b]	No growth	0	—
SA	Growth (0.64)	66.1204	115
MCD	Growth (0.70)	87.7897	95
MS10R	Growth (0.50)	63.1722	95
MS15	Growth (0.37)	66.6537	95
ZBM (aerobiosis)	Growth	66.7389	96
ZBM (anaerobiosis)	Growth	69.9846	96
BS1	Growth (0.78)	66.1202	97
BS7[c]	Growth (0.72)	1.0470	97
MCD[d] (glucose)	Growth (0.81)	44.6944	116
MCD[d] (galactose)	Growth (0.26)	43.881	116
MS10R[d] (glucose)	Growth (0.55)	31.974	116
MS10R[d] (galactose)	Growth (0.17)	31.2584	116
CDM[e] (D = 0.09 h^{-1})	Growth (0.09)	87.2985	117
CDM[e] (D = 0.24 h^{-1})	Growth (0.24)	87.3167	117
CDM[e] (D = 0.35 h^{-1})	Growth (0.35)	87.3275	117
CDM[e] (D = 0.47 h^{-1})	Growth (0.47)	87.3446	117

The different sets of constraints used for each media impose limitations on the conclusions that can be drawn between the different *in silico* conditions. Nevertheless, some relevant analysis is possible.

Firstly, regarding the fully unconstrained media (SA, MCD, MS10R, MS15, ZBM, and BS1) it is observed that the highest growth was attained in MCD, a result in agreement with what was expected. The medium MCD has the most complete composition of the unconstrained ones, accounting for all amino acids but glutamate, a large number of vitamins, micronutrients, minerals, and, most importantly, a series of nucleotide bases (95) (known as a complete medium). As discussed above, while not essential for growth, nucleotide bases have been shown to stimulate *L. lactis* IL1403 growth in chemically defined media (95, 96). This result suggested the metabolic model could be

simulating said effect. In order to further confirm this hypothesis, growth was again tested for, only this time without the nucleotide bases (adenine, guanine, inosine, uracil, and xanthine) in the medium composition. Indeed, the metabolic model simulated a lower growth rate, of 86.9055 h^{-1}. This result seems to confirm its ability to simulate the stimulatory effect of nucleotide bases reported in the literature (95, 96). Nevertheless, future works should aim to further confirm this capability with experimental data testing both conditions, while also determining full macronutrient consumption rates for realistic *in silico* constraints.

Still regarding the unconstrained results, both ZBM media led to unexpected and conflicting results. Firstly, much like MCD, these are complete media, containing virtually all building blocks for biomass production (96), including nucleotide bases. Yet their respective simulated growth rate was lower than that of MCD. Furthermore, these media allowed for the correct prediction of the reported inhibitory effect by air on *L. lactis* IL1403 growth (95). Yet this result was not reproducible in any other medium, indicating the predictions in ZBM as false-positives. Future works should further investigate the mechanisms behind the results for these media. Nonetheless, it is, again, stressed that particular reservation must be had when analysing unconstrained results, as these *in silico* settings do not permit proper realistic simulations and may overshadow metabolic mechanisms much more subtle than simple Boolean nutrient consumptions.

The results for the constraints collected from the work by Dressaire *et al*. (117) in a complete chemically defined medium (much like MCD or ZBM), also offer valuable insight. Firstly, it was again demonstrated and verified the stimulatory effect of nucleotide bases. The *a priori* inclusion of said nutrients leads to unconstrained growth rates similar to those in MCD, while their exclusion also lowers the simulated growth rate; in this case proportionally for each dilution rate (*in silico* μ_{max} equal to 86.4048, 86.4227, 86.4335, and 86.4504 h^{-1} for the respective dilution rates of 0.09, 0.24, 0.35, and 0.47 h^{-1}). Secondly, these results serve to show that, for realistic *in silico* predictions, specific flux rate constraints are necessary for all macronutrients and not just the carbon source and the major metabolism by-product. The application of the consumption and production rates determined by the authors (117) allowed distinguishing growth rates between the different dilution rates and even from the absence of specific constraints (where the substitution of the reported glucose and lactate flux rates with unconstrained values leads to an *in silico* μ_{max} of 87.7897 h^{-1}). However, those flux rates did not sufficiently constrain the metabolic network for realistic growth rates to be simulated.

On the subject of constraints, the results for the data reported by Even *et al*. (116) also enable relevant conclusions. Firstly, they demonstrate that the model here developed is capable of simulating lower growth rates for less energetically efficient carbon sources, such as galactose when compared to glucose. Secondly, when comparing these partially constrained results with the previously discussed ones for unconstrained media, it becomes clear how the application of realistic flux constraints further limits simulations into more realistic values. By applying *in silico* the rates measured by Even *et al*. (116) for carbon source consumption, by-product formation (more specifically, lactate, formate, acetate, and ethanol), and enzyme activities, it was possible to halve the simulated growth rates for the same exact media without specific constraints.

The possibly most prominent result was observed for medium BS7, by Aller *et al*. (97). This rich, chemically defined medium differs very little from BS1 (97) *in vitro* and even less so *in silico*, where it only contains a single more nutrient (lipoate). However, the results for BS7 were drastically different from those for BS1. This was due to the application of amino acid consumption rate constraints, which allowed to lower the predicted growth rate to actually realistic values. The simulated value was not yet equal to the specific growth rate calculated by the authors (97), but this is most likely due to the missing measurement of the carbon source consumption rate (and, of course, any metabolic inaccuracies still remaining in the model). Nevertheless, this result demonstrates the

fundamental value of constraining the appropriate exchange reactions in a GEM with realistic, experimentally determined flux rates, which then allow for proper simulations of expected phenotypes and the safe application of these models for prospective uses.

Finally, a passing mention is made to the results in MS15. This is a minimal medium specifically developed for *L. lactis* IL1403 (95). The fact that simulated growth is achieved in its composition, even if unconstrained, demonstrates how the GEM here developed accounts for the previously discussed prototrophic capabilities of *L. lactis* IL1403. The positive result in this medium also highlight the importance of previous network evaluation and validation steps. By correcting network errors and further analysing pathways associated to the nutritional requirements of this strain, the reconstruction progressively gained greater realistic capabilities, not exclusive to the minimal MS15 medium.

3.6. Model validation: exometabolomics data

In the previously mentioned multi-omics study of *L. lactis* IL1403, Lahtvee *et al*. (100) determine, amongst other parameters, the rates of amino acid and carbon source consumption and metabolic by-product formation in continuous culture. The authors obtained this data in accelerostat experiments at varying dilution rates, and also in chemostat experiments, at the single dilution rate of 0.45 h^{-1} (100). Using the raw data kindly provided by Dr. Petri-Jaan Lahtvee, from the University of Tartu (Tartu, Estonia), the metabolic model was constrained to those conditions. More specifically, the values measured by the authors were set as flux rates for the respective exchange reactions and the model was evaluated on the ability to match expected growth rates.

Analysing the data more thoroughly, however, revealed the low confidence measurements reported by the authors for aspartate, histidine, and proline. The case of histidine was particularly problematic, as consumptions were often measured at very low values and sometimes even registered as production, a finding at odds with the previously discussed histidine auxotrophy. Considering these measurements were reported as erroneous by the authors themselves, a tentative solution was applied to the histidine values, in which these were replaced by estimated minimal consumption rates. As previously reported, Lahtvee *et al*. (100) determined the chemical composition of *L. lactis* IL1403 cells grown in these same continuous culture experiments. Furthermore, the authors detail, amongst other things, the amino acid composition of the protein fraction at dilution rates (h^{-1}) of 0.1, 0.15, 0.20, 0.25, 0.30, 0.35, 0.40, 0.45, 0.50, 0.55, and 0.60 (100). Thus, taking into consideration each of the histidine values of cellular compositions, minimal consumptions fluxes were estimated at the mentioned dilution rates (calculated to units of mmol g_{DW}^{-1} h^{-1}). The original histidine consumption rates kindly provided by Dr. Petri-Jaan Lahtvee and the estimated solution are presented in Table 3.13.

Table 3.13: L-histidine consumption rates kindly provided by Dr. Petri-Jaan Lahtvee. The shared values are presented, along with their respective percentage deviations calculated by the original authors, and the tentative estimation of minimal consumption rates here calculated for the amino acid. a: the original values are the mean of 6 independent experiments; however, in the provided unpublished data, many replicates suffered failures to measure. b: a negative value indicates a measurement of production by the original authors (100).

Dilution rate	**Original L-histidine consumption rates (mmol g_{DW}^{-1} h^{-1})[a]**	**Original % SD**	**Tentative minimal estimation (mmol g_{DW}^{-1} h^{-1})**
A-stat (D = 0.10 h^{-1})	-0.00172[b]	183.59	0.00692
A-stat (D = 0.15 h^{-1})	-0.00144[b]	309.40	0.01036
A-stat (D = 0.20 h^{-1})	0.00474	109.59	0.01378
A-stat (D = 0.25 h^{-1})	0.00824	61.83	0.01718
A-stat (D = 0.30 h^{-1})	0.01097	45.09	0.02056
A-stat (D = 0.35 h^{-1})	0.01484	42.43	0.02392
A-stat (D = 0.40 h^{-1})	0.01814	42.15	0.02726
A-stat (D = 0.45 h^{-1})	0.01949	71.66	0.03059
A-stat (D = 0.50 h^{-1})	0.01940	83.77	0.03390
A-stat (D = 0.55 h^{-1})	0.01210	82.95	0.03719
A-stat (D = 0.60 h^{-1})	0.00862	37.18	0.04046

Using the assembled sets of constraints, the model was thus tested for the ability to match expected specific growth rates. These results are presented in Table 3.14.

Table 3.14: *L. lactis* IL1403 growth simulations under exometabolomics constraints. Results are shown for when using the values kindly provided by Dr. Petri-Jaan Lahtvee as exchange constraints, as well alternatively using a minimal estimation of histidine consumption values. a: No-growth predictions were determined to be consequence of the histidine exchange constraint, which demanded biosynthesis and excretion of the amino acid.

Growth conditions	**Growth rate under the original constraints (h^{-1})**	**Growth rate under histidine-corrected constraints (h^{-1})**
A-stat (D = 0.10 h^{-1})	0[a]	0.0905
A-stat (D = 0.15 h^{-1})	0[a]	0.1516
A-stat (D = 0.20 h^{-1})	0.0694	0.2016
A-stat (D = 0.25 h^{-1})	0.1206	0.2513
A-stat (D = 0.30 h^{-1})	0.1606	0.3008
A-stat (D = 0.35 h^{-1})	0.2171	0.3500
A-stat (D = 0.40 h^{-1})	0.2654	0.3989
A-stat (D = 0.45 h^{-1})	0.2851	0.4435
A-stat (D = 0.50 h^{-1})	0.2838	0.4579
A-stat (D = 0.55 h^{-1})	0.1771	0.4508
A-stat (D = 0.60 h^{-1})	0.1262	0.4803
C-stat (D = 0.45 h^{-1})	0.2634	0.4476

The results for simulations using the exometabolomics data by Lahtvee *et al*. (100) show the GEM to be capable of achieving growth when using detailed sets of constraints. Furthermore, when correcting the histidine consumption rates by applying tentative estimated values (as described above), the model also shows the ability to predict accurate growth rates for dilution rates 0.10 h^{-1} through 0.45 h^{-1}. For dilution rates 0.50 h^{-1} through 0.60 h^{-1}, it is clear further network evaluation is necessary on the metabolic reconstruction here presented. Future works should inspect in greater detail any of the remaining pathways not covered in previous steps, such as the ones reported to have possible excessive reaction inclusions. Naturally, this is particularly important for energy producing pathways such as the central metabolism. However, it is also relevant to peripheral pathways that might be behind excessive energy dissipation and, thus, resulting in the lower than expected simulated growth

rates at higher dilution rates (Table 3.14). Finally, future works should also aim to perform exometabolic studies using methodologies more precise than the ones applied by Lahtvee *et al*. (100). As shown, proper model validation absolutely requires the accurate determination of all macronutrient consumption rates, for even a single erroneous nutrient measurement risks making the entire dataset unusable.

3.7. Model validation: carbon source utilization

Another method to validate a GEM is by assessing growth capability on different experimentally determined carbon sources. As such, the literature was scanned for *L. lactis* IL1403 growth reported in chemically defined media supplemented with different carbon sources.

In the characterization of a newly isolated *L. lactis* strain, Passerini *et al*. (118) also evaluate strain IL1403 as a point of reference. Amongst the tests conducted, the authors assess the growth capabilities of both strains on 28 different carbon sources, supplemented on a chemically defined medium in batch conditions. Using this substrate list as a starting point, the literature was then searched for any evidence in disagreement with the mentioned findings.

Passerini *et al*. (118) determined strain IL1403 to be incapable of growing in a medium where galactose is the sole carbon source. However, the previously mentioned study by Even *et al*. (116) reported this strain growing in two different chemically defined media where this sugar was the sole carbon source. Given the latter study provides a much more comprehensive analysis of growth on galactose, its results were considered over the ones by Passerini *et al*. (118) for the purpose of model validation. The mentioned authors also determine the strain as incapable of growing on lactose as the only carbon source (118). However, in a study characterizing *L. lactis* IL1403 isolates with a β-galactosidase-negative phenotype, Aleksandrzak-Piekarczyk *et al.* (119) report the strain to grow on lactose, albeit at a very slow rate. More specifically, in a chemically defined broth medium supplemented with lactose, the authors observed growth of strain IL1403 only after 40 h and maximum OD values only after 80 h (119). The fact that Passerini *et al*. (118) only followed incubations for 24 h could explain their observation on lactose as a false-negative.

After collecting published experimental data, the model developed for *L. lactis* IL1403 was then tested on the capability of matching those expected phenotypes. The network was constrained to a chemically defined medium and, successively, each carbon source was added and followed by a growth test. More specifically, the medium CDM, developed by Poolman and Konings (120) and used by Passerini *et al*. (118), was set as the *in silico* constraints. Seeing as the experiments by the latter authors took place in batch conditions, the exchange lower boundaries for each compound present in the medium were set to unconstrained uptake. However, the fact that these simulations are not in nutrient limited conditions unavoidably leads to simulated growth even in the absence of a carbon source. No literature was found reporting *L. lactis* IL1403 growth in the absence of carbon source compounds. As such, any value equal to or lower than the growth rate obtained without a carbon source was considered as a negative result. Conversely, any value greater than the mentioned cut-off was considered a positive result. Furthermore, any failure to test a compound due to the absence of a transport reaction was also considered a negative result. Table 3.15 lists the possible carbon sources collected from the literature and the respective model result after the final tests.

Table 3.15: Final *in silico* results on carbon source utilization. The substrate list is based on the work by Passerini *et al*. (118). In the second column ("Expected result"), parenthesis indicate the specific growth rate reported by Passerini *et al.* (118). a: some compounds were absent from the GEM and are also currently absent from the BiGG database (74); they were considered as negative results. b: expected phenotype corrected based on the work by Even *et al.* (116). c: expected phenotype corrected based on the work by Aleksandrzak-Piekarczyk *et al.* (119).

Carbon source	**Expected result (reported μ_{max} at h^{-1})**	**Model result (h^{-1})**	**Result *vs.* no carbon source (%)**	**Result *vs.* glucose (%)**
No carbon source	No growth	83.2506	—	—
Glucose	Growth (0.63)	87.7897	105.45	100.00
Galactose	Growth[b]	87.1004	104.62	99.21
Fructose	Growth (0.35)	87.9256	105.62	100.15
L-Arabinose	No growth	0	0	0
D-Xylose	No growth	0	0	0
Rhamnose	No growth	0[a]	—	—
Sucrose	No growth	0	0	0.00
D-Melibiose	No growth	0[a]	—	—
Gentiobiose	Growth (0.03)	0[a]	—	—
D-Cellobiose	Growth (0.54)	87.6146	105.24	99.80
D-Maltose	Growth (0.35)	87.6146	105.24	99.80
Trehalose	Growth (0.66)	88.6754	106.52	101.01
Palatinose	No growth	0[a]	—	—
Lactose	Growth[c]	87.2667	104.82	99.40
D-Raffinose	No growth	0[a]	—	—
Maltotriose	Growth (0.36)	88.4968	106.30	100.81
Melezitose	No growth	0[a]	—	—
Stachyose	No growth	0[a]	—	—
Dextran	No growth	0[a]	—	—
Pectin	No growth	0[a]	—	—
Xylan	No growth	0[a]	—	—
Hydroxycellulose	No growth	0[a]	—	—
Inulin	No growth	0[a]	—	—
Starch	No growth	0[a]	—	—
D-Glucuronate	No growth	0	0	0
D-Galacturonate	No growth	0[a]	—	—
D-Gluconate	Growth (0.06)	86.5448	103.96	98.58
Amygdalin	No growth	0[a]	—	—

After the first round of tests, the metabolic model was capable of matching 23 carbon source utilization phenotypes, covering both simple and complex sugars. Most growth phenotypes, however, were observed for simple sugars. This is in line with expected available carbon sources in the dairy environments from which the parent strain of *L. lactis* IL1403 was originally isolated from (121). Nevertheless, many of the carbon source substrates the strain can utilize are also not typically present in dairy products, such as fructose, cellobiose, maltotriose and others. *L. lactis* plant isolates typically display much greater metabolic plasticity than their dairy relatives (95). As such, the ability of *L. lactis* IL1403 to grow on the mentioned substrates might be due to residual genes originating from ancestral wild type strains, generally thought to have inhabited plant environments (16). Conversely, the

inability to use many other polysaccharides typically found in plant tissues could be due to a progressive loss of metabolic functions as the parent strain was cultivated in rich dairy environments. Furthermore, seeing as bacterial plasmids typically harbour genes for carbohydrate degradation pathways, the fact that *L. lactis* IL1403 is plasmid-free could also explain its inability to use many of the tested carbon sources.

The model initially performed incorrect predictions for carbon sources L-arabinose, D-xylose, sucrose, gentiobiose, and D-glucuronate. As such, their metabolic pathways were reviewed. Analysing the metabolic and transport reactions for L-arabinose, D-xylose, sucrose and D-glucuronate revealed low confidence inclusions, wrongfully added in the reconstruction process. These reactions were therefore removed. Regarding gentiobiose, no metabolic information involving this compound was found in any of the target models used in the network reconstruction step (Chapter 2.1). Consequently, the pathway responsible for metabolising this compound in *L. lactis* IL1403 could not be determined.

After the application of all possible network corrections, the model here developed now matches 27 carbon source utilization phenotypes. Only the gentiobiose test leads to an incorrect result. Table 3.16 summarizes the model's performance on carbon source utilization, from which a sensitivity of 90%, a specificity of 100%, and an accuracy of 96.43% were inferred. Regarding these results, it is important to note, however, that the GEM accounts for the transport of 11 other sugars or amino sugars for which no experimental data was found. Consequently, the predictive performance here reported could be an overestimation of the model's true capabilities. Future works aiming to further curate this metabolic reconstruction should examine its transport reactions more thoroughly. Ideally, they should also conduct parallel experiments in which it is investigated the ability of *L. lactis* IL1403 to utilize the compounds for which no published data was found.

Table 3.16: Confusion matrix for the GEM's capability of predicting *L. lactis* IL1403 carbon source utilization. Tests were conducted in a chemically defined medium, as determined by Even *et al.* (116), Passerini *et al.* (118) and Aleksandrzak-Piekarczyk *et al.* (119).

		Experimentally determined carbon source utilization (116, 118, 119)	
		Growth	No growth
Model prediction of carbon source utilization	Growth	9	0
	No growth	1	18

3.8. *L. lactis* LMG 19460 metabolic reconstruction and evaluation

L. lactis LMG 19460 is a recently sequenced, plasmid-free strain of particular biotechnological interest (75), but for which no published experimental metabolic data is yet available. This lack of experimental data precludes the direct reconstruction and validation of its metabolic network. Therefore, having developed a functional and mostly validated GEM for *L. lactis* IL1403 (though not yet at the level of published reconstructions), the model was then used to infer metabolic functions in *L. lactis* LMG 19460. The methodology used was the same as when assembling the prior reconstruction, only this time the model for *L. lactis* IL1403 was the sole target of sequence homology analysis.

The metabolic model here developed for *L. lactis* LMG 19460 accounts for 570 genes, 916 reactions and 638 metabolites. It is presented in Supplementary Table S1, in parallel to the model developed for *L. lactis* IL1403. This model is identical to the reconstruction for IL1403 in everything

other than 1 metabolite, 5 reactions, and 5 metabolic genes for which no orthologous was found in *L. lactis* LMG 19460. Of those genes for which no homology was detected, only 3 coded the unique enzymes catalysing the 5 removed reactions, which are presented in Table 3.17.

Table 3.17: Reactions in the metabolic reconstruction for *L. lactis* IL1403 for which no homology was found with *L. lactis* LMG 19460.

Model ID	Reaction name	Reaction equation	Subsystem
ACONTa	Aconitase (half-reaction A, Citrate hydro-lyase)	cit[c] ⇌ acon_C[c] + h2o[c]	Citric Acid Cycle
ACONTb	Aconitase (half-reaction B, Isocitrate hydro-lyase)	acon_C[c] + h2o[c] ⇌ icit[c]	Citric Acid Cycle
PKETF	Phosphoketolase (fructose-6-phosphate utilizing)	f6p[c] + pi[c] → actp[c] + e4p[c] + h2o[c]	Pentose Phosphate Pathway
PKETX	Phosphoketolase (xylulose-5-phosphate utilizing)	pi[c] + xu5p__D[c] → actp[c] + g3p[c] + h2o[c]	Pentose Phosphate Pathway
ALDD2y	Aldehyde dehydrogenase (acetaldehyde, NADP)	nadp[c] + h2o[c] + acald[c] → ac[c] + 2 h[c] + nadph[c]	Pyruvate Metabolism

Distinct conclusions can be drawn when analysing the reactions product of genes without an orthologous gene in *L. lactis* LMG 19460. Firstly, it is apparent this strain possesses fewer reactions in the central metabolism pathways than strain IL1403, which could be in line with the lower number of protein coding genes found in the former organism (Table 2.1).

Furthermore, the lack of an orthologous gene for reactions ACONTa and ACONTb is particularly interesting, as these are central reactions in the citric acid cycle. While well supported in the reconstruction for strain IL1403 (having been inferred and confirmed through positive homologies with 3 and 4 organisms, respectively), these aconitase reactions are clearly absent from the TCA cycle of strain LMG 19460. The citric acid cycle reconstructed for *L. lactis* IL1403 is itself already incomplete, a finding in line with thorough work done on the central metabolism of another *L. lactis* strain (102). However, these results suggest this cycle is even less complete in *L. lactis* LMG 19460.

Regarding reactions PKETF, PKETX, and ALDD2y, it is suggested that strain LMG 19460 might also have a less complete pentose phosphate pathway and pyruvate metabolism. However, it is important to note these reactions were included in the *L. lactis* IL1403 reconstruction through homologies with only a single organism each. More specifically, reactions PKETF and PKETX are product of identifying an orthologous gene between *L. lactis* IL1403 and *Leuconostoc mesenteroides* subsp. *mesenteroides* ATCC-8923, while reaction ALDD2y was inferred from an orthologous with *E. coli* str. K-12 substr. MG1655. These homologies were inferred from strong sequence alignment results, as it is shown in Table 3.18. Furthermore, the fact that these reactions were deducted from single organisms only does not necessarily rule them out. The GEMs for *L. mesenteroids*, *i*LME620 (88) and *E. coli*, *i*ML1515 (85), are very recent developments, having both been published in 2017. As such, they might detail functions present but not yet uncovered in *L. lactis*. Nevertheless, seeing as these reactions refer to central metabolism pathways, future works in the GEM here developed for *L. lactis* IL1403 should aim to better elucidate the validity of these inclusions.

Table 3.18: Protein sequence alignment results between *L. lactis* IL1403 and the genes coding for reactions PKETF, PKETX, and ALDD2y, in their respective original GEMs. These alignments were performed using the software tool Proteinortho (79), with BLASTp+ as the search option and remaining settings as default.

Reaction(s)	Query sequence ID	Subject sequence ID	Forward e-value	Forward bitscore	Reverse e-value	Reverse bitscore
PKETF, PKETX	L_RS07840	LEUM_1961	0.0	1235	0.0	1235
ALDD2y	L_RS06850	b0493	8.18e-42	141	3.96e-42	141

Finally, seeing as the differences between the two *L. lactis* strains here discussed concern, at least, the central metabolic pathways, it could be expected for strain LMG 19460 to generally have a slower growth profile. As such, future works regarding these two organisms should compare their growth kinetics to discern whether the genetic differences here reported have any phenotypical effect.

Evaluation of the metabolic network reconstructed for *L. lactis* LMG 19460 was performed through the same methodology as for the model developed for strain IL1403. However, seeing as the reconstruction for strain LMG 19460 was based on a single, already reviewed model, and considering the few differences above reported between the two models, no particular further network errors were expected.

This was confirmed when repeating the search for mass-imbalanced reactions, dead-end metabolites, network gaps, blocked reactions and SBCs. The only additional errors present in the model developed for *L. lactis* LMG 19460 are a single new dead-end metabolite and a single blocked reaction, leading to said dead-end. The additional blocked reaction is ICDHyr, catalysed by the isocitrate dehydrogenase enzyme in the citric acid cycle, and the dead-end metabolite is isocitrate, a substrate of the prior enzyme. These results are expected as they are a direct consequence of the previously discussed absence of aconitase reactions in the citric acid cycle. Overall, these network evaluation results highlight the advantages of using a curated model as the starting point for metabolic reconstructions, namely in more quickly achieving a working model free of the most possible amount of errors.

3.9. Performance of the model for *L. lactis* LMG 19460

As previously discussed, the validation of a GEM requires evaluating its ability to simulate experimentally determined, organism-specific phenotypes. However, no such published data is currently available for *L. lactis* LMG 19460. Nevertheless, the previous validation tests performed on the metabolic model developed for *L. lactis* IL1403 were repeated on the model for strain LMG 19460. This had the aim of elucidating what might be the strain's behaviour when subject to similar constraints in the future. Furthermore, these tests also aimed to evaluate whether the small, but metabolically central differences observed between the two models resulted in any different *in silico* predictions.

The tests conducted were, thus, those of nutritional requirements, carbon source utilization and growth in published chemically defined media. Regarding the essentiality of medium components, the metabolic model for *L. lactis* LMG 19460 displays no difference from that of strain IL1403. The model retains the same prototrophic capabilities and the same auxotrophies, namely those for histidine, isoleucine, leucine, valine, and magnesium. It also retains the predictions determined as incorrect in the reconstruction for *L. lactis* IL1403, namely those of higher growth rates in aerobiosis than anaerobiosis and the ability to biosynthesise arginine and methionine.

However, it must be stressed that without experimental evidence, none of these essentiality predictions are final. For instance, the results determined to be incorrect for *L. lactis* IL1403 might be true phenotypes in strain LMG 19460. Conversely, various cellular mechanisms (such as gene regulation) in the latter organism might result in auxotrophic phenotypes invisible to the mere determination of orthologous genes. Furthermore, the point mutations reported in the histidine operon of *L. lactis* IL1403 might not be present in strain LMG 19460, thus, enabling it to be a prototroph for histidine. Likewise, the network gap filling performed in various vitamin and cofactor pathways might not apply to strain LMG 19460, as the experimental determination of its nutritional requirements might reveal that no biosynthetic phenotype needed to be matched.

The metabolic model for *L. lactis* LMG 19460 also retains the same behaviour as the one developed for strain IL1403 regarding carbon source utilization and growth in chemically defined media. Nevertheless, what was said for the validity of the previous essentiality predictions also applies to these results. Future works with the GEM for this strain should aim to validate these results by experimentally determining nutritional requirements, carbon source utilization, and the rates of nutrient consumption and metabolic by-product formation in chemically defined media.

Besides the unchanged results when applying *L. lactis* IL1403 validation tests to the metabolic reconstruction for strain LMG 19460, one difference is, however, observed. That difference is in the simulated growth rates under unconstrained or partially constrained exchange flux rates. More specifically, compared to strain IL1403, the model for *L. lactis* LMG 19460 achieves a slightly lower growth rate under the following sets of constraints: when unbounded flux is allowed on all exchange reactions; when unbounded flux is allowed only on exchange reactions representing a medium composition; and when under minimal specific flux rate constrains, such as those only on metabolic by-product secretion or carbon source consumption (Table 3.19).

Table 3.19: Growth comparison between the two GEMs in the collected published synthetic media. None of the works behind these media determined full macronutrient consumption rates. Therefore, the application of their composition as model constraints took the form of unbounded nutrient uptake, with the exception of some partial rates as previously detailed in Table 3.12.

Medium	***L. lactis* IL1403 model result (h^{-1})**	***L. lactis* LMG 19460 model result (h^{-1})**	**Reference**
Unconstrained	137.7528	134.2484	—
SA	66.1204	63.1170	115
MCD	87.7897	87.6995	95
MS10R	63.1722	62.8858	95
MS15	66.6537	63.3034	95
ZBM (aerobiosis)	66.7389	64.1747	96
ZBM (anaerobiosis)	69.9846	68.9580	96
BS1	66.1202	63.3778	97
MCD (glucose)	44.6944	44.6092	116
MCD (galactose)	43.881	43.8143	116
MS10R (glucose)	31.974	31.8820	116
MS10R (galactose)	31.2584	31.1685	116
CDM ($D = 0.09\ h^{-1}$)	87.2985	87.1847	117
CDM ($D = 0.24\ h^{-1}$)	87.3167	87.2042	117
CDM ($D = 0.35\ h^{-1}$)	87.3275	87.2158	117
CDM ($D = 0.47\ h^{-1}$)	87.3446	87.2341	117

Previously, it was discussed how the metabolic reconstruction for *L. lactis* LMG 19460 has a slightly reduced central metabolism when compared to the one for strain IL1403, particularly noticeable in the citric acid cycle. The results presented in Table 3.19 suggest that the network differences may indeed impact the growth capabilities of strain LMG 19460.

When under the same specific rate constraints as the ones applied to the metabolic model for *L. lactis* IL1403, namely the previously discussed fluxes measured by Lahtvee *et al*. (100), the model for strain LMG 19460 achieves the exact same growth rates. However, limited conclusions can be drawn from these results, as all determined rates are specific to strain IL1403. Furthermore, the flux rates determined by Lahtvee *et al*. (100) were not determined in carbon limited conditions and, as such, may represent excessive nutrient consumption for other cellular functions besides growth. The same issue does not happen when testing both models with the flux rates determined by Flahaut *et al*. (73) for macronutrient consumption and by-product secretion rates, in carbon-limited continuous cultures of *L. lactis* MG1363. Using those sets of constraints, the same previously discussed growth rate differences are, again, observed (Table 3.20). This reaffirms the possible physiological consequences of the differences registered between the GEMs for strains IL1403 and LMG 19460. Furthermore, it demonstrates how even nutrient flux data can have limited applications if not determined under strict conditions.

Table 3.20: Growth comparison between the two GEMs using the consumption and production rates determined by Flahaut e*t al.* (73).

Growth conditions	***L. lactis* IL1403 model result (h^{-1})**	***L. lactis* LMG 19460 model result (h^{-1})**
CDM. (D = 0.05 h^{-1})-A	0.0987	0.0986
CDM. (D = 0.05 h^{-1})-B	0.0882	0.0876
CDM. (D = 0.25 h^{-1})-A	0.2981	0.2953
CDM. (D = 0.25 h^{-1})-B	0.2701	0.2692
CDM. (D = 0.40 h^{-1})-A	0.5722	0.5709
CDM. (D = 0.40 h^{-1})-B	0.5430	0.5381
CDM. (D = 0.50 h^{-1})	0.7367	0.7077

These results then further highlight the need for future studies on *L. lactis* LMG 19460, where its rates of nutrient consumption and by-product formation are experimentally determined in carbon-limited continuous cultures. However, it also highlights how the same studies should be conducted for strain IL1403, which still lacks proper fluxomic data in carbon-limited growth conditions. Future works involving the metabolic models here developed should determine those rates for *L. lactis* IL1403 and strain LMG 19460, ideally, in parallel and under the same exact conditions.

3.10. *L. lactis* LMG 19460 growth assays in chemically defined media

It has already been established that proper GEM validation requires organism-specific experimental data. As such, and as a first step in furthering the metabolic knowledge on *L. lactis* LMG 19460, a series of batch growth assays in chemically defined media were performed. These media were composed in this work. In order to evaluate their performance, growth experiments in the rich complex medium M17, using the same strain, were also performed in parallel.

The first chemically defined medium, CDM1, is a rich medium based on the work by Cocaign-Bousquet *et al*. (95), Zhang *et al*. (96) and Aller *et al*. (97). It contains glucose as the sole carbon source, all amino acids, multiple buffers and a series of vitamins, minerals and other micronutrients (Table 2.2). Unlike the media developed by Cocaign-Bousquet *et al*. (95) and Zhang *et al*. (96) however, it does not contain any nucleotide base. Two sets of growth assays were conducted in CDM1 using *L. lactis* LMG 19460. For the second of these sets, the strain was also grown in parallel in the complex medium M17. The results of these experiments are shown in Figure 3.3.

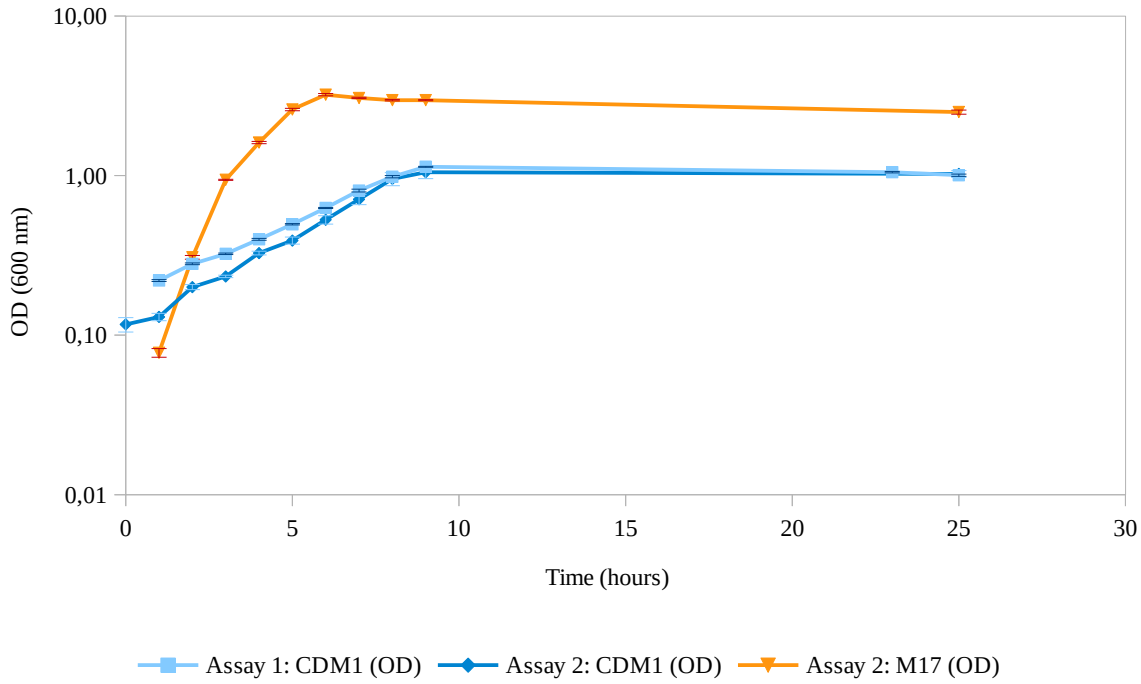

Figure 3.3: Growth curves for *L. lactis* LMG 19460 cultivated in CDM1 and in M17. The complex medium assay was conducted in parallel to the second CDM1 experiment. The error bars represent the standard error of the mean. Experiments were conducted in negative-controlled triplicates.

The two growth experiments conducted in CDM1 demonstrate, first and foremost, that the medium here assembled is capable of supporting growth of *L. lactis* LMG 19460. Analysing the strain's growth kinetics in this medium, it is observed that the first assay resulted in a measured maximum OD_{600} of 1.14, a calculated specific growth rate of 0.23 h^{-1}, and a duplication time of 2.95 h (Figure 3.3). The second growth assay resulted in a maximum OD_{600} of 1.05, a specific growth rate of 0.30 h^{-1}, and duplication time of 2.34 h (Figure 3.3). The first experiment led to a slightly better growth performance, as observed by the growth rates, but, nevertheless, the maximum biomass formation was similar both times. For both experiments, no true exponential phase was observed and, instead, the strain followed something more akin to cubic growth. When compared to growth in the complex M17 medium, the limitations of CDM1 become even more apparent. In the parallel M17 assay conducted during the second experiment, *L. lactis* LMG 19460 achieved a maximum OD_{600} of 3.21, a specific growth rate of 1.25 h^{-1}, and duplication time of 0.56 h (Figure 3.3). Furthermore, maximum cell density was achieved 3 h earlier than that in CDM1.

These results show that the laborious process of composing a rich chemically defined medium hardly results in a medium of comparable performance to complex ones. While Zhang *et al*. (96) report better performances in their chemically defined ZMB media than in M17, those authors added virtually every possible nutritional compound to their media, resulting in a total of 57 chemically defined constituents. Nevertheless, the goal of a chemically defined medium is not necessarily to match performances in complex media, and they allow for a far wider range of metabolic studies.

With the goal of improving the performance of CDM1, the concentration of glucose, the sole carbon source, was increased (from 3.5 to 10 g L^{-1}) and ascorbic acid was added to its composition (at 0.5 g L^{-1}). The increase in glucose concentration was to determine whether the sugar was present in carbon-limiting concentrations and, thus, whether it was the medium's growth-limiting factor. Ascorbic acid, an antioxidant, was added with the goal of counteracting or, at least, minimizing the

documented inhibitory effect of an aerobic environment on *L. lactis* growth (95, 98, 99). This new composition is regarded as a separate medium, CDM2.

As previously, two sets of experiments were conducted in CDM2. In the second assay, however, the culture volume was increased from the initial 10 mL to 40 mL, in order to evaluate the medium's performance in upscaled conditions. Additionally, the same cells were also inoculated in parallel M17 cultures, in order to properly compare the upscaled performance of CDM2 to the complex medium. Finally, in the same second assay, cultures in both media also had their pH followed in order to investigate it as a growth-limiting factor. Figure 3.4 shows the results of this set of experiments.

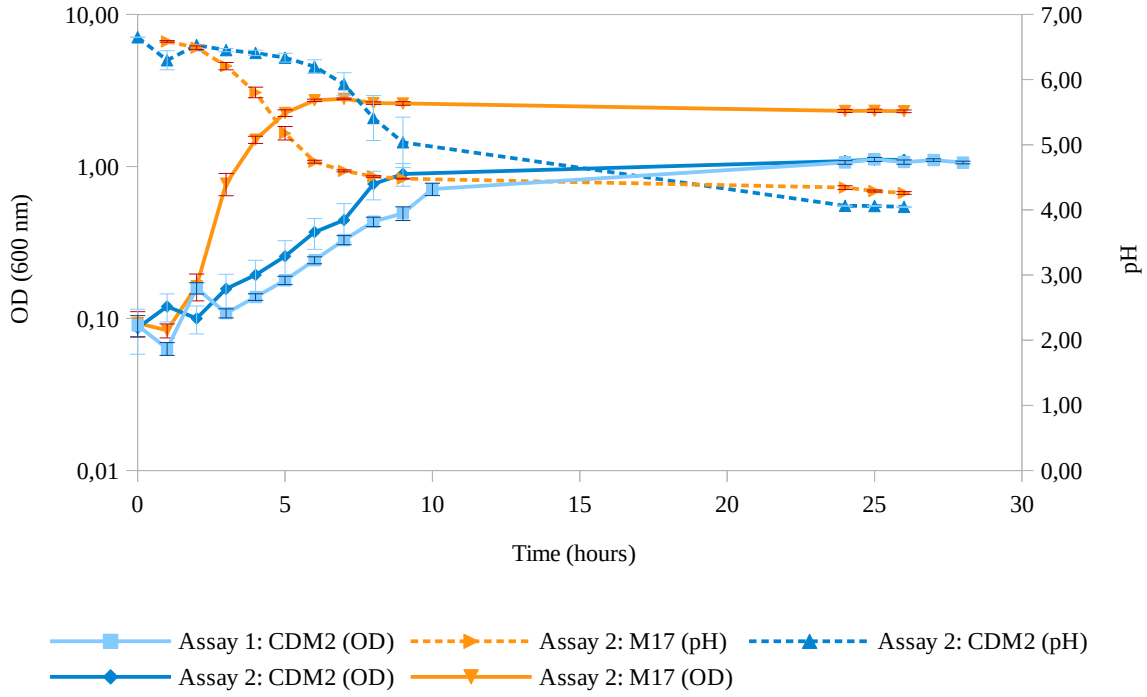

Figure 3.4: Growth and pH curves for *L. lactis* LMG 19460 cultivated in CDM2 and in M17. Complex medium assays were conducted in parallel to the second CDM2 experiment. The second assays took place in upscaled culture volumes of 40 mL; their pH curves are also presented. The error bars represent the standard error of the mean. Experiments were conducted in negative-controlled triplicates.

The *L. lactis* LMG 19460 growth assays in CDM2 revealed similar results to the previous medium composition (Figure 3.4). Despite the mentioned modification of CDM1, no particular increase was observed in either final cellular concentration or specific growth rates. More specifically, in the first experiment (in cultures of 10 mL) the maximum registered OD_{600} was 1.11, while the specific growth rate and duplication time were calculated at 0.28 h^{-1} and 2.46 h, respectively. For the second experiment, upscaled to 40 mL, the maximum measured OD_{600} was also 1.11, and the calculated specific growth rate and duplication time were 0.29 h^{-1} and 2.42 h, respectively. Despite the different culture volumes used, both experiments show very similar growth kinetics. Nonetheless, when again compared to growth in the complex medium M17, the results show CDM2 to still be noticeably far from the best performances registered for the strain. In the M17 assay, maximum OD_{600} was registered at 2.79 and, respectively, the calculated specific growth rate and duplication time were 1.11 h^{-1} and 0.62 h. Evaluating the changes in CDM2, it is concluded neither the increase in glucose concentration or culture volume seem to have improved the strain's growth in CDM2. Furthermore, it is concluded that glucose at the previous concentration (of 3.5 g L^{-1}) was not growth-limiting.

Analysing the pH measurements, however, did allow to identify the likely growth-limiting factor, both in CDM2 and M17. Following the growth and pH curves presented for both media (Figure 3.4), it can be observed that growth rates in both environments start decreasing in parallel to the decrease in medium pH. Furthermore, it becomes apparent that there is a point in pH values after which cells enter stationary phase. In CDM2 the point of maximum cell density corresponded to a medium pH value of 4.06, while in M17 that value corresponded to a pH of 4.60. After the drastic changes in medium pH up to those points, values do not decrease much more. The final pH value measured for CDM2 was 4.05, while for M17 it was 4.26. Both media started at similar pH values, more specifically 6.65 for CDM2 and 6.59 for M17 (although the latter was measured 1 h after incubation). Although not investigated, the main cause behind the decrease in medium pH is thought to be most certainly the excretion of lactic acid by *L. lactis* LMG 19460, the main by-product of its homofermentative metabolism.

The clear effect of medium pH on growth permitted another conclusion beyond identifying the growth-limiting factor. While both media reached similar final pH values once *L. lactis* LMG 19460 entered stationary phase, M17 did it only after sustaining almost three times the cellular concentration. As such, it was concluded that the complex medium clearly had much higher buffer capabilities.

In the continuous attempt to optimise the originally assembled synthetic medium, further modifications were applied to CDM2, now based on the previously reported findings. More specifically, the initial pH value was adjusted to 7.0 and the concentration of the buffer MOPS was increased substantially (from 7.5 to 26.16 g L^{-1}), in what is referred as CDM3. MOPS, or 3-(N-morpholino)propanesulfonic acid, is a buffer commonly used in LAB synthetic media assays, first applied in growth of *L. lactis* by Jensen and Hammer (115). In the mentioned work, the authors demonstrate how MOPS can sustain much higher *L. lactis* biomass yields than traditional buffers (such as phosphate buffers) (115), a finding corroborated by the work of Aller *et al*. (97).

The effect of the changes introduced in CDM3 were, again, investigated in two sets of experiments. In the first one, a different culture volume was also investigated, this time decreased to 35 mL. In the second one, a further lower culture volume of 20 mL was tested. In both experiments, the synthetic medium was compared to parallel growth in M17. The results of these assays are presented in Figure 3.5.

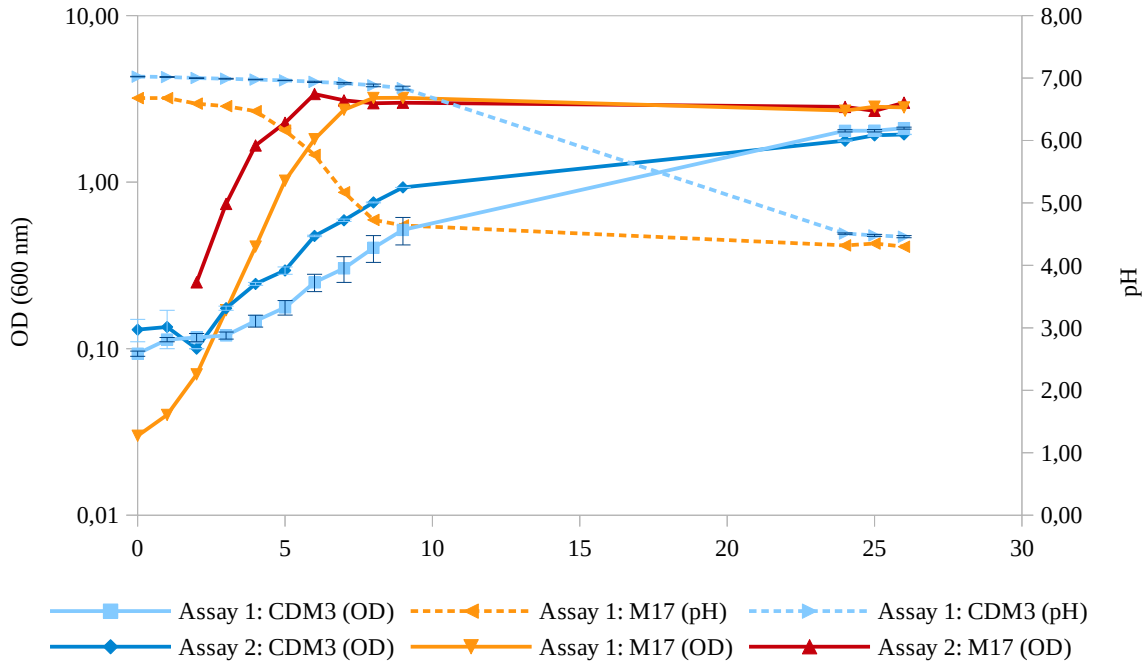

Figure 3.5: Growth and pH curves for *L. lactis* LMG 19460 cultivated in CDM3 and in M17. Complex medium assays were conducted in parallel to both CDM3 experiments. The first assays took place in culture volumes of 35 mL; their pH curves are also presented. The second assays took place in culture volumes of 20 mL. The error bars represent the standard error of the mean.

When analysing the results for CDM3, it becomes apparent that the increased concentration of MOPS had a significant effect on growth of *L. lactis* LMG 19460. The previous maximum OD_{600} of 1.11, registered in CDM2, was raised, respectively, to 2.11 and 1.94 in the first and second experiments in CDM3. These values were now closer to the ones observed for M17, respectively 3.21 and 3.38 in the first and second assays parallel to CDM3. As for medium pH in the first assay, CDM3 maintained high values throughout all the initially measured points. In the last measurement of the first day of growth, pH in the synthetic medium was registered still at 6.84, barely lower than the initial value of 7.0, while OD_{600} was already at 0.52. Comparing these results with the previous ones, when the strain achieved a similar OD_{600} in CDM2 (0.44, the closest available measurement), pH was already at 5.93. These results for maximum OD_{600} and medium pH are well in line with the mentioned positive result MOPS is reported to have on maximum biomass production (115).

As for the remaining growth kinetics in CDM3, no significant difference was observed on specific growth rate nor, consequently, duplication times. The first experiment registered a specific growth rate of 0.27 h^{-1} and duplication time of 2.56 h, while the second one registered a specific growth rate and duplication time of 0.30 h^{-1} and 2.28 h, respectively. Both these values are still noticeably lower than the ones for M17. Specific growth rates in the first and second M17 assays were determined to be 0.89 and 0.95 h^{-1}, respectively, while duplication times were calculated at 0.78 and 0.73 h, also respectively.

Finally, regarding the tested different volumes, a somewhat slower growth rate was observed in the larger volume of 35 mL than the one of 20 mL. These findings are possibly at odds with the previously presented growths in 10 mL and 40 mL (Figure 3.4), where *L. lactis* LMG 19460 achieved better growth kinetics on a lower volume. Nevertheless, not enough consistency was applied when evaluating the volume parameter, which led to low comparability between the results. For the proper investigation of the effect of culture volume on growth, future works should evaluate this parameter singly.

Overall, the chemically defined media here evaluated permit well-defined growth of *L. lactis* LMG 19460. Through the variation of some parameters, such as constituents, concentrations, and pH, it was possible to further optimise the synthetic medium. This optimization was only mostly noticed on biomass production, however, as specific growth rates and duplication times never varied much from the calculated averages of 0.28 h^{-1} and 2.51 h, respectively. This is further noticed when comparing the performance of the media here developed with published chemically defined media for *L. lactis* (Table 3.21). Generally speaking, most published synthetic media for the species report much higher specific growth rates than the ones achieved in the various iterations of CDM. However, none of those media seem to have reached the biomass formation achieved in CDM3, other than the ones by Zhang *et al*. (96), where the authors report biomass yields even higher than those in complex media. It was not possible, however, to include those results for biomass formation in Table 3.21, as the specific OD values are never shared by the authors (96).

Table 3.21: Comparison between average growth kinetics in the synthetic media developed for *L. lactis* LMG 19460 and published values for *L. lactis*. Certain works measured optical densities at wavelengths other than 600 nm and, as such, those results were excluded (N/A).

Synthetic medium	**CDM1**	**CDM2**	**CDM3**	**SA**	**MCD**	**MS10**	**BS3**	**BS6**	**BS7**
Reference	This work	This work	This work	115	95	95	97	97	97
Growth rate (h^{-1})	0.27	0.28	0.29	0.64	0.70	0.50	0.52	0.49	0.72
Final biomass (OD_{600})	1.09	1.11	2.02	N/A	N/A	N/A	1.26	0.91	1.38
Duplication time (h)	2.65	2.45	2.42	1.08	0.99	1.39	1.34	1.40	0.96

Nevertheless, the possible comparisons with published chemically defined media for *L. lactis* suggest possible routes for future works with the synthetic medium here developed (Table 3.21). On one hand, the parameters behind higher specific growth rates should be investigated and the appropriate changes introduced, to further optimise these media. Further optimization might also pass by identifying unnecessary medium components and having them remove, both to simplify the process of preparing the medium and also develop a more cost-effective one. Finally, on the subject of component removal, after having permitted growth of *L. lactis* LMG 19460, the media here developed should next be used to infer the strain's nutritional requirements and, consequently, a minimal medium which can sustain its growth. These last two applications of chemically defined media are particularly important for the development of GEMs, as previously discussed in this work.

3.11. Application of CDM1 in the GEM for *L. lactis* LMG 19460

After experimentally determining growth of *L. lactis* LMG 19460 in a chemical defined medium, this data could then be applied to the GEM developed for the strain.

As previously done, the composition of the synthetic media was loaded into the model as constraints on its exchange reactions. However, as the previous wet work did not determine yields for nutrient consumption and metabolic by-product formation, no specific flux rate constraints could be applied to those reactions. Consequently, and as described above for batch results, the reaction boundaries were set to unconstrained values, and the model's ability to match growth was evaluated as Boolean data only.

When carried over to the *in silico* environment, compositions of CDM1 and CDM2 corresponded to 55 and 56 exchange constraints, respectively. However, not all media components have an exchange reaction and, consequently, a pathway accounted for in the metabolic model for *L.*

lactis LMG 19460. More specifically, the metabolites MOPS, iodide, molybdate, ascorbic acid, and cobalamin are not currently included in the mentioned metabolic model. The case of ascorbic acid is particularly relevant, as it means there was no difference *in silico* between loading the constraints representing CDM1 and CDM2. Also limiting the computational representation of these media is the previously detailed steady-state assumption behind FBA. As metabolites are presumed to be at fixed concentrations when cells are under maximum growth rate (that is, they are consumed at the same rate as they are produced), differences in medium constituent concentrations are lost to simulations depending on said mathematical method. Therefore, the distinctions in concentrations between CDM1, CDM2, and CDM3 were also not carried over to the *in silico* environment.

With that in mind, a single composition representing the CDM media was set as the model constraints (Table 2.2) and growth was simulated. The result of performing FBA on the loaded set of constraints, was a simulated specific growth rate of 88.6395 h^{-1}, an expected unrealistically high value (due to the mentioned constraints type) which, nevertheless, demonstrates the metabolic reconstruction can predict growth in an experimentally validated medium. This value is in line with the previously reported predictions under unconstrained exchange rates representing published synthetic media for *L. lactis* IL1403 (Table 3.12).

While this result is a good first step in validating and curating the metabolic model here developed for *L. lactis* LMG 19460, much more work must still be done to fully turn it into a high-quality GEM. Future works have already been suggested, both regarding the development of the two metabolic reconstructions here presented and experimental work for their respective strains. Nonetheless, the result presented in this chapter, in particular, further highlights the priority need for experimental data detailing rates of nutrient consumption and by-product formation for *L. lactis* LMG 19460 cells grown in chemically defined media. This is the type of data that will allow to realistically constrain the GEM and, thus, evaluate its ability to meet not only Boolean growth, but also expected specific growth rates. Furthermore, the mentioned data should also be determined in carbon-limited conditions, in order to properly estimate the energetic parameters of the strain’s growth and non-associated growth functions.

4. Conclusions and future prospects

In this work, two GEMs were developed for the LAB *L. lactis* IL1403 and *L. lactis* LMG 19460. Furthermore, chemically defined media were developed for the latter strain and the organism's growth capabilities in said media were evaluated.

The first metabolic network, that of strain IL1403, was reconstructed through comparative genomics with organisms for which published GEMs are available. Through the determination of orthologous genes with each chosen target, the metabolic functions of *L. lactis* IL1403 were progressively inferred and new hypothesis were created for expanding its metabolic knowledge. After its assembly, the metabolic network was cleared of various errors and issues. Finally, the process of validating the developed GEM was commenced, by comparing its predictive capabilities with expected published phenotypes.

The GEM developed for *L. lactis* IL1403 demonstrates good capabilities in simulating most of the organism's reported nutritional requirements and possible carbon sources. Furthermore, it is able to achieve growth in all published chemically defined media specific to the strain, both in minimal nutrient compositions and when under specific rate constraints for nutrient consumption and by-product formation.

Nevertheless, more iterative steps in model refinement are still necessary before the GEM for strain IL1403 can be considered of high-quality. The methodology here applied to infer metabolic functions often led to false-positive inclusions during the reconstruction process. These were point inclusions, product of lower confidence bidirectional sequence homology results. They were not immediately detected due to the employed semi-automated addition of reactions determined to be new to the reconstruction. Many of these reactions were removed through the retroactive revision of their respective pathways. However, this generally only took place whenever said pathways were brought up for inspection in the process of correcting network errors or inconsistent predictions. As such, it is reported and acknowledged that this GEM likely still contains excessive inclusions.

The data kindly provided by Dr. Petri-Jaan Lahtvee was, without any doubt, fundamental to the proper validation of the *L. lactis* IL1403 model under specific environmental flux rate constraints. However, the unfortunate difficulties which the authors had in measuring consumption rates of certain amino acids came to limit the usability of said data (100). These data types are essential for proper GEM validation, and they become even more crucial when regarding organisms known to be auxotrophic. As such, the mentioned measurement errors were particularly critical due to L-histidine, a known auxotrophy in strain IL1403, being one of said errors. While a practical solution was applied for said erroneous values, it remains unknown how a realistic flux rate constraint on L-histidine uptake would affect the model's predictive capabilities in the tested conditions.

Taking into consideration the acknowledged limitations of the GEM developed for *L. lactis* IL1403, clear goals can be determined for future works using the model. Firstly, future developments on this GEM should aim to further manually curate the metabolic network, in order to continue in clearing it of the largest possible number of erroneous inclusions. Furthermore, some validation tests remain to be performed on the metabolic network, such as, for instance, evaluating its correct prediction of gene-deletion phenotypes and the ability to simulate the shift from homolactic to heterolactic metabolism, experimentally observed (and characterised) in *L. lactis* IL1403 (13). Future works should also aim to perform high-quality exometabolomic experiments for the strain, in order to assemble sets of constraints that enable both further model validation and prospective uses under realistic conditions. For the same purpose of validation, the characterisation of lethal mutants at the species level, at least, would also be of great use in order to ensure realistic predictions by the GEM. Finally on the subject of experimental work, future works should eventually also aim to obtain a

highly detailed chemical composition of *L. lactis* IL1403 cells. This experimental data could then be applied to the BOF here developed as to impart it with greater realism and strain-specificity.

Finally, when refined into a high-quality, manually curated GEM, the reconstruction may then be used in a myriad of applications. One example of said prospective uses is the simulation of the metabolic behaviour associated with the production of recombinant protein coded in exogenous plasmids (62). This is particularly relevant to GEMs for LAB, even more so *L. lactis*, which are progressively finding greater applications in the biotechnological roles associated with the production of recombinant protein (84, 8).

Having developed a partially curated and validated working GEM for *L. lactis* IL1403, it was then possible to use this model to infer the metabolic network of the lesser characterised strain LMG 19460. This was achieved through the same comparative genomics approach used before, this time between the two strains. Consequently, the GEM developed for *L. lactis* LMG 19460 is, in almost its entirety, identical to the one developed for strain IL1403. As such, everything said regarding the characteristics and performance of the first model also applies to the one for *L. lactis* LMG 19460. The two reconstructions differ only in 5 reactions, which were removed in the model for strain LMG 19460 due to a lack of homology with their respective genes in strain IL1403. Curiously, however, these reactions refer to central metabolic pathways and seem to affect the second model's growth capabilities.

Every suggestion for future applications of the GEM developed for *L. lactis* IL1403 applies to the one developed for strain LMG 19460, and more. The metabolic reconstruction for *L. lactis* LMG 19460 requires not only every improvement and further validation listed for the first model, but also the more elementary validation here carried on the model for strain IL1403. This is due to the fact that strain LMG 19460 currently does not yet have any available metabolically-relevant published data. As such, any further improvement on its model requires first a series of experimental assays. With that in mind, future experimental works with the strain should first aim to perform the most fundamental phenotypic characterisations, such as determining nutritional requirements and carbon source utilization capabilities. Afterwards, these works should move on the same goals described for strain IL1403, such as obtaining high quality exometabolomic data, determining gene essentiality and cellular composition, and more.

Many of the suggested future works require assays in a chemically defined medium. Here, it was developed and improved one of such synthetic media. This medium and its iterative versions contain, generally, a carbon source, all amino acids and a wide range of vitamins, minerals, and micronutrients. They all enabled growth of *L. lactis* LMG 19460 and the last version, in which the concentration of the buffer MOPS was substantially increased, also supports significant biomass production. Nevertheless, all registered specific growth rates were noticeable lower than other chemically defined media reported for *L. lactis* IL1403.

With these considerations in mind, future works and improvements are clearly possible on the medium here reported. First and foremost, the mechanics behind the noted slower growth rates should be determined, by investigating alternative medium compositions, but also the metabolic capabilities of *L. lactis* LMG 19460. As mentioned, it was noted in its GEM that this strain has fewer reactions in some central metabolic pathways. While this cannot yet be a strong enough indication of the slower rate observed *in vitro*, particularly given the refinement still necessary on the model, it does offer a suggestion of where to drive future works.

Besides further optimization leading to better growth rates, the synthetic medium can also be applied to numerous other goals directly related to the strain. It may serve as the base for the mentioned nutrient essentiality tests, from which a minimal medium specific to the strain can then be

investigated. Furthermore, the medium here developed can be used in carbon source utilization tests, exometabolomics assays, and any other application requiring a chemically defined medium.

Either way, it is clear that building the metabolic knowledge on *L. lactis* LMG 19460 will greatly benefit from a parallel development of the GEM and the synthetic medium here developed for the strain. Together, these developments will then allow for better pursuing all the potential applications of *L. lactis* LMG 19460 in biotechnology.

References

1. Wood, Brian JB, and W. H. N. Holzapfel, eds. *The genera of lactic acid bacteria*. Vol. 2. Springer Science & Business Media, 1992.

2. Liu, W., et al. "Lactic acid bacteria: fundamentals and practice." *Amsterdam: Springer, doi* 10 (2014): 978-94.

3. Vinderola, Gabriel, et al., eds. *Lactic Acid Bacteria: Microbiological and Functional Aspects*. CRC Press, 2019.

4. Quinto, Emiliano J., et al. "Probiotic lactic acid bacteria: a review." *Food and Nutrition Sciences* 5.18 (2014): 1765.

5. Mays, Zachary JS, and Nikhil U. Nair. "Synthetic biology in probiotic lactic acid bacteria: At the frontier of living therapeutics." *Current opinion in biotechnology* 53 (2018): 224-231.

6. Michon, Christophe, et al. "Display of recombinant proteins at the surface of lactic acid bacteria: strategies and applications." *Microbial cell factories* 15.1 (2016): 1-16.

7. García-Fruitós, Elena. "Lactic acid bacteria: a promising alternative for recombinant protein production." (2012): 1-3.

8. Wells, Jerry. "Mucosal vaccination and therapy with genetically modified lactic acid bacteria." *Annual review of food science and technology* 2 (2011): 423-445.

9. Gaudu, Philippe, et al. "Respiration capacity and consequences in Lactococcus lactis." *Lactic Acid Bacteria: Genetics, Metabolism and Applications*. Springer, Dordrecht, 2002. 263-269.

10. Narvhus, J. A., and L. Axelsson. "Encyclopedia of food science and nutrition." (2003): 3465-3472.

11. Zaidi, Arsalan Haseeb, et al. "The ABC-type multidrug resistance transporter LmrCD is responsible for an extrusion-based mechanism of bile acid resistance in Lactococcus lactis." *Journal of bacteriology* 190.22 (2008): 7357-7366.

12. Neves, Ana Rute, et al. "Overview on sugar metabolism and its control in Lactococcus lactis—the input from in vivo NMR." *FEMS microbiology reviews* 29.3 (2005): 531-554.

13. Garrigues, Christel, et al. "Control of the shift from homolactic acid to mixed-acid fermentation in Lactococcus lactis: predominant role of the NADH/NAD+ ratio." *Journal of Bacteriology* 179.17 (1997): 5282-5287.

14. Bolotin, Alexander, et al. "The complete genome sequence of the lactic acid bacterium Lactococcus lactis ssp. lactis IL1403." *Genome research* 11.5 (2001): 731-753.

15. Cavanagh, Daniel, Gerald F. Fitzgerald, and Olivia McAuliffe. "From field to fermentation: the origins of Lactococcus lactis and its domestication to the dairy environment." *Food microbiology* 47 (2015): 45-61.

16. Kelly, William J., Lawrence JH Ward, and Sinead C. Leahy. "Chromosomal diversity in Lactococcus lactis and the origin of dairy starter cultures." *Genome biology and evolution* 2 (2010): 729-744.

17. Ayad, Eman HE, et al. "Flavour forming abilities and amino acid requirements of Lactococcus lactis strains isolated from artisanal and non-dairy origin." *International Dairy Journal* 9.10 (1999): 725-735.

18. Yvon, Mireille, et al. "An aminotransferase from Lactococcus lactis initiates conversion of amino acids to cheese flavor compounds." *Applied and Environmental Microbiology* 63.2 (1997): 414-419.

19. Law, B. A., Emel Sezgin, and M. Elisabeth Sharpe. "Amino acid nutrition of some commercial cheese starters in relation to their growth in peptone-supplemented whey media." *Journal of Dairy Research* 43.2 (1976): 291-300.

20. Siezen, Roland J., et al. "Genome-scale genotype-phenotype matching of two Lactococcus lactis isolates from plants identifies mechanisms of adaptation to the plant niche." *Applied and environmental microbiology* 74.2 (2008): 424-436.
21. Ainsworth, Stuart, et al. "The Lactococcus lactis plasmidome: much learnt, yet still lots to discover." *FEMS microbiology reviews* 38.5 (2014): 1066-1088.
22. Morello, Eric, et al. "Lactococcus lactis, an efficient cell factory for recombinant protein production and secretion." *Journal of molecular microbiology and biotechnology* 14.1-3 (2008): 48-58.
23. Song, Adelene Ai-Lian, et al. "A review on Lactococcus lactis: from food to factory." *Microbial cell factories* 16.1 (2017): 55.
24. Klijn, Nicolette, Anton H. Weerkamp, and W. M. De Vos. "Genetic marking of Lactococcus lactis shows its survival in the human gastrointestinal tract." *Applied and environmental microbiology* 61.7 (1995): 2771-2774.
25. Pontes, Daniela Santos, et al. "Lactococcus lactis as a live vector: heterologous protein production and DNA delivery systems." *Protein expression and purification* 79.2 (2011): 165-175.
26. Lister, Joseph Baron. *On the lactic fermentation and its bearings on pathology*. JE Adlard, 1878.
27. Wels, Michiel, et al. "Comparative genome analysis of Lactococcus lactis indicates niche adaptation and resolves genotype/phenotype disparity." *Frontiers in microbiology* 10 (2019): 4.
28. Palsson, Bernhard. "Metabolic systems biology." *FEBS letters* 583.24 (2009): 3900-3904.
29. Covert, Markus W., et al. "Metabolic modeling of microbial strains in silico." *Trends in biochemical sciences* 26.3 (2001): 179-186.
30. Papoutsakis, Eleftherios Terry. "Equations and calculations for fermentations of butyric acid bacteria." *Biotechnology and bioengineering* 67.6 (2000): 813-826.
31. Papoutsakis, Eleftherios Terry, and Charles L. Meyer. "Equations and calculations of product yields and preferred pathways for butanediol and mixed-acid fermentations." *Biotechnology and bioengineering* 27.1 (1985): 50-66.
32. Edwards, Jeremy S., and Bernhard O. Palsson. "Systems properties of the Haemophilus influenzae Rd metabolic genotype." *Journal of Biological Chemistry* 274.25 (1999): 17410-17416.
33. Fleischmann, Robert D., et al. "Whole-genome random sequencing and assembly of Haemophilus influenzae Rd." *Science* 269.5223 (1995): 496-512.
34. Gu, Changdai, et al. "Current status and applications of genome-scale metabolic models." *Genome biology* 20.1 (2019): 121.
35. Reed, Jennifer L., et al. "Towards multidimensional genome annotation." *Nature Reviews Genetics* 7.2 (2006): 130-141.
36. Durot, Maxime, Pierre-Yves Bourguignon, and Vincent Schachter. "Genome-scale models of bacterial metabolism: reconstruction and applications." *FEMS microbiology reviews* 33.1 (2008): 164-190.
37. Feist, Adam M., et al. "Reconstruction of biochemical networks in microorganisms." *Nature Reviews Microbiology* 7.2 (2009): 129-143.
38. Baart, Gino JE, and Dirk E. Martens. "Genome-scale metabolic models: reconstruction and analysis." *Neisseria meningitidis*. Humana Press, (2012): 107-126.
39. Santos, Filipe, Joost Boele, and Bas Teusink. "A practical guide to genome-scale metabolic models and their analysis." *Methods in enzymology*. Vol. 500. Academic Press, (2011): 509-532.
40. Thiele, Ines, and Bernhard Ø. Palsson. "A protocol for generating a high-quality genome-scale metabolic reconstruction." *Nature protocols* 5.1 (2010): 93.
41. Monk, Jonathan, Juan Nogales, and Bernhard O. Palsson. "Optimizing genome-scale network reconstructions." *Nature biotechnology* 32.5 (2014): 447-452.

42. Sauls, John T., and Joerg M. Buescher. "Assimilating genome-scale metabolic reconstructions with modelBorgifier." *Bioinformatics* 30.7 (2014): 1036-1038.
43. Mendoza, Sebastián N., et al. "A systematic assessment of current genome-scale metabolic reconstruction tools." *Genome biology* 20.1 (2019): 1-20.
44. Feist, Adam M., and Bernhard O. Palsson. "The biomass objective function." *Current opinion in microbiology* 13.3 (2010): 344-349.
45. Russell, James B., and Gregory M. Cook. "Energetics of bacterial growth: balance of anabolic and catabolic reactions." *Microbiological reviews* 59.1 (1995): 48-62.
46. Palsson, Bernhard. *Systems biology*. Cambridge university press, 2015.
47. Terzer, Marco, et al. "Genome-scale metabolic networks." *Wiley Interdisciplinary Reviews: Systems Biology and Medicine* 1.3 (2009): 285-297.
48. Durot, Maxime, Pierre-Yves Bourguignon, and Vincent Schachter. "Genome-scale models of bacterial metabolism: reconstruction and applications." *FEMS microbiology reviews* 33.1 (2008): 164-190.
49. Orth, Jeffrey D., Ines Thiele, and Bernhard Ø. Palsson. "What is flux balance analysis?." *Nature biotechnology* 28.3 (2010): 245-248.
50. García Sánchez, Carlos Eduardo, and Rodrigo Gonzalo Torres Sáez. "Comparison and analysis of objective functions in flux balance analysis." *Biotechnology progress* 30.5 (2014): 985-991.
51. Medema, Marnix H., et al. "Computational tools for the synthetic design of biochemical pathways." *Nature Reviews Microbiology* 10.3 (2012): 191-202.
52. Kim, Do-Gyun, et al. "Review of current approaches for implementing metabolic reconstruction." *Journal of Biosystems Engineering* 43.1 (2018): 45-58.
53. Mackie, Amanda, et al. "Dead end metabolites-defining the known unknowns of the E. coli metabolic network." *PloS one* 8.9 (2013): e75210.
54. Price, Nathan D., et al. "Extreme pathways and Kirchhoff's second law." *Biophysical journal* 83.5 (2002): 2879-2882.
55. Pan, Shu, and Jennifer L. Reed. "Advances in gap-filling genome-scale metabolic models and model-driven experiments lead to novel metabolic discoveries." *Current opinion in biotechnology* 51 (2018): 103-108.
56. Hucka, Michael, et al. "The systems biology markup language (SBML): a medium for representation and exchange of biochemical network models." *Bioinformatics* 19.4 (2003): 524-531.
57. Durot, Maxime, Pierre-Yves Bourguignon, and Vincent Schachter. "Genome-scale models of bacterial metabolism: reconstruction and applications." *FEMS microbiology reviews* 33.1 (2008): 164-190.
58. Patil, Kiran Raosaheb, Mats Åkesson, and Jens Nielsen. "Use of genome-scale microbial models for metabolic engineering." *Current opinion in biotechnology* 15.1 (2004): 64-69.
59. Zhang, Cheng, and Qiang Hua. "Applications of genome-scale metabolic models in biotechnology and systems medicine." *Frontiers in physiology* 6 (2016): 413.
60. Oberhardt, Matthew A., Bernhard Ø. Palsson, and Jason A. Papin. "Applications of genome-scale metabolic reconstructions." *Molecular systems biology* 5.1 (2009): 320.
61. Bordbar, Aarash, et al. "Constraint-based models predict metabolic and associated cellular functions." *Nature Reviews Genetics* 15.2 (2014): 107-120.
62. Ow, Dave Siak-Wei, et al. "Identification of cellular objective for elucidating the physiological state of plasmid-bearing Escherichia coli using genome-scale in silico analysis." *Biotechnology progress* 25.1 (2009): 61-67.

63. Norsigian, Charles J., et al. "A workflow for generating multi-strain genome-scale metabolic models of prokaryotes." *Nature Protocols* (2019): 1-14.
64. Fang, Xin, Colton J. Lloyd, and Bernhard O. Palsson. "Reconstructing organisms in silico: genome-scale models and their emerging applications." *Nature Reviews Microbiology* (2020): 1-13.
65. Lewis, Nathan E., Harish Nagarajan, and Bernhard O. Palsson. "Constraining the metabolic genotype–phenotype relationship using a phylogeny of in silico methods." *Nature Reviews Microbiology* 10.4 (2012): 291-305.
66. King, Zachary A., et al. "Next-generation genome-scale models for metabolic engineering." *Current opinion in biotechnology* 35 (2015): 23-29.
67. Lerman, Joshua A., et al. "In silico method for modelling metabolism and gene product expression at genome scale." *Nature communications* 3.1 (2012): 1-10.
68. Seif, Yara, et al. "A computational knowledge-base elucidates the response of Staphylococcus aureus to different media types." *PLoS computational biology* 15.1 (2019): e1006644.
69. Chandrasekaran, Sriram, and Nathan D. Price. "Probabilistic integrative modeling of genome-scale metabolic and regulatory networks in Escherichia coli and Mycobacterium tuberculosis." *Proceedings of the National Academy of Sciences* 107.41 (2010): 17845-17850.
70. O'brien, Edward J., et al. "Genome-scale models of metabolism and gene expression extend and refine growth phenotype prediction." *Molecular systems biology* 9.1 (2013): 693.
71. Oliveira, Ana Paula, Jens Nielsen, and Jochen Förster. "Modeling Lactococcus lactis using a genome-scale flux model." *BMC microbiology* 5.1 (2005): 39.
72. Cavanagh, Daniel, Gerald F. Fitzgerald, and Olivia McAuliffe. "From field to fermentation: the origins of Lactococcus lactis and its domestication to the dairy environment." *Food microbiology* 47 (2015): 45-61.
73. Flahaut, Nicolas AL, et al. "Genome-scale metabolic model for Lactococcus lactis MG1363 and its application to the analysis of flavor formation." *Applied microbiology and biotechnology* 97.19 (2013): 8729-8739.
74. Norsigian, Charles J., et al. "BiGG Models 2020: multi-strain genome-scale models and expansion across the phylogenetic tree." *Nucleic acids research* 48.D1 (2020): D402-D406.
75. Silva, Inês N., et al. "Draft Genome Sequence of the Plasmid-Free Lactococcus lactis subsp. lactis Strain LMG 19460." *Genome Announcements* 5.16 (2017).
76. Monk, Jonathan M., et al. "Genome-scale metabolic reconstructions of multiple Escherichia coli strains highlight strain-specific adaptations to nutritional environments." *Proceedings of the National Academy of Sciences* 110.50 (2013): 20338-20343.
77. Bosi, Emanuele, et al. "Comparative genome-scale modelling of Staphylococcus aureus strains identifies strain-specific metabolic capabilities linked to pathogenicity." *Proceedings of the National Academy of Sciences* 113.26 (2016): E3801-E3809.
78. Seif, Yara, et al. "Genome-scale metabolic reconstructions of multiple Salmonella strains reveal serovar-specific metabolic traits." *Nature communications* 9.1 (2018): 1-12.
79. Lechner, Marcus, et al. "Proteinortho: detection of (co-) orthologs in large-scale analysis." *BMC bioinformatics* 12.1 (2011): 1-9.
80. Camacho, Christiam, et al. "BLAST+: architecture and applications." *BMC bioinformatics* 10.1 (2009): 421.
81. Ogata, Hiroyuki, et al. "KEGG: Kyoto encyclopedia of genes and genomes." *Nucleic acids research* 27.1 (1999): 29-34.
82. Caspi, Ron, et al. "The MetaCyc database of metabolic pathways and enzymes." *Nucleic acids research* 46.D1 (2018): D633-D639.

83. Devoid, Scott, et al. "Automated genome annotation and metabolic model reconstruction in the SEED and Model SEED." *Systems Metabolic Engineering*. Humana Press, Totowa, NJ, 2013. 17-45.
84. King, Zachary A., et al. "BiGG Models: A platform for integrating, standardizing and sharing genome-scale models." *Nucleic acids research* 44.D1 (2016): D515-D522.
85. Monk, Jonathan M., et al. "i ML1515, a knowledgebase that computes Escherichia coli traits." *Nature biotechnology* 35.10 (2017): 904-908.
86. Jensen, Christian S., et al. "Reconstruction and validation of a genome-scale metabolic model of Streptococcus oralis (iCJ415), a human commensal and opportunistic pathogen." *Frontiers in Genetics* 11 (2020): 116.
87. Levering, Jennifer, et al. "Genome-scale reconstruction of the Streptococcus pyogenes M49 metabolic network reveals growth requirements and indicates potential drug targets." *Journal of biotechnology* 232 (2016): 25-37.
88. Koduru, Lokanand, et al. "Genome-scale modeling and transcriptome analysis of Leuconostoc mesenteroides unravel the redox governed metabolic states in obligate heterofermentative lactic acid bacteria." *Scientific reports* 7.1 (2017): 1-15.
89. Veith, Nadine, et al. "Using a genome-scale metabolic model of Enterococcus faecalis V583 to assess amino acid uptake and its impact on central metabolism." *Applied and Environmental Microbiology* 81.5 (2015): 1622-1633.
90. Machado, Daniel, et al. "Fast automated reconstruction of genome-scale metabolic models for microbial species and communities." *Nucleic acids research* 46.15 (2018): 7542-7553.
91. Buchfink, Benjamin, Chao Xie, and Daniel H. Huson. "Fast and sensitive protein alignment using DIAMOND." *Nature methods* 12.1 (2015): 59-60.
92. Elbourne, Liam DH, et al. "TransportDB 2.0: a database for exploring membrane transporters in sequenced genomes from all domains of life." *Nucleic Acids Research* 45.D1 (2017): D320-D324.
93. Saier Jr, Milton H., Can V. Tran, and Ravi D. Barabote. "TCDB: the Transporter Classification Database for membrane transport protein analyses and information." *Nucleic acids research* 34.suppl_1 (2006): D181-D186.
94. Heirendt, Laurent, et al. "Creation and analysis of biochemical constraint-based models using the COBRA Toolbox v. 3.0." *Nature protocols* 14.3 (2019): 639-702.
95. Cocaign-Bousquet, M., et al. "Rational development of a simple synthetic medium for the sustained growth of Lactococcus lactis." *Journal of applied bacteriology* 79.1 (1995): 108-116.
96. Zhang, Guiying, David A. Mills, and David E. Block. "Development of chemically defined media supporting high-cell-density growth of lactococci, enterococci, and streptococci." *Applied and environmental microbiology* 75.4 (2009): 1080-1087.
97. Aller, Kadri, et al. "Nutritional requirements and media development for Lactococcus lactis IL1403." *Applied microbiology and biotechnology* 98.13 (2014): 5871-5881.
98. Nordkvist, Mikkel, Niels Bang Siemsen Jensen, and John Villadsen. "Glucose metabolism in Lactococcus lactis MG1363 under different aeration conditions: requirement of acetate to sustain growth under microaerobic conditions." *Applied and Environmental Microbiology* 69.6 (2003): 3462-3468.
99. Van Niel, E. W. J., and Bärbel Hahn-Hägerdal. "Nutrient requirements of lactococci in defined growth media." *Applied Microbiology and Biotechnology* 52.5 (1999): 617-627.
100. Lahtvee, Petri-Jaan, et al. "Multi-omics approach to study the growth efficiency and amino acid metabolism in Lactococcus lactis at various specific growth rates." *Microbial Cell Factories* 10.1 (2011): 1-12.

101. Xavier, Joana C., Kiran Raosaheb Patil, and Isabel Rocha. "Integration of biomass formulations of genome-scale metabolic models with experimental data reveals universally essential cofactors in prokaryotes." *Metabolic engineering* 39 (2017): 200-208.
102. Novak, L., and Pascal Loubiere. "The metabolic network of Lactococcus lactis: distribution of 14C-labeled substrates between catabolic and anabolic pathways." *Journal of bacteriology* 182.4 (2000): 1136-1143.
103. Reed, Jennifer L., et al. "An expanded genome-scale model of Escherichia coli K-12 (iJR904 GSM/GPR)." *Genome biology* 4.9 (2003): R54.
104. Jeske, Lisa, et al. "BRENDA in 2019: a European ELIXIR core data resource." *Nucleic acids research* 47.D1 (2019): D542-D549.
105. Flamholz, Avi, et al. "eQuilibrator—the biochemical thermodynamics calculator." *Nucleic acids research* 40.D1 (2012): D770-D775.
106. Noor, Elad, et al. "Consistent estimation of Gibbs energy using component contributions." *PLoS Comput Biol* 9.7 (2013): e1003098.
107. Price, Nathan D., Jennifer L. Reed, and Bernhard Ø. Palsson. "Genome-scale models of microbial cells: evaluating the consequences of constraints." *Nature Reviews Microbiology* 2.11 (2004): 886-897.
108. Navarro-González, R., and C. Ponnamperuma. "Role of trace metal ions in chemical evolution. The case of free-radical reactions." *Advances in Space Research* 15.3 (1995): 357-364.
109. Delorme, C. H. R. I. S. T. I. N. E., et al. "Gene inactivation in Lactococcus lactis: histidine biosynthesis." *Journal of bacteriology* 175.14 (1993): 4391-4399.
110. Sperandio, Brice, et al. "Sulfur amino acid metabolism and its control in Lactococcus lactis IL1403." *Journal of bacteriology* 187.11 (2005): 3762-3778.
111. Chopin, Alain. "Organization and regulation of genes for amino acid biosynthesis in lactic acid bacteria." *FEMS microbiology reviews* 12.1-3 (1993): 21-37.
112. Godon, Jean-Jacques, et al. "Gene inactivation in Lactococcus lactis: branched-chain amino acid biosynthesis." *Journal of bacteriology* 175.14 (1993): 4383-4390.
113. Dias, Oscar, et al. "iDS372, a phenotypically reconciled model for the metabolism Streptococcus pneumoniae strain R6." *Frontiers in microbiology* 10 (2019): 1283.
114. Pastink, Margreet I., et al. "Genome-scale model of Streptococcus thermophilus LMG18311 for metabolic comparison of lactic acid bacteria." *Applied and environmental microbiology* 75.11 (2009): 3627-3633.
115. Jensen, Peter Ruhdal, and Karin Hammer. "Minimal requirements for exponential growth of Lactococcus lactis." *Applied and Environmental Microbiology* 59.12 (1993): 4363-4366.
116. Even, Sergine, Nic D. Lindley, and Muriel Cocaign-Bousquet. "Molecular physiology of sugar catabolism in Lactococcus lactis IL1403." *Journal of Bacteriology* 183.13 (2001): 3817-3824.
117. Dressaire, Clémentine, et al. "Growth rate regulated genes and their wide involvement in the Lactococcus lactis stress responses." *BMC genomics* 9.1 (2008): 343.
118. Passerini, Delphine, et al. "The carbohydrate metabolism signature of Lactococcus lactis strain A12 reveals its sourdough ecosystem origin." *Applied and environmental microbiology* 79.19 (2013): 5844-5852.
119. Aleksandrzak-Piekarczyk, Tamara, et al. "Alternative lactose catabolic pathway in Lactococcus lactis IL1403." *Applied and environmental microbiology* 71.10 (2005): 6060-6069.
120. Poolman, Bert, and Wil N. Konings. "Relation of growth of Streptococcus lactis and Streptococcus cremoris to amino acid transport." *Journal of bacteriology* 170.2 (1988): 700-707.
121. Chopin, Alain, et al. "Two plasmid-determined restriction and modification systems in Streptococcus lactis." *Plasmid* 11.3 (1984): 260-263.

Supplementary Materials

Supplementary Table S1: Tabular representation of the two GEMs developed in this work, for better convenience and visualisation. The models for *L. lactis* IL1403 and *L. lactis* LMG 19460 are differentiated by the GPR columns.

Abbreviation	Description	Reaction	GPR (IL1403)	GPR (LMG 19460)	Lower bound	Upper bound	Objective	Subsystem	EC Number	KEGG ID	SEED ID	BioCyc ID
ALAR	Alanine racemase	ala__L[c] <=> ala__D[c]	L_RS04450	BZO99_RS05260	-1000	1000	0	Amino Acid Metabolism: Alanine and Aspartate Metabolism	5.1.1.1	R00401	rxn00283	META:ALARACECAT-RXN
ALATA_L	L-alanine transaminase	akg[c] + ala__L[c] <=> glu__L[c] + pyr[c]	L_RS00880 or L_RS00345	BZO99_RS03090 or BZO99_RS08730	-1000	1000	0	Amino Acid Metabolism: Alanine and Aspartate Metabolism	2.6.1.2	R00258	rxn00191	META:ALANINE-AMINOTRANSFERASE-RXN; META:RXN-13698
ASNN	L-asparaginase	asn__L[c] + h2o[c] -> asp__L[c] + nh4[c]	L_RS03920	BZO99_RS10860	0	1000	0	Amino Acid Metabolism: Alanine and Aspartate Metabolism	3.5.1.1; 3.5.1.38; 3.5.5.4	R00485	rxn00342	META:ASPARAGHYD-RXN
ASNS1	Asparagine synthase (glutamine-hydrolysing)	asp__L[c] + atp[c] + gln__L[c] + h2o[c] -> amp[c] + asn__L[c] + ppi[c] + glu__L[c] + h[c]	L_RS01860 or L_RS11695	BZO99_RS02110 or BZO99_RS09890	0	1000	0	Amino Acid Metabolism: Alanine and Aspartate Metabolism	6.3.5.4	R00578	rxn00416; rxn11214	META:ASNSYNB-RXN
ASPTA	Aspartate transaminase	akg[c] + asp__L[c] <=> glu__L[c] + oaa[c]	L_RS10040 or L_RS09535 or L_RS00880	BZO99_RS10380 or BZO99_RS03470 or BZO99_RS03090	-1000	1000	0	Amino Acid Metabolism: Alanine and Aspartate Metabolism	2.6.1.1	R00355	rxn00260	META:ASPAMINOTRANS-RXN; META:RXN-13697
ACGK	Acetylglutamate kinase	acglu[c] + atp[c] -> acg5p[c] + adp[c]	L_RS04240	BZO99_RS07145	0	1000	0	Amino Acid Metabolism: Arginine and Proline Metabolism	2.7.2.8	R02649	rxn01917	META:ACETYLGLUTKIN-RXN
ACGS	N-acetylglutamate synthase	accoa[c] + glu__L[c] <=> acglu[c] + coa[c] + h[c]	L_RS04230	BZO99_RS07135	-1000	1000	0	Amino Acid Metabolism: Arginine and Proline Metabolism	2.3.1.1	R00259	rxn00192	META:N-ACETYLTRANSFER-RXN
ACODA_1	Acetylornithine deacetylase	acorn[c] + h2o[c] -> ac[c] + orn__L[c]	L_RS03045	BZO99_RS06240	0	1000	0	Amino Acid Metabolism: Arginine and Proline Metabolism	3.5.1.14; 3.5.1.16	R00669	rxn00469	META:ACETYLORNDEACET-RXN
ACOTA	Acetylornithine transaminase	acorn[c] + akg[c] <=> acg5sa[c] + glu__L[c]	L_RS04235	BZO99_RS07140	-1000	1000	0	Amino Acid Metabolism: Arginine and Proline Metabolism	2.6.1.11	R02283	rxn01637	META:ACETYLORNTRANSAM-RXN
AGPR	N-acetyl-g-glutamyl-phosphate reductase	acg5sa[c] + pi[c] + nadp[c] <=> acg5p[c] + h[c] + nadph[c]	L_RS04225	BZO99_RS07130	-1000	1000	0	Amino Acid Metabolism: Arginine and Proline Metabolism	1.2.1.38	R03443	rxn02465	META:N-ACETYLGLUTPREDUCT-RXN
ARGDr	Arginine deiminase	arg__L[c] + h2o[c] -> citr__L[c] + nh4[c]	L_RS10705	BZO99_RS07745	0	1000	0	Amino Acid Metabolism: Arginine and Proline Metabolism	3.5.3.6	R00552	rxn00395	META:ARGININE-DEIMINASE-RXN
ARGSL	Argininosuccinate lyase	argsuc[c] <=> arg__L[c] + fum[c]	L_RS00705	BZO99_RS08510	-1000	1000	0	Amino Acid Metabolism: Arginine and Proline Metabolism	4.3.2.1	R01086	rxn00802	META:ARGSUCCINLYA-RXN
ARGSS	Argininosuccinate synthase	citr__L[c] + asp__L[c] + atp[c] -> amp[c] + argsuc[c] + ppi[c] + h[c]	L_RS00700	BZO99_RS08515	0	1000	0	Amino Acid Metabolism: Arginine and Proline Metabolism	6.3.4.5	R01954	rxn01434	META:ARGSUCCINSYN-RXN
CBMKr	Carbamate kinase	co2[c] + atp[c] + nh4[c] <=> adp[c] + cbp[c] + 2 h[c]	L_RS08850 or L_RS10685 or L_RS10680	BZO99_RS11430 or BZO99_RS07760 or BZO99_RS07765	-1000	1000	0	Amino Acid Metabolism: Arginine and Proline Metabolism	2.7.2.2	R00150	rxn00114	META:CARBAMATE-KINASE-RXN
G5SADs	L-glutamate 5-semialdehyde dehydratase (spontaneous)	glu5sa[c] <=> 1pyr5c[c] + h2o[c] + h[c]	s0001	s0001	-1000	1000	0	Amino Acid Metabolism: Arginine and Proline Metabolism	Non-enzymatic	R03314	rxn02374; rxn11220	META:SPONTPRO-RXN
G5SD	Glutamate-5-semialdehyde dehydrogenase	glu5p[c] + h[c] + nadph[c] -> pi[c] + glu5sa[c] + nadp[c]	L_RS08385	BZO99_RS01740	0	1000	0	Amino Acid Metabolism: Arginine and Proline Metabolism	1.2.1.41	R03313	rxn02373	META:GLUTSEMIALDEHYDROG-RXN
GLU5K	Glutamate 5-kinase	atp[c] + glu__L[c] -> adp[c] + glu5p[c]	L_RS08390	BZO99_RS01745	0	1000	0	Amino Acid Metabolism: Arginine and Proline Metabolism	2.7.2.11	R00239	rxn00179	META:GLUTKIN-RXN
MTAN	Methylthioadenosine nucleosidase	5mta[c] + h2o[c] -> ade[c] + 5mtr[c]	L_RS09790	BZO99_RS03215	0	1000	0	Amino Acid Metabolism: Arginine and Proline Metabolism	3.2.2.9; 3.2.2.16	R01401	rxn01021	META:METHYLTHIOADENOSINE-NUCLEOSIDASE-RXN
OCBT_1	Ornithine	cbp[c] + orn__L[c]	L_RS10700 or	BZO99_RS07750 or	-1000	1000	0	Amino Acid Metabolism: Arginine and	2.1.3.3	R01398	rxn01019	META:ORNCARBA

	carbamoyltransferase	<=> citr__L[c] + pi[c] + h[c]	L_RS04245	BZO99_RS07150				Proline Metabolism				MTRANSFER-RXN; META:RXN-13482
ORNTAC_1	Ornithine transacetylase	acorn[c] + glu__L[c] <=> acglu[c] + orn__L[c]	L_RS04230	BZO99_RS07135	-1000	1000	0	Amino Acid Metabolism: Arginine and Proline Metabolism	2.3.1.35	R02282	rxn01636; rxn38121	META:GLUTAMATE-N-ACETYLTRANSFERASE-RXN
P5CR	Pyrroline-5-carboxylate reductase	1pyr5c[c] + 2 h[c] + nadph[c] -> pro__L[c] + nadp[c]	L_RS09810	BZO99_RS03195	0	1000	0	Amino Acid Metabolism: Arginine and Proline Metabolism	1.5.1.2	R01251	rxn00931	META:PYRROLINECARBREDUCT-RXN
SPMDAT1	Spermidine acetyltransferase	accoa[c] + spmd[c] -> coa[c] + N1aspmd[c] + h[c]	L_RS08420	BZO99_RS01775	0	1000	0	Amino Acid Metabolism: Arginine and Proline Metabolism	2.3.1.57		rxn09264	META:SPERMACTRAN-RXN
SPMDAT2	Spermidine acetyltransferase (N8)	accoa[c] + spmd[c] -> coa[c] + n8aspmd[c] + h[c]	L_RS08420	BZO99_RS01775	0	1000	0	Amino Acid Metabolism: Arginine and Proline Metabolism	2.3.1.57		rxn09265	META:RXN0-7165
AHSERL2	O acetylhomoserine thiol lyase	achms[c] + h2s[c] <=> ac[c] + h[c] + hcys__L[c]	L_RS00430	BZO99_RS08815	-1000	1000	0	Amino Acid Metabolism: Cysteine Metabolism	2.5.1.48; 2.5.1.49	R01287	rxn00952	META:ACETYLHOMOSER-CYS-RXN
CYSDS	Cysteine desulfhydrase	cys__L[c] + h2o[c] -> pyr[c] + h2s[c] + nh4[c]	L_RS04145 or L_RS03365	BZO99_RS07045 or BZO99_RS05920	0	1000	0	Amino Acid Metabolism: Cysteine Metabolism	4.4.1.28; 4.4.1.8; 4.4.1.1	R00782	rxn00566	META:LCYSDESULF-RXN
CYSS	Cysteine synthase	acser[c] + h2s[c] -> ac[c] + cys__L[c] + h[c]	L_RS02835 or L_RS04150	BZO99_RS04195 or BZO99_RS07050	0	1000	0	Amino Acid Metabolism: Cysteine Metabolism	2.5.1.47; 2.5.1.65	R00897	rxn00649	META:ACSERLY-RXN
CYSTGL	Cystathionine g lyase	cyst__L[c] + h2o[c] -> 2obut[c] + cys__L[c] + nh4[c]	L_RS04145 or L_RS03365	BZO99_RS07045 or BZO99_RS05920	0	1000	0	Amino Acid Metabolism: Cysteine Metabolism	4.4.1.1	R01001	rxn33428	META:CYSTAGLY-RXN; META:RXN-15130
HSERTA	Homoserine O trans acetylase	accoa[c] + hom__L[c] <=> coa[c] + achms[c]	L_RS10050	BZO99_RS10390	-1000	1000	0	Amino Acid Metabolism: Cysteine Metabolism	2.3.1.31	R01776	rxn01303	META:HOMOSERINE-O-ACETYLTRANSFERASE-RXN
METB1	Metb1 (rev)	cys__L[c] + achms[c] -> ac[c] + cyst__L[c] + h[c]	L_RS10045	BZO99_RS10385	0	1000	0	Amino Acid Metabolism: Cysteine Metabolism	2.5.1.48	R03217	rxn02302	META:RXN-721
MHPGLUT2	5-methyltetrahydropteroyltriglutamate methyltransferase	ahcys[c] + h[c] + mhpglu[c] <=> amet[c] + hpglu[c]	L_RS06580	BZO99_RS08140	-1000	1000	0	Amino Acid Metabolism: Cysteine Metabolism	2.1.1.13; 2.1.1.14	R09365	rxn16206; rxn23136	META:RXN-12730
RHCCE	S-ribosylhomocysteine cleavage enzyme	rhcys[c] -> dhptd[c] + hcys__L[c]	L_RS01410	BZO99_RS02560	0	1000	0	Amino Acid Metabolism: Cysteine Metabolism	4.4.1.21	R01291	rxn05958	META:RIBOSYLHOMOCYSTEINASE-RXN
RHCYS	5 deoxyribos 5 ylhomocysteinase	rhcys[c] + h2o[c] -> rib__D[c] + hcys__L[c]	L_RS01410	BZO99_RS02560	0	1000	0	Amino Acid Metabolism: Cysteine Metabolism	4.4.1.21		rxn00955	
SERAT	Serine O-acetyltransferase	accoa[c] + ser__L[c] <=> coa[c] + acser[c]	L_RS09650	BZO99_RS03355	-1000	1000	0	Amino Acid Metabolism: Cysteine Metabolism	2.3.1.30	R00586	rxn00423	META:SERINE-O-ACETTRAN-RXN
SHSL2r	O-succinylhomoserine lyase (H2S)	h2s[c] + suchms[c] -> h[c] + hcys__L[c] + succ[c]	L_RS00430	BZO99_RS08815	0	1000	0	Amino Acid Metabolism: Cysteine Metabolism	2.5.1.48	R01288	rxn05957	META:RXN-9384
SHSL4r	O succinylhomoserine lyase elimination (reversible)	h2o[c] + suchms[c] -> 2obut[c] + h[c] + nh4[c] + succ[c]	L_RS10045	BZO99_RS10385	0	1000	0	Amino Acid Metabolism: Cysteine Metabolism	2.5.1.48; 4.2.99.9; 4.3.1	R00999	rxn00740	META:METBALT-RXN
2H3MBDH	2 hydroxy 3 methylbutanoate dehydrogenase	3mob[c] + h[c] + nadh[c] <=> 2hiv[c] + nad[c]	L_RS06920	BZO99_RS08355	-1000	1000	0	Amino Acid Metabolism: Flavour Forming Pathways				
2H3MPDH	2 hydroxy 3 methylpentanoate dehydrogenase	3mop[c] + h[c] + nadh[c] <=> 2h3mv[c] + nad[c]	L_RS06920	BZO99_RS08355	-1000	1000	0	Amino Acid Metabolism: Flavour Forming Pathways				
2MBALDH	2 methylbutanal dehydrogenase acid forming	2mbald[c] + h2o[c] + nad[c] <=> h[c] + m2but[c] + nadh[c]			-1000	1000	0	Amino Acid Metabolism: Flavour Forming Pathways				
ACKILE	2 methylbutanoyl p acyl kinase	m2butp[c] + adp[c] -> m2but[c] + atp[c]	L_RS10575 or L_RS10580	BZO99_RS07865 or BZO99_RS07860	0	1000	0	Amino Acid Metabolism: Flavour Forming Pathways				
ACKLEU	Isovaleryl p acyl	adp[c] + ppap[c] ->	L_RS10575 or	BZO99_RS07865 or	0	1000	0	Amino Acid Metabolism: Flavour				

	kinase	3mb[c] + atp[c]	L_RS10580	BZO99_RS07860				Forming Pathways				
ACKVAL	Isobutyryl p acyl kinase	adp[c] + isobutp[c] + h[c] -> atp[c] + isobuta[c]	L_RS10575 or L_RS10580	BZO99_RS07865 or BZO99_RS07860	0	1000	0	Amino Acid Metabolism: Flavour Forming Pathways				
PTAILE	2 oxobutanoyl coa phosphotransacetylation	2mbcoa[c] + pi[c] + h[c] -> coa[c] + m2butp[c]	L_RS08650	BZO99_RS02000	0	1000	0	Amino Acid Metabolism: Flavour Forming Pathways				
PTALEU	Isovaleryl coa phosphotransacetylation	pi[c] + ivcoa[c] -> coa[c] + ppap[c]	L_RS08650	BZO99_RS02000	0	1000	0	Amino Acid Metabolism: Flavour Forming Pathways				
PTAVAL	Isobutyryl phosphotransacetylase	pi[c] + ibcoa[c] -> coa[c] + isobutp[c]	L_RS08650	BZO99_RS02000	0	1000	0	Amino Acid Metabolism: Flavour Forming Pathways				
CBPS	Carbamoyl-phosphate synthase (glutamine-hydrolysing)	2 atp[c] + gln__L[c] + h2o[c] + hco3[c] -> 2 adp[c] + cbp[c] + pi[c] + glu__L[c] + 2 h[c]	L_RS08350 and L_RS07125	BZO99_RS01705 and BZO99_RS05365	0	1000	0	Amino Acid Metabolism: Glutamate Metabolism	6.3.5.5	R00575	rxn00414	META:CARBPSYN-RXN
GF6PTA	Glutamine-fructose-6-phosphate transaminase	f6p[c] + gln__L[c] -> gam6p[c] + glu__L[c]	L_RS05265	BZO99_RS00380	0	1000	0	Amino Acid Metabolism: Glutamate Metabolism	2.6.1.16	R00768	rxn15064	META:L-GLN-FRUCT-6-P-AMINOTRANS-RXN
GLNS	Glutamine synthetase	atp[c] + glu__L[c] + nh4[c] -> adp[c] + pi[c] + gln__L[c] + h[c]	L_RS11545	BZO99_RS09460	0	1000	0	Amino Acid Metabolism: Glutamate Metabolism	6.3.1.2	R00253	rxn00187	META:GLUTAMINESYN-RXN
GLUDC	Glutamate Decarboxylase	glu__L[c] + h[c] -> co2[c] + 4abut[c]	L_RS06760	BZO99_RS07960	0	1000	0	Amino Acid Metabolism: Glutamate Metabolism	4.1.1.15	R00261	rxn00194	META:GLUTDECARBOX-RXN
GLUPRT	Cofactor and Prosthetic Group Biosynthesis: Folate Salvage Pathway	gln__L[c] + prpp[c] + h2o[c] -> ppi[c] + pram[c] + glu__L[c]	L_RS07970	BZO99_RS10280	0	1000	0	Amino Acid Metabolism: Glutamate Metabolism	2.4.2.14	R01072	rxn00790	META:PRPPAMIDOTRANS-RXN
GLUSy	Glutamate synthase (NADPH)	akg[c] + gln__L[c] + h[c] + nadph[c] -> 2 glu__L[c] + nadp[c]	L_RS06735 and L_RS06740	BZO99_RS07985 and BZO99_RS07980	0	1000	0	Amino Acid Metabolism: Glutamate Metabolism	1.4.1.13	R00114	rxn00085	META:GLUTAMATESYN-RXN
BETALDHx	Betaine-aldehyde dehydrogenase	betald[c] + h2o[c] + nad[c] -> 2 h[c] + glyb[c] + nadh[c]	L_RS02565	BZO99_RS04475	0	1000	0	Amino Acid Metabolism: Glycine and Serine Metabolism	1.2.1.8	R02565	rxn01867	META:BADH-RXN
CHOLD	Choline dehydrogenase	nad[c] + chol[c] -> h[c] + nadh[c] + betald[c]	L_RS11295	BZO99_RS09350	0	1000	0	Amino Acid Metabolism: Glycine and Serine Metabolism	1.1.1.1	R08557	rxn10770	META:RXN-6021
GLYCK2	Glycerate 2-kinase	atp[c] + glyc__R[c] -> 2pg[c] + h[c] + adp[c]	L_RS04515	BZO99_RS05190	0	1000	0	Amino Acid Metabolism: Glycine and Serine Metabolism	2.7.1.31; 2.7.1.165	R08572	rxn08647	META:GKI-RXN
HPYRRx	Hydroxypyruvate reductase (NADH)	h[c] + hpyr[c] + nadh[c] -> nad[c] + glyc__R[c]	L_RS10450	BZO99_RS07540	0	1000	0	Amino Acid Metabolism: Glycine and Serine Metabolism	1.1.1.26; 1.1.1.29; 1.1.1.81	R01388	rxn01011	META:GLYCERATE-DEHYDROGENASE-RXN
HPYRRy	Hydroxypyruvate reductase (NADPH)	h[c] + hpyr[c] + nadph[c] -> nadp[c] + glyc__R[c]	L_RS10450	BZO99_RS07540	0	1000	0	Amino Acid Metabolism: Glycine and Serine Metabolism	1.1.1; 1.1.1.79; 1.1.1.81	R01392	rxn01013	META:RXN0-300
PGCD	Phosphoglycerate dehydrogenase	3pg[c] + nad[c] -> 3php[c] + h[c] + nadh[c]	L_RS03250 or L_RS10450	BZO99_RS06035 or BZO99_RS07540	0	1000	0	Amino Acid Metabolism: Glycine and Serine Metabolism	1.1.1.95	R01513	rxn01101	META:PGLYCDEHYDROG-RXN
PSERT	Phosphoserine transaminase	3php[c] + glu__L[c] -> akg[c] + pser__L[c]	L_RS03245	BZO99_RS06040	0	1000	0	Amino Acid Metabolism: Glycine and Serine Metabolism	2.6.1.52	R04173	rxn02914	META:PSERTRANSAM-RXN
PSP_L	Phosphoserine phosphatase (L-serine)	pser__L[c] + h2o[c] -> pi[c] + ser__L[c]	L_RS03255	BZO99_RS06030	0	1000	0	Amino Acid Metabolism: Glycine and Serine Metabolism	3.1.3.3	R00582	rxn00420	META:RXN0-5114
SERD_L	L-serine deaminase	ser__L[c] -> pyr[c] + nh4[c]	(L_RS04375 and L_RS04370) or L_RS06435	(BZO99_RS05330 and BZO99_RS05335) or BZO99_RS09955	0	1000	0	Amino Acid Metabolism: Glycine and Serine Metabolism	4.3.1.15; 4.3.1.17; 4.3.1.19	R00220	rxn00165	META:4.3.1.17-RXN
SPTc	Serine-pyruvate	pyr[c] + ser__L[c]	L_RS02580	BZO99_RS04460	-1000	1000	0	Amino Acid Metabolism: Glycine and	2.6.1.51	R00585	rxn00422	META:SERINE--

	aminotransferase	<=> ala__L[c] + hpyr[c]						Serine Metabolism				PYRUVATE-AMINOTRANSFERASE-RXN
HISTP	Histidinol-phosphatase	h2o[c] + hisp[c] -> pi[c] + histd[c]	L_RS06375	BZO99_RS11075	0	1000	0	Amino Acid Metabolism: Histidine Metabolism	3.1.3.15	R03013	rxn02160	META:HISTIDPHOS-RXN
PRAMPC_1	Phosphoribosyl AMP cyclohydrolase	prbamp[c] + h2o[c] + h[c] -> prfp[c]	L_RS06370	BZO99_RS11070	0	1000	0	Amino Acid Metabolism: Histidine Metabolism	3.5.4.19	R04037	rxn02835	META:HISTCYCLOHYD-RXN
PRATPP	Phosphoribosyl-ATP pyrophosphatase	prbatp[c] + h2o[c] -> ppi[c] + prbamp[c] + h[c]	L_RS06370	BZO99_RS11070	0	1000	0	Amino Acid Metabolism: Histidine Metabolism	3.6.1.31	R04035	rxn02834	META:HISTPRATPHYD-RXN
AHCYSNS	S-adenosylhomocysteine nucleosidase	ahcys[c] + h2o[c] -> ade[c] + rhcys[c]	L_RS09790	BZO99_RS03215	0	1000	0	Amino Acid Metabolism: Methionine Metabolism	3.2.2.9	R00194	rxn00143	META:ADENOSYLHOMOCYSTEINE-NUCLEOSIDASE-RXN
CYSTL	Cystathionine b-lyase	cyst__L[c] + h2o[c] -> pyr[c] + hcys__L[c] + nh4[c]	L_RS04145 or L_RS03365	BZO99_RS07045 or BZO99_RS05920	0	1000	0	Amino Acid Metabolism: Methionine Metabolism	4.4.1.13	R01286	rxn15166	META:CYSTATHIONINE-BETA-LYASE-RXN
DHPTDCs2	4,5-dihydroxy-2,3-pentanedione cyclization (spontaneous)	dhptd[c] -> mdhdhf[c]	s0001	s0001	0	1000	0	Amino Acid Metabolism: Methionine Metabolism				
HSST	Homoserine O-succinyltransferase	hom__L[c] + succoa[c] -> coa[c] + suchms[c]	L_RS10050	BZO99_RS10390	0	1000	0	Amino Acid Metabolism: Methionine Metabolism	2.3.1.46	R01777	rxn01304	META:HOMSUCTRAN-RXN
METAT	Methionine adenosyltransferase	atp[c] + met__L[c] + h2o[c] -> amet[c] + pi[c] + ppi[c]	L_RS09905	BZO99_RS10605	0	1000	0	Amino Acid Metabolism: Methionine Metabolism	2.5.1.6	R00177	rxn00126	META:S-ADENMETSYN-RXN
METGL	Methionine g lyase	met__L[c] + h2o[c] -> 2obut[c] + ch4s[c] + nh4[c]	L_RS04145	BZO99_RS07045	0	1000	0	Amino Acid Metabolism: Methionine Metabolism	4.4.1.11	R00654	rxn00456	META:METHIONINE-GAMMA-LYASE-RXN
METOX1s	Methionine oxidation (spontaneous)	met__L[c] + h2o2[c] -> h2o[c] + metsox_S__L[c]	s0001	s0001	0	1000	0	Amino Acid Metabolism: Methionine Metabolism				
METOX2s	Methionine oxidation 2 (spontaneous)	met__L[c] + h2o2[c] -> h2o[c] + metsox_R__L[c]	s0001	s0001	0	1000	0	Amino Acid Metabolism: Methionine Metabolism				
METS	Methionine synthase	5mthf[c] + hcys__L[c] -> met__L[c] + h[c] + thf[c]	L_RS06580	BZO99_RS08140	0	1000	0	Amino Acid Metabolism: Methionine Metabolism	2.1.1.13	R00946	rxn00693	META:HOMOCYSMETB12-RXN
METSOXR1	L-methionine-S-oxide reductase	metsox_S__L[c] + trdrd[c] <=> h2o[c] + met__L[c] + trdox[c]	L_RS08575 and (L_RS08105 or L_RS10545)	BZO99_RS01925 and (BZO99_RS01450 or BZO99_RS07895)	-1000	1000	0	Amino Acid Metabolism: Methionine Metabolism	1.8.4.13; 1.8.4.14	R02025	rxn06077; rxn08918	
METSOXR2	L-methionine-R-sulfoxide reductase	trdrd[c] + metsox_R__L[c] -> met__L[c] + trdox[c] + h2o[c]	(L_RS08575 and L_RS01025) or (L_RS11525 and L_RS08575)	(BZO99_RS01925 and BZO99_RS02945) or (BZO99_RS09440 and BZO99_RS01925)	0	1000	0	Amino Acid Metabolism: Methionine Metabolism	1.8.4.14	R07608	rxn07439; rxn08919	META:1.8.4.14-RXN
MHPGLUT	5 methyltetrahydropteroyltriglutamate homocysteine S methyltransferase	mhpglu[c] + hcys__L[c] -> met__L[c] + hpglu[c]	L_RS06580	BZO99_RS08140	0	1000	0	Amino Acid Metabolism: Methionine Metabolism	2.1.1.14	R04405	rxn03052	META:HOMOCYSMET-RXN
MTHTHFSs	(2R,4S)-2-methyl-2,3,3,4-tetrahydroxytetrahydrofuran synthesis (spontaneous)	mdhdhf[c] + h2o[c] -> mththf[c]	s0001	s0001	0	1000	0	Amino Acid Metabolism: Methionine Metabolism				
SHSL1	O-succinylhomoserine lyase (L-cysteine)	cys__L[c] + suchms[c] <=> cyst__L[c] + h[c] + succ[c]	L_RS10045 or L_RS04145	BZO99_RS10385 or BZO99_RS07045	-1000	1000	0	Amino Acid Metabolism: Methionine Metabolism	2.5.1.48	R03260	rxn15395	META:O-SUCCHOMOSERLYASE-RXN
ADAPAT	E N-acetyl-L,L-	glu__L[c] +	L_RS00345	BZO99_RS08730	-1000	1000	0	Amino Acid Metabolism: Threonine and	2.6.1.-	R04467	rxn03086	META:RXN-4822

	diaminopimelate aminotransferase	nal2a6o[c] <=> akg[c] + n6all26d[c]						Lysine Metabolism				
ASAD	Aspartate-semialdehyde dehydrogenase	aspsa[c] + pi[c] + nadp[c] <=> 4pasp[c] + h[c] + nadph[c]	L_RS08455	BZO99_RS01810	-1000	1000	0	Amino Acid Metabolism: Threonine and Lysine Metabolism	1.2.1.11	R02291	rxn01643	META:ASPARTATE-SEMIALDEHYDE-DEHYDROGENASE-RXN
ASPK	Aspartate kinase	asp__L[c] + atp[c] <=> adp[c] + 4pasp[c]	L_RS03940	BZO99_RS10880	-1000	1000	0	Amino Acid Metabolism: Threonine and Lysine Metabolism	2.7.2.4	R00480	rxn00337	META:ASPARTATEKIN-RXN
DAPDA	N-acetyl-L,L-diaminopimelate deacetylase	h2o[c] + n6all26d[c] <=> 26dap_LL[c] + ac[c]	L_RS01495 or L_RS05020	BZO99_RS02475 or BZO99_RS00125	-1000	1000	0	Amino Acid Metabolism: Threonine and Lysine Metabolism	3.5.1.47	R02733	rxn01972	META:N-ACETYLDIAMINOPIMELATE-DEACETYLASE-RXN
DAPDC	Diaminopimelate decarboxylase	26dap__M[c] + h[c] -> co2[c] + lys__L[c]	L_RS06730	BZO99_RS07990	0	1000	0	Amino Acid Metabolism: Threonine and Lysine Metabolism	4.1.1.20	R00451	rxn00313	META:DIAMINOPIMDECARB-RXN
DAPE	Diaminopimelate epimerase	26dap_LL[c] <=> 26dap__M[c]	L_RS06730	BZO99_RS07990	-1000	1000	0	Amino Acid Metabolism: Threonine and Lysine Metabolism	5.1.1.7	R02735	rxn01974	META:DIAMINOPIMEPIM-RXN
DHDPRy	Dihydrodipicolinate reductase (NADPH)	23dhdp[c] + h[c] + nadph[c] -> nadp[c] + thdp[c]	L_RS08155	BZO99_RS01505	0	1000	0	Amino Acid Metabolism: Threonine and Lysine Metabolism	1.3.1.26; 1.17.1.8	R04199	rxn02929	META:DIHYDROPICRED-RXN
DHDPS	Dihydrodipicolinate synthase	aspsa[c] + pyr[c] -> 23dhdp[c] + h[c] + 2.0 h2o[c]	L_RS08445	BZO99_RS01800	0	1000	0	Amino Acid Metabolism: Threonine and Lysine Metabolism	4.3.3.7	R10147	rxn01644; rxn40037	META:DIHYDRODIPICSYN-RXN
HSDy	Homoserine dehydrogenase (NADPH)	nadp[c] + hom__L[c] <=> aspsa[c] + h[c] + nadph[c]	L_RS06075	BZO99_RS01215	-1000	1000	0	Amino Acid Metabolism: Threonine and Lysine Metabolism	1.1.1.3	R01775	rxn01302	META:HOMOSERDEHYDROG-RXN
HSK	Homoserine kinase	atp[c] + hom__L[c] -> adp[c] + phom[c] + h[c]	L_RS06080	BZO99_RS01220	0	1000	0	Amino Acid Metabolism: Threonine and Lysine Metabolism	2.7.1.39	R01771	rxn01300	META:HOMOSERKIN-RXN
SDPDS	Succinyl-diaminopimelate desuccinylase	h2o[c] + sl26da[c] -> 26dap_LL[c] + succ[c]	L_RS03045	BZO99_RS06240	0	1000	0	Amino Acid Metabolism: Threonine and Lysine Metabolism	3.5.1.18	R02734	rxn01973	META:SUCCDIAMINOPIMDESUCC-RXN
SDPTA	Succinyldiaminopimelate transaminase	akg[c] + sl26da[c] <=> glu__L[c] + sl2a6o[c]	L_RS04235	BZO99_RS07140	-1000	1000	0	Amino Acid Metabolism: Threonine and Lysine Metabolism	2.6.1.17	R04475	rxn03087	META:SUCCINYLDIAMINOPIMTRANS-RXN
THDPS	Tetrahydrodipicolinate succinylase	h2o[c] + succoa[c] + thdp[c] -> coa[c] + sl2a6o[c]	L_RS01490	BZO99_RS02480	0	1000	0	Amino Acid Metabolism: Threonine and Lysine Metabolism	2.3.1.117	R04365	rxn03031	META:TETHYDPICSUCC-RXN
THPAT	L-2,3,4,5-tetrahydrodipicolinate N2-acetyltransferase	accoa[c] + h2o[c] + thdp[c] -> coa[c] + nal2a6o[c]	L_RS01490	BZO99_RS02480	-1000	1000	0	Amino Acid Metabolism: Threonine and Lysine Metabolism	2.3.1.-; 2.3.1.89	R04364	rxn03030	META:2.3.1.89-RXN
THRA	Threonine aldolase	thr__L[c] <=> acald[c] + gly[c]	L_RS03235	BZO99_RS06050	-1000	1000	0	Amino Acid Metabolism: Threonine and Lysine Metabolism	4.1.2.48; 4.1.2.5	R00751	rxn00541	META:THREONINE-ALDOLASE-RXN
THRD_L	L-threonine deaminase	thr__L[c] -> 2obut[c] + nh4[c]	L_RS06425 or L_RS06435	BZO99_RS09945 or BZO99_RS09955	0	1000	0	Amino Acid Metabolism: Threonine and Lysine Metabolism	4.3.1.19	R00996	rxn00737	META:THREDEHYD-RXN
THRS	Threonine synthase	phom[c] + h2o[c] -> pi[c] + thr__L[c]	L_RS11030	BZO99_RS06785	0	1000	0	Amino Acid Metabolism: Threonine and Lysine Metabolism	4.2.3.1	R01466	rxn01069	META:THRESYN-RXN
AALDH	Aryl alcohol dehydrogenase	h[c] + nadh[c] + pacald[c] <=> nad[c] + pea[c]	L_RS09420	BZO99_RS03585	-1000	1000	0	Amino Acid Metabolism: Tyrosine, Tryptophan, and Phenylalanine Metabolism	1.1.1.90; 1.1.1.1	R02611	rxn01902	META:RXN-7700
ANPRT	Anthranilate phosphoribosyltransferase	anth[c] + prpp[c] -> ppi[c] + pran[c]	L_RS07670	BZO99_RS05630	0	1000	0	Amino Acid Metabolism: Tyrosine, Tryptophan, and Phenylalanine Metabolism	2.4.2.18	R01073	rxn00791	META:PRTRANS-RXN
ANS	Anthranilate synthase	chor[c] + gln__L[c] -> anth[c] + glu__L[c] + pyr[c] + h[c]	L_RS07680 and (L_RS07675 or L_RS06880)	BZO99_RS05640 and (BZO99_RS05635 or BZO99_RS08395)	0	1000	0	Amino Acid Metabolism: Tyrosine, Tryptophan, and Phenylalanine Metabolism	4.1.3.27	R00986	rxn00727	META:ANTHRANSYN-RXN
ANS2	Anthranilate synthase 2	chor[c] + nh4[c] <=> anth[c] + h2o[c] + h[c] + pyr[c]	L_RS07680 and (L_RS07675 or L_RS06880) and (L_RS07675 or L_RS06880)	BZO99_RS05640 and (BZO99_RS05635 or BZO99_RS08395) and (BZO99_RS05635 or BZO99_RS08395)	-1000	1000	0	Amino Acid Metabolism: Tyrosine, Tryptophan, and Phenylalanine Metabolism	4.1.3.27	R00985	rxn00726; rxn11283	
CHORM	Chorismate mutase	chor[c] -> pphn[c]	L_RS11530	BZO99_RS09445	0	1000	0	Amino Acid Metabolism: Tyrosine,	5.4.99.5	R01715	rxn01256	META:CHORISMAT

								Tryptophan, and Phenylalanine Metabolism				EMUT-RXN
CHORS	Chorismate synthase	3psme[c] -> chor[c] + pi[c]	L_RS09135	BZO99_RS03870	0	1000	0	Amino Acid Metabolism: Tyrosine, Tryptophan, and Phenylalanine Metabolism	4.2.3.5	R01714	rxn01255	META:CHORISMATE-SYNTHASE-RXN
DDPA	3-deoxy-D-arabino-heptulosonate 7-phosphate synthetase	e4p[c] + h2o[c] + pep[c] -> 2dda7p[c] + pi[c]	L_RS00655 or L_RS06570	BZO99_RS08565 or BZO99_RS08150	0	1000	0	Amino Acid Metabolism: Tyrosine, Tryptophan, and Phenylalanine Metabolism	2.5.1.54	R01826	rxn01332	META:DAHPSYN-RXN
DHQS	3-dehydroquinate synthase	2dda7p[c] -> 3dhq[c] + pi[c]	L_RS09155	BZO99_RS03850	0	1000	0	Amino Acid Metabolism: Tyrosine, Tryptophan, and Phenylalanine Metabolism	4.2.3.4	R03083	rxn02212	META:3-DEHYDROQUINATE-SYNTHASE-RXN
DHQTi	3-dehydroquinate dehydratase, irreversible	3dhq[c] <=> 3dhsk[c] + h2o[c]	L_RS08560	BZO99_RS01910	-1000	1000	0	Amino Acid Metabolism: Tyrosine, Tryptophan, and Phenylalanine Metabolism	4.2.1.10	R03084	rxn02213	META:3-DEHYDROQUINATE-DEHYDRATASE-RXN
IGPS	Indole-3-glycerol-phosphate synthase	2cpr5p[c] + h[c] -> co2[c] + 3ig3p[c] + h2o[c]	L_RS07665	BZO99_RS05625	0	1000	0	Amino Acid Metabolism: Tyrosine, Tryptophan, and Phenylalanine Metabolism	4.1.1.48	R03508	rxn02507	META:IGPSYN-RXN
INDPYRD	Indole 3 pyruvate decarboxylase	h[c] + indpyr[c] <=> co2[c] + id3acald[c]	L_RS06825	BZO99_RS08450	-1000	1000	0	Amino Acid Metabolism: Tyrosine, Tryptophan, and Phenylalanine Metabolism	4.1.1.43; 4.1.1.74	R01974	rxn01450	META:4.1.1.74-RXN
PHETA1	Phenylalanine transaminase	akg[c] + phe__L[c] <=> phpyr[c] + glu__L[c]	L_RS00345 or L_RS09535	BZO99_RS08730 or BZO99_RS03470	-1000	1000	0	Amino Acid Metabolism: Tyrosine, Tryptophan, and Phenylalanine Metabolism	2.6.1.57; 2.6.1.5; 2.6.1.9; 2.6.1.1	R00694	rxn00493	META:PHEAMINOTRANS-RXN; META:RXN-10814
PPND	Prephenate dehydrogenase	pphn[c] + nad[c] -> co2[c] + 34hpp[c] + nadh[c]	L_RS09095	BZO99_RS03905	0	1000	0	Amino Acid Metabolism: Tyrosine, Tryptophan, and Phenylalanine Metabolism	1.3.1.12	R01728	rxn01268	META:PREPHENATEDEHYDROG-RXN
PPNDH	Prephenate dehydratase	pphn[c] + h[c] -> co2[c] + phpyr[c] + h2o[c]	L_RS09080	BZO99_RS03920	0	1000	0	Amino Acid Metabolism: Tyrosine, Tryptophan, and Phenylalanine Metabolism	4.2.1.51; 4.2.1.91	R01373	rxn01000	META:PREPHENATEDEHYDRAT-RXN
PPYRDC	Phenylpyruvate decarboxylase	phpyr[c] + h[c] -> co2[c] + pacald[c]	L_RS10120	BZO99_RS10460	0	1000	0	Amino Acid Metabolism: Tyrosine, Tryptophan, and Phenylalanine Metabolism	4.1.1.-; 4.1.1.43	R01377	rxn01003	META:PHENYLPYRUVATE-DECARBOXYLASE-RXN
PRAIi	Phosphoribosylanthranilate isomerase (irreversible)	pran[c] <=> 2cpr5p[c]	L_RS07660	BZO99_RS05620	-1000	1000	0	Amino Acid Metabolism: Tyrosine, Tryptophan, and Phenylalanine Metabolism	5.3.1.24	R03509	rxn02508	META:PRAISOM-RXN
PSCVT	3-phosphoshikimate 1-carboxyvinyltransferase	skm5p[c] + pep[c] <=> 3psme[c] + pi[c]	L_RS09090	BZO99_RS03910	-1000	1000	0	Amino Acid Metabolism: Tyrosine, Tryptophan, and Phenylalanine Metabolism	2.5.1.19	R03460	rxn02476	META:2.5.1.19-RXN
SHK3Dr	Shikimate dehydrogenase	3dhsk[c] + h[c] + nadph[c] <=> skm[c] + nadp[c]	L_RS09160	BZO99_RS03845	-1000	1000	0	Amino Acid Metabolism: Tyrosine, Tryptophan, and Phenylalanine Metabolism	1.1.1.25; 1.1.1.282	R02413	rxn01740	META:SHIKIMATE-5-DEHYDROGENASE-RXN
SHKK	Shikimate kinase	atp[c] + skm[c] -> adp[c] + h[c] + skm5p[c]	L_RS09085	BZO99_RS03915	0	1000	0	Amino Acid Metabolism: Tyrosine, Tryptophan, and Phenylalanine Metabolism	2.7.1.71	R02412	rxn01739	META:SHIKIMATE-KINASE-RXN
TRPS1	Tryptophan synthase (indoleglycerol phosphate)	3ig3p[c] + ser__L[c] -> g3p[c] + h2o[c] + trp__L[c]	L_RS07650 and L_RS07645	BZO99_RS05610 and BZO99_RS05605	0	1000	0	Amino Acid Metabolism: Tyrosine, Tryptophan, and Phenylalanine Metabolism	4.2.1.20	R02722	rxn01964	META:TRYPSYN-RXN
TRPS2	Tryptophan synthase (indole)	indole[c] + ser__L[c] -> h2o[c] + trp__L[c]	L_RS07650 and L_RS07645	BZO99_RS05610 and BZO99_RS05605	0	1000	0	Amino Acid Metabolism: Tyrosine, Tryptophan, and Phenylalanine Metabolism	4.2.1.122; 4.2.1.20	R00674	rxn00474	META:RXN0-2382
TRPS3	Tryptophan synthase (subunit alpha)	3ig3p[c] -> g3p[c] + indole[c]	L_RS07645 and L_RS07650	BZO99_RS05605 and BZO99_RS05610	0	1000	0	Amino Acid Metabolism: Tyrosine, Tryptophan, and Phenylalanine Metabolism	4.1.2.8; 4.2.1.20	R02340	rxn01682	META:RXN0-2381
TRPTA	Tryptophan transaminase	akg[c] + trp__L[c] <=> indpyr[c] + glu__L[c]	L_RS00345	BZO99_RS08730	-1000	1000	0	Amino Acid Metabolism: Tyrosine, Tryptophan, and Phenylalanine Metabolism	2.6.1.27	R00684	rxn00483	META:TRYPTOPHAN-AMINOTRANSFERASE-RXN
TYRTA	Tyrosine transaminase	akg[c] + tyr__L[c] <=> 34hpp[c] + glu__L[c]	L_RS00345 or L_RS09535	BZO99_RS08730 or BZO99_RS03470	-1000	1000	0	Amino Acid Metabolism: Tyrosine, Tryptophan, and Phenylalanine Metabolism	2.6.1.57; 2.6.1.5; 2.6.1.9; 2.6.1.1	R00734	rxn00527	META:TYROSINE-AMINOTRANSFERASE-RXN

2HXICDH	L-2-hydroxyisocaproate dehydrogenase	4mop[c] + h[c] + nadh[c] <=> 2hxic__L[c] + nad[c]	L_RS06920	BZO99_RS08355	-1000	1000	0	Amino Acid Metabolism: Valine, Leucine and Isoleucine Metabolism	1.1.1.345		rxn45233	META:RXN-16245
3MOPDC	3 Methyl 2 oxopentanoate decarboxylase	3mop[c] + h[c] -> 2mbald[c] + co2[c]			0	1000	0	Amino Acid Metabolism: Valine, Leucine and Isoleucine Metabolism	4.1.1.72	R03894	rxn02748	META:4.1.1.72-RXN
ACHBS	2-aceto-2-hydroxybutanoate synthase	2obut[c] + pyr[c] + h[c] -> 2ahbut[c] + co2[c]	L_RS06420 and L_RS06425 and L_RS06195	BZO99_RS09945 and BZO99_RS01335	0	1000	0	Amino Acid Metabolism: Valine, Leucine and Isoleucine Metabolism	2.2.1.6	R08648	rxn08043	META:ACETOOHBUTSYN-RXN
ACLS	Acetolactate synthase	2 pyr[c] + h[c] -> co2[c] + alac__S[c]	L_RS06420 and L_RS06425 and L_RS06195	BZO99_RS09945 and BZO99_RS01335	0	1000	0	Amino Acid Metabolism: Valine, Leucine and Isoleucine Metabolism	2.2.1.6	R00226	rxn15021	META:ACETOLACTSYN-RXN
DHAD1	Dihydroxy-acid dehydratase (2,3-dihydroxy-3-methylbutanoate)	23dhmb[c] -> 3mob[c] + h2o[c]	L_RS06415	BZO99_RS09935	0	1000	0	Amino Acid Metabolism: Valine, Leucine and Isoleucine Metabolism	4.2.1.9	R04441	rxn15467	META:DIHYDROXYISOVALDEHYDRAT-RXN
DHAD2	Dihydroxy-acid dehydratase (2,3-dihydroxy-3-methylpentanoate)	23dhmp[c] -> 3mop[c] + h2o[c]	L_RS06415	BZO99_RS09935	0	1000	0	Amino Acid Metabolism: Valine, Leucine and Isoleucine Metabolism	4.2.1.9	R05070	rxn03437	META:DIHYDROXYMETVALDEHYDRAT-RXN
ILETA	Isoleucine transaminase	akg[c] + ile__L[c] -> 3mop[c] + glu__L[c]	L_RS06750	BZO99_RS07970	0	1000	0	Amino Acid Metabolism: Valine, Leucine and Isoleucine Metabolism	2.6.1.42	R02199	rxn01575	META:BRANCHED-CHAINAMINOTRANSFERILEU-RXN
IPPMIa	3-isopropylmalate dehydratase	3c2hmp[c] <=> 2ippm[c] + h2o[c]	L_RS06405 and L_RS06400	BZO99_RS09925 and BZO99_RS09920	-1000	1000	0	Amino Acid Metabolism: Valine, Leucine and Isoleucine Metabolism	4.2.1.33	R04001	rxn02811	META:RXN-8991
IPPMIb	2-isopropylmalate hydratase	2ippm[c] + h2o[c] <=> 3c3hmp[c]	L_RS06405 and L_RS06400	BZO99_RS09925 and BZO99_RS09920	-1000	1000	0	Amino Acid Metabolism: Valine, Leucine and Isoleucine Metabolism	4.2.1.33	R03968	rxn02789	META:3-ISOPROPYLMALISOM-RXN
KARA1	Ketol-acid reductoisomerase (2,3-dihydroxy-3-methylbutanoate)	23dhmb[c] + nadp[c] <=> alac__S[c] + h[c] + nadph[c]	L_RS06430	BZO99_RS09950	-1000	1000	0	Amino Acid Metabolism: Valine, Leucine and Isoleucine Metabolism	1.1.1.383; 1.1.1.86	R04439	rxn15466	META:ACETOLACTREDUCTOISOM-RXN
KARA2	Ketol-acid reductoisomerase (2-Acetolactate)	2ahbut[c] + h[c] + nadph[c] <=> 23dhmp[c] + nadp[c]	L_RS06430	BZO99_RS09950	-1000	1000	0	Amino Acid Metabolism: Valine, Leucine and Isoleucine Metabolism	1.1.1.86		rxn08764	META:ACETOOHBUTREDUCTOISOM-RXN
LEUTA	Leucine transaminase	akg[c] + leu__L[c] -> 4mop[c] + glu__L[c]	L_RS06750	BZO99_RS07970	0	1000	0	Amino Acid Metabolism: Valine, Leucine and Isoleucine Metabolism	2.6.1.42; 2.6.1.6; 2.6.1.67	R01090	rxn00806	META:BRANCHED-CHAINAMINOTRANSFERLEU-RXN
OIVD1r	2-oxoisovalerate dehydrogenase (acylating; 4-methyl-2-oxopentaoate)	coa[c] + 4mop[c] + nad[c] -> co2[c] + ivcoa[c] + nadh[c]	L_RS00370 and L_RS00375 and L_RS00365 and L_RS00360	BZO99_RS08755 and BZO99_RS08760 and BZO99_RS08750 and BZO99_RS08745	0	1000	0	Amino Acid Metabolism: Valine, Leucine and Isoleucine Metabolism	1.2.1.25; 1.2.1	R01651	rxn01207	META:2KETO-4METHYL-PENTANOATE-DEHYDROG-RXN
OIVD2	2-oxoisovalerate dehydrogenase (acylating; 3-methyl-2-oxobutanoate)	coa[c] + 3mob[c] + nad[c] -> co2[c] + nadh[c] + ibcoa[c]	L_RS00370 and L_RS00375 and L_RS00365 and L_RS00360	BZO99_RS08755 and BZO99_RS08760 and BZO99_RS08750 and BZO99_RS08745	0	1000	0	Amino Acid Metabolism: Valine, Leucine and Isoleucine Metabolism	1.2.1.25	R01210	rxn00899	META:1.2.1.25-RXN
OIVD3	2-oxoisovalerate dehydrogenase (acylating; 3-methyl-2-oxopentanoate)	coa[c] + 3mop[c] + nad[c] -> 2mbcoa[c] + co2[c] + nadh[c]	L_RS00370 and L_RS00375 and L_RS00365 and L_RS00360	BZO99_RS08755 and BZO99_RS08760 and BZO99_RS08750 and BZO99_RS08745	0	1000	0	Amino Acid Metabolism: Valine, Leucine and Isoleucine Metabolism	1.2.1.25; 1.2.1		rxn02269	META:2KETO-3METHYLVALERATE-RXN
OMCDC	2-Oxo-4-methyl-3-carboxypentanoate decarboxylation	3c4mop[c] + h[c] -> 4mop[c] + co2[c]	s0001	s0001	0	1000	0	Amino Acid Metabolism: Valine, Leucine and Isoleucine Metabolism	Non-enzymatic	R01652	rxn01208	META:RXN-7800
VALTA	Valine transaminase	akg[c] + val__L[c] -> 3mob[c] + glu__L[c]	L_RS06750	BZO99_RS07970	0	1000	0	Amino Acid Metabolism: Valine, Leucine and Isoleucine Metabolism	2.6.1.42; 2.6.1.6	R01214	rxn00903	META:BRANCHED-CHAINAMINOTRANSFERVAL-RXN
AB6PGH	Arbutin 6-phosphate glucohydrolase	arbt6p[c] + h2o[c] -> g6p[c] + hqn[c]	L_RS02175 or L_RS08720	BZO99_RS04590 or BZO99_RS09685	0	1000	0	Carbohydrate Metabolism: Alternative Carbon Metabolism	3.2.1.86	R05133	rxn08025	META:RXN0-5295
ACTD2	Acetoin dehydrogenase (Coenzyme A)	actn__R[c] + coa[c] + nad[c] -> acald[c] + accoa[c] + h[c] + nadh[c]	L_RS00375 and L_RS00370 and L_RS00365 and L_RS00360	BZO99_RS08760 and BZO99_RS08755 and BZO99_RS08750 and BZO99_RS08745	0	1000	0	Carbohydrate Metabolism: Alternative Carbon Metabolism	2.3.1.190	R09524	rxn16365	META:RXN-9718
BGLA1	6-phospho-beta-glucosidase	6pgg[c] + h2o[c] -> g6p[c] + glc__D[c]	L_RS02175 or L_RS04330 or	BZO99_RS04590 or BZO99_RS07235 or	0	1000	0	Carbohydrate Metabolism: Alternative Carbon Metabolism	3.2.1.86	R00839	rxn00608	META:6-PHOSPHO-BETA-

			L_RS08720	BZO99_RS09685								GLUCOSIDASE-RXN
GUI1	Glucuronate isomerase (D-glucuronate)	glcur[c] <=> fruur[c]	L_RS08485	BZO99_RS01840	-1000	1000	0	Carbohydrate Metabolism: Alternative Carbon Metabolism	5.3.1.12	R01482	rxn01080	META:GLUCUROISOM-RXN
MANAO	Mannonate oxidoreductase	mana[c] + nad[c] <=> fruur[c] + h[c] + nadh[c]	L_RS08510	BZO99_RS01860	-1000	1000	0	Carbohydrate Metabolism: Alternative Carbon Metabolism	1.1.1.57	R02454	rxn01775	META:MANNONOXIDOREDUCT-RXN
MNNH	D-mannonate hydrolyase	mana[c] -> 2ddglcn[c] + h2o[c]	L_RS08500	BZO99_RS01855	0	1000	0	Carbohydrate Metabolism: Alternative Carbon Metabolism	4.2.1.8	R05606	rxn03885	META:MANNONDEHYDRAT-RXN
PGMT	Phosphoglucomutase	g1p[c] <=> g6p[c]	L_RS02245	BZO99_RS04520	-1000	1000	0	Carbohydrate Metabolism: Alternative Carbon Metabolism	5.4.2.2; 5.4.2.5; 5.4.2.8	R08639	rxn00704	META:PHOSPHOGLUCMUT-RXN; META:RXN-16999
R5PP	Ribose 5-phosphate phosphatase	r5p[c] + h2o[c] -> rib__D[c] + pi[c]	L_RS00420 or L_RS05995 or L_RS05660	BZO99_RS08805 or BZO99_RS01130 or BZO99_RS00790	0	1000	0	Carbohydrate Metabolism: Alternative Carbon Metabolism	3.1.3.23			
XYLI1	Xylose isomerase	xyl__D[c] <=> xylu__D[c]	L_RS07875	BZO99_RS05835	-1000	1000	0	Carbohydrate Metabolism: Alternative Carbon Metabolism	5.3.1.5	R01432	rxn01044	META:XYLISOM-RXN
XYLK	Xylulokinase	atp[c] + xylu__D[c] -> adp[c] + h[c] + xu5p__D[c]	L_RS07870	BZO99_RS05830	0	1000	0	Carbohydrate Metabolism: Alternative Carbon Metabolism	2.7.1.17	R01639	rxn01199	META:XYLULOKIN-RXN
ACM6PH	N-acetylmuramate 6-phosphate hydrolase	acmum6p[c] + h2o[c] -> acgam6p[c] + lac__D[c]	L_RS05930	BZO99_RS01065	0	1000	0	Carbohydrate Metabolism: Aminosugars Metabolism	4.2.1.126	R08555	rxn08044	RXN0-4641
AGDC	N-acetylglucosamine-6-phosphate deacetylase	acgam6p[c] + h2o[c] -> ac[c] + gam6p[c]	L_RS06990	BZO99_RS08285	0	1000	0	Carbohydrate Metabolism: Aminosugars Metabolism	3.5.1.25	R02059	rxn01484	META:NAG6PDEACET-RXN
AMANAPEr	N-acetylmannosamine 6-phosphate epimerase	acmanap[c] -> acgam6p[c]	L_RS06155	BZO99_RS01295	0	1000	0	Carbohydrate Metabolism: Aminosugars Metabolism	5.1.3.9	R02087	rxn01506	META:NANE-RXN
AMANK	N-acetyl-D-mannosamine kinase	acmana[c] + atp[c] -> acmanap[c] + adp[c] + h[c]	L_RS07775 or L_RS03315	BZO99_RS05735 or BZO99_RS05970	0	1000	0	Carbohydrate Metabolism: Aminosugars Metabolism	2.7.1.60	R02705	rxn01951	META:NANK-RXN
G1PACT	Glucosamine-1-phosphate N-acetyltransferase	accoa[c] + gam1p[c] -> coa[c] + acgam1p[c] + h[c]	L_RS09805	BZO99_RS03200	0	1000	0	Carbohydrate Metabolism: Aminosugars Metabolism	2.3.1.157; 2.3.1.4	R05332	rxn03638	META:2.3.1.157-RXN
G6PDA	Glucosamine-6-phosphate deaminase	gam6p[c] + h2o[c] -> f6p[c] + nh4[c]	L_RS08215	BZO99_RS01565	0	1000	0	Carbohydrate Metabolism: Aminosugars Metabolism	3.5.99.6	R00765	rxn00552	META:GLUCOSAMINE-6-P-DEAMIN-RXN
PGAMT	Phosphoglucosamine mutase	gam1p[c] <=> gam6p[c]	L_RS02220	BZO99_RS04545	-1000	1000	0	Carbohydrate Metabolism: Aminosugars Metabolism	5.4.2.10	R02060	rxn01485	META:5.4.2.10-RXN
UAG2EMA	UDP-N-acetyl-D-glucosamine 2-epimerase (Hydrolysis)	h2o[c] + uacgam[c] <=> acmana[c] + h[c] + udp[c]	L_RS06640	BZO99_RS08080	-1000	1000	0	Carbohydrate Metabolism: Aminosugars Metabolism	5.1.3.14	R00414	rxn00292	
UAG4Ei	UDP-N-acetylglucosamine 4-epimerase	uacgam[c] -> udpacgal[c]	L_RS10400 or L_RS01135	BZO99_RS07485 or BZO99_RS02835	0	1000	0	Carbohydrate Metabolism: Aminosugars Metabolism	5.1.3.2	R00418	rxn00295	META:UDP-N-ACETYLGLUCOSAMINE-4-EPIMERASE-RXN
UAGCVT	UDP-N-acetylglucosamine 1-carboxyvinyltransferase	pep[c] + uacgam[c] -> pi[c] + uaccg[c]	L_RS02880 or L_RS01655	BZO99_RS04150 or BZO99_RS02315	0	1000	0	Carbohydrate Metabolism: Aminosugars Metabolism	2.5.1.7	R00660	rxn00461	META:UDPNACETYLGLUCOSAMENOLPYRTRANS-RXN
UAGDP	UDP-N-acetylglucosamine diphosphorylase	acgam1p[c] + h[c] + utp[c] -> ppi[c] + uacgam[c]	L_RS09805	BZO99_RS03200	0	1000	0	Carbohydrate Metabolism: Aminosugars Metabolism	2.7.7.23	R00416	rxn00293	META:2.7.7.64-RXN; META:NAG1P-URIDYLTRANS-RXN
UAPGR	UDP-N-acetylenolpyruvoylglucosamine reductase	h[c] + nadph[c] + uaccg[c] -> nadp[c] + uamr[c]	L_RS06090	BZO99_RS01230	0	1000	0	Carbohydrate Metabolism: Aminosugars Metabolism	1.3.1.98	R03192	rxn02285	META:UDPNACETYLMURAMATEDEHYDROG-RXN
UDPACGLP	UDP N acetylglucosamine	acgam1p[c] + h[c] + utp[c] <=> ppi[c] +	L_RS09805	BZO99_RS03200	-1000	1000	0	Carbohydrate Metabolism: Aminosugars Metabolism	2.7.7.23; 2.7.7.64		rxn09486	META:2.7.7.64-RXN

	diphosphorylase (galactosamine)	udpacgal[c]									
BG_CELLB	Beta glucosidase cellobiose	cellb[e] + h2o[e] -> 2 glc__D[e]	L_RS00965	BZO99_RS03005	0	1000	0	Carbohydrate Metabolism: Complex Sugar Metabolism	3.2.1.21	R00306; R06104	rxn00222; rxn15033	META:RXN-10773
GALUi	UTP-glucose-1-phosphate uridylyltransferase (irreversible)	g1p[c] + h[c] + utp[c] <=> ppi[c] + udpg[c]	L_RS07010	BZO99_RS08265	-1000	1000	0	Carbohydrate Metabolism: Complex Sugar Metabolism	2.7.7.9; 2.7.7.64	R00289	rxn00213	META:GLUC1PURIDYLTRANS-RXN
GLCS1	Glycogen synthase (ADPGlc)	adpglc[c] -> adp[c] + glycogen[c] + h[c]	L_RS03730	BZO99_RS10555	0	1000	0	Carbohydrate Metabolism: Complex Sugar Metabolism	2.4.1.21	R02421; R06049	rxn13643	META:GLYCOGENSYN-RXN
GLGC	Glucose-1-phosphate adenylyltransferase	atp[c] + g1p[c] + h[c] -> adpglc[c] + ppi[c]	L_RS03720 and L_RS03725	BZO99_RS10545 and BZO99_RS10550	0	1000	0	Carbohydrate Metabolism: Complex Sugar Metabolism	2.7.7.27	R00948	rxn00695	META:GLUC1PADENYLTRANS-RXN
MAL6PG	Maltose 6 phosphate glucosidase	h2o[c] + malt6p[c] -> g6p[c] + glc__D[c]	L_RS08750	BZO99_RS09655	0	1000	0	Carbohydrate Metabolism: Complex Sugar Metabolism	3.2.1.122	R00838; R06115	rxn00607	META:MALTOSE-6-PHOSPHATE-GLUCOSIDASE-RXN
MALT	Alpha glucosidase	malt[c] + h2o[c] -> 2 glc__D[c]	L_RS08770 or L_RS08755	BZO99_RS09635 or BZO99_RS09650	0	1000	0	Carbohydrate Metabolism: Complex Sugar Metabolism	3.2.1.20	R00028	rxn00022	META:RXN-15910
MALTATr	Maltose O-acetyltransferase	accoa[c] + malt[c] -> coa[c] + acmalt[c]	L_RS06745 or L_RS08765	BZO99_RS07975 or BZO99_RS09640	0	1000	0	Carbohydrate Metabolism: Complex Sugar Metabolism	2.3.1.79	R01556; R06251	rxn01133	META:MALTACETYLTRAN-RXN
MLTG1	Maltodextrin glucosidase (maltotriose)	h2o[c] + malttr[c] -> malt[c] + glc__D[c]	L_RS03740	BZO99_RS10565	0	1000	0	Carbohydrate Metabolism: Complex Sugar Metabolism	3.2.1.20			
MLTG2	Maltodextrin glucosidase (maltotetraose)	maltttr[c] + h2o[c] -> glc__D[c] + malttr[c]	L_RS03740	BZO99_RS10565	0	1000	0	Carbohydrate Metabolism: Complex Sugar Metabolism				
MLTG3	Maltodextrin glucosidase (maltopentaose)	maltpt[c] + h2o[c] -> glc__D[c] + maltttr[c]	L_RS03740	BZO99_RS10565	0	1000	0	Carbohydrate Metabolism: Complex Sugar Metabolism	3.2.1.20; 3.2.1.74			
MLTG4	Maltodextrin glucosidase (maltohexaose)	malthx[c] + h2o[c] -> glc__D[c] + maltpt[c]	L_RS03740	BZO99_RS10565	0	1000	0	Carbohydrate Metabolism: Complex Sugar Metabolism	3.2.1.20			
MLTG5	Maltodextrin glucosidase (maltoheptaose)	h2o[c] + malthp[c] -> glc__D[c] + malthx[c]	L_RS03740	BZO99_RS10565	0	1000	0	Carbohydrate Metabolism: Complex Sugar Metabolism	3.2.1.20			
MLTP0_1	Maltodextrin phosphorylase (maltose)	malt[c] + pi[c] -> g1p[c] + glc__D[c]	L_RS03735	BZO99_RS10560	0	1000	0	Carbohydrate Metabolism: Complex Sugar Metabolism	2.4.1.1			
MLTP0_2	Maltodextrin phosphorylase (maltotriose)	malttr[c] + pi[c] -> g1p[c] + malt[c]	L_RS03735	BZO99_RS10560	0	1000	0	Carbohydrate Metabolism: Complex Sugar Metabolism	2.4.1.1			
MLTP0_3	Maltodextrin phosphorylase (maltotetraose)	maltttr[c] + pi[c] -> g1p[c] + malttr[c]	L_RS03735	BZO99_RS10560	0	1000	0	Carbohydrate Metabolism: Complex Sugar Metabolism	2.4.1.1			
MLTP1	Maltodextrin phosphorylase (maltopentaose)	maltpt[c] + pi[c] <=> g1p[c] + maltttr[c]	L_RS03735	BZO99_RS10560	-1000	1000	0	Carbohydrate Metabolism: Complex Sugar Metabolism	2.4.1.1		rxn08941	META:RXN-14284
MLTP2	Maltodextrin phosphorylase (maltohexaose)	malthx[c] + pi[c] <=> g1p[c] + maltpt[c]	L_RS03735	BZO99_RS10560	-1000	1000	0	Carbohydrate Metabolism: Complex Sugar Metabolism	2.4.1.1		rxn08942	META:RXN-14285
MLTP3	Maltodextrin phosphorylase (maltoheptaose)	malthp[c] + pi[c] <=> g1p[c] + malthx[c]	L_RS03735	BZO99_RS10560	-1000	1000	0	Carbohydrate Metabolism: Complex Sugar Metabolism	2.4.1.1		rxn08943	META:RXN-14286
MPL	Maltose phosphorylase	pi[c] + malt[c] <=> g1p_B[c] + glc__D[c]	L_RS08750 or L_RS02240	BZO99_RS09655 or BZO99_RS04525	-1000	1000	0	Carbohydrate Metabolism: Complex Sugar Metabolism	2.4.1.8	R01555; R06040	rxn01132	META:MALTOSE-PHOSPHORYLASE-RXN
T6PGD	Trehalose-6-phosphate glycosidase	pi[c] + tre6p[c] <=> g1p_B[c] + g6p[c]	L_RS02240	BZO99_RS04525	-1000	1000	0	Carbohydrate Metabolism: Complex Sugar Metabolism	2.4.1.216	R05767; R06044	rxn15551	META:2.4.1.216-RXN
TRE6PH	Trehalose-6-phosphate hydrolase	h2o[c] + tre6p[c] -> g6p[c] + glc__D[c]	L_RS08770 or L_RS07795	BZO99_RS09635 or BZO99_RS05755	0	1000	0	Carbohydrate Metabolism: Complex Sugar Metabolism	3.2.1.93; 3.2.1.122	R06113; R00837	rxn00606	META:TRE6PHYDRO-RXN
ALLULEP	Allulose 6 phosphate epimerase	allul6p[c] <=> f6p[c]			-1000	1000	0	Carbohydrate Metabolism: Fructose and Mannose Metabolism	5.1.3.-			
F1PP	D-fructose 1-phosphate	f1p[c] + h2o[c] -> fru[c] + pi[c]	L_RS00420 or L_RS05660	BZO99_RS08805 or BZO99_RS00790	0	1000	0	Carbohydrate Metabolism: Fructose and Mannose Metabolism				

	phosphatase											
F6PP	D-fructose 6-phosphate phosphatase	h2o[c] + f6p[c] -> fru[c] + pi[c]	L_RS00420 or L_RS05660	BZO99_RS08805 or BZO99_RS00790	0	1000	0	Carbohydrate Metabolism: Fructose and Mannose Metabolism	3.1.3.23			
FBA2	D Fructose 1 phosphate D glyceraldehyde 3 phosphate lyase	f1p[c] <=> dhap[c] + glyald[c]	L_RS09945	BZO99_RS11540	-1000	1000	0	Carbohydrate Metabolism: Fructose and Mannose Metabolism	4.1.2.13	R02568	rxn01870	META:RXN-8631
FRUK	Fructose-1-phosphate kinase	atp[c] + f1p[c] -> adp[c] + fdp[c] + h[c]	L_RS05030	BZO99_RS00135	0	1000	0	Carbohydrate Metabolism: Fructose and Mannose Metabolism	2.7.1.56	R02071	rxn01492	META:1PFRUCTPHOSN-RXN
HEX7	Hexokinase (D-fructose:ATP)	atp[c] + fru[c] -> adp[c] + f6p[c] + h[c]	L_RS07770	BZO99_RS05730	0	1000	0	Carbohydrate Metabolism: Fructose and Mannose Metabolism	2.7.1.1; 2.7.1.4	R00867	rxn15081	META:HEXOKINASE-RXN
M1PD	Mannitol-1-phosphate 5-dehydrogenase	mnl1p[c] + nad[c] <=> f6p[c] + h[c] + nadh[c]	L_RS00170	BZO99_RS09035	-1000	1000	0	Carbohydrate Metabolism: Fructose and Mannose Metabolism	1.1.1.17	R02703	rxn15354	META:MANNPDEHYDROG-RXN
MAN6PI	Mannose-6-phosphate isomerase	man6p[c] <=> f6p[c]	L_RS04085	BZO99_RS06980	-1000	1000	0	Carbohydrate Metabolism: Fructose and Mannose Metabolism	5.3.1.8	R01819	rxn15270	META:MANNPISOM-RXN
SBTPD	Sorbitol-6-phosphate dehydrogenase	nad[c] + sbt6p[c] <=> h[c] + f6p[c] + nadh[c]	L_RS04715	BZO99_RS04995	-1000	1000	0	Carbohydrate Metabolism: Fructose and Mannose Metabolism	1.1.1.140	R05607		
TRIOK	Triokinase	atp[c] + glyald[c] -> adp[c] + g3p[c] + h[c]	L_RS01305	BZO99_RS02660	0	1000	0	Carbohydrate Metabolism: Fructose and Mannose Metabolism	2.7.1.28	R01059	rxn00780	META:TRIOKINASE-RXN
XYLI2	Xylose isomerase (D-glucose)	glc__D[c] <=> fru[c]	L_RS07875	BZO99_RS05835	-1000	1000	0	Carbohydrate Metabolism: Fructose and Mannose Metabolism	5.3.1.5	R00307	rxn00223	META:GLUCISOM-RXN
GALK2	Galactokinase	atp[c] + a_gal__D[c] <=> adp[c] + gal1p[c] + h[c]	L_RS10420	BZO99_RS07510	-1000	1000	0	Carbohydrate Metabolism: Galactose Metabolism	2.7.1.6	R01092	rxn00808; rxn15121	META:GALACTOKIN-RXN
GALM	Aldose 1 epimerase	gal[c] <=> a_gal__D[c]	L_RS07865 or L_RS10425 or L_RS08490	BZO99_RS05825 or BZO99_RS07515 or BZO99_RS01845	-1000	1000	0	Carbohydrate Metabolism: Galactose Metabolism	5.1.3.3	R10619	rxn08582	META:ALDOSE1EPIM-RXN
GALT	Galactose 1 phosphate uridylyltransferase	gal1p[c] + h[c] + utp[c] <=> ppi[c] + udpgal[c]	L_RS10415	BZO99_RS07505	-1000	1000	0	Carbohydrate Metabolism: Galactose Metabolism	2.7.7.10; 2.7.7.64	R00502	rxn00355	META:UTPHEXPURIDYLYLTRANS-RXN
LACZ	B-galactosidase	lcts[c] + h2o[c] -> gal[c] + glc__D[c]	L_RS10405	BZO99_RS07490	0	1000	0	Carbohydrate Metabolism: Galactose Metabolism	3.2.1.108; 3.2.1.23	R01100; R06114	rxn00816; rxn11244	META:BETAGALACTOSID-RXN; META:3.2.1.23-RXN
PFK_2	Phosphofructokinase (D-tagatose 6-phosphate)	atp[c] + tag6p__D[c] -> adp[c] + h[c] + tagdp__D[c]	L_RS05030 or L_RS06985	BZO99_RS00135 or BZO99_RS08295	0	1000	0	Carbohydrate Metabolism: Galactose Metabolism	2.7.1.11; 2.7.1.144; 2.7.1.56	R03236	rxn02314	META:TAGAKIN-RXN
UDPG4E	UDPglucose 4-epimerase	udpg[c] <=> udpgal[c]	L_RS10400 or L_RS01135	BZO99_RS07485 or BZO99_RS02835	-1000	1000	0	Carbohydrate Metabolism: Galactose Metabolism	5.1.3.2	R00291	rxn00214	META:UDPGLUCEPIM-RXN
UGLT	UDPglucose--hexose-1-phosphate uridylyltransferase	gal1p[c] + udpg[c] -> g1p[c] + udpgal[c]	L_RS10415	BZO99_RS07505	0	1000	0	Carbohydrate Metabolism: Galactose Metabolism	2.7.7.12	R00955	rxn00701	META:GALACTURIDYLYLTRANS-RXN
INS2D	Inositol 2-dehydrogenase	inost[c] + nad[c] -> h[c] + nadh[c] + 2ins[c]	L_RS08110	BZO99_RS01455	0	1000	0	Carbohydrate Metabolism: Inositol Phosphate Metabolism	1.1.1.18	R01183	rxn00879	META:MYO-INOSITOL-2-DEHYDROGENASE-RXN
INSCR	Inositol catabolic reactions lumped	atp[c] + 2ins[c] -> adp[c] + dhap[c] + 2.0 h[c] + msa[c]	L_RS09945	BZO99_RS11540	0	1000	0	Carbohydrate Metabolism: Inositol Phosphate Metabolism			rxn05743	
MI1PP	Myo-inositol 1-phosphatase	h2o[c] + mi1p__D[c] -> inost[c] + pi[c]	L_RS02875	BZO99_RS04155	0	1000	0	Carbohydrate Metabolism: Inositol Phosphate Metabolism	3.1.3.25	R01185	rxn00881	META:RXN0-5408
MI1PS	Myo Inositol 1 phosphate synthase	g6p[c] -> mi1p__D[c]			0	1000	0	Carbohydrate Metabolism: Inositol Phosphate Metabolism	5.5.1.4		rxn00609	
DAGGT_LLA	1 2 diacylglycerol 3 glucosyltransferase Lactis specific	0.01 12dgr_LLA[c] + 2 udpg[c] -> 0.01 d12dg_LLA[c] + 2 h[c] + 2 udp[c]	L_RS11195 and L_RS11200	BZO99_RS11325 and BZO99_RS11330	0	1000	0	Cell Envelope Biosynthesis: Lipoteichoic Acid	2.4.1.337; 2.4.1.208	R10850	rxn17534; rxn41394	META:2.4.1.157-RXN
DALTAL_LLA	D Alanine lipoteichoic acid ligase	6 ala__D[c] + 6 atp[c] + 0.01 LTA_LLA[c] -> 6 adp[c] + 0.01 LTAala_LLA[c] + 6 pi[c]	L_RS06610 and L_RS06605 and L_RS06600 and L_RS06595	BZO99_RS08110 and BZO99_RS08115 and BZO99_RS08120 and BZO99_RS08125	0	1000	0	Cell Envelope Biosynthesis: Lipoteichoic Acid				

GALTAL	Galactose lipoteichoic acid ligase	0.01 LTAala_LLA[c] + 9.8 udpgal[c] -> 0.01 LTAAlaGal_LLA[c] + 9.8 h[c] + 9.8 udp[c]	L_RS06595 and L_RS06600 and L_RS06605 and L_RS06610	BZO99_RS08125 and BZO99_RS08120 and BZO99_RS08115 and BZO99_RS08110	0	1000	0	Cell Envelope Biosynthesis: Lipoteichoic Acid	6.3.2.16			
LTAS_LLA	Lipoteichoic acid synthase LPL specific	0.01 d12dg_LLA[c] + 0.16 pg_LLA[c] -> 0.16 12dgr_LLA[c] + 0.01 LTA_LLA[c]	L_RS04260	BZO99_RS07165	0	1000	0	Cell Envelope Biosynthesis: Lipoteichoic Acid	2.7.8.20			
ALAALAr	D-alanine-D-alanine ligase (reversible)	2 ala__D[c] + atp[c] <=> adp[c] + alaala[c] + pi[c] + h[c]	L_RS01805	BZO99_RS02165	-1000	1000	0	Cell Envelope Biosynthesis: Peptidoglycan Biosynthesis	6.3.2.4	R01150	rxn00851; rxn13802	META:DALADALALIG-RXN
GLUR	Glutamate racemase	glu__D[c] <=> glu__L[c]	L_RS06720	BZO99_RS08000	-1000	1000	0	Cell Envelope Biosynthesis: Peptidoglycan Biosynthesis	5.1.1.3	R00260	rxn00193	META:GLUTRACE-RXN
PAPPT1	Phospho N acetylmuramoyl pentapeptide transferase alpha glutamate	uAgla[c] + udcpp[c] -> uaAgla[c] + ump[c]	L_RS04570	BZO99_RS05130	0	1000	0	Cell Envelope Biosynthesis: Peptidoglycan Biosynthesis	2.7.8.13	R05629	rxn03902; rxn03903; rxn39510	META:PHOSNACMURPENTATRANS-RXN; META:RXN-11347; META:RXN-8975
PGGT2	Peptidoglycan glycosyltransferase	uaaAgla[c] -> PG[c] + udcpdp[c]	(L_RS11055 and L_RS04565) or (L_RS11055 and L_RS01795)	(BZO99_RS06760 and BZO99_RS05135) or (BZO99_RS06760 and BZO99_RS02175)	0	1000	0	Cell Envelope Biosynthesis: Peptidoglycan Biosynthesis	2.4.1.129	R06178; R04519	rxn06718; rxn07070	META:RXN-15521
UAAGLS1_1	UDP N acetylmuramoyl L alanyl D glutamate lysine synthetase alpha glutamate	atp[c] + lys__L[c] + uamag[c] -> adp[c] + pi[c] + 2 h[c] + uAgl[c]	L_RS05810 or L_RS09410	BZO99_RS00945 or BZO99_RS03595	0	1000	0	Cell Envelope Biosynthesis: Peptidoglycan Biosynthesis	6.3.2.7	R02786	rxn02009; rxn11253	META:6.3.2.7-RXN
UAGPT1	UDP N acetylglucosamine N acetylmuramyl pentapeptide pyrophosphoryl undecaprenol N acetylglucosamine transferase	uaAgla[c] + uacgam[c] -> h[c] + uaaAgla[c] + udp[c]	L_RS08290	BZO99_RS01640	0	1000	0	Cell Envelope Biosynthesis: Peptidoglycan Biosynthesis	2.4.1.227	R05662; R05032	rxn03405; rxn03408; rxn03933; rxn25276	META:RXN-8976
UAMAGS	UDP-N-acetylmuramoyl-L-alanyl-D-glutamate synthetase	atp[c] + glu__D[c] + uama[c] -> adp[c] + pi[c] + h[c] + uamag[c]	L_RS08295	BZO99_RS01645	0	1000	0	Cell Envelope Biosynthesis: Peptidoglycan Biosynthesis	6.3.2.9	R02783	rxn02008; rxn11252	META:UDP-NACMURALA-GLU-LIG-RXN
UAMAS	UDP-N-acetylmuramoyl-L-alanine synthetase	ala__L[c] + atp[c] + uamr[c] -> adp[c] + pi[c] + h[c] + uama[c]	L_RS10720	BZO99_RS07730	0	1000	0	Cell Envelope Biosynthesis: Peptidoglycan Biosynthesis	6.3.2.8	R03193	rxn02286; rxn11251	META:UDP-NACMUR-ALA-LIG-RXN
UDCPDP	Undecaprenyl-diphosphatase	h2o[c] + udcpdp[c] -> pi[c] + h[c] + udcpp[c]	L_RS05260 or L_RS11505	BZO99_RS00375 or BZO99_RS09420	0	1000	0	Cell Envelope Biosynthesis: Peptidoglycan Biosynthesis	3.6.1.27	R05627	rxn03901	META:UNDECAPRENYL-DIPHOSPHATASE-RXN
UDCPKr	Undecaprenol kinase (reversible)	atp[c] + udcp[c] -> adp[c] + h[c] + udcpp[c]	L_RS11505	BZO99_RS09420	0	1000	0	Cell Envelope Biosynthesis: Peptidoglycan Biosynthesis	2.7.1.66	R05626	rxn03900; rxn39509	META:UNDECAPRENOL-KINASE-RXN
UGLDDS1	UDP N acetylmuramoyl L alanyl D glutamyl L lysyl D alanyl D alanine synthetase alpha glutamate	alaala[c] + atp[c] + uAgl[c] -> adp[c] + pi[c] + uAgla[c]	L_RS01810	BZO99_RS02160	0	1000	0	Cell Envelope Biosynthesis: Peptidoglycan Biosynthesis	6.3.2.10	R04573	rxn03140; rxn03141; rxn11254	META:6.3.2.10-RXN
CPSS_LLA	CPS synthase complex LLA specific	4.0 h2o[c] + 2.0 udpg[c] + udpgal[c] + dtdprmn[c] <=> dtdp[c] + 5.0 h[c] +			-1000	1000	0	Cell Envelope Biosynthesis: Surface Polysaccharides				

		2.0 udp[c] + ump[c] + CPS_LLA[c]									
BACCL	Biotin acetyl CoA carboxylase ligase	atp[c] + btn[c] + h[c] -> btamp[c] + ppi[c]	L_RS09915 or L_RS09280	BZO99_RS10595 or BZO99_RS03725	0	1000	0	Cofactor and Prosthetic Group Biosynthesis: Biotin Metabolism	6.3.4.15	R01074	rxn00792	META:RXN0-7192
ADCL	4-aminobenzoate synthase	4adcho[c] -> 4abz[c] + pyr[c] + h[c]	L_RS06880 and L_RS06875	BZO99_RS08395 and BZO99_RS08400	0	1000	0	Cofactor and Prosthetic Group Biosynthesis: Folate Metabolism	4.1.3.38	R05553	rxn03841	META:ADCLY-RXN
ADCS	4-amino-4-deoxychorismate synthase	chor[c] + gln__L[c] -> 4adcho[c] + glu__L[c]	(L_RS06880 or L_RS07675) and L_RS06875	(BZO99_RS08395 or BZO99_RS05635) and BZO99_RS08400	0	1000	0	Cofactor and Prosthetic Group Biosynthesis: Folate Metabolism	2.6.1.85	R01716	rxn01257	META:PABASYN-RXN
DHFS	Dihydrofolate synthase	dhpt[c] + atp[c] + glu__L[c] -> adp[c] + dhf[c] + pi[c] + h[c]	L_RS06065	BZO99_RS01205	0	1000	0	Cofactor and Prosthetic Group Biosynthesis: Folate Metabolism	6.3.2.12; 6.3.2.17	R02237	rxn01603	META:DIHYDROFOLATESYNTH-RXN
DHNPA2r	Dihydroneopterin aldolase reversible	dhnpt[c] -> 6hmhpt[c] + gcald[c]	L_RS06045	BZO99_RS01185	0	1000	0	Cofactor and Prosthetic Group Biosynthesis: Folate Metabolism	4.1.2.25	R03504	rxn02504	META:H2NEOPTERINALDOL-RXN
DHPS2	Dihydropteroate synthase	4abz[c] + 6hmhptpp[c] -> dhpt[c] + ppi[c]	L_RS06055	BZO99_RS01195	0	1000	0	Cofactor and Prosthetic Group Biosynthesis: Folate Metabolism	2.5.1.15	R03067	rxn12954	META:H2PTEROATESYNTH-RXN
DNMPPA	Dihydroneopterin monophosphate dephosphorylase	h2o[c] + dhpmp[c] -> pi[c] + dhnpt[c]	L_RS03030 or L_RS09425	BZO99_RS06255 or BZO99_RS03580	0	1000	0	Cofactor and Prosthetic Group Biosynthesis: Folate Metabolism	3.6.1; 3.6.1.-	R04621	rxn03168	META:DIHYDRONEOPTERIN-MONO-P-DEPHOS-RXN
DNTPPA	Dihydroneopterin triphosphate pyrophosphatase	h2o[c] + ahdt[c] -> h[c] + ppi[c] + dhpmp[c]	L_RS03030 or L_RS09425	BZO99_RS06255 or BZO99_RS03580	0	1000	0	Cofactor and Prosthetic Group Biosynthesis: Folate Metabolism	3.6.1.67	R04638	rxn03173	META:H2NEOPTERINP3PYROPHOSPHOHYDRO-RXN
FTHFCL	5 formethyltetrahydrofolate cyclo ligase	5fthf[c] + atp[c] -> adp[c] + methf[c] + pi[c]	L_RS00925	BZO99_RS03045	0	1000	0	Cofactor and Prosthetic Group Biosynthesis: Folate Metabolism	6.3.3.2	R02301	rxn01653	META:5-FORMYL-THF-CYCLO-LIGASE-RXN
GLYCL	Glycine Cleavage System	gly[c] + nad[c] + thf[c] -> co2[c] + mlthf[c] + nadh[c] + nh4[c]	L_RS00360	BZO99_RS08745	0	1000	0	Cofactor and Prosthetic Group Biosynthesis: Folate Metabolism	1.4.4.2; 1.8.1.4; 2.1.2.10	R01221	rxn00908	META:GCVMULTI-RXN
GTPCI	GTP cyclohydrolase I	gtp[c] + h2o[c] -> ahdt[c] + for[c] + h[c]	L_RS06050	BZO99_RS01190	0	1000	0	Cofactor and Prosthetic Group Biosynthesis: Folate Metabolism	3.5.4.16	R00424	rxn00299; rxn11232	META:GTP-CYCLOHYDRO-I-RXN
HPPK2	6-hydroxymethyl-dihydropterin pyrophosphokinase	6hmhpt[c] + atp[c] -> 6hmhptpp[c] + amp[c] + h[c]	L_RS06050	BZO99_RS01190	0	1000	0	Cofactor and Prosthetic Group Biosynthesis: Folate Metabolism	2.7.6.3	R03503	rxn02503	META:H2PTERIDINEPYROPHOSPHOKIN-RXN
MTHFC	Methenyltetrahydrofolate cyclohydrolase	methf[c] + h2o[c] <=> 10fthf[c] + h[c]	L_RS04500	BZO99_RS05205	-1000	1000	0	Cofactor and Prosthetic Group Biosynthesis: Folate Metabolism	1.5.1.15; 3.5.4.9	R01655	rxn01211	META:METHENYLTHFCYCLOHYDRO-RXN
MTHFD	Methylenetetrahydrofolate dehydrogenase (NADP)	mlthf[c] + nadp[c] <=> methf[c] + nadph[c]	L_RS04500	BZO99_RS05205	-1000	1000	0	Cofactor and Prosthetic Group Biosynthesis: Folate Metabolism	1.5.1.5	R01220	rxn00907	META:METHYLENETHFDEHYDROG-NADP-RXN
MTHFR2	5,10-methylenetetrahydrofolate reductase (NADH)	2.0 h[c] + mlthf[c] + nadh[c] -> 5mthf[c] + nad[c]	L_RS06575	BZO99_RS08145	0	1000	0	Cofactor and Prosthetic Group Biosynthesis: Folate Metabolism	1.5.1.20	R07168	rxn04954	META:1.5.1.20-RXN
THFAT	Tetrahydrofolate aminomethyltransferase	h2o[c] + methf[c] -> h[c] + 5fthf[c]	L_RS03235	BZO99_RS06050	0	1000	0	Cofactor and Prosthetic Group Biosynthesis: Folate Metabolism	2.1.2.10	R02300	rxn01652	
DHFR	Dihydrofolate reductase	dhf[c] + h[c] + nadph[c] <=> nadp[c] + thf[c]	L_RS10300 or L_RS06030	BZO99_RS07385 or BZO99_RS01165	-1000	1000	0	Cofactor and Prosthetic Group Biosynthesis: Folate Salvage Pathway	1.5.1.3	R00939	rxn00686	META:DIHYDROFOLATEREDUCT-RXN; META:RXN-19329
FOLR2	Folate reductase	fol[c] + nadph[c] <=> dhf[c] + nadp[c]	L_RS10300 or L_RS06030	BZO99_RS07385 or BZO99_RS01165	-1000	1000	0	Cofactor and Prosthetic Group Biosynthesis: Folate Salvage Pathway	1.5.1.3	R02236	rxn01602	META:RXN-18357
FTHFLi	Formate-tetrahydrofolate ligase	atp[c] + for[c] + thf[c] -> 10fthf[c] + adp[c] + pi[c]	L_RS04910	BZO99_RS00015	0	1000	0	Cofactor and Prosthetic Group Biosynthesis: Folate Salvage Pathway	6.3.4.3	R00943	rxn00690	META:FORMATETHFLIG-RXN
GHMT2r	Glycine hydroxymethyltransferase, reversible	ser__L[c] + thf[c] <=> gly[c] + h2o[c] + mlthf[c]	L_RS03235	BZO99_RS06050	-1000	1000	0	Cofactor and Prosthetic Group Biosynthesis: Folate Salvage Pathway	2.1.2.1	R00945	rxn00692	META:GLYOHMETRANS-RXN
THFGLUS	TetrahydrofolateL glutamate gamma ligase ADP forming	atp[c] + glu__L[c] + thf[c] <=> adp[c] + pi[c] + h[c] +	L_RS06065	BZO99_RS01205	-1000	1000	0	Cofactor and Prosthetic Group Biosynthesis: Folate Salvage Pathway	6.3.2.17	R00942	rxn00689	META:FOLYLPOLYGLUTAMATESYNTH-RXN

		thfglu[c]										
THFOR1	5,6,7,8-Tetrahydrofolate:NAD+ oxidoreductase	fol[c] + h[c] + 2 nadh[c] -> 2 nad[c] + thf[c]	L_RS10300 or L_RS06030	BZO99_RS07385 or BZO99_RS01165	0	1000	0	Cofactor and Prosthetic Group Biosynthesis: Folate Salvage Pathway	1.5.1.3	R00937	rxn14120	
GTHOr	Glutathione oxidoreductase	gthox[c] + h[c] + nadph[c] <=> 2 gthrd[c] + nadp[c]	L_RS04460	BZO99_RS05250	-1000	1000	0	Cofactor and Prosthetic Group Biosynthesis: Glutathione Metabolism	1.8.1.7	R00115	rxn00086	META:GLUTATHIONE-REDUCT-NADPH-RXN
GTHPi	Glutathione peridoxase	2 gthrd[c] + h2o2[c] -> gthox[c] + 2 h2o[c]	L_RS07130	BZO99_RS05370	0	1000	0	Cofactor and Prosthetic Group Biosynthesis: Glutathione Metabolism	1.11.1.9	R00274	rxn00205	META:GLUTATHIONE-PEROXIDASE-RXN
DMATT	Dimethylallyltranstransferase	dmpp[c] + ipdp[c] -> ppi[c] + grdp[c]	L_RS04520 or L_RS03360	BZO99_RS05185 or BZO99_RS05925	0	1000	0	Cofactor and Prosthetic Group Biosynthesis: Isoprenoid Biosynthesis	2.5.1.1	R01658	rxn01213	META:GPPSYN-RXN
DPMVD	Diphosphomevalonate decarboxylase	5dpmev[c] + atp[c] -> co2[c] + adp[c] + pi[c] + ipdp[c]	L_RS02115	BZO99_RS04655	0	1000	0	Cofactor and Prosthetic Group Biosynthesis: Isoprenoid Biosynthesis	4.1.1.33	R01121	rxn00829	META:DIPHOSPHOMEVALONTE-DECARBOXYLASE-RXN
GRTT	Geranyltranstransferase	ipdp[c] + grdp[c] -> frdp[c] + ppi[c]	L_RS04520	BZO99_RS05185	0	1000	0	Cofactor and Prosthetic Group Biosynthesis: Isoprenoid Biosynthesis	2.5.1.10	R02003	rxn01466	META:FPPSYN-RXN
HMGCOAR	Hydroxymethylglutaryl CoA reductase	coa[c] + mev__R[c] + 2 nadp[c] <=> 2 h[c] + hmgcoa[c] + 2 nadph[c]	L_RS08200	BZO99_RS01550	-1000	1000	0	Cofactor and Prosthetic Group Biosynthesis: Isoprenoid Biosynthesis	1.1.1.34	R02082	rxn01501	META:1.1.1.34-RXN
IPDDI	Isopentenyl-diphosphate D-isomerase	ipdp[c] <=> dmpp[c]	L_RS02125	BZO99_RS04645	-1000	1000	0	Cofactor and Prosthetic Group Biosynthesis: Isoprenoid Biosynthesis	5.3.3.2	R01123	rxn00830	META:IPPISOM-RXN
MEVK1	Mevalonate kinase (ATP)	atp[c] + mev__R[c] -> adp[c] + 5pmev[c] + h[c]	L_RS02110	BZO99_RS04660	0	1000	0	Cofactor and Prosthetic Group Biosynthesis: Isoprenoid Biosynthesis	2.7.1.36	R02245	rxn01607	META:MEVALONATE-KINASE-RXN
MEVK2	Mevalonate kinase (CTP)	ctp[c] + mev__R[c] -> h[c] + cdp[c] + 5pmev[c]	L_RS02110	BZO99_RS04660	0	1000	0	Cofactor and Prosthetic Group Biosynthesis: Isoprenoid Biosynthesis	2.7.1.36		rxn09616	
MEVK3	Mevalonate kinase (GTP)	gtp[c] + mev__R[c] -> h[c] + gdp[c] + 5pmev[c]	L_RS02110	BZO99_RS04660	0	1000	0	Cofactor and Prosthetic Group Biosynthesis: Isoprenoid Biosynthesis	2.7.1.36		rxn09615	
MEVK4	Mevalonate kinase (UTP)	utp[c] + mev__R[c] -> h[c] + udp[c] + 5pmev[c]	L_RS02110	BZO99_RS04660	0	1000	0	Cofactor and Prosthetic Group Biosynthesis: Isoprenoid Biosynthesis	2.7.1.36		rxn09614	
OCTDPS	Octaprenyl pyrophosphate synthase	frdp[c] + 5.0 ipdp[c] -> octdp[c] + 5.0 ppi[c]	L_RS00995 or L_RS07025 or L_RS04520	BZO99_RS02975 or BZO99_RS08250 or BZO99_RS05185	0	1000	0	Cofactor and Prosthetic Group Biosynthesis: Isoprenoid Biosynthesis	2.5.1.90	R09248	rxn09037	META:RXN-8992
PMEVK	Phosphomevalonate kinase	5pmev[c] + atp[c] -> adp[c] + 5dpmev[c]	L_RS02120	BZO99_RS04650	0	1000	0	Cofactor and Prosthetic Group Biosynthesis: Isoprenoid Biosynthesis	2.7.4.2	R03245	rxn02322	META:PHOSPHOMEVALONATE-KINASE-RXN
UDCPDPS	Undecaprenyl diphosphate synthase	frdp[c] + 8 ipdp[c] -> 8 ppi[c] + udcpdp[c]	L_RS07025 and L_RS11165	BZO99_RS08250 and BZO99_RS06410	0	1000	0	Cofactor and Prosthetic Group Biosynthesis: Isoprenoid Biosynthesis	2.5.1; 2.5.1.31; 2.5.1.M1	R06447	rxn04308	META:RXN-9138; META:RXN-8999
LIPAMPL	Lipoyl-adenylate protein ligase	lipoamp[c] -> lipopb[c] + amp[c]	L_RS00380	BZO99_RS08765	0	1000	0	Cofactor and Prosthetic Group Biosynthesis: Lipoic Acid Metabolism				
LIPATPT	Lipoate-ATP adenylate transferase	atp[c] + lipoate[c] -> ppi[c] + lipoamp[c]	L_RS00380	BZO99_RS08765	0	1000	0	Cofactor and Prosthetic Group Biosynthesis: Lipoic Acid Metabolism	6.3.1.20; 2.7.7.63	R07770	rxn07584	META:RXN-8654
AMMQLT8	S-adenosylmethione:2-demthylmenaquinole methyltransferase (menaquinone 8)	amet[c] + 2dmmql8[c] -> h[c] + ahcys[c] + mql8[c]	L_RS06180	BZO99_RS01320	0	1000	0	Cofactor and Prosthetic Group Biosynthesis: Menaquinone Biosynthesis	2.1.1.163			
AMMQT8_2	S-adenosylmethione:2-demethylmenaquinone methyltransferase	2dmmq8[c] + amet[c] -> h[c] + ahcys[c] + mqn8[c]	L_RS06180	BZO99_RS01320	0	1000	0	Cofactor and Prosthetic Group Biosynthesis: Menaquinone Biosynthesis			rxn10094	
DHNAOT	1,4-dihydroxy-2-naphthoate octaprenyltransferase	dhna[c] + octdp[c] -> h[c] + ppi[c] + co2[c] + 2dmmq8[c]	L_RS01000 or L_RS08675	BZO99_RS02970 or BZO99_RS09730	0	1000	0	Cofactor and Prosthetic Group Biosynthesis: Menaquinone Biosynthesis			rxn05267	
DHNCOAS	1,4-dihydroxy-2-napthoyl-CoA synthase	h[c] + sbzcoa[c] -> 14dhncoa[c] + h2o[c]	L_RS03885	BZO99_RS10825	0	1000	0	Cofactor and Prosthetic Group Biosynthesis: Menaquinone Biosynthesis	4.1.3.36	R07263	rxn05024	META:NAPHTHOATE-SYN-RXN

DHNCOAT	1,4-dihydroxy-2-napthoyl-CoA thioesterase	h2o[c] + 14dhncoa[c] -> h[c] + dhna[c] + coa[c]	L_RS03870	BZO99_RS10810	0	1000	0	Cofactor and Prosthetic Group Biosynthesis: Menaquinone Biosynthesis				
ICHORS	Isochorismate synthase	chor[c] <=> ichor[c]	L_RS03900	BZO99_RS10840	-1000	1000	0	Cofactor and Prosthetic Group Biosynthesis: Menaquinone Biosynthesis	5.4.4.2	R01717	rxn01258	META:ISOCHORSYN-RXN
NPHS	Naphthoate synthase	sbzcoa[c] -> coa[c] + dhna[c]	L_RS03885	BZO99_RS10825	0	1000	0	Cofactor and Prosthetic Group Biosynthesis: Menaquinone Biosynthesis	4.1.3.36	R04150	rxn02898	
SEPHCHCS	2-succinyl-5-enolpyruvyl-6-hydroxy-3-cyclohexene-1-carboxylate synthase	akg[c] + h[c] + ichor[c] -> 2sephchc[c] + co2[c]	L_RS03895	BZO99_RS10835	0	1000	0	Cofactor and Prosthetic Group Biosynthesis: Menaquinone Biosynthesis	4.1.1.71; 4.2.99.20; 2.5.1.64; 2.2.1.9; 4.1.3.-	R08165	rxn04675	META:2.5.1.64-RXN
SHCHCS3	2-succinyl-6-hydroxy-2,4-cyclohexadiene 1-carboxylate synthase	2sephchc[c] -> 2shchc[c] + pyr[c]	L_RS03890	BZO99_RS10830	0	1000	0	Cofactor and Prosthetic Group Biosynthesis: Menaquinone Biosynthesis	4.2.99.20	R08166	rxn11703	META:RXN-9310
SUCBZL	O-succinylbenzoate-CoA ligase	coa[c] + atp[c] + sucbz[c] -> amp[c] + ppi[c] + sbzcoa[c]	L_RS03880	BZO99_RS10820	0	1000	0	Cofactor and Prosthetic Group Biosynthesis: Menaquinone Biosynthesis	6.2.1.26	R04030	rxn02831	META:O-SUCCINYLBENZOATE-COA-LIG-RXN
SUCBZS	O-succinylbenzoate-CoA synthase	2shchc[c] -> h2o[c] + sucbz[c]	L_RS03875	BZO99_RS10815	0	1000	0	Cofactor and Prosthetic Group Biosynthesis: Menaquinone Biosynthesis	4.2.1.113	R04031	rxn02832	META:O-SUCCINYLBENZOATE-COA-SYN-RXN
ASPO6	L-aspartate oxidase	asp__L[c] + o2[c] -> h[c] + h2o2[c] + iasp[c]	L_RS05900	BZO99_RS01035	0	1000	0	Cofactor and Prosthetic Group Biosynthesis: Nicotinate and Nicotinamide Metabolism	1.4.3.16	R00481	rxn00338	META:L-ASPARTATE-OXID-RXN
NADK	NAD kinase	atp[c] + nad[c] -> adp[c] + h[c] + nadp[c]	L_RS01915	BZO99_RS02050	0	1000	0	Cofactor and Prosthetic Group Biosynthesis: Nicotinate and Nicotinamide Metabolism	2.7.1.23	R00104	rxn00077	META:NAD-KIN-RXN
NADN	NAD nucleosidase	h2o[c] + nad[c] -> adprib[c] + h[c] + ncam[c]			0	1000	0	Cofactor and Prosthetic Group Biosynthesis: Nicotinate and Nicotinamide Metabolism	3.5.1.-; 3.2.2.5; 3.2.2.6	R00102	rxn00075; rxn13106	META:NADNUCLEOSID-RXN; META:RXN-13859
NADS1	NAD synthase (nh3)	dnad[c] + atp[c] + nh4[c] -> amp[c] + ppi[c] + h[c] + nad[c]	L_RS05790	BZO99_RS00925	0	1000	0	Cofactor and Prosthetic Group Biosynthesis: Nicotinate and Nicotinamide Metabolism	6.3.1.5; 6.3.5.1	R00189	rxn00138	META:NAD-SYNTH-NH3-RXN
NADS2	Nicotinate-mononucleotide adenylyltransferase	h2o[c] + dnad[c] + gln__L[c] + atp[c] -> glu__L[c] + amp[c] + h[c] + nad[c] + ppi[c]	L_RS05790	BZO99_RS00925	0	1000	0	Cofactor and Prosthetic Group Biosynthesis: Nicotinate and Nicotinamide Metabolism	6.3.5.1	R00257	rxn00190	META:NAD-SYNTH-GLN-RXN
NAMNPP	Nicotinic acid mononucleotide pyrophosphorylase	atp[c] + h2o[c] + nac[c] + prpp[c] -> adp[c] + nicrnt[c] + pi[c] + ppi[c]	L_RS05780	BZO99_RS00915	0	1000	0	Cofactor and Prosthetic Group Biosynthesis: Nicotinate and Nicotinamide Metabolism	6.3.4.21; 2.4.2.11	R01724	rxn08981; rxn01265	META:NICOTINATEPRIBOSYLTRANS-RXN
NMNAT	Nicotinamide-nucleotide adenylyltransferase	atp[c] + h[c] + nmn[c] -> ppi[c] + nad[c]	L_RS10445 or L_RS01205 or L_RS05775	BZO99_RS07535 or BZO99_RS02765 or BZO99_RS00905	0	1000	0	Cofactor and Prosthetic Group Biosynthesis: Nicotinate and Nicotinamide Metabolism	2.7.7.1; 2.7.7.18	R00137	rxn00105	META:2.7.7.1-RXN
NNAM	Nicotinamidase	h2o[c] + ncam[c] <=> nac[c] + nh4[c]	L_RS01425 or L_RS10790	BZO99_RS02545 or BZO99_RS07660	-1000	1000	0	Cofactor and Prosthetic Group Biosynthesis: Nicotinate and Nicotinamide Metabolism	3.5.1.19	R01268	rxn00938	META:NICOTINAMID-RXN
NNATr	Nicotinate-nucleotide adenylyltransferase	atp[c] + h[c] + nicrnt[c] -> dnad[c] + ppi[c]	L_RS01205 or L_RS05775 or L_RS10445	BZO99_RS02765 or BZO99_RS00905 or BZO99_RS07535	0	1000	0	Cofactor and Prosthetic Group Biosynthesis: Nicotinate and Nicotinamide Metabolism	2.7.7.1; 2.7.7.18	R03005	rxn02155	META:NICONUCADENYLYLTRAN-RXN
NNDPR	Nicotinate-nucleotide diphosphorylase (carboxylating)	2 h[c] + quln[c] + prpp[c] -> ppi[c] + nicrnt[c] + co2[c]			0	1000	0	Cofactor and Prosthetic Group Biosynthesis: Nicotinate and Nicotinamide Metabolism	2.4.2.19	R03348	rxn02402	META:QUINOPRIBOTRANS-RXN
PNP	Purine nucleoside phosphorylase	pi[c] + rnam[c] <=> h[c] + ncam[c] + r1p[c]	L_RS04890	BZO99_RS04825	-1000	1000	0	Cofactor and Prosthetic Group Biosynthesis: Nicotinate and Nicotinamide Metabolism	2.4.2; 2.4.2.1	R02294	rxn01646	META:RXN0-7092
QULNS	Quinolinate synthase	dhap[c] + iasp[c] -> quln[c] + pi[c] + 2 h2o[c]			0	1000	0	Cofactor and Prosthetic Group Biosynthesis: Nicotinate and Nicotinamide Metabolism	2.5.1.72	R04292	rxn02988	META:QUINOLINATE-SYNTHA-RXN
RNMK	Ribosylnicotinamide kinase	atp[c] + rnam[c] -> adp[c] + h[c] + nmn[c]	L_RS10445	BZO99_RS07535	0	1000	0	Cofactor and Prosthetic Group Biosynthesis: Nicotinate and Nicotinamide Metabolism	2.7.1.22	R02324	rxn01671	META:RIBOSYLNICOTINAMIDE-KINASE-RXN
ACPpds	[acyl-carrier-protein]	ACP[c] + h2o[c] ->	L_RS01995 or	BZO99_RS04775 or	0	1000	0	Cofactor and Prosthetic Group	3.1.4.14	R01623	rxn06022	META:3.1.4.14-RXN

	phosphodiesterase	apoACP[c] + h[c] + pan4p[c]	L_RS00645	BZO99_RS08575				Biosynthesis: Pantothenate and CoA Biosynthesis				
ACPS1	Acyl-carrier protein synthase	apoACP[c] + coa[c] -> ACP[c] + h[c] + pap[c]	L_RS04100 and L_RS04445	BZO99_RS06995 and BZO99_RS05265	0	1000	0	Cofactor and Prosthetic Group Biosynthesis: Pantothenate and CoA Biosynthesis	2.7.8.7	R01625	rxn06023	META:HOLO-ACP-SYNTH-RXN
APATr	B alanine pyruvate aminotransferase	ala_B[c] + pyr[c] <=> ala__L[c] + msa[c]	L_RS01845	BZO99_RS02125	-1000	1000	0	Cofactor and Prosthetic Group Biosynthesis: Pantothenate and CoA Biosynthesis	2.6.1.18	R00907	rxn00656	META:2.6.1.18-RXN
DPCOAK	Dephospho-CoA kinase	dpcoa[c] + atp[c] -> coa[c] + adp[c] + h[c]	L_RS03560	BZO99_RS10150	0	1000	0	Cofactor and Prosthetic Group Biosynthesis: Pantothenate and CoA Biosynthesis	2.7.1.24	R00130	rxn00100	META:DEPHOSPHOCOAKIN-RXN
DPR	2-dehydropantoate 2-reductase	h[c] + 2dhp[c] + nadph[c] -> nadp[c] + pant__R[c]	L_RS06920 or L_RS06430	BZO99_RS08355 or BZO99_RS09950	0	1000	0	Cofactor and Prosthetic Group Biosynthesis: Pantothenate and CoA Biosynthesis	1.1.1.169	R02472	rxn01790	META:2-DEHYDROPANTOATE-REDUCT-RXN
MOHMT	3-methyl-2-oxobutanoate hydroxymethyltransferase	3mob[c] + mlthf[c] + h2o[c] -> thf[c] + 2dhp[c]			0	1000	0	Cofactor and Prosthetic Group Biosynthesis: Pantothenate and CoA Biosynthesis	2.1.2.11	R01226	rxn00912	META:3-CH3-2-OXOBUTANOATE-OH-CH3-XFER-RXN
PANTS	Pantothenate synthase	ala_B[c] + atp[c] + pant__R[c] -> h[c] + pnto__R[c] + ppi[c] + amp[c]	L_RS09810	BZO99_RS03195	0	1000	0	Cofactor and Prosthetic Group Biosynthesis: Pantothenate and CoA Biosynthesis	6.3.2.1	R02473	rxn01791	META:PANTOATE-BETA-ALANINE-LIG-RXN
PNTK	Pantothenate kinase	atp[c] + pnto__R[c] -> adp[c] + 4ppan[c] + h[c]	L_RS07550	BZO99_RS05510	0	1000	0	Cofactor and Prosthetic Group Biosynthesis: Pantothenate and CoA Biosynthesis	2.7.1.33	R03018	rxn12510	META:PANTOTHENATE-KIN-RXN
PPCDC	Phosphopantothenoyl cysteine decarboxylase	4ppcys[c] + h[c] -> co2[c] + pan4p[c]	L_RS03090	BZO99_RS06195	0	1000	0	Cofactor and Prosthetic Group Biosynthesis: Pantothenate and CoA Biosynthesis	4.1.1.36	R03269	rxn02341	META:P-PANTOCYSDECARB-RXN
PPNCL2	Phosphopantothenate-cysteine ligase	4ppan[c] + ctp[c] + cys__L[c] -> 4ppcys[c] + cmp[c] + h[c] + ppi[c]	L_RS03095	BZO99_RS06190	0	1000	0	Cofactor and Prosthetic Group Biosynthesis: Pantothenate and CoA Biosynthesis	6.3.2.5	R04231	rxn09177	META:P-PANTOCYSLIG-RXN
PTPATi	Pantetheine-phosphate adenylyltransferase	atp[c] + h[c] + pan4p[c] <=> dpcoa[c] + ppi[c]	L_RS11330	BZO99_RS09315	-1000	1000	0	Cofactor and Prosthetic Group Biosynthesis: Pantothenate and CoA Biosynthesis	2.7.7.3	R03035	rxn02175	META:PANTEPADENYLYLTRAN-RXN
ALATA_D2	D-alanine transaminase	pydx5p[c] + ala__D[c] -> pyam5p[c] + pyr[c]	L_RS03235	BZO99_RS06050	0	1000	0	Cofactor and Prosthetic Group Biosynthesis: Pyridoxine Metabolism		R01147		
ALATA_L2	Alanine transaminase	pydx5p[c] + ala__L[c] -> pyam5p[c] + pyr[c]	L_RS03235	BZO99_RS06050	0	1000	0	Cofactor and Prosthetic Group Biosynthesis: Pyridoxine Metabolism				
E4PD	Erythrose 4-phosphate dehydrogenase	e4p[c] + h2o[c] + nad[c] <=> 4per[c] + 2.0 h[c] + nadh[c]	L_RS11785	BZO99_RS09800	-1000	1000	0	Cofactor and Prosthetic Group Biosynthesis: Pyridoxine Metabolism	1.2.1.72	R01825	rxn01331	META:ERYTH4PDEHYDROG-RXN
HYPOE	Hypothetical enyme	h2o[c] + pyam5p[c] -> pi[c] + pydam[c]	L_RS05995	BZO99_RS01130	0	1000	0	Cofactor and Prosthetic Group Biosynthesis: Pyridoxine Metabolism	3.1.3.74	R02494	rxn01808	META:RXN-14046
OHPBAT	O-Phospho-4-hydroxy-L-threonine:2-oxoglutarate aminotransferase	glu__L[c] + ohpb[c] <=> akg[c] + phthr[c]	L_RS03245	BZO99_RS06040	-1000	1000	0	Cofactor and Prosthetic Group Biosynthesis: Pyridoxine Metabolism	2.6.1.52	R05085	rxn03445	META:PSERTRANSAMPYR-RXN
PDX5PO2	Pyridoxine 5'-phosphate oxidase (anaerboic)	nad[c] + pdx5p[c] -> h[c] + nadh[c] + pydx5p[c]			0	1000	0	Cofactor and Prosthetic Group Biosynthesis: Pyridoxine Metabolism			rxn09071	
PDX5PS	Pyridoxine 5'-phosphate synthase	dxyl5p[c] + nad[c] + phthr[c] -> co2[c] + h[c] + 2.0 h2o[c] + nadh[c] + pdx5p[c] + pi[c]			0	1000	0	Cofactor and Prosthetic Group Biosynthesis: Pyridoxine Metabolism			rxn09072	
PERD	Erythronate 4-phosphate (4per) dehydrogenase	4per[c] + nad[c] -> h[c] + nadh[c] + ohpb[c]			0	1000	0	Cofactor and Prosthetic Group Biosynthesis: Pyridoxine Metabolism	1.1.1.290	R04210	rxn02939	META:ERYTHRON4PDEHYDROG-RXN
PYAM5PO	Pyridoxamine 5'-phosphate oxidase	h2o[c] + o2[c] + pyam5p[c] -> h2o2[c]	L_RS04890 or L_RS04890	BZO99_RS04825 or BZO99_RS04825	0	1000	0	Cofactor and Prosthetic Group Biosynthesis: Pyridoxine Metabolism				

		+ nh4[c] + pydx5p[c]										
PYDAMK	Pyridoxamine kinase	atp[c] + pydam[c] -> adp[c] + h[c] + pyam5p[c]	L_RS02565	BZO99_RS04475	0	1000	0	Cofactor and Prosthetic Group Biosynthesis: Pyridoxine Metabolism	2.7.1.35	R02493	rxn01807	META:PYRAMKIN-RXN
PYDXK	Pyridoxal kinase	atp[c] + pydx[c] -> adp[c] + h[c] + pydx5p[c]	L_RS02565	BZO99_RS04475	0	1000	0	Cofactor and Prosthetic Group Biosynthesis: Pyridoxine Metabolism	2.7.1.35	R00174	rxn00124	META:PYRIDOXKIN-RXN
PYDXNK	Pyridoxine kinase	atp[c] + pydxn[c] <=> adp[c] + h[c] + pdx5p[c]	L_RS02565	BZO99_RS04475	-1000	1000	0	Cofactor and Prosthetic Group Biosynthesis: Pyridoxine Metabolism	2.7.1.35	R01909	rxn01396	META:PNKIN-RXN
PYDXPP	Pyridoxal 5-phosphate phosphatase	pydx5p[c] + h2o[c] -> pi[c] + pydx[c]	L_RS05995	BZO99_RS01130	0	1000	0	Cofactor and Prosthetic Group Biosynthesis: Pyridoxine Metabolism	3.1.3.74	R00173	rxn00123	META:3.1.3.74-RXN
APRAUR	5-amino-6-(5-phosphoribosylamino)uracil reductase	5apru[c] + h[c] + nadph[c] -> 5aprbu[c] + nadp[c]	L_RS05200	BZO99_RS00315	0	1000	0	Cofactor and Prosthetic Group Biosynthesis: Riboflavin Metabolism	1.1.1.193	R03458	rxn02474	META:RIBOFLAVINSYNREDUC-RXN
DB4PS	3,4-Dihydroxy-2-butanone-4-phosphate synthase	ru5p__D[c] -> db4p[c] + for[c] + h[c]	L_RS05210	BZO99_RS00325	0	1000	0	Cofactor and Prosthetic Group Biosynthesis: Riboflavin Metabolism	4.1.99.12	R07281	rxn05040	META:DIOHBUTANONEPSYN-RXN
DHPPDA2	Diaminohydroxyphosphoribosylaminopyrimidine deaminase (25drapp)	h[c] + h2o[c] + 25drapp[c] -> 5apru[c] + nh4[c]	L_RS05200	BZO99_RS00315	0	1000	0	Cofactor and Prosthetic Group Biosynthesis: Riboflavin Metabolism	3.5.4.26	R03459	rxn30012; rxn30309; rxn02475	META:RIBOFLAVINSYNDEAM-RXN
FMNAT	FMN adenylyltransferase	atp[c] + fmn[c] + h[c] -> fad[c] + ppi[c]	L_RS05915	BZO99_RS01050	0	1000	0	Cofactor and Prosthetic Group Biosynthesis: Riboflavin Metabolism	2.7.7.2	R00161	rxn00122	META:FADSYN-RXN
GTPCII2	GTP cyclohydrolase II (25drapp)	gtp[c] + 3.0 h2o[c] -> 25drapp[c] + for[c] + 2.0 h[c] + ppi[c]	L_RS05210	BZO99_RS00325	0	1000	0	Cofactor and Prosthetic Group Biosynthesis: Riboflavin Metabolism	3.5.4.25	R00425	rxn00300	META:GTP-CYCLOHYDRO-II-RXN
PMDPHT	Pyrimidine phosphatase	5aprbu[c] + h2o[c] <=> 4r5au[c] + pi[c]	L_RS00420	BZO99_RS08805	-1000	1000	0	Cofactor and Prosthetic Group Biosynthesis: Riboflavin Metabolism	3.1.3.-; 3.1.3.104	R07280	rxn05039	META:RIBOPHOSPHAT-RXN
RBFK	Riboflavin kinase	atp[c] + ribflv[c] -> adp[c] + fmn[c] + h[c]	L_RS05915	BZO99_RS01050	0	1000	0	Cofactor and Prosthetic Group Biosynthesis: Riboflavin Metabolism	2.7.1.26	R00549	rxn00392	META:RIBOFLAVINKIN-RXN
RBFSa	6,7-Dimethyl-8-ribityllumazine synthase	db4p[c] + 4r5au[c] -> dmlz[c] + pi[c] + 2 h2o[c]	L_RS05215 or L_RS05205	BZO99_RS00330 or BZO99_RS00320	0	1000	0	Cofactor and Prosthetic Group Biosynthesis: Riboflavin Metabolism	2.5.1.78; 2.5.1.9	R04457	rxn03080	META:LUMAZINESYN-RXN
RBFSb	Riboflavin synthase	2 dmlz[c] -> 4r5au[c] + ribflv[c]	L_RS05205	BZO99_RS00320	0	1000	0	Cofactor and Prosthetic Group Biosynthesis: Riboflavin Metabolism	2.5.1.9	R00066	rxn00048	META:RIBOFLAVIN-SYN-RXN
AHMMPS_1	4 amino 5 hydroxymethyl 2 methylpyrimidine synthetase	air[c] + h2o[c] -> 4ahmmp[c] + pi[c] + gcald[c] + 0.5 o2[c]	L_RS05840 or L_RS01940	BZO99_RS00975 or BZO99_RS02025	0	1000	0	Cofactor and Prosthetic Group Biosynthesis: Thiamine Metabolism			rxn09633	
DXPS	1-deoxy-D-xylulose 5-phosphate synthase	g3p[c] + pyr[c] + h[c] -> co2[c] + dxyl5p[c]	L_RS07740 or L_RS08730	BZO99_RS05700 or BZO99_RS09675	0	1000	0	Cofactor and Prosthetic Group Biosynthesis: Thiamine Metabolism	2.2.1.7	R05636	rxn03909	META:DXS-RXN
HETZK	Hydroxyethylthiazole kinase	4mhetz[c] + atp[c] -> adp[c] + 4mpetz[c] + h[c]	L_RS06630	BZO99_RS08090	0	1000	0	Cofactor and Prosthetic Group Biosynthesis: Thiamine Metabolism	2.7.1.50	R04448	rxn03075	META:THIAZOLSYN3-RXN
HMPK1	Hydroxymethylpyrimidine kinase (ATP)	4ahmmp[c] + atp[c] -> adp[c] + 4ampm[c] + h[c]	L_RS02565 or L_RS06625	BZO99_RS04475 or BZO99_RS08095	0	1000	0	Cofactor and Prosthetic Group Biosynthesis: Thiamine Metabolism	2.7.1.49	R03471	rxn02484	META:OHMETPYRKIN-RXN
PMPK	Phosphomethylpyrimidine kinase	4ampm[c] + atp[c] -> 2mahmp[c] + adp[c]	L_RS02565 or L_RS06625	BZO99_RS04475 or BZO99_RS08095	0	1000	0	Cofactor and Prosthetic Group Biosynthesis: Thiamine Metabolism	2.7.4.7	R04509	rxn03108	META:PYRIMSYN3-RXN
TDP	Thiamin pyrophosphatase	h2o[c] + thmpp[c] -> h[c] + pi[c] + thmmp[c]	L_RS01835	BZO99_RS02135	0	1000	0	Cofactor and Prosthetic Group Biosynthesis: Thiamine Metabolism	3.6.1; 3.6.1.-; 3.6.1.15	R00615	rxn00436	META:RXN0-3542
THMP	Thiamin phosphatase	h2o[c] + thmmp[c] -> pi[c] + thm[c]	L_RS10100	BZO99_RS10440	0	1000	0	Cofactor and Prosthetic Group Biosynthesis: Thiamine Metabolism	3.1.3.100	R02135	rxn01539	MEtA:RXNQT-4191
THZPSN	Thiazole phosphate synthesis	atp[c] + cys__L[c] + dxyl5p[c] + tyr__L[c] -> h2o[c] + h[c] + amp[c] + ppi[c] + co2[c] + ala__L[c] + 4mpetz[c] + 4hba[c]	L_RS01985 or L_RS02820 or L_RS05125	BZO99_RS04785 or BZO99_RS04210 or BZO99_RS00235	0	1000	0	Cofactor and Prosthetic Group Biosynthesis: Thiamine Metabolism			rxn09310	
TMDPK	Thiamine	atp[c] + thm[c] ->	L_RS09505	BZO99_RS03500	0	1000	0	Cofactor and Prosthetic Group	2.7.6.2	R00619	rxn00440	META:THIAMIN-

	diphosphokinase	amp[c] + h[c] + thmpp[c]						Biosynthesis: Thiamine Metabolism				PYROPHOSPHOKINASE-RXN
TMN	Thiaminase	h2o[c] + thm[c] -> 4ahmmp[c] + 4mhetz[c] + h[c]	L_RS09270	BZO99_RS03735	0	1000	0	Cofactor and Prosthetic Group Biosynthesis: Thiamine Metabolism	3.5.99.2	R02133	rxn01537	META:THIAMINASE-RXN
TMPPP	Thiamine-phosphate diphosphorylase	2mahmp[c] + 4mpetz[c] + h[c] -> ppi[c] + thmmp[c]	L_RS06620	BZO99_RS08100	0	1000	0	Cofactor and Prosthetic Group Biosynthesis: Thiamine Metabolism	2.5.1.3	R03223	rxn02305	META:THI-P-SYN-RXN
ATPS4r	ATP synthase (four protons for one ATP)	adp[c] + pi[c] + 4.0 h[e] <=> atp[c] + 3.0 h[c] + h2o[c]	L_RS09190 and L_RS09195 and L_RS09200 and L_RS09205 and L_RS09210 and L_RS09215 and L_RS09220 and L_RS09225	BZO99_RS03815 and BZO99_RS03810 and BZO99_RS03805 and BZO99_RS03800 and BZO99_RS03795 and BZO99_RS03790 and BZO99_RS03785 and BZO99_RS03780	-1000	1000	0	Energy Production and Conversion: Anaplerotic Reactions	7.1.2.2; 3.6.3.14		rxn08173	META:ATPSYN-RXN
ME1	Malic enzyme (NAD)	mal__L[c] + nad[c] -> co2[c] + nadh[c] + pyr[c]	L_RS04730	BZO99_RS04985	0	1000	0	Energy Production and Conversion: Anaplerotic Reactions	1.1.1.38; 1.1.1.39	R00214	rxn00159	META:1.1.1.39-RXN
NOX	NADH oxidase	h[c] + nadh[c] + o2[c] -> h2o2[c] + nad[c]	L_RS04170 or L_RS02045	BZO99_RS07070 or BZO99_RS04725	0	1000	0	Energy Production and Conversion: Anaplerotic Reactions	1.6.3.1; 1.6.3.3	R07171	rxn04957	META:RXN-14691
NOX2	NADH oxidase H2O forming	2 h[c] + 2 nadh[c] + o2[c] -> 2 h2o[c] + 2 nad[c]	L_RS02045 or L_RS04170	BZO99_RS04725 or BZO99_RS07070	0	1000	0	Energy Production and Conversion: Anaplerotic Reactions	1.6.3.4	R10517	rxn13771	META:RXN-14692
PPA	Inorganic diphosphatase	ppi[c] + h2o[c] -> 2 pi[c] + h[c]	L_RS09445	BZO99_RS03560	0	1000	0	Energy Production and Conversion: Anaplerotic Reactions	3.6.1.1	R00004	rxn00001; rxn11226	META:INORGPYROPHOSPHAT-RXN
ACONTa	Aconitase (half-reaction A, Citrate hydro-lyase)	cit[c] <=> acon_C[c] + h2o[c]	L_RS03590	Err:520	-1000	1000	0	Energy Production and Conversion: Citric Acid Cycle	4.2.1.3	R01325	rxn00974	META:ACONITATEDEHYDR-RXN
ACONTb	Aconitase (half-reaction B, Isocitrate hydro-lyase)	acon_C[c] + h2o[c] <=> icit[c]	L_RS03590	Err:520	-1000	1000	0	Energy Production and Conversion: Citric Acid Cycle	4.2.1.3	R01900	rxn01388	META:ACONITATEHYDR-RXN
AKGDH	2-Oxogluterate dehydrogenase	akg[c] + coa[c] + nad[c] <=> co2[c] + nadh[c] + succoa[c]	L_RS00360	BZO99_RS08745	-1000	1000	0	Energy Production and Conversion: Citric Acid Cycle	1.2.1.52; 1.2.4.2; 1.8.1.4; 2.3.1.61	R08549	rxn08094	META:2OXOGLUTARATEDEH-RXN
CITL	Citrate lyase	cit[c] -> ac[c] + oaa[c]	L_RS06215 and L_RS06220 and L_RS06225 and L_RS06230	BZO99_RS01355 and BZO99_RS01360 and BZO99_RS01365 and BZO99_RS01370	0	1000	0	Energy Production and Conversion: Citric Acid Cycle	4.1.3.6	R00362	rxn00265	META:CITLY-RXN
CS	Citrate synthase	accoa[c] + h2o[c] + oaa[c] -> coa[c] + cit[c] + h[c]	L_RS03585	BZO99_RS10120	0	1000	0	Energy Production and Conversion: Citric Acid Cycle	2.3.3.1; 2.3.3.3; 2.3.3.16	R00351	rxn00256	META:CITSYN-RXN; META:RXN-14905
FRD2	Fumarate reductase	fum[c] + mql8[c] <=> mqn8[c] + succ[c]	L_RS05900	BZO99_RS01035	-1000	1000	0	Energy Production and Conversion: Citric Acid Cycle			rxn08527	
FRDx	Fumarate reductase NADH	fum[c] + h[c] + nadh[c] <=> nad[c] + succ[c]	L_RS05900	BZO99_RS01035	-1000	1000	0	Energy Production and Conversion: Citric Acid Cycle	1.3.1.6	R02164	rxn00284	META:FUMARATE-REDUCTASE-NADH-RXN
ICDHyr	Isocitrate dehydrogenase (NADP)	nadp[c] + icit[c] <=> co2[c] + akg[c] + nadph[c]	L_RS03595	BZO99_RS10110	-1000	1000	0	Energy Production and Conversion: Citric Acid Cycle	1.1.1.42	R00267	rxn00198	META:ISOCITDEH-RXN
MDH	Malate dehydrogenase	mal__L[c] + nad[c] <=> h[c] + nadh[c] + oaa[c]	L_RS01970 or L_RS04730	BZO99_RS04800 or BZO99_RS04985	-1000	1000	0	Energy Production and Conversion: Citric Acid Cycle	1.1.1.299; 1.1.1.37	R00342	rxn00248	META:MALATE-DEH-RXN
SUCOAS	Succinyl-CoA synthetase (ADP-forming)	atp[c] + coa[c] + succ[c] <=> adp[c] + pi[c] + succoa[c]	L_RS00855	BZO99_RS03115	-1000	1000	0	Energy Production and Conversion: Citric Acid Cycle	6.2.1.5	R00405	rxn00285	META:SUCCCOASYN-RXN
ACYP	Acylphosphatase	h2o[c] + 13dpg[c] -> 3pg[c] + pi[c] + h[c]	L_RS03260	BZO99_RS06025	0	1000	0	Energy Production and Conversion: Glycolysis/Gluconeogenesis	3.6.1.7	R01515	rxn01103	
ENO	Enolase	2pg[c] <=> h2o[c] + pep[c]	L_RS03450	BZO99_RS10775	-1000	1000	0	Energy Production and Conversion: Glycolysis/Gluconeogenesis	4.2.1.11	R00658	rxn00459	META:2PGADEHYDRAT-RXN
FBA	Fructose-bisphosphate aldolase	fdp[c] <=> dhap[c] + g3p[c]	L_RS09945	BZO99_RS11540	-1000	1000	0	Energy Production and Conversion: Glycolysis/Gluconeogenesis	4.1.2.13	R01068	rxn00786	META:F16ALDOLASE-RXN
FBP	Fructose-bisphosphatase	fdp[c] + h2o[c] -> f6p[c] + pi[c]	L_RS01360	BZO99_RS02605	0	1000	0	Energy Production and Conversion: Glycolysis/Gluconeogenesis	3.1.3.11	R00762	rxn00549	META:F16BDEPHOS-RXN

G1PP	Glucose-1-phosphatase	g1p[c] + h2o[c] -> pi[c] + glc__D[c]	L_RS00625 or L_RS05660	BZO99_RS08595 or BZO99_RS00790	0	1000	0	Energy Production and Conversion: Glycolysis/Gluconeogenesis	3.1.3.10	R00304	rxn00221	META:GLUCOSE-1-PHOSPHAT-RXN
G6PI	Glucose 6 phosphate isomerase	g6p[c] <=> g6p_B[c]	L_RS11360	BZO99_RS09285	-1000	1000	0	Energy Production and Conversion: Glycolysis/Gluconeogenesis	5.1.3.15; 5.3.1.9	R02739	rxn01977	META:GLUCOSE-6-PHOSPHATE-1-EPIMERASE-RXN
G6PP	Glucose-6-phosphate phosphatase	h2o[c] + g6p[c] -> pi[c] + glc__D[c]	L_RS00420	BZO99_RS08805	0	1000	0	Energy Production and Conversion: Glycolysis/Gluconeogenesis	3.1.3.9; 3.1.3.58	R00303	rxn00220	META:RXN66-526
GAPD	Glyceraldehyde-3-phosphate dehydrogenase	g3p[c] + pi[c] + nad[c] <=> 13dpg[c] + h[c] + nadh[c]	L_RS03020 or L_RS11785	BZO99_RS06265 or BZO99_RS09800	-1000	1000	0	Energy Production and Conversion: Glycolysis/Gluconeogenesis	1.2.1.12	R01061	rxn00781	META:GAPOXNPHOSPHN-RXN
GLCP	Glycogen phosphorylase	pi[c] + glycogen[c] -> g1p[c]	L_RS03740 and L_RS03735	BZO99_RS10565 and BZO99_RS10560	0	1000	0	Energy Production and Conversion: Glycolysis/Gluconeogenesis	2.4.1.1	R06050; R01821	rxn13299	META:GLYCOPHOSPHORYL-RXN; META:GLYMALTOPHOSPHORYL-RXN
HEX1	Hexokinase (D-glucose:ATP)	atp[c] + glc__D[c] -> adp[c] + g6p[c] + h[c]	L_RS10635	BZO99_RS07805	0	1000	0	Energy Production and Conversion: Glycolysis/Gluconeogenesis	2.7.1.2	R00299	rxn00216	META:GLUCOKIN-RXN
PC	Pyruvate carboxylase	atp[c] + pyr[c] + hco3[c] -> adp[c] + pi[c] + h[c] + oaa[c]	L_RS03580	BZO99_RS10125	0	1000	0	Energy Production and Conversion: Glycolysis/Gluconeogenesis	6.4.1.1	R00344	rxn00250	META:PYRUVATE-CARBOXYLASE-RXN
PDH	Pyruvate dehydrogenase	coa[c] + pyr[c] + nad[c] -> co2[c] + accoa[c] + nadh[c]	L_RS00370 and L_RS00375 and L_RS00365 and L_RS00360	BZO99_RS08755 and BZO99_RS08760 and BZO99_RS08750 and BZO99_RS08745	0	1000	0	Energy Production and Conversion: Glycolysis/Gluconeogenesis	1.2.1; 1.8.1.4; 1.2.1.51; 1.2.4.1; 2.3.1.12	R00209	rxn00154	META:PYRUVDEH-RXN
PFK	Phosphofructokinase	atp[c] + f6p[c] -> adp[c] + fdp[c] + h[c]	L_RS06985	BZO99_RS08295	0	1000	0	Energy Production and Conversion: Glycolysis/Gluconeogenesis	2.7.1.11	R00756	rxn00545	META:6PFRUCTPHOS-RXN
PGI	Glucose-6-phosphate isomerase	g6p[c] <=> f6p[c]	L_RS11360	BZO99_RS09285	-1000	1000	0	Energy Production and Conversion: Glycolysis/Gluconeogenesis	5.3.1.9	R00771	rxn00558	META:PGLUCISOM-RXN
PGK	Phosphoglycerate kinase	3pg[c] + atp[c] <=> 13dpg[c] + adp[c]	L_RS01300	BZO99_RS02665	-1000	1000	0	Energy Production and Conversion: Glycolysis/Gluconeogenesis	2.7.2.3	R01512	rxn01100	META:PHOSGLYPHOS-RXN
PGM	Phosphoglycerate mutase	2pg[c] <=> 3pg[c]	L_RS01780 or L_RS09075 or L_RS04985	BZO99_RS02190 or BZO99_RS03925 or BZO99_RS00090	-1000	1000	0	Energy Production and Conversion: Glycolysis/Gluconeogenesis	5.4.2.1	R01518	rxn01106	META:3PGAREARR-RXN; META:RXN-15513
PGMT_B	B phosphoglucomutase	g6p_B[c] <=> g1p_B[c]	L_RS02245	BZO99_RS04520	-1000	1000	0	Energy Production and Conversion: Glycolysis/Gluconeogenesis	5.4.2.6	R02728	rxn01967	META:BETA-PHOSPHOGLUCOMUTASE-RXN
PYK	Pyruvate kinase	adp[c] + h[c] + pep[c] -> atp[c] + pyr[c]	L_RS06980	BZO99_RS08300	0	1000	0	Energy Production and Conversion: Glycolysis/Gluconeogenesis	2.7.1.40	R00200	rxn00148	META:PEPDEPHOS-RXN
PYK2	Pyruvate kinase (2)	h[c] + pep[c] + udp[c] -> pyr[c] + utp[c]	L_RS06980	BZO99_RS08300	0	1000	0	Energy Production and Conversion: Glycolysis/Gluconeogenesis	2.7.1.40	R00659	rxn00460	
PYK3	Pyruvate kinase (3)	h[c] + gdp[c] + pep[c] -> gtp[c] + pyr[c]	L_RS06980	BZO99_RS08300	0	1000	0	Energy Production and Conversion: Glycolysis/Gluconeogenesis	2.7.1.40	R00430	rxn00304	META:RXN-14117
PYK4	Pyruvate kinase (4)	h[c] + cdp[c] + pep[c] -> pyr[c] + ctp[c]	L_RS06980	BZO99_RS08300	0	1000	0	Energy Production and Conversion: Glycolysis/Gluconeogenesis	2.7.1.40	R00572	rxn00411	
PYK5	Pyruvate kinase (5)	h[c] + pep[c] + idp[c] -> pyr[c] + itp[c]	L_RS06980	BZO99_RS08300	0	1000	0	Energy Production and Conversion: Glycolysis/Gluconeogenesis	2.7.1.40	R00724	rxn00517	
TPI	Triose-phosphate isomerase	dhap[c] <=> g3p[c]	L_RS05950	BZO99_RS01085	-1000	1000	0	Energy Production and Conversion: Glycolysis/Gluconeogenesis	5.3.1.1	R01015	rxn00747	META:TRIOSEPISOMERIZATION-RXN
DDGLK	2-dehydro-3-deoxygluconokinase	2ddglcn[c] + atp[c] <=> 2ddg6p[c] + adp[c] + h[c]	L_RS08480	BZO99_RS01835	-1000	1000	0	Energy Production and Conversion: Pentose Phosphate Pathway	2.7.1.178; 2.7.1.45	R01541	rxn01123	META:DEOXYGLUCONOKIN-RXN
DRBK	Deoxyribokinase	drib[c] + atp[c] -> 2dr5p[c] + adp[c] + h[c]	L_RS08545	BZO99_RS01895	0	1000	0	Energy Production and Conversion: Pentose Phosphate Pathway	2.7.1.15; 2.7.1.229	R02750	rxn01987	META:RXN-14223
DRPA	Deoxyribose-phosphate aldolase	2dr5p[c] -> acald[c] + g3p[c]	L_RS07530	BZO99_RS05490	0	1000	0	Energy Production and Conversion: Pentose Phosphate Pathway	4.1.2.4	R01066	rxn00784	META:DEOXYRIBOSE-P-ALD-RXN
EDA	2-dehydro-3-deoxy-phosphogluconate aldolase	2ddg6p[c] -> g3p[c] + pyr[c]	L_RS08475	BZO99_RS01830	0	1000	0	Energy Production and Conversion: Pentose Phosphate Pathway	4.1.2.14; 4.1.2.55	R05605	rxn03884	META:KDPGALDOL-RXN
FBA3	Sedoheptulose 1,7-bisphosphate D-glyceraldehyde-3-phosphate-lyase	s17bp[c] <=> dhap[c] + e4p[c]	L_RS09945	BZO99_RS11540	-1000	1000	0	Energy Production and Conversion: Pentose Phosphate Pathway	4.1.2.13	R01829	rxn01334	META:SEDOBISALDOL-RXN
G6PDH2r	Glucose 6-phosphate dehydrogenase	g6p[c] + nadp[c] <=> 6pgl[c] + h[c] +	L_RS11655	BZO99_RS09565	-1000	1000	0	Energy Production and Conversion: Pentose Phosphate Pathway	1.1.1.363; 1.1.1.49	R00835; R02736	rxn00604; rxn01975	META:GLU6PDEHYDROG-RXN

		nadph[c]									
GND	Phosphogluconate dehydrogenase	6pgc[c] + nadp[c] -> co2[c] + ru5p__D[c] + nadph[c]	L_RS11470 or L_RS03335	BZO99_RS09385 or BZO99_RS05950	0	1000	0	Energy Production and Conversion: Pentose Phosphate Pathway	1.1.1.44; 1.1.1.351	R01528	rxn01115	META:RXN-9952
GNK	Gluconokinase	atp[c] + glcn[c] -> adp[c] + h[c] + 6pgc[c]	L_RS11465	BZO99_RS09380	0	1000	0	Energy Production and Conversion: Pentose Phosphate Pathway	2.7.1.12	R01737	rxn01275	META:GLUCONOKIN-RXN
PFK_3	Phosphofructokinase (s7p)	atp[c] + s7p[c] -> adp[c] + h[c] + s17bp[c]	L_RS06985	BZO99_RS08295	0	1000	0	Energy Production and Conversion: Pentose Phosphate Pathway	2.7.1.11	R01843	rxn01343	META:RXN0-6541
PGL	6-phosphogluconolactonase	6pgl[c] + h2o[c] -> 6pgc[c] + h[c]	L_RS11290	BZO99_RS09355	0	1000	0	Energy Production and Conversion: Pentose Phosphate Pathway	3.1.1.31	R02035	rxn01476	META:6PGLUCONOLACT-RXN
PKETF	Phosphoketolase (fructose-6-phosphate utilizing)	f6p[c] + pi[c] -> actp[c] + e4p[c] + h2o[c]	L_RS07840	Err:520	0	1000	0	Energy Production and Conversion: Pentose Phosphate Pathway				
PKETX	Phosphoketolase (xylulose-5-phosphate utilizing)	pi[c] + xu5p__D[c] -> actp[c] + g3p[c] + h2o[c]	L_RS07840	Err:520	0	1000	0	Energy Production and Conversion: Pentose Phosphate Pathway				
PPM2	Phosphopentomutase 2 (deoxyribose)	2dr1p[c] <=> 2dr5p[c]	L_RS04880	BZO99_RS04835	-1000	1000	0	Energy Production and Conversion: Pentose Phosphate Pathway	5.4.2.7	R02749	rxn01986	META:D-PPENTOMUT-RXN
PRPPS	Phosphoribosylpyrophosphate synthetase	atp[c] + r5p[c] <=> amp[c] + prpp[c] + h[c]	L_RS04305 or L_RS09670	BZO99_RS07210 or BZO99_RS03335	-1000	1000	0	Energy Production and Conversion: Pentose Phosphate Pathway	2.7.6.1	R01049	rxn15108; rxn00770	META:PRPPSYN-RXN
RBK	Ribokinase	atp[c] + rib__D[c] -> adp[c] + r5p[c] + h[c]	L_RS08545	BZO99_RS01895	0	1000	0	Energy Production and Conversion: Pentose Phosphate Pathway	2.7.1.15	R01051	rxn00772	META:RIBOKIN-RXN
RPE	Ribulose 5-phosphate 3-epimerase	ru5p__D[c] <=> xu5p__D[c]	L_RS10085	BZO99_RS10425	-1000	1000	0	Energy Production and Conversion: Pentose Phosphate Pathway	5.1.3.1	R01529	rxn01116	META:RIBULP3EPIM-RXN
RPI	Ribose-5-phosphate isomerase	r5p[c] <=> ru5p__D[c]	L_RS11720	BZO99_RS09865	-1000	1000	0	Energy Production and Conversion: Pentose Phosphate Pathway	5.3.1.6	R01056	rxn00777	META:RIB5PISOM-RXN
TKT1	Transketolase (alpha-D-ribose 5-phosphate)	r5p[c] + xu5p__D[c] <=> g3p[c] + s7p[c]	L_RS08470	BZO99_RS01825	-1000	1000	0	Energy Production and Conversion: Pentose Phosphate Pathway	2.2.1.1	R01641	rxn15228; rxn01200	META:1TRANSKETO-RXN
TKT2	Transketolase (D-erythrose 4-phosphate)	e4p[c] + xu5p__D[c] <=> f6p[c] + g3p[c]	L_RS08470	BZO99_RS01825	-1000	1000	0	Energy Production and Conversion: Pentose Phosphate Pathway	2.2.1.1	R01067; R01830	rxn31366	META:2TRANSKETO-RXN
ACALD	Acetaldehyde dehydrogenase (acetylating)	acald[c] + coa[c] + nad[c] <=> accoa[c] + h[c] + nadh[c]	L_RS11295	BZO99_RS09350	-1000	1000	0	Energy Production and Conversion: Pyruvate Metabolism	1.2.1.10	R00228	rxn00171	META:ACETALD-DEHYDROG-RXN
ACKr	Acetate kinase	ac[c] + atp[c] <=> actp[c] + adp[c]	L_RS10575 or L_RS10580	BZO99_RS07865 or BZO99_RS07860	-1000	1000	0	Energy Production and Conversion: Pyruvate Metabolism	2.7.2.1; 2.7.2.15	R00315	rxn00225	META:ACETATEKIN-RXN
ACLDC	Acetolactate decarboxylase	alac__S[c] + h[c] -> co2[c] + actn__R[c]	L_RS05815 or L_RS06440	BZO99_RS00950 or BZO99_RS09960	0	1000	0	Energy Production and Conversion: Pyruvate Metabolism	4.1.1.5	R02948	rxn15383	META:ACETOLACTATE-DECARBOXYLASE-RXN
ACTD	Acetoin dehydrogenase	actn__R[c] + nad[c] <=> diact[c] + h[c] + nadh[c]	L_RS04715	BZO99_RS04995	-1000	1000	0	Energy Production and Conversion: Pyruvate Metabolism	1.1.1.303; 1.1.1.304	R02343; R02855; R09078	rxn15373; rxn01685	META:ACETOINDEHYDROG-RXN; META:RXN-11032; META:RXN-11036
ACYP_2	Acylphosphatase (2)	actp[c] + h2o[c] -> ac[c] + h[c] + pi[c]	L_RS03260	BZO99_RS06025	0	1000	0	Energy Production and Conversion: Pyruvate Metabolism	3.6.1.7	R00317	rxn00227	META:ACYLPHOSPHATASE-RXN
ALCD2x	Alcohol dehydrogenase (ethanol)	etoh[c] + nad[c] <=> acald[c] + h[c] + nadh[c]	L_RS08085 or L_RS11295 or L_RS09420	BZO99_RS01430 or BZO99_RS09350 or BZO99_RS03585	-1000	1000	0	Energy Production and Conversion: Pyruvate Metabolism	1.1.1.1; 1.1.1.71	R00754	rxn00543	META:ALCOHOL-DEHYDROG-RXN
ALDD2y	Aldehyde dehydrogenase (acetaldehyde, NADP)	nadp[c] + h2o[c] + acald[c] -> ac[c] + 2 h[c] + nadph[c]	L_RS06850	Err:520	0	1000	0	Energy Production and Conversion: Pyruvate Metabolism	1.2.1.-; 1.2.1.4; 1.2.1.5	R00711	rxn00507	META:RXN0-3962
ALOX	Oxidative decarboxylation of acetolacate chemical	alac__S[c] + h[c] + 0.5 o2[c] -> co2[c] + diact[c] + h2o[c]	s0001	s0001	0	1000	0	Energy Production and Conversion: Pyruvate Metabolism	Non-enzymatic	R10506	rxn40288	META:RXN-6081
BTDD_RR	R R butanediol dehydrogenase	btd_RR[c] + nad[c] <=> actn__R[c] + h[c] + nadh[c]	L_RS04710	BZO99_RS05000	-1000	1000	0	Energy Production and Conversion: Pyruvate Metabolism	1.1.1.4	R02946	rxn39373	META:RR-BUTANEDIOL-DEHYDROGENASE-RXN

LACOX	L-lactate oxidase	lac__L[c] + o2[c] -> h2o2[c] + pyr[c]	L_RS06565	BZO99_RS08155	0	1000	0	Energy Production and Conversion: Pyruvate Metabolism	1.1.3.2	R11996	rxn41759	LACTATE-2-MONOOXYGENASE-RXN
LDH_D	D-lactate dehydrogenase	lac__D[c] + nad[c] <=> h[c] + nadh[c] + pyr[c]	L_RS03250	BZO99_RS06035	-1000	1000	0	Energy Production and Conversion: Pyruvate Metabolism	1.1.1.28	R00704	rxn00500	META:DLACTDEHYDROGNAD-RXN
LDH_L	L-lactate dehydrogenase	lac__L[c] + nad[c] <=> pyr[c] + h[c] + nadh[c]	L_RS01970 or L_RS05920 or L_RS06975	BZO99_RS04800 or BZO99_RS01055 or BZO99_RS08305	-1000	1000	0	Energy Production and Conversion: Pyruvate Metabolism	1.1.1.27	R00703	rxn00499	META:L-LACTATE-DEHYDROGENASE-RXN
MALLAC	Malolactic enzyme	mal__L[c] + h[c] -> co2[c] + lac__L[c]	L_RS04730	BZO99_RS04985	0	1000	0	Energy Production and Conversion: Pyruvate Metabolism	4.1.1.101	R11074	rxn11132	META:RXN-16819
MDHy	MDHy	nadp[c] + mal__L[c] <=> oaa[c] + nadph[c] + h[c]	L_RS04730	BZO99_RS04985	-1000	1000	0	Energy Production and Conversion: Pyruvate Metabolism	1.1.1.299; 1.1.1.82	R00343	rxn00249	META:MALATE-DEHYDROGENASE-NADP+-RXN
ME2	Malic enzyme (NADP)	mal__L[c] + nadp[c] -> co2[c] + nadph[c] + pyr[c]	L_RS04730 or L_RS06200	BZO99_RS04985 or BZO99_RS01340	0	1000	0	Energy Production and Conversion: Pyruvate Metabolism	1.1.1.40	R00216	rxn00161	META:MALIC-NADP-RXN
OAADC	Oxaloacetate decarboxylase	h[c] + oaa[c] -> co2[c] + pyr[c]	L_RS06200	BZO99_RS01340	0	1000	0	Energy Production and Conversion: Pyruvate Metabolism	1.1.1.38; 1.1.1.40; 4.1.1.3	R00217	rxn00162	META:OXALODECARB-RXN
PDHa	Pyruvate dehydrogenase (lipoamide)	pyr[c] + lpam[c] + h[c] -> co2[c] + adhlam[c]	L_RS00375 and L_RS00370	BZO99_RS08760 and BZO99_RS08755	0	1000	0	Energy Production and Conversion: Pyruvate Metabolism	1.2.4.1		rxn01242	
PDHbr	Pyruvate dehydrogenase (dihydrolipoamide) reversible	coa[c] + adhlam[c] <=> dhlam[c] + accoa[c]	L_RS00365	BZO99_RS08750	-1000	1000	0	Energy Production and Conversion: Pyruvate Metabolism	2.3.1.12; 2.3.1.168		rxn01871	META:DIHYDLIPACETRANS-RXN
PDHcr	Pyruvate dehydrogenase (dihydrolipoamide dehydrogenase) reversible	dhlam[c] + nad[c] <=> h[c] + lpam[c] + nadh[c]	L_RS00360	BZO99_RS08745	-1000	1000	0	Energy Production and Conversion: Pyruvate Metabolism	1.8.1; 1.8.1.4	R01698	rxn01241	META:RXN-18331
PFL	Pyruvate formate lyase	coa[c] + pyr[c] <=> accoa[c] + for[c]	L_RS03555 and L_RS09450	BZO99_RS10155 and BZO99_RS03555	-1000	1000	0	Energy Production and Conversion: Pyruvate Metabolism	2.3.1.54	R00212	rxn00157	META:PYRUVFORMLY-RXN
POR	Pyruvate synthase	coa[c] + fdxo_42[c] + pyr[c] <=> co2[c] + accoa[c] + fdxr_42[c] + h[c]	L_RS02205	BZO99_RS04560	-1000	1000	0	Energy Production and Conversion: Pyruvate Metabolism				
POX3_1	Pyruvate:menaquinone oxidoreductase	h2o[c] + pyr[c] + mqn8[c] -> ac[c] + co2[c] + mql8[c]	L_RS10740	BZO99_RS07710	0	1000	0	Energy Production and Conversion: Pyruvate Metabolism				
PTAr	Phosphotransacetylase	accoa[c] + pi[c] <=> coa[c] + actp[c]	L_RS08650	BZO99_RS02000	-1000	1000	0	Energy Production and Conversion: Pyruvate Metabolism	2.3.1.8	R00230	rxn00173	META:PHOSACETYLTRANS-RXN
PYROX_1	Pyruvate oxidase	pi[c] + pyr[c] + h[c] + o2[c] -> co2[c] + actp[c] + h2o2[c]	L_RS10740	BZO99_RS07710	0	1000	0	Energy Production and Conversion: Pyruvate Metabolism	1.2.3.3	R00207	rxn10878; rxn00152	META:1.2.3.3-RXN
CYTBD2	CYTBD2	2.0 h[c] + mql8[c] + 0.5 o2[c] -> h2o[c] + mqn8[c] + 2.0 h[e]	L_RS03760 and L_RS03755 and L_RS03770	BZO99_RS10980 and BZO99_RS10985 and BZO99_RS10970	0	1000	0	Energy Production and Conversion: Respiration	7.1.1.5	R09492	rxn10045; rxn16334	META:RXN-12164
G3PD6	Glycerol-3-phosphate dehydrogenase (menaquinone-8)	mqn8[c] + glyc3p[c] -> dhap[c] + mql8[c]	L_RS06535	BZO99_RS10060	0	1000	0	Energy Production and Conversion: Respiration			rxn08557	
G3PD7	Glycerol-3-phosphate dehydrogenase (demethylmenaquinone-8)	2dmmq8[c] + glyc3p[c] -> dhap[c] + 2dmmql8[c]	L_RS06535	BZO99_RS10060	0	1000	0	Energy Production and Conversion: Respiration	1.1.99.5		rxn08558	META:RXN0-5260
L_LACD3	L-Lactate dehydrogenase (menaquinone)	mqn8[c] + lac__L[c] -> mql8[c] + pyr[c]	(L_RS09035 and L_RS09045 and L_RS09040) or L_RS06565	(BZO99_RS03965 and BZO99_RS03955 and BZO99_RS03960) or BZO99_RS08155	0	1000	0	Energy Production and Conversion: Respiration	1.1.2.3			
NADH10	NADH dehydrogenase (menaquinone-8 & 0 protons)	h[c] + mqn8[c] + nadh[c] -> nad[c] + mql8[c]	L_RS04365 or L_RS01935	BZO99_RS05340 or BZO99_RS02030	0	1000	0	Energy Production and Conversion: Respiration				
NADH9	NADH	h[c] + 2dmmq8[c] +	L_RS04365 or	BZO99_RS05340 or	0	1000	0	Energy Production and Conversion:				

	dehydrogenase (demethylmenaquinone-8 & 0 protons)	nadh[c] -> nad[c] + 2dmmql8[c]	L_RS01935	BZO99_RS02030				Respiration				
NADHPO	NADH peroxidase	h[c] + h2o2[c] + nadh[c] -> 2.0 h2o[c] + nad[c]	(L_RS01790 and L_RS01785) or L_RS02045	(BZO99_RS02180 and BZO99_RS02185) or BZO99_RS04725	0	1000	0	Energy Production and Conversion: Respiration	1.11.1.1	R00090	rxn00066	META:NADH-PEROXIDASE-RXN
SUCD1	Succinate dehydrogenase	fad[c] + succ[c] <=> fadh2[c] + fum[c]	L_RS01935	BZO99_RS02030	-1000	1000	0	Energy Production and Conversion: Respiration	1.3.5.1	R00408	rxn00288	META:RXN-14971
3HAD100	3-hydroxyacyl-[acyl-carrier-protein] dehydratase (n-C10:0)	3hdecACP[c] -> h2o[c] + tdec2eACP[c]	L_RS04125 or L_RS03050	BZO99_RS07020 or BZO99_RS06235	0	1000	0	Lipid Metabolism: Fatty Acid Metabolism	4.2.1.59	R04535	rxn05333	META:RXN-9655
3HAD120	3-hydroxyacyl-[acyl-carrier-protein] dehydratase (n-C12:0)	3hddecACP[c] -> h2o[c] + tddec2eACP[c]	L_RS04125 or L_RS03050	BZO99_RS07020 or BZO99_RS06235	0	1000	0	Lipid Metabolism: Fatty Acid Metabolism	4.2.1.59	R04965	rxn05331	META:RXN-9533
3HAD121	3-hydroxyacyl-[acyl-carrier-protein] dehydratase (n-C12:1)	3hcddec5eACP[c] -> h2o[c] + t3c5ddeceACP[c]	L_RS04125 or L_RS03050	BZO99_RS07020 or BZO99_RS06235	0	1000	0	Lipid Metabolism: Fatty Acid Metabolism	4.2.1.59		rxn07976	META:RXN0-2144
3HAD140	3-hydroxyacyl-[acyl-carrier-protein] dehydratase (n-C14:0)	3hmrsACP[c] -> h2o[c] + tmrs2eACP[c]	L_RS04125 or L_RS03050	BZO99_RS07020 or BZO99_RS06235	0	1000	0	Lipid Metabolism: Fatty Acid Metabolism	4.2.1.59	R04568	rxn05335	META:RXN-9537
3HAD141	3-hydroxyacyl-[acyl-carrier-protein] dehydratase (n-C14:1)	3hcmrs7eACP[c] -> h2o[c] + t3c7mrseACP[c]	L_RS04125 or L_RS03050	BZO99_RS07020 or BZO99_RS06235	0	1000	0	Lipid Metabolism: Fatty Acid Metabolism	4.2.1.59		rxn07977	META:RXN-10656
3HAD160	3-hydroxyacyl-[acyl-carrier-protein] dehydratase (n-C16:0)	3hpalmACP[c] -> h2o[c] + tpalm2eACP[c]	L_RS04125 or L_RS03050	BZO99_RS07020 or BZO99_RS06235	0	1000	0	Lipid Metabolism: Fatty Acid Metabolism	4.2.1.59	R04544	rxn05332	META:4.2.1.61-RXN
3HAD161	3-hydroxyacyl-[acyl-carrier-protein] dehydratase (n-C16:1)	3hcpalm9eACP[c] -> h2o[c] + t3c9palmeACP[c]	L_RS04125 or L_RS03050	BZO99_RS07020 or BZO99_RS06235	0	1000	0	Lipid Metabolism: Fatty Acid Metabolism	4.2.1.59		rxn07978	META:RXN-10660
3HAD180	3-hydroxyacyl-[acyl-carrier-protein] dehydratase (n-C18:0)	3hoctaACP[c] -> h2o[c] + toctd2eACP[c]	L_RS04125 or L_RS03050	BZO99_RS07020 or BZO99_RS06235	0	1000	0	Lipid Metabolism: Fatty Acid Metabolism	4.2.1.59	R07764	rxn07979	META:RXN-9634
3HAD181	3-hydroxyacyl-[acyl-carrier-protein] dehydratase (n-C18:1)	3hcvac11eACP[c] -> h2o[c] + t3c11vaceACP[c]	L_RS04125 or L_RS03050	BZO99_RS07020 or BZO99_RS06235	0	1000	0	Lipid Metabolism: Fatty Acid Metabolism	4.2.1.59		rxn07980	META:RXN-9557
3HAD40	3-hydroxyacyl-[acyl-carrier-protein] dehydratase (n-C4:0)	3haACP[c] -> but2eACP[c] + h2o[c]	L_RS04125 or L_RS03050	BZO99_RS07020 or BZO99_RS06235	0	1000	0	Lipid Metabolism: Fatty Acid Metabolism	4.2.1.59	R04428	rxn07981	META:3-HYDROXYDECANOYL-ACP-DEHYDR-RXN
3HAD60	3-hydroxyacyl-[acyl-carrier-protein] dehydratase (n-C6:0)	3hhexACP[c] -> h2o[c] + thex2eACP[c]	L_RS04125 or L_RS03050	BZO99_RS07020 or BZO99_RS06235	0	1000	0	Lipid Metabolism: Fatty Acid Metabolism	4.2.1.59	R04954	rxn05330	META:RXN-9520
3HAD80	3-hydroxyacyl-[acyl-carrier-protein] dehydratase (n-C8:0)	3hoctACP[c] -> h2o[c] + toct2eACP[c]	L_RS04125 or L_RS03050	BZO99_RS07020 or BZO99_RS06235	0	1000	0	Lipid Metabolism: Fatty Acid Metabolism	4.2.1.59	R04537	rxn05334	META:4.2.1.59-RXN
3OAR100	3-oxoacyl-[acyl-carrier-protein] reductase (n-C10:0)	3odecACP[c] + h[c] + nadph[c] <=> 3hdecACP[c] + nadp[c]	L_RS04110 or L_RS04210	BZO99_RS07005 or BZO99_RS07110	-1000	1000	0	Lipid Metabolism: Fatty Acid Metabolism	1.1.1.100	R04534	rxn05338	META:RXN-9528
3OAR120	3-oxoacyl-[acyl-carrier-protein] reductase (n-C12:0)	3oddecACP[c] + h[c] + nadph[c] <=> 3hddecACP[c] + nadp[c]	L_RS04110 or L_RS04210	BZO99_RS07005 or BZO99_RS07110	-1000	1000	0	Lipid Metabolism: Fatty Acid Metabolism	1.1.1.100	R04964	rxn05340	META:RXN-9532
3OAR121	3-oxoacyl-[acyl-carrier-protein] reductase (n-C12:1)	3ocddec5eACP[c] + h[c] + nadph[c] -> 3hcddec5eACP[c] + nadp[c]	L_RS04110 or L_RS04210	BZO99_RS07005 or BZO99_RS07110	0	1000	0	Lipid Metabolism: Fatty Acid Metabolism	1.1.1.100		rxn07987	META:RXN0-2142
3OAR140	3-oxoacyl-[acyl-carrier-protein] reductase (n-C14:0)	3omrsACP[c] + h[c] + nadph[c] <=> 3hmrsACP[c] + nadp[c]	L_RS04110 or L_RS04210	BZO99_RS07005 or BZO99_RS07110	-1000	1000	0	Lipid Metabolism: Fatty Acid Metabolism	1.1.1.100	R04566	rxn05342	META:RXN-9536
3OAR141	3-oxoacyl-[acyl-carrier-protein]	3ocmrs7eACP[c] + h[c] + nadph[c] ->	L_RS04110 or L_RS04210	BZO99_RS07005 or BZO99_RS07110	0	1000	0	Lipid Metabolism: Fatty Acid Metabolism	1.1.1.100		rxn07989	META:RXN-10655

	reductase (n-C14:1)	3hcmrs7eACP[c] + nadp[c]									
3OAR160	3-oxoacyl-[acyl-carrier-protein] reductase (n-C16:0)	3opalmACP[c] + h[c] + nadph[c] <=> 3hpalmACP[c] + nadp[c]	L_RS04110 or L_RS04210	BZO99_RS07005 or BZO99_RS07110	-1000	1000	0	Lipid Metabolism: Fatty Acid Metabolism 1.1.1.100	R04543	rxn05336	META:RXN-9540
3OAR161	3-oxoacyl-[acyl-carrier-protein] reductase (n-C16:1)	3ocpalm9eACP[c] + h[c] + nadph[c] -> 3hcpalm9eACP[c] + nadp[c]	L_RS04110 or L_RS04210	BZO99_RS07005 or BZO99_RS07110	0	1000	0	Lipid Metabolism: Fatty Acid Metabolism 1.1.1.100		rxn07991	META:RXN-10659
3OAR180	3-oxoacyl-[acyl-carrier-protein] reductase (n-C18:0)	3ooctdACP[c] + h[c] + nadph[c] <=> 3hoctaACP[c] + nadp[c]	L_RS04110 or L_RS04210	BZO99_RS07005 or BZO99_RS07110	-1000	1000	0	Lipid Metabolism: Fatty Acid Metabolism 1.1.1.100	R07763	rxn07992	META:RXN-9633
3OAR181	3-oxoacyl-[acyl-carrier-protein] reductase (n-C18:1)	3ocvac11eACP[c] + h[c] + nadph[c] -> 3hcvac11eACP[c] + nadp[c]	L_RS04110 or L_RS04210	BZO99_RS07005 or BZO99_RS07110	0	1000	0	Lipid Metabolism: Fatty Acid Metabolism 1.1.1.100		rxn07993	META:RXN-9556
3OAR40	3-oxoacyl-[acyl-carrier-protein] reductase (n-C4:0)	actACP[c] + h[c] + nadph[c] <=> 3haACP[c] + nadp[c]	L_RS04110 or L_RS04210	BZO99_RS07005 or BZO99_RS07110	-1000	1000	0	Lipid Metabolism: Fatty Acid Metabolism 1.1.1.100	R04533	rxn07994	META:3-OXOACYL-ACP-REDUCT-RXN
3OAR60	3-oxoacyl-[acyl-carrier-protein] reductase (n-C6:0)	3ohexACP[c] + h[c] + nadph[c] <=> 3hhexACP[c] + nadp[c]	L_RS04110 or L_RS04210	BZO99_RS07005 or BZO99_RS07110	-1000	1000	0	Lipid Metabolism: Fatty Acid Metabolism 1.1.1.100	R04953	rxn05337	META:RXN-9518
3OAR80	3-oxoacyl-[acyl-carrier-protein] reductase (n-C8:0)	3ooctACP[c] + h[c] + nadph[c] <=> 3hoctACP[c] + nadp[c]	L_RS04110 or L_RS04210	BZO99_RS07005 or BZO99_RS07110	-1000	1000	0	Lipid Metabolism: Fatty Acid Metabolism 1.1.1.100	R04536	rxn05341	META:RXN-9524
3OAS100	3-oxoacyl-[acyl-carrier-protein] synthase (n-C10:0)	h[c] + malACP[c] + ocACP[c] -> 3odecACP[c] + ACP[c] + co2[c]	L_RS04115	BZO99_RS07010	0	1000	0	Lipid Metabolism: Fatty Acid Metabolism 2.3.1.179	R04960	rxn05343	META:RXN-9527
3OAS120	3-oxoacyl-[acyl-carrier-protein] synthase (n-C12:0)	dcaACP[c] + h[c] + malACP[c] -> 3oddecACP[c] + ACP[c] + co2[c]	L_RS04115	BZO99_RS07010	0	1000	0	Lipid Metabolism: Fatty Acid Metabolism 2.3.1.179	R04963	rxn05348	META:RXN-9531
3OAS121	3-oxoacyl-[acyl-carrier-protein] synthase (n-C12:1)	cdec3eACP[c] + h[c] + malACP[c] -> 3ocddec5eACP[c] + ACP[c] + co2[c]	L_RS04115	BZO99_RS07010	0	1000	0	Lipid Metabolism: Fatty Acid Metabolism 2.3.1.179		rxn07997	META:RXN0-2141
3OAS140	3-oxoacyl-[acyl-carrier-protein] synthase (n-C14:0)	ddcaACP[c] + h[c] + malACP[c] -> 3omrsACP[c] + ACP[c] + co2[c]	L_RS04115	BZO99_RS07010	0	1000	0	Lipid Metabolism: Fatty Acid Metabolism 2.3.1.179	R04726	rxn05345	META:RXN-9535
3OAS141	3-oxoacyl-[acyl-carrier-protein] synthase (n-C14:1)	cddec5eACP[c] + h[c] + malACP[c] -> 3ocmrs7eACP[c] + ACP[c] + co2[c]	L_RS04115	BZO99_RS07010	0	1000	0	Lipid Metabolism: Fatty Acid Metabolism 2.3.1.179		rxn07998	META:RXN-10654
3OAS160	3-oxoacyl-[acyl-carrier-protein] synthase (n-C16:0)	h[c] + malACP[c] + myrsACP[c] -> 3opalmACP[c] + ACP[c] + co2[c]	L_RS04115	BZO99_RS07010	0	1000	0	Lipid Metabolism: Fatty Acid Metabolism 2.3.1.179	R04968	rxn25647	META:RXN-9539
3OAS161	3-oxoacyl-[acyl-carrier-protein] synthase (n-C16:1)	h[c] + malACP[c] + tdeACP[c] -> 3ocpalm9eACP[c] + ACP[c] + co2[c]	L_RS04115	BZO99_RS07010	0	1000	0	Lipid Metabolism: Fatty Acid Metabolism 2.3.1.179		rxn08000	META:RXN-10658
3OAS180	3-oxoacyl-[acyl-carrier-protein] synthase (n-C18:0)	h[c] + malACP[c] + palmACP[c] -> 3ooctdACP[c] + ACP[c] + co2[c]	L_RS04115	BZO99_RS07010	0	1000	0	Lipid Metabolism: Fatty Acid Metabolism 2.3.1.179	R07762	rxn08001	META:RXN3O-1803
3OAS181	3-oxoacyl-[acyl-carrier-protein] synthase (n-C18:1)	h[c] + hdeACP[c] + malACP[c] -> 3ocvac11eACP[c] +	L_RS04115	BZO99_RS07010	0	1000	0	Lipid Metabolism: Fatty Acid Metabolism 2.3.1.179		rxn08002	META:2.3.1.179-RXN

3OAS60	3-oxoacyl-[acyl-carrier-protein] synthase (n-C6:0)	ACP[c] + co2[c] butACP[c] + h[c] + malACP[c] -> 3ohexACP[c] + ACP[c] + co2[c]	L_RS04115	BZO99_RS07010	0	1000	0	Lipid Metabolism: Fatty Acid Metabolism	2.3.1.179	R04952	rxn05346	META:RXN-9516
3OAS80	3-oxoacyl-[acyl-carrier-protein] synthase (n-C8:0)	h[c] + hexACP[c] + malACP[c] -> 3ooctACP[c] + ACP[c] + co2[c]	L_RS04115	BZO99_RS07010	0	1000	0	Lipid Metabolism: Fatty Acid Metabolism	2.3.1.179	R04957	rxn05350	META:RXN-9523
ACACT1r	Acetyl-CoA C-acetyltransferase	2 accoa[c] <=> aacoa[c] + coa[c]	L_RS08205	BZO99_RS01555	-1000	1000	0	Lipid Metabolism: Fatty Acid Metabolism	2.3.1.9	R00238	rxn00178	META:ACETYL-COA-ACETYLTRANSFER-RXN
ACCOAC	Acetyl-CoA carboxylase	accoa[c] + atp[c] + hco3[c] -> adp[c] + pi[c] + malcoa[c] + h[c]	L_RS04140 and L_RS04120 and L_RS04130 and L_RS04135 and (L_RS09280 or L_RS09915)	BZO99_RS07040 and BZO99_RS07015 and BZO99_RS07030 and BZO99_RS07035 and (BZO99_RS03725 or BZO99_RS10595)	0	1000	0	Lipid Metabolism: Fatty Acid Metabolism	6.4.1.2	R00742	rxn00533	META:ACETYL-COA-CARBOXYLTRANSFER-RXN
ACOATA	Acetyl-CoA ACP transacylase	ACP[c] + accoa[c] <=> acACP[c] + coa[c]	(L_RS04100 and L_RS04095) or L_RS04115	(BZO99_RS06995 and BZO99_RS06990) or BZO99_RS07010	-1000	1000	0	Lipid Metabolism: Fatty Acid Metabolism	2.3.1.180; 2.3.1.85; 2.3.1.86; 2.3.1.179; 2.3.1.-; 2.3.1.38; 2.3.1.41	R01624	rxn05349	META:ACP-S-ACETYLTRANSFER-RXN
BPNT	3',5'-bisphosphate nucleotidase	h2o[c] + pap[c] -> amp[c] + pi[c]	L_RS03915	BZO99_RS10855	0	1000	0	Lipid Metabolism: Fatty Acid Metabolism	3.1.3.97	R00188	rxn00137; rxn11357	META:325-BISPHOSPHATE-NUCLEOTIDASE-RXN
C190cSN	Cyclopropane fatty acid synthase (n-C19:0)	amet[c] + octeACP[c] -> ahcys[c] + h[c] + c190cACP[c]	L_RS07545	BZO99_RS05505	0	1000	0	Lipid Metabolism: Fatty Acid Metabolism	2.1.1.79		rxn10925	
EAR100x	Enoyl-[acyl-carrier-protein] reductase (NADH) (n-C10:0)	h[c] + nadh[c] + tdec2eACP[c] -> dcaACP[c] + nad[c]	L_RS03055 or L_RS09315	BZO99_RS06230 or BZO99_RS03690	0	1000	0	Lipid Metabolism: Fatty Acid Metabolism	1.3.1.9	R04961	rxn05327	META:RXN-9530
EAR100y	Enoyl-[acyl-carrier-protein] reductase (NADPH) (n-C10:0)	h[c] + nadph[c] + tdec2eACP[c] -> dcaACP[c] + nadp[c]	L_RS03055	BZO99_RS06230	0	1000	0	Lipid Metabolism: Fatty Acid Metabolism	2.3.1.86			
EAR120x	Enoyl-[acyl-carrier-protein] reductase (NADH) (n-C12:0)	h[c] + nadh[c] + tddec2eACP[c] -> ddcaACP[c] + nad[c]	L_RS03055 or L_RS09315	BZO99_RS06230 or BZO99_RS03690	0	1000	0	Lipid Metabolism: Fatty Acid Metabolism	1.3.1.9	R04724	rxn05324	META:RXN-9661
EAR120y	Enoyl-[acyl-carrier-protein] reductase (NADPH) (n-C12:0)	h[c] + nadph[c] + tddec2eACP[c] -> ddcaACP[c] + nadp[c]	L_RS03055	BZO99_RS06230	0	1000	0	Lipid Metabolism: Fatty Acid Metabolism	2.3.1.86			
EAR121x	Enoyl-[acyl-carrier-protein] reductase (NADH) (n-C12:1)	h[c] + nadh[c] + t3c5ddeceACP[c] -> cddec5eACP[c] + nad[c]	L_RS03055 or L_RS09315	BZO99_RS06230 or BZO99_RS03690	0	1000	0	Lipid Metabolism: Fatty Acid Metabolism	1.3.1.9		rxn08386	META:RXN0-2145
EAR121y	Enoyl-[acyl-carrier-protein] reductase (NADPH) (n-C12:1)	h[c] + t3c5ddeceACP[c] + nadph[c] -> nadp[c] + cddec5eACP[c]	L_RS03055	BZO99_RS06230	0	1000	0	Lipid Metabolism: Fatty Acid Metabolism	1.3.1.10			
EAR140x	Enoyl-[acyl-carrier-protein] reductase (NADH) (n-C14:0)	h[c] + nadh[c] + tmrs2eACP[c] -> myrsACP[c] + nad[c]	L_RS03055 or L_RS09315	BZO99_RS06230 or BZO99_RS03690	0	1000	0	Lipid Metabolism: Fatty Acid Metabolism	1.3.1.9	R04966	rxn25750	META:RXN-9662
EAR140y	Enoyl-[acyl-carrier-protein] reductase (NADPH) (n-C14:0)	h[c] + nadph[c] + tmrs2eACP[c] -> nadp[c] + myrsACP[c]	L_RS03055	BZO99_RS06230	0	1000	0	Lipid Metabolism: Fatty Acid Metabolism	2.3.1.86			
EAR141x	Enoyl-[acyl-carrier-protein] reductase (NADH) (n-C14:1)	h[c] + nadh[c] + t3c7mrseACP[c] -> nad[c] + tdeACP[c]	L_RS03055 or L_RS09315	BZO99_RS06230 or BZO99_RS03690	0	1000	0	Lipid Metabolism: Fatty Acid Metabolism	1.3.1.9		rxn08390	META:RXN-10657
EAR141y	Enoyl-[acyl-carrier-protein] reductase (NADPH) (n-C14:1)	h[c] + t3c7mrseACP[c] + nadph[c] ->	L_RS03055	BZO99_RS06230	0	1000	0	Lipid Metabolism: Fatty Acid Metabolism	1.3.1.10			

		tdeACP[c] + nadp[c]									
EAR160x	Enoyl-[acyl-carrier-protein] reductase (NADH) (n-C16:0)	h[c] + nadh[c] + tpalm2eACP[c] -> nad[c] + palmACP[c]	L_RS03055 or L_RS09315	BZO99_RS06230 or BZO99_RS03690	0	1000	0	Lipid Metabolism: Fatty Acid Metabolism 1.3.1.9	R04969	rxn08392	META:RXN-9663
EAR160y	Enoyl-[acyl-carrier-protein] reductase (NADPH) (n-C16:0)	h[c] + nadph[c] + tpalm2eACP[c] -> nadp[c] + palmACP[c]	L_RS03055	BZO99_RS06230	0	1000	0	Lipid Metabolism: Fatty Acid Metabolism 1.3.1.10			
EAR161x	Enoyl-[acyl-carrier-protein] reductase (NADH) (n-C16:1)	h[c] + nadh[c] + t3c9palmeACP[c] -> hdeACP[c] + nad[c]	L_RS03055 or L_RS09315	BZO99_RS06230 or BZO99_RS03690	0	1000	0	Lipid Metabolism: Fatty Acid Metabolism 1.3.1.9		rxn08394	META:RXN-10661
EAR161y	Enoyl-[acyl-carrier-protein] reductase (NADPH) (n-C16:1)	h[c] + t3c9palmeACP[c] + nadph[c] -> hdeACP[c] + nadp[c]	L_RS03055	BZO99_RS06230	0	1000	0	Lipid Metabolism: Fatty Acid Metabolism 1.3.1.10			
EAR180x	Enoyl-[acyl-carrier-protein] reductase (NADH) (n-C18:0)	h[c] + nadh[c] + toctd2eACP[c] -> nad[c] + ocdcaACP[c]	L_RS03055 or L_RS09315	BZO99_RS06230 or BZO99_RS03690	0	1000	0	Lipid Metabolism: Fatty Acid Metabolism 1.3.1.9	R07765	rxn08396	META:RXN-9635
EAR180y	Enoyl-[acyl-carrier-protein] reductase (NADPH) (n-C18:0)	h[c] + nadph[c] + toctd2eACP[c] -> nadp[c] + ocdcaACP[c]	L_RS03055	BZO99_RS06230	0	1000	0	Lipid Metabolism: Fatty Acid Metabolism 1.3.1.10			
EAR181x	Enoyl-[acyl-carrier-protein] reductase (NADH) (n-C18:1)	h[c] + nadh[c] + t3c11vaceACP[c] -> nad[c] + octeACP[c]	L_RS03055 or L_RS09315	BZO99_RS06230 or BZO99_RS03690	0	1000	0	Lipid Metabolism: Fatty Acid Metabolism 1.3.1.9		rxn08398	META:RXN-9558
EAR181y	Enoyl-[acyl-carrier-protein] reductase (NADPH) (n-C18:1)	h[c] + t3c11vaceACP[c] + nadph[c] -> nadp[c] + octeACP[c]	L_RS03055	BZO99_RS06230	0	1000	0	Lipid Metabolism: Fatty Acid Metabolism 1.3.1.10			
EAR40x	Enoyl-[acyl-carrier-protein] reductase (NADH) (n-C4:0)	but2eACP[c] + h[c] + nadh[c] -> butACP[c] + nad[c]	L_RS03055 or L_RS09315	BZO99_RS06230 or BZO99_RS03690	0	1000	0	Lipid Metabolism: Fatty Acid Metabolism 1.3.1.9	R04429	rxn05322	META:RXN-9515
EAR40y	Enoyl-[acyl-carrier-protein] reductase (NADPH) (n-C4:0)	but2eACP[c] + h[c] + nadph[c] -> butACP[c] + nadp[c]	L_RS03055	BZO99_RS06230	0	1000	0	Lipid Metabolism: Fatty Acid Metabolism 2.3.1.86			
EAR60x	Enoyl-[acyl-carrier-protein] reductase (NADH) (n-C6:0)	h[c] + nadh[c] + thex2eACP[c] -> hexACP[c] + nad[c]	L_RS03055 or L_RS09315	BZO99_RS06230 or BZO99_RS03690	0	1000	0	Lipid Metabolism: Fatty Acid Metabolism 1.3.1.9	R04955	rxn05326	META:RXN-9658
EAR60y	Enoyl-[acyl-carrier-protein] reductase (NADPH) (n-C6:0)	h[c] + nadph[c] + thex2eACP[c] -> hexACP[c] + nadp[c]	L_RS03055	BZO99_RS06230	0	1000	0	Lipid Metabolism: Fatty Acid Metabolism 2.3.1.86			
EAR80x	Enoyl-[acyl-carrier-protein] reductase (NADH) (n-C8:0)	h[c] + nadh[c] + toct2eACP[c] -> nad[c] + ocACP[c]	L_RS03055 or L_RS09315	BZO99_RS06230 or BZO99_RS03690	0	1000	0	Lipid Metabolism: Fatty Acid Metabolism 1.3.1.9	R04958	rxn05325	META:RXN-9659
EAR80y	Enoyl-[acyl-carrier-protein] reductase (NADPH) (n-C8:0)	h[c] + nadph[c] + toct2eACP[c] -> nadp[c] + ocACP[c]	L_RS03055	BZO99_RS06230	0	1000	0	Lipid Metabolism: Fatty Acid Metabolism 2.3.1.86			
HMGCOAS	Hydroxymethylglutaryl CoA synthase	coa[c] + h[c] + hmgcoa[c] <=> aacoa[c] + accoa[c] + h2o[c]	L_RS08210	BZO99_RS01560	-1000	1000	0	Lipid Metabolism: Fatty Acid Metabolism 2.3.3.10	R01978	rxn01454	META:HYDROXYMETHYLGLUTARYL-COA-SYNTHASE-RXN
KAS14	Beta-ketoacyl-ACP synthase	acACP[c] + h[c] + malACP[c] -> ACP[c] + actACP[c] + co2[c]	L_RS04115	BZO99_RS07010	0	1000	0	Lipid Metabolism: Fatty Acid Metabolism 2.3.1.179	R04355	rxn05347	META:3-OXOACYL-ACP-SYNTH-BASE-RXN
KAS15	Beta-ketoacyl-ACP synthase (2)	accoa[c] + h[c] + malACP[c] -> actACP[c] + co2[c] + coa[c]	L_RS04095	BZO99_RS06990	0	1000	0	Lipid Metabolism: Fatty Acid Metabolism 2.3.1.180	R10707	rxn08766	META:2.3.1.180-RXN
KAS16	3-hydroxy-myristoyl-ACP synthesis	ddcaACP[c] + 2 h[c] + malACP[c] + nadph[c] -> 3hmrsACP[c] + ACP[c] + co2[c] +	L_RS04110 and L_RS04095 and L_RS04115	BZO99_RS07005 and BZO99_RS06990 and BZO99_RS07010	0	1000	0	Lipid Metabolism: Fatty Acid Metabolism		rxn10100	

		nadp[c]										
MCOATA	Malonyl-CoA-ACP transacylase	ACP[c] + malcoa[c] <=> coa[c] + malACP[c]	L_RS04100 and L_RS04105	BZO99_RS06995 and BZO99_RS07000	-1000	1000	0	Lipid Metabolism: Fatty Acid Metabolism	2.3.1.39; 2.3.1.85; 2.3.1.86	R01626	rxn05465	META:MALONYL-COA-ACP-TRANSACYL-RXN
T2DECAI	Trans-2-decenoyl-ACP isomerase	tdec2eACP[c] <=> cdec3eACP[c]	L_RS03885	BZO99_RS10825	-1000	1000	0	Lipid Metabolism: Fatty Acid Metabolism	5.3.3.14	R07639	rxn09280	META:5.3.3.14-RXN
T2DODECAI	Trans-2-dodecenoyl-ACP isomerase	tddec2eACP[c] -> cddec5eACP[c]	L_RS03885	BZO99_RS10825	0	1000	0	Lipid Metabolism: Fatty Acid Metabolism				
ALCD19	Alcohol dehydrogenase (glycerol)	glyald[c] + h[c] + nadh[c] <=> glyc[c] + nad[c]	L_RS08085 or L_RS08130	BZO99_RS01430 or BZO99_RS01480	-1000	1000	0	Lipid Metabolism: Glycerolipid Metabolism	1.1.1.21; 1.1.1.72	R01036	rxn00763	META:RXN-11709
DHAPT	Dihydroxyacetone phosphotransferase	dha[c] + pep[c] -> dhap[c] + pyr[c]	L_RS01315 and L_RS01320 and L_RS01325 and L_RS00665 and L_RS00660	BZO99_RS02650 and BZO99_RS02645 and BZO99_RS02640 and BZO99_RS08555 and BZO99_RS08560	0	1000	0	Lipid Metabolism: Glycerolipid Metabolism	2.7.1.121	R01012	rxn00745	META:2.7.1.121-RXN
G3PT	Glycerol-3-phosphatase	glyc3p[c] + h2o[c] -> pi[c] + glyc[c]	L_RS00420 or L_RS05995	BZO99_RS08805 or BZO99_RS01130	0	1000	0	Lipid Metabolism: Glycerolipid Metabolism	3.1.3.2; 3.1.3.21	R00841	rxn00610	META:RXN-14965
GLYCK	Glycerate 3-kinase	atp[c] + glyc__R[c] -> 3pg[c] + adp[c] + h[c]	L_RS04515	BZO99_RS05190	0	1000	0	Lipid Metabolism: Glycerolipid Metabolism	2.7.1.31	R01514	rxn01102	META:GLY3KIN-RXN
AGAT_LLA	1 Acyl glycerol 3 phosphate acyltransferase lactis specific specific	0.03 hdeACP[c] + 0.44 octeACP[c] + 0.005 tdeACP[c] + 0.13 c190cACP[c] + 0.01 agly3p_LLA[c] + 0.295 palmACP[c] + 0.01 ocdcaACP[c] + 0.09 myrsACP[c] -> ACP[c] + 0.01 pa_LLA[c]	L_RS00635	BZO99_RS08585	0	1000	0	Lipid Metabolism: Glycerophospholipids	2.3.1.51		rxn09555	
ALKP	Alkaline phosphatase	dhap[c] + h2o[c] -> dha[c] + pi[c]	L_RS03800	BZO99_RS10940	0	1000	0	Lipid Metabolism: Glycerophospholipids	3.1.3; 3.1.3.2; 3.1.3.1	R01010	rxn00743	META:RXN0-7249
CLPNS_LLA	Cardiolipin Synthase lactis specific	0.02 pg_LLA[c] <=> 0.01 clpn_LLA[c] + glyc[c]	L_RS05040 or L_RS06145	BZO99_RS00145 or BZO99_RS01285	-1000	1000	0	Lipid Metabolism: Glycerophospholipids	2.7.8.-	R07390	rxn07267	META:CARDIOLIPSYN-RXN
DAGK_LLA	Diacylglycerol kinase Lactis specific	0.01 12dgr_LLA[c] + atp[c] -> adp[c] + h[c] + 0.01 pa_LLA[c]	L_RS05715	BZO99_RS00845	0	1000	0	Lipid Metabolism: Glycerophospholipids	2.7.1.107	R02240	rxn06139	META:DIACYLGLYKIN-RXN
DASYN_LLA	CDP Diacylglycerol synthetase Lactis specific	ctp[c] + h[c] + 0.01 pa_LLA[c] <=> 0.01 cdpdag_LLA[c] + ppi[c]	L_RS11160	BZO99_RS06415	-1000	1000	0	Lipid Metabolism: Glycerophospholipids	2.7.7.41	R01799	rxn06043	CDPDIGLYSYN-RXN
G3PD	Glycerol-3-phosphate dehydrogenase (FAD)	fad[c] + glyc3p[c] <=> dhap[c] + fadh2[c]	L_RS06535	BZO99_RS10060	-1000	1000	0	Lipid Metabolism: Glycerophospholipids	1.1.99.5; 1.1.5.3	R00848	rxn00616	
G3PD1ir	Glycerol 3 phosphate dehydrogenase (NAD)	dhap[c] + h[c] + nadh[c] <=> glyc3p[c] + nad[c]	L_RS07005	BZO99_RS08270	-1000	1000	0	Lipid Metabolism: Glycerophospholipids	1.1.1.8; 1.1.1.94	R00842	rxn00611	META:1.1.1.8-RXN
G3PD2	Glycerol-3-phosphate dehydrogenase (NADP)	glyc3p[c] + nadp[c] <=> dhap[c] + h[c] + nadph[c]	L_RS07005	BZO99_RS08270	-1000	1000	0	Lipid Metabolism: Glycerophospholipids	1.1.1.94	R00844	rxn00612	META:GLYC3PDEHYDROGBIOSYN-RXN
GAT1_LLA	Glycerol 3 phosphate acyltransferase Lactis specific	0.03 hdeACP[c] + 0.44 octeACP[c] + 0.005 tdeACP[c] + 0.13 c190cACP[c] + glyc3p[c] + 0.295 palmACP[c] + 0.01 ocdcaACP[c] + 0.09 myrsACP[c] -> ACP[c] + 0.01 agly3p_LLA[c]	L_RS04100 and L_RS00415 and L_RS05130	BZO99_RS06995 and BZO99_RS08800 and BZO99_RS00240	0	1000	0	Lipid Metabolism: Glycerophospholipids	2.3.1.275; 2.3.1.15		rxn09548	
GLYK	Glycerol kinase	atp[c] + glyc[c] -> adp[c] + glyc3p[c] +	L_RS07585 or L_RS06540	BZO99_RS05545 or BZO99_RS10065	0	1000	0	Lipid Metabolism: Glycerophospholipids	2.7.1.30	R00847	rxn00615	META:GLYCEROL-KIN-RXN

		h[c]										
GPDDA1	Glycerophosphodiesteg r phosphodiesterase (Glycerophosphocholin e)	3pc[c] + h2o[c] -> chol[c] + glyc3p[c] + h[c]	L_RS10495 or L_RS00385	BZO99_RS07585 or BZO99_RS08770	0	1000	0	Lipid Metabolism: Glycerophospholipids	3.1.4.46	R01030	rxn00758	META:3.1.4.2-RXN
GPDDA2	Glycerophosphodiesteg r phosphodiesterase (Glycerophosphoetha nolamine)	3pe[c] + h2o[c] -> etha[c] + glyc3p[c] + h[c]	L_RS10495 or L_RS00385	BZO99_RS07585 or BZO99_RS08770	0	1000	0	Lipid Metabolism: Glycerophospholipids	3.1.4.46	R01470	rxn01073	META:RXN-14160
GPDDA3	Glycerophosphodiesteg r phosphodiesterase (Glycerophosphoserin e)	3ps[c] + h2o[c] -> glyc3p[c] + h[c] + ser__L[c]	L_RS10495 or L_RS00385	BZO99_RS07585 or BZO99_RS08770	0	1000	0	Lipid Metabolism: Glycerophospholipids	3.1.4.46		rxn08668	META:RXN-14136
GPDDA4	Glycerophosphodiesteg r phosphodiesterase (Glycerophosphoglyc erol)	3pg[c] + h2o[c] -> glyc3p[c] + glyc[c] + h[c]	L_RS10495 or L_RS00385	BZO99_RS07585 or BZO99_RS08770	0	1000	0	Lipid Metabolism: Glycerophospholipids	3.1.4.46		rxn08669	META:RXN-14073
GPDDA5	Glycerophosphodiesteg r phosphodiesterase (Glycerophosphoinosi tol)	3pi[c] + h2o[c] -> inost[c] + glyc3p[c] + h[c]	L_RS10495 or L_RS00385	BZO99_RS07585 or BZO99_RS08770	0	1000	0	Lipid Metabolism: Glycerophospholipids	3.1.4.44	R01193	rxn00889	META:3.1.4.44-RXN
LPGS_LLA	Lysylphosphatidyl glycerol synthetase	lystrna[c] + 0.01 pg_LLA[c] -> 0.01 lyspg_LLA[c] + trnalys[c]			0	1000	0	Lipid Metabolism: Glycerophospholipids	2.7.8.5			
PAP_LLA	Phosphatidic acid phosphatase	h2o[c] + 0.01 pa_LLA[c] -> 0.01 12dgr_LLA[c] + pi[c]	L_RS05260	BZO99_RS00375	0	1000	0	Lipid Metabolism: Glycerophospholipids	3.1.3.4; 3.1.3.81	R02239; R09644	rxn05270; rxn16488; rxn06138	META:PHOSPHATIDATE-PHOSPHATASE-RXN; META:RXN-11277
PGPP_LLA	Phosphatidylglycerol phosphate phosphatase Lactis specific	h2o[c] + 0.01 pgp_LLA[c] -> pi[c] + 0.01 pg_LLA[c]	L_RS02220	BZO99_RS04545	0	1000	0	Lipid Metabolism: Glycerophospholipids	3.1.3.27	R02029	rxn06080	META:PGPPHOSPHA-RXN
PGSA_LLA	Phosphatidylglycerol synthase lactis specific	0.01 cdpdag_LLA[c] + glyc3p[c] <=> cmp[c] + h[c] + 0.01 pgp_LLA[c]	L_RS10355	BZO99_RS07440	-1000	1000	0	Lipid Metabolism: Glycerophospholipids	2.7.8.5	R01801	rxn06045	META:PHOSPHAGLYPSYN-RXN
UGT1_LLA	UDP glucosyltransferase monoacylglycerol	0.01 12dgr_LLA[c] + udpg[c] -> 0.01 m12dg_LLA[c] + h[c] + udp[c]	L_RS08290	BZO99_RS01640	0	1000	0	Lipid Metabolism: Glycerophospholipids	2.4.1.315; 2.4.1.336	R02689	rxn06219; rxn05283	META:RXN-16648
UGT2_LLA	UDP glucosyltransferase diacylglycerol	0.01 m12dg_LLA[c] + udpg[c] -> 0.01 d12dg_LLA[c] + h[c] + udp[c]	L_RS08290	BZO99_RS01640	0	1000	0	Lipid Metabolism: Glycerophospholipids	2.4.1.315	R04377	rxn06671; rxn12668; rxn05284	META:RXN-15117; META:RXN-15118
OBTFL	2-Oxobutanoate formate lyase	2obut[c] + coa[c] -> ppcoa[c] + for[c]	L_RS09450 and L_RS03555	BZO99_RS03555 and BZO99_RS10155	0	1000	0	Lipid Metabolism: Propanoate Metabolism	2.3.1; 2.3.1.54	R06987	rxn04794	META:KETOBUTFORMLY-RXN
PTA2	Phosphate acetyltransferase	pi[c] + ppcoa[c] <=> coa[c] + ppap[c]	L_RS08650	BZO99_RS02000	-1000	1000	0	Lipid Metabolism: Propanoate Metabolism	2.3.1.8; 2.3.1.222	R00921	rxn00670	META:PTAALT-RXN
ALAt2r	L alanine reversible transport via proton symport	ala__L[e] + h[e] <=> ala__L[c] + h[c]	L_RS01875 or L_RS01880	BZO99_RS02090 or BZO99_RS02085	-1000	1000	0	Membrane Transport: Amino acids and Peptides	2.A.3; 2.A.25		rxn05496; rxn08101	META:RXN0-5202
ARGabc	L-arginine transport via ABC system	arg__L[e] + atp[c] + h2o[c] -> adp[c] + arg__L[c] + pi[c] + h[c]	L_RS09365 and L_RS09360 and L_RS03040	BZO99_RS03640 and BZO99_RS03645 and BZO99_RS06245	0	1000	0	Membrane Transport: Amino acids and Peptides	7.4.2.1; 3.A.1		rxn05154; rxn08151; rxn11236	META:ABC-4-RXN
ARGORNt3	Arginineornithine antiporter	arg__L[e] + orn__L[c] <=> arg__L[c] + orn__L[e]	L_RS10670 or L_RS10695	BZO99_RS07775 or BZO99_RS07755	-1000	1000	0	Membrane Transport: Amino acids and Peptides	2.A.3.2.10; 2.A.3.2.11		rxn10131	
ARGt2r	L arganine reversible transport via proton symport	arg__L[e] + h[e] -> arg__L[c] + h[c]			0	1000	0	Membrane Transport: Amino acids and Peptides			rxn05303	META:RXN66-448

ASNt2r	L asparagine reversible transport via proton symport	asn__L[e] + h[e] -> asn__L[c] + h[c]			0	1000	0	Membrane Transport: Amino acids and Peptides	2.A.3	rxn05508; rxn08161; rxn09782; rxn11321; rxn13230	
ASPabc	L-aspartate transport via ABC system	asp__L[e] + atp[c] + h2o[c] -> adp[c] + asp__L[c] + h[c] + pi[c]	L_RS09360 and L_RS09170	BZO99_RS03645 and BZO99_RS03835	0	1000	0	Membrane Transport: Amino acids and Peptides	7.4.2.1; 3.6.3.21	rxn05152	META:TRANS-RXN0-222
ASPt2r	L aspartate reversible transport via proton symport	asp__L[e] + h[e] -> asp__L[c] + h[c]			0	1000	0	Membrane Transport: Amino acids and Peptides	2.A.3	rxn05217; rxn09781; rxn09825; rxn13233	META:TRANS-RXN-122A
CYSt2r	L cysteine reversible transport via proton symport	cys__L[e] + h[e] -> cys__L[c] + h[c]			0	1000	0	Membrane Transport: Amino acids and Peptides	2.A.3	rxn09690; rxn11324	META:TRANS-RXN-287
DALAt2r	D-alanine transport via proton symport	ala__D[e] + h[e] <=> ala__D[c] + h[c]	L_RS01875 or L_RS01880 or L_RS04280	BZO99_RS02090 or BZO99_RS02085 or BZO99_RS07185	-1000	1000	0	Membrane Transport: Amino acids and Peptides	2.A.3.1.-	rxn05494	META:TRANS-RXN-62A
GLNabc	L-glutamine transport via ABC system	atp[c] + gln__L[e] + h2o[c] -> adp[c] + pi[c] + gln__L[c] + h[c]	L_RS03040 and L_RS09170 and L_RS09175 and L_RS09360 and L_RS09365	BZO99_RS06245 and BZO99_RS03835 and BZO99_RS03830 and BZO99_RS03645 and BZO99_RS03640	0	1000	0	Membrane Transport: Amino acids and Peptides	7.4.2.1; 3.A.1	rxn05155; rxn05196; rxn08624; rxn11101; rxn11233	META:ABC-12-RXN
GLUabc	L-glutamate transport via ABC system	atp[c] + glu__L[e] + h2o[c] -> adp[c] + pi[c] + glu__L[c] + h[c]	L_RS09365 and L_RS09360 and L_RS09170	BZO99_RS03640 and BZO99_RS03645 and BZO99_RS03835	0	1000	0	Membrane Transport: Amino acids and Peptides	2.A.23.1	rxn05146; rxn08627; rxn11235	META:ABC-13-RXN
GLUABUTt7	4-aminobutyrate/ glutamate antiport	4abut[c] + glu__L[e] <=> 4abut[e] + glu__L[c]	L_RS06765	BZO99_RS07955	-1000	1000	0	Membrane Transport: Amino acids and Peptides	2.A.3.7.1	rxn08628; rxn10136	
GLYt2r	Glycine reversible transport via proton symport	gly[e] + h[e] <=> gly[c] + h[c]	L_RS01875 or L_RS01880	BZO99_RS02090 or BZO99_RS02085	-1000	1000	0	Membrane Transport: Amino acids and Peptides	2.A.3; 2.A.3.1	rxn05582; rxn08660; rxn09748	META:TRANS-RXN-62B
HISt2r	L histidine reversible transport via proton symport	h[e] + his__L[e] -> h[c] + his__L[c]	L_RS01875 or L_RS01880	BZO99_RS02090 or BZO99_RS02085	0	1000	0	Membrane Transport: Amino acids and Peptides	2.A.3	rxn05299; rxn08719; rxn09744; rxn11327	META:RXN-14653
ILEt2r	L isoleucine reversible transport via proton symport	h[e] + ile__L[e] <=> h[c] + ile__L[c]	L_RS08410	BZO99_RS01765	-1000	1000	0	Membrane Transport: Amino acids and Peptides	2.A.3	rxn05244; rxn08746; rxn13322	META:TRANS-RXN-126
LEUt2r	L leucine reversible transport via proton symport	leu__L[e] + h[e] <=> leu__L[c] + h[c]	L_RS00630	BZO99_RS08590	-1000	1000	0	Membrane Transport: Amino acids and Peptides	2.A.3	rxn05243; rxn08785; rxn13340	META:RXN-14649
LYSt2r	L lysine reversible transport via proton symport	lys__L[e] + h[e] <=> lys__L[c] + h[c]	L_RS11510 or L_RS01930	BZO99_RS09425 or BZO99_RS02035	-1000	1000	0	Membrane Transport: Amino acids and Peptides	2.A.3.1.2	rxn08854; rxn09674; rxn09740	META:TRANS-RXN-58
METabc	L-methionine transport via ABC system	atp[c] + met__L[e] + h2o[c] -> adp[c] + pi[c] + met__L[c] + h[c]	(L_RS01710 and L_RS01705 and L_RS01695) or (L_RS01710 and L_RS01705 and L_RS01690) or (L_RS01710 and L_RS01705 and L_RS01685) or (L_RS01710 and L_RS01705 and L_RS01700)	(BZO99_RS02260 and BZO99_RS02265 and BZO99_RS02275) or (BZO99_RS02260 and BZO99_RS02265 and BZO99_RS02280) or (BZO99_RS02260 and BZO99_RS02265 and BZO99_RS02285) or (BZO99_RS02260 and BZO99_RS02265 and BZO99_RS02270)	0	1000	0	Membrane Transport: Amino acids and Peptides	7.4.2.2; 3.6.3.22	rxn05219	META:3.6.3.22-RXN; META:RXN0-4522
METt2r	L methionine reversible transport via proton symport	met__L[e] + h[e] -> met__L[c] + h[c]			0	1000	0	Membrane Transport: Amino acids and Peptides	2.A.3	rxn09672; rxn09738	META:RXN-14652
PHEt2r	L phenylalanine reversible transport	h[e] + phe__L[e] <=> h[c] + phe__L[c]	L_RS01875 or L_RS01880	BZO99_RS02090 or BZO99_RS02085	-1000	1000	0	Membrane Transport: Amino acids and Peptides	2.A.3	rxn05306; rxn09117; rxn09724; rxn11337	META:TRANS-RXN-56

	via proton symport											
PROabc	L-proline transport via ABC system	atp[c] + pro__L[e] + h2o[c] -> adp[c] + pi[c] + pro__L[c] + h[c]	L_RS04470 and L_RS04465 and L_RS07595 and L_RS07590	BZO99_RS05240 and BZO99_RS05245 and BZO99_RS05555 and BZO99_RS05550	0	1000	0	Membrane Transport: Amino acids and Peptides	3.6.3.22		rxn05165	META:3.6.3.22-RXN; META:ABC-26-RXN
PROt2r	L proline reversible transport via proton symport	h[e] + pro__L[e] <=> h[c] + pro__L[c]	L_RS04280 or L_RS05830	BZO99_RS07185 or BZO99_RS00965	-1000	1000	0	Membrane Transport: Amino acids and Peptides			rxn05638	META:TRANS-RXN-29
PROt3	L proline transport out via proton antiport	pro__L[c] + h[e] -> pro__L[e] + h[c]			0	1000	0	Membrane Transport: Amino acids and Peptides				
SERt2r	L serine reversible transport via proton symport	h[e] + ser__L[e] <=> h[c] + ser__L[c]	L_RS01875 or L_RS01880	BZO99_RS02090 or BZO99_RS02085	-1000	1000	0	Membrane Transport: Amino acids and Peptides	2.A.3		rxn05307; rxn09246; rxn09714	META:TRANS-RXN-71
THRt2r	L threonine reversible transport via proton symport	h[e] + thr__L[e] <=> h[c] + thr__L[c]			-1000	1000	0	Membrane Transport: Amino acids and Peptides	2.A.3; 2.A.42		rxn05300; rxn09305; rxn09710	META:TRANS-RXN-72
TRPt2r	L tryptophan reversible transport via proton symport	h[e] + trp__L[e] <=> h[c] + trp__L[c]	L_RS01875 or L_RS01880	BZO99_RS02090 or BZO99_RS02085	-1000	1000	0	Membrane Transport: Amino acids and Peptides	2.A.3		rxn05663; rxn09326; rxn09709	META:TRANS-RXN-76
TYRt2r	L tyrosine reversible transport via proton symport	h[e] + tyr__L[e] <=> h[c] + tyr__L[c]	L_RS01875 or L_RS01880	BZO99_RS02090 or BZO99_RS02085	-1000	1000	0	Membrane Transport: Amino acids and Peptides	2.A.3		rxn05301; rxn09338; rxn09708; rxn09831; rxn13412	META:TRANS-RXN-77
VALt2r	L valine reversible transport via proton symport	h[e] + val__L[e] <=> h[c] + val__L[c]	L_RS00630	BZO99_RS08590	-1000	1000	0	Membrane Transport: Amino acids and Peptides	2.A.3		rxn05669; rxn09374; rxn09707	META:TRANS-RXN-126A
ACGApts	N-Acetyl-D-glucosamine transport via PEP:Pyr PTS	acgam[e] + pep[c] -> acgam6p[c] + pyr[c]	L_RS08910 and L_RS08905 and L_RS08900 and L_RS00665 and L_RS00660	BZO99_RS04090 and BZO99_RS04095 and BZO99_RS04100 and BZO99_RS08555 and BZO99_RS08560	0	1000	0	Membrane Transport: Amino sugars	2.7.1.193		rxn05485; rxn08041	META:TRANS-RXN-167
ACMANApts	N-acetyl-D-mannosamine transport via PTS	acmana[e] + pep[c] -> acmanap[c] + pyr[c]	L_RS00660 and L_RS00665	BZO99_RS08560 and BZO99_RS08555	0	1000	0	Membrane Transport: Amino sugars	2.7.1.-		rxn08046; rxn10183	
GAMpts	D-glucosamine transport via PEP:Pyr PTS	pep[c] + gam[e] -> gam6p[c] + pyr[c]	L_RS08910 and L_RS08905 and L_RS08900 and L_RS00665 and L_RS00660	BZO99_RS04090 and BZO99_RS04095 and BZO99_RS04100 and BZO99_RS08555 and BZO99_RS08560	0	1000	0	Membrane Transport: Amino sugars	2.7.1.-	R10407	rxn05569; rxn08592	META:TRANS-RXN-167A
ALLULpts	Allulose transport via ABC system (import)	allul[e] + pep[c] -> allul6p[c] + pyr[c]	L_RS00665 and L_RS00660 and L_RS05035	BZO99_RS08555 and BZO99_RS08560 and BZO99_RS00140	0	1000	0	Membrane Transport: Carbohydrates	7.5.2.-			
CELBpts	Cellobiose transport via PEPPyr PTS	cellb[e] + pep[c] -> 6pgg[c] + pyr[c]	L_RS02155 and L_RS02160 and L_RS04325 and L_RS00660 and L_RS00665	BZO99_RS04615 and BZO99_RS04610 and BZO99_RS07230 and BZO99_RS08560 and BZO99_RS08555	0	1000	0	Membrane Transport: Carbohydrates	2.7.1.205; 4.A	R11172	rxn05518	META:RXN-15086
DRIBabc	Deoxyribose transport via ABC system	atp[c] + h2o[c] + drib[e] -> adp[c] + h[c] + pi[c] + drib[c]	L_RS06960 and L_RS06965 and L_RS06970	BZO99_RS08320 and BZO99_RS08315 and BZO99_RS08310	0	1000	0	Membrane Transport: Carbohydrates	7.5.2.-		rxn05549	META:3.6.3.17-RXN
DRIBt2	Deoxyribose transport in via proton symporter	drib[e] + h[e] -> drib[c] + h[c]			0	1000	0	Membrane Transport: Carbohydrates	2.A.3		rxn12579	
FRUpts	D-fructose transport via PEP:Pyr PTS	fru[e] + pep[c] -> f1p[c] + pyr[c]	(L_RS05035 and L_RS00660 and L_RS00665) or ((L_RS08905 or L_RS08900 or L_RS08910) and L_RS00660 and L_RS00665)	(BZO99_RS00140 and BZO99_RS08560 and BZO99_RS08555) or ((BZO99_RS04095 or BZO99_RS04100 or BZO99_RS04090) and BZO99_RS08560 and BZO99_RS08555)	0	1000	0	Membrane Transport: Carbohydrates	2.7.1.202; 4.A	R03232	rxn05560; rxn08536	META:RXN-15084
FRUpts2	D-fructose transport via PEP:Pyr PTS (f6p	fru[e] + pep[c] -> f6p[c] + pyr[c]	L_RS08910 and L_RS08905 and	BZO99_RS04090 and BZO99_RS04095 and	0	1000	0	Membrane Transport: Carbohydrates	2.7.1.-		rxn08535	

	generating)		L_RS08900 and L_RS00665 and L_RS00660	BZO99_RS04100 and BZO99_RS08555 and BZO99_RS08560								
GALabc	Galactose transport via the ABC system	atp[c] + gal[e] + h2o[c] -> adp[c] + gal[c] + h[c] + pi[c]	L_RS07805 and L_RS07810 and L_RS07815	BZO99_RS05765 and BZO99_RS05770 and BZO99_RS05775	0	1000	0	Membrane Transport: Carbohydrates	7.5.2.-		rxn05162	META:ABC-18-RXN
GALt2	D galactose transport in via proton symport	gal[e] + h[e] -> gal[c] + h[c]			0	1000	0	Membrane Transport: Carbohydrates	2.A.1.1		rxn05566; rxn08584	META:TRANS-RXN-21
GLCpts	D-glucose transport via PEP:Pyr PTS	glc__D[e] + pep[c] -> g6p[c] + pyr[c]	(((L_RS02230 or L_RS05940) and L_RS05935) or L_RS02230 or L_RS05940) and L_RS00660 and L_RS00665	(((BZO99_RS04535 or BZO99_RS01075) and BZO99_RS01070) or BZO99_RS04535 or BZO99_RS01075) and BZO99_RS08560 and BZO99_RS08555	0	1000	0	Membrane Transport: Carbohydrates	2.7.1.199; 4.A	R02738	rxn05226; rxn08612	META:RXN-15083
GLCt2	D-glucose transport in via proton symport	glc__D[e] + h[e] <=> h[c] + glc__D[c]	L_RS11925	BZO99_RS11210	-1000	1000	0	Membrane Transport: Carbohydrates			rxn05573	META:RXN0-7077
LCTSt	Lactose transport via proton symport	lcts[e] + h[e] <=> lcts[c] + h[c]			-1000	1000	0	Membrane Transport: Carbohydrates	2.A.14		rxn08781; rxn10169	META:TRANS-RXN-24
MALt2r	L malate reversible transport via proton symport	mal__L[e] + h[e] -> mal__L[c] + h[c]	L_RS04735	BZO99_RS04980	0	1000	0	Membrane Transport: Carbohydrates	2.A.24		rxn05605	META:TRANS-RXN-121A
MALTabc	Maltose transport via ABC system	atp[c] + malt[e] + h2o[c] -> adp[c] + pi[c] + malt[c] + h[c]	L_RS02200 and L_RS08790 and L_RS08785 and L_RS08780	BZO99_RS04565 and BZO99_RS09615 and BZO99_RS09620 and BZO99_RS09625	0	1000	0	Membrane Transport: Carbohydrates	7.5.2.1; 3.A.1		rxn05170; rxn08867	META:3.6.3.19-RXN; META:ABC-16-RXN
MALTHPabc	Maltoheptaose transport via ABC system	atp[c] + h2o[c] + malthp[e] -> adp[c] + h[c] + malthp[c] + pi[c]	L_RS02200 and L_RS08790 and L_RS08785 and L_RS08780	BZO99_RS04565 and BZO99_RS09615 and BZO99_RS09620 and BZO99_RS09625	0	1000	0	Membrane Transport: Carbohydrates	7.5.2.2		rxn10833	META:3.6.3.18-RXN
MALTHXabc	Maltohexaose transport via ABC system	atp[c] + h2o[c] + malthx[e] -> adp[c] + h[c] + malthx[c] + pi[c]	L_RS02200 and L_RS08790 and L_RS08785 and L_RS08780	BZO99_RS04565 and BZO99_RS09615 and BZO99_RS09620 and BZO99_RS09625	0	1000	0	Membrane Transport: Carbohydrates	7.5.2.2		rxn08869	META:3.6.3.18-RXN
MALTPTabc	Maltopentose transport via ABC system	atp[c] + h2o[c] + maltpt[e] -> adp[c] + h[c] + maltpt[c] + pi[c]	L_RS02200 and L_RS08790 and L_RS08785 and L_RS08780	BZO99_RS04565 and BZO99_RS09615 and BZO99_RS09620 and BZO99_RS09625	0	1000	0	Membrane Transport: Carbohydrates	7.5.2.2		rxn08871	META:3.6.3.18-RXN
MALTpts	Maltose transport via PEP:Pyr PTS	malt[e] + pep[c] -> malt6p[c] + pyr[c]	L_RS00660 and L_RS00665 and (L_RS02230 or L_RS05940)	BZO99_RS08560 and BZO99_RS08555 and (BZO99_RS04535 or BZO99_RS01075)	0	1000	0	Membrane Transport: Carbohydrates		R04111; R06236	rxn05607	META:RXN-15092; META:RXN-15166
MALTTRabc	Maltotriose transport via ABC system	atp[c] + h2o[c] + malttr[e] -> adp[c] + h[c] + malttr[c] + pi[c]	L_RS02200 and L_RS08790 and L_RS08785 and L_RS08780	BZO99_RS04565 and BZO99_RS09615 and BZO99_RS09620 and BZO99_RS09625	0	1000	0	Membrane Transport: Carbohydrates	7.5.2.1		rxn05608	META:TRANS-RXN0-503
MALTTTRabc	Maltotetraose transport via ABC system	atp[c] + h2o[c] + malttttr[e] -> adp[c] + h[c] + malttttr[c] + pi[c]	L_RS02200 and L_RS08790 and L_RS08785 and L_RS08780	BZO99_RS04565 and BZO99_RS09615 and BZO99_RS09620 and BZO99_RS09625	0	1000	0	Membrane Transport: Carbohydrates	7.5.2.1		rxn08877	META:TRANS-RXN0-504
MANpts	D-mannose transport via PEP:Pyr PTS	man[e] + pep[c] -> pyr[c] + man6p[c]	(L_RS08905 or L_RS08900 or L_RS08910) and L_RS00660 and L_RS00665	(BZO99_RS04095 or BZO99_RS04100 or BZO99_RS04090) and BZO99_RS08560 and BZO99_RS08555	0	1000	0	Membrane Transport: Carbohydrates	2.7.1.191; 4.A	R02630	rxn05610; rxn08885	META:RXN-15087
RIBabc	D-ribose transport via ABC system	atp[c] + rib__D[e] + h2o[c] -> adp[c] + pi[c] + rib__D[c] + h[c]	L_RS08535 and L_RS08530 and L_RS08525	BZO99_RS01885 and BZO99_RS01880 and BZO99_RS01875	0	1000	0	Membrane Transport: Carbohydrates	3.A.1		rxn05160; rxn09227	META:ABC-28-RXN
RIBabc1	D ribose transport out via ABC system	atp[c] + h2o[c] + rib__D[c] -> adp[c] + pi[c] + h[c] + rib__D[e]	(L_RS08525 and L_RS08530 and L_RS08535 and L_RS08540)	(BZO99_RS01875 and BZO99_RS01880 and BZO99_RS01885 and BZO99_RS01890	0	1000	0	Membrane Transport: Carbohydrates			rxn05644	

				)								
RIBt2	Ribose transport in via proton symporter	rib__D[e] + h[e] -> rib__D[c] + h[c]	L_RS11925	BZO99_RS11210	0	1000	0	Membrane Transport: Carbohydrates			rxn09663	
TREpts	Trehalose transport via PEP:Pyr PTS	pep[c] + tre[e] -> pyr[c] + tre6p[c]	L_RS02235 and L_RS00660 and L_RS00665 and L_RS07635	BZO99_RS04530 and BZO99_RS08560 and BZO99_RS08555 and BZO99_RS05595	0	1000	0	Membrane Transport: Carbohydrates	2.7.1.201; 4.A	R02780	rxn02005; rxn09322	META:RXN-15095
CA2abc	Calcium transport via ABC system	atp[c] + ca2[e] + h2o[c] -> adp[c] + ca2[c] + h[c] + pi[c]	L_RS07140	BZO99_RS05380	0	1000	0	Membrane Transport: Ions and Gases	7.2.2.10; 3.6.3.8		rxn10447	META:TRANS-RXN-193
Clt	Major Facilitator(MFS) TCDB:2.A.1.14.6	cl[e] <=> cl[c]	L_RS05770	BZO99_RS00900	-1000	1000	0	Membrane Transport: Ions and Gases			rxn08234; rxn10473	META:TRANS-RXN-139
CO2t	CO2 transporter via diffusion	co2[e] <=> co2[c]	s0001	s0001	-1000	1000	0	Membrane Transport: Ions and Gases	Non-enzymatic		rxn05467; rxn08237; rxn08238; rxn09706; rxn09775; rxn09821; rxn09860; rxn09876	META:TRANS-RXN0-545
COabc	Cobalt transport via ABC system	atp[c] + cobalt2[e] + h2o[c] -> adp[c] + cobalt2[c] + h[c] + pi[c]	(L_RS01720 and L_RS01725 and L_RS01480 and L_RS01475 and L_RS01470) or (L_RS11795 and L_RS07140 and L_RS04490) or L_RS08380	(BZO99_RS02250 and BZO99_RS02245 and BZO99_RS02490 and BZO99_RS02495 and BZO99_RS02500) or (BZO99_RS09785 and BZO99_RS05380 and BZO99_RS05215) or BZO99_RS01735	0	1000	0	Membrane Transport: Ions and Gases			rxn05166	
COBALTt5	Cobalt (Co+2) transport via diffusion (extracellular to cytoplasm)	cobalt2[c] <=> cobalt2[e]	L_RS01635 or L_RS07750	BZO99_RS02335 or BZO99_RS05710	-1000	1000	0	Membrane Transport: Ions and Gases			rxn08241; rxn08242; rxn10474	META:TRANS-RXN-141A
Cuabc	Cuabc	atp[c] + h2o[c] + cu2[e] -> adp[c] + pi[c] + h[c] + cu2[c]	L_RS04390	BZO99_RS05315	0	1000	0	Membrane Transport: Ions and Gases	3.6.3.4; 3.A.3.5.1		rxn10481	
Cut1	Copper export via ATPase	atp[c] + h2o[c] + cu2[c] -> adp[c] + pi[c] + h[c] + cu2[e]	(L_RS04490 or L_RS10845)	(BZO99_RS05215 or BZO99_RS11410)	0	1000	0	Membrane Transport: Ions and Gases	7.2.2.9; 3.6.3.4; 3.A.3.5.2		rxn05528	META:TRANS-RXN-178
DHAt	Dihydroxyacetone transport via facilitated diffusion	dha[e] <=> dha[c]	s0001	s0001	-1000	1000	0	Membrane Transport: Ions and Gases	Non-enzymatic		rxn05532	META:TRANS-RXN0-559
FE2abc	Iron (II) transport via ABC system	atp[c] + fe2[e] + h2o[c] -> adp[c] + fe2[c] + pi[c] + h[c]	L_RS01015 and L_RS01740	BZO99_RS02955 and BZO99_RS02230	0	1000	0	Membrane Transport: Ions and Gases	3.A.1.-		rxn05555	
FE3abc	Iron (III) transport via ABC system	atp[c] + fe3[e] + h2o[c] -> adp[c] + fe3[c] + pi[c] + h[c]	L_RS01740 and L_RS01745 and L_RS01750	BZO99_RS02230 and BZO99_RS02225 and BZO99_RS02220	0	1000	0	Membrane Transport: Ions and Gases	7.2.2.7; 3.6.3.30; 3.A.1.14.28		rxn05195	META:3.6.3.30-RXN
FE3DCITexs	Dicitrate Fe(III) binding (spontaneous)	2 cit[e] + fe3[e] -> fe3dcit[e]	s0001	s0001	0	1000	0	Membrane Transport: Ions and Gases				
H2Ot	H2O transport via diffusion	h2o[e] <=> h2o[c]	s0001	s0001	-1000	1000	0	Membrane Transport: Ions and Gases	Non-enzymatic		rxn05319; rxn08686; rxn08687; rxn09643; rxn09745; rxn09812; rxn09838; rxn09874	META:TRANS-RXN0-547; META:TRANS-RXN-145
H2St1	H2s transport (diffusion)	h2s[c] <=> h2s[e]	s0001	s0001	-1000	1000	0	Membrane Transport: Ions and Gases	Non-enzymatic		rxn08689	META:TRANS-RXN-310
Kt1	Potassium transport via uniport (facilitated diffusion)	k[e] -> k[c]	L_RS04805	BZO99_RS04910	0	1000	0	Membrane Transport: Ions and Gases	1.A.1.1.1		rxn05206	META:TRANS-RXN-185
Kt2r	Potassium reversible transport via proton symport	h[e] + k[e] -> h[c] + k[c]	L_RS03340	BZO99_RS05945	0	1000	0	Membrane Transport: Ions and Gases	2.A.72.1.3		rxn05595	META:TRANS-RXN-3
MG2abc	Magnesium transport via ABC system	atp[c] + h2o[c] + mg2[e] -> adp[c] + h[c] + mg2[c] + pi[c]	L_RS06590	BZO99_RS08130	0	1000	0	Membrane Transport: Ions and Gases	3.6.3.2		rxn08924	META:3.6.3.2-RXN; META:TRANS-RXN-250

MGt5	Magnesium transport in/out via permease (no H+)	mg2[c] <=> mg2[e]	L_RS01635 or L_RS07750	BZO99_RS02335 or BZO99_RS05710	-1000	1000	0	Membrane Transport: Ions and Gases		rxn05616; rxn08922; rxn08923	META:TRANS-RXN-141
MNabc	Manganese transport via ABC system	atp[c] + h2o[c] + mn2[e] -> adp[c] + pi[c] + h[c] + mn2[c]	L_RS06895 and L_RS06890 and L_RS06885 and L_RS11080	BZO99_RS08380 and BZO99_RS08385 and BZO99_RS08390 and BZO99_RS06735	0	1000	0	Membrane Transport: Ions and Gases	3.6.3.35	rxn05149	META:3.6.3.35-RXN
NAt3_1	Sodium proton antiporter HNA is 11	na1[c] + h[e] <=> h[c] + na1[e]	L_RS02005 or RS10035	BZO99_RS04765 or RS10035	-1000	1000	0	Membrane Transport: Ions and Gases		rxn05209; rxn08984	META:TRANS-RXN-101
NH4t	Ammonia reversible transport	nh4[e] <=> nh4[c]	L_RS08305	BZO99_RS01655	-1000	1000	0	Membrane Transport: Ions and Gases	1.A.11	rxn05466; rxn08986; rxn08987; rxn09736; rxn09835; rxn13364	META:RXN-9615; META:TRANS-RXN0-206; META:TRANS-RXN0-544
O2t	O2 transport diffusion	o2[e] -> o2[c]	s0001	s0001	-1000	1000	0	Membrane Transport: Ions and Gases	Non-enzymatic	rxn05468; rxn09031; rxn09032; rxn09641; rxn09734	META:TRANS-RXN0-474
PIabc	Phosphate transport via ABC system	atp[c] + pi[e] + h2o[c] -> adp[c] + 2 pi[c] + h[c]	(L_RS08950 or L_RS08955) and L_RS08960 and L_RS08965 and L_RS08970 and L_RS08975	(BZO99_RS04050 or BZO99_RS04045) and BZO99_RS04040 and BZO99_RS04035 and BZO99_RS04030 and BZO99_RS04025	0	1000	0	Membrane Transport: Ions and Gases	7.3.2.1; 3.A.1	rxn05145; rxn09122	META:ABC-27-RXN
PPIabc	Diphosphate transport in via ABC system	atp[c] + ppi[e] + h2o[c] -> adp[c] + pi[c] + ppi[c] + h[c]	L_RS08950 and L_RS08955 and L_RS08960 and L_RS08965 and L_RS08970 and L_RS08975	BZO99_RS04050 and BZO99_RS04045 and BZO99_RS04040 and BZO99_RS04035 and BZO99_RS04030 and BZO99_RS04025	0	1000	0	Membrane Transport: Ions and Gases	3.A.1	rxn05635	
SO4t2	sulphate transport in via proton symport	h[e] + so4[e] -> h[c] + so4[c]			0	1000	0	Membrane Transport: Ions and Gases		rxn05651	
ZN2t4	Zinc transport out via antiport	h[e] + k[e] + zn2[c] -> h[c] + k[c] + zn2[e]	L_RS08380	BZO99_RS01735	0	1000	0	Membrane Transport: Ions and Gases	2.A.4.1.7	rxn05315	
ZNabc	Zinc transport via ABC system	atp[c] + h2o[c] + zn2[e] -> adp[c] + pi[c] + h[c] + zn2[c]	L_RS11080 and L_RS11085 and L_RS11090	BZO99_RS06735 and BZO99_RS06730 and BZO99_RS06725	0	1000	0	Membrane Transport: Ions and Gases	7.2.2.12; 3.6.3.5	rxn05150	META:ABC-63-RXN
2H3MBt	2-Hydroxy-Isovalerate transport	2hiv[c] + h[c] -> 2hiv[e] + h[e]			0	1000	0	Membrane Transport: Metabolism Products			
2H3MPt	2-Hydroxy-3-Methyl-Valerate transport	2h3mv[c] + h[c] -> 2h3mv[e] + h[e]			0	1000	0	Membrane Transport: Metabolism Products			
2HXICt	L-2-hydroxycaproate transport	2hxic__L[c] + h[c] <=> 2hxic__L[e] + h[e]			-1000	1000	0	Membrane Transport: Metabolism Products	2.A.3		
2MBALDt	2 Methylbutanal transport extracellular	2mbald[c] <=> 2mbald[e]			-1000	1000	0	Membrane Transport: Metabolism Products		rxn13189	
2MBAt6	2-Methylbutyric acid transport H symport	m2but[c] + h[c] <=> m2but[e] + h[e]			-1000	1000	0	Membrane Transport: Metabolism Products			
2MPAt6	Isobutyric acid transport H symport	isobuta[c] + h[c] <=> isobuta[e] + h[e]			-1000	1000	0	Membrane Transport: Metabolism Products			
3MBAt6	3-Methylbutanoic acid transport H symport	3mb[c] + h[c] <=> 3mb[e] + h[e]			-1000	1000	0	Membrane Transport: Metabolism Products			
ABUTt2r	4 aminobutyrate reversible transport in via proton symport	4abut[e] + h[e] <=> 4abut[c] + h[c]			-1000	1000	0	Membrane Transport: Metabolism Products	2.A.3	rxn05564; rxn08027	META:TRANS-RXN-57
ACALDt	Acetaldehyde reversible transport	acald[e] <=> acald[c]	s0001	s0001	-1000	1000	0	Membrane Transport: Metabolism Products	Non-enzymatic	rxn08032; rxn08033; rxn09700; rxn13212	
ACt2r	Acetate reversible transport via proton symport	ac[e] + h[e] <=> ac[c] + h[c]			-1000	1000	0	Membrane Transport: Metabolism Products	2.A.21	rxn05488; rxn08061	META:TRANS-RXN0-571
ACTNdiff	R acetoin diffusion	actn__R[e] <=> actn__R[c]	s0001	s0001	-1000	1000	0	Membrane Transport: Metabolism Products	Non-enzymatic		
AKGt2r	2 oxoglutarate reversible transport	akg[e] + h[e] <=> akg[c] + h[c]			-1000	1000	0	Membrane Transport: Metabolism Products		rxn05493	META:TRANS-RXN-23

	via symport										
BTDt_RR	R R butanediol transport	btd_RR[c] <=> btd_RR[e]			-1000	1000	0	Membrane Transport: Metabolism Products		rxn11322	
CH4St	Methanethiol diffusion	ch4s[e] <=> ch4s[c]	s0001	s0001	-1000	1000	0	Membrane Transport: Metabolism Products	Non-enzymatic	rxn10470	
D_LACt2	D-lactate transport via proton symport	h[e] + lac__D[e] <=> h[c] + lac__D[c]			-1000	1000	0	Membrane Transport: Metabolism Products		rxn08350	META:TRANS-RXN0-515
DIACTt	Diacetyl diffusion	diact[c] <=> diact[e]	s0001	s0001	-1000	1000	0	Membrane Transport: Metabolism Products	Non-enzymatic	rxn11325	
ETOHt	Ethanol reversible transport	etoh[e] <=> etoh[c]			-1000	1000	0	Membrane Transport: Metabolism Products		rxn08428; rxn09683; rxn09764	META:TRANS-RXN0-546
FORt2	Formate transport in via proton symport	for[e] + h[e] <=> for[c] + h[c]	L_RS05080	BZO99_RS00185	-1000	1000	0	Membrane Transport: Metabolism Products	1.A.16	rxn05559; rxn08524	
GCALDt	Glycoaldehydye reversible transport	gcald[e] <=> gcald[c]			-1000	1000	0	Membrane Transport: Metabolism Products		rxn09680	
GLYBabc	Glycine betaine transport via ABC system	atp[c] + glyb[e] + h2o[c] -> adp[c] + pi[c] + glyb[c] + h[c]	(L_RS04470 and L_RS04465) or (L_RS07595 and L_RS07590)	(BZO99_RS05240 and BZO99_RS05245) or (BZO99_RS05555 and BZO99_RS05550)	0	1000	0	Membrane Transport: Metabolism Products		rxn05181	META:TRANS-RXN-283
GLYBt2r	Glycine betaine transport via proton symport, reversible	h[e] + glyb[e] <=> h[c] + glyb[c]	L_RS04465	BZO99_RS05245	-1000	1000	0	Membrane Transport: Metabolism Products		rxn05579	META:TRANS-RXN-29A
GLYC3Pt6	Glycerol-3-phosphate : phosphate antiporter	pi[c] + glyc3p[e] -> pi[e] + glyc3p[c]	L_RS03000	BZO99_RS06285	0	1000	0	Membrane Transport: Metabolism Products	2.A.1.4	rxn08642; rxn10165	META:TRANS-RXN-22
GLYCt	Glycerol transport via channel	glyc[c] <=> glyc[e]	L_RS06530 or L_RS08460 or L_RS10760	BZO99_RS10055 or BZO99_RS01815 or BZO99_RS07690	-1000	1000	0	Membrane Transport: Metabolism Products	2.A.50	rxn05581; rxn08654; rxn08658	META:TRANS-RXN-131
L_LACt2r	L lactate reversible transport via proton symport	lac__L[e] + h[e] <=> lac__L[c] + h[c]			-1000	1000	0	Membrane Transport: Metabolism Products	2.A.1	rxn05602; rxn08794; rxn13334	META:TRANS-RXN-104
PACALDt	Phenylacetaldehyde transport extracellular	pacald[c] <=> pacald[e]			-1000	1000	0	Membrane Transport: Metabolism Products		rxn09061	META:META:TRANS-RXN0-284
PEAt	Phenylethylalcohol transport	pea[c] <=> pea[e]			-1000	1000	0	Membrane Transport: Metabolism Products		rxn13196	
PYRt2	Pyruvate transport in via proton symport	pyr[e] + h[e] <=> pyr[c] + h[c]			-1000	1000	0	Membrane Transport: Metabolism Products	2.A.21	rxn05469; rxn09217; rxn09717; rxn09832	META:TRANS-RXN-335
SUCCt2r	Succinate transport via proton symport	h[e] + succ[e] <=> h[c] + succ[c]			-1000	1000	0	Membrane Transport: Metabolism Products		rxn05654	
ADEt2	Adenine transport in via proton symport	ade[e] + h[e] <=> ade[c] + h[c]			-1000	1000	0	Membrane Transport: Nucleosides, Vitamins and Fatty Acids	2.A.39	rxn05491; rxn08064	META:TRANS-RXN0-447; META:TRANS-RXN-198
BTNt2i	Biotin uptake	btn[e] + h[e] -> btn[c] + h[c]	L_RS01670 or L_RS09285	BZO99_RS02300 or BZO99_RS03720	0	1000	0	Membrane Transport: Nucleosides, Vitamins and Fatty Acids		rxn09693	
CHLabc	Choline transport via ABC system	atp[c] + chol[e] + h2o[c] -> adp[c] + chol[c] + pi[c] + h[c]	L_RS04470 and L_RS04465	BZO99_RS05240 and BZO99_RS05245	0	1000	0	Membrane Transport: Nucleosides, Vitamins and Fatty Acids	3.A.1	rxn05159; rxn08212	META:TRANS-RXN-319
CITt2r	Citrate reversible transport via symport	cit[e] + h[e] <=> cit[c] + h[c]	L_RS04735	BZO99_RS04980	-1000	1000	0	Membrane Transport: Nucleosides, Vitamins and Fatty Acids		rxn05211	
FOLt	Folate transport via proton simport	fol[e] + h[e] <=> fol[c] + h[c]			-1000	1000	0	Membrane Transport: Nucleosides, Vitamins and Fatty Acids	2.A	rxn05255	
GUAt2r	Guanine reversible transport via proton symport	gua[e] + h[e] -> gua[c] + h[c]	L_RS09025	BZO99_RS03975	0	1000	0	Membrane Transport: Nucleosides, Vitamins and Fatty Acids	2.A.39	rxn05203; rxn08681	
HXANt2r	Hypoxanthine reversible transport via proton symport	h[e] + hxan[e] -> h[c] + hxan[c]	L_RS09025	BZO99_RS03975	0	1000	0	Membrane Transport: Nucleosides, Vitamins and Fatty Acids	2.A	rxn05201	
INOST_Et	Myo-Inositol transport	inost[e] <=> inost[c]	L_RS01180	BZO99_RS02790	-1000	1000	0	Membrane Transport: Nucleosides, Vitamins and Fatty Acids			
INSt2	Inosine transport in via proton symport	ins[e] + h[e] <=> ins[c] + h[c]	L_RS06960 and L_RS06965	BZO99_RS08320 and BZO99_RS08315	-1000	1000	0	Membrane Transport: Nucleosides, Vitamins and Fatty Acids		rxn05316	META:TRANS-RXN-108G

LIPOPBt	Lipoate transport via proton symport	h[e] + lipoate[e] -> h[c] + lipoate[c]	L_RS00380	BZO99_RS08765	0	1000	0	Membrane Transport: Nucleosides, Vitamins and Fatty Acids					
NACt	Nicotinic acid transport	nac[e] -> nac[c]	L_RS06085	BZO99_RS01225	0	1000	0	Membrane Transport: Nucleosides, Vitamins and Fatty Acids			rxn05310		
NCAMUP	Nicotinamide acid uptake	ncam[e] -> ncam[c]	L_RS06085	BZO99_RS01225	0	1000	0	Membrane Transport: Nucleosides, Vitamins and Fatty Acids			rxn10867		
OROATP	Orotic acid transport inout via proton symporter	h[e] + orot[e] <=> h[c] + orot[c]			-1000	1000	0	Membrane Transport: Nucleosides, Vitamins and Fatty Acids			rxn10978		
PDXt2	Pyridoxin transport via proton symport	h[e] + pydxn[e] -> h[c] + pydxn[c]	L_RS02570	BZO99_RS04470	0	1000	0	Membrane Transport: Nucleosides, Vitamins and Fatty Acids					
PNTOt2	Pantothenate reversible transport via proton symport	pnto__R[e] + h[e] <=> pnto__R[c] + h[c]	L_RS03085	BZO99_RS06200	-1000	1000	0	Membrane Transport: Nucleosides, Vitamins and Fatty Acids	2.A.1		rxn05308		
PYDAMt	Pyridoxamine transport	h[e] + pydam[e] <=> h[c] + pydam[c]			-1000	1000	0	Membrane Transport: Nucleosides, Vitamins and Fatty Acids					
PYDXtr	Pyridoxal transport via diffusion	pydx[e] <=> pydx[c]			-1000	1000	0	Membrane Transport: Nucleosides, Vitamins and Fatty Acids			rxn12666	META:TRANS-RXN0-214	
RIBFLVt2	Riboflavin transport in via proton symport	ribflv[e] + h[e] -> ribflv[c] + h[c]	L_RS06680	BZO99_RS08040	0	1000	0	Membrane Transport: Nucleosides, Vitamins and Fatty Acids	2.A.87		rxn05645		
RNAMTPP_1	Nicotinamide riboside transport	rnam[e] -> rnam[c]			0	1000	0	Membrane Transport: Nucleosides, Vitamins and Fatty Acids			rxn10181		
THMabc	Thiamine transport via ABC system	atp[c] + h2o[c] + thm[e] -> adp[c] + pi[c] + h[c] + thm[c]	L_RS01725 and L_RS01720 and L_RS01680	BZO99_RS02245 and BZO99_RS02250 and BZO99_RS02290	0	1000	0	Membrane Transport: Nucleosides, Vitamins and Fatty Acids	2.A.88.3.2		rxn05177; rxn09297	META:ABC-32-RXN	
THMDt2	Thymidine transport in via proton symport	h[e] + thymd[e] -> h[c] + thymd[c]			0	1000	0	Membrane Transport: Nucleosides, Vitamins and Fatty Acids			rxn05200; rxn09298	META:TRANS-RXN-108H	
THYMt	Thymine reversible transport via facilated diffusion	thym[e] <=> thym[c]			-1000	1000	0	Membrane Transport: Nucleosides, Vitamins and Fatty Acids			rxn09309	META:TRANS-RXN0-524	
URAt2	Uracil transport in via proton symport	h[e] + ura[e] -> h[c] + ura[c]	L_RS09025 or L_RS08360 or L_RS06015	BZO99_RS03975 or BZO99_RS01715 or BZO99_RS01150	0	1000	0	Membrane Transport: Nucleosides, Vitamins and Fatty Acids	2.A.40.1.2		rxn05197; rxn09365	META:TRANS-RXN-132	
XANt2	Xanthine transport in via proton symport	h[e] + xan[e] -> h[c] + xan[c]	L_RS09025 or L_RS08360 or L_RS06015	BZO99_RS03975 or BZO99_RS01715 or BZO99_RS01150	0	1000	0	Membrane Transport: Nucleosides, Vitamins and Fatty Acids	2.A.40.3.1		rxn05202; rxn09377	META:RXN-5076; META:TRANS-RXN-206	
4ABZt	4 Aminobenzoate mitochondrial transport via diffusion	4abz[c] <=> 4abz[e]	s0001	s0001	-1000	1000	0	Membrane Transport: Organic Acids	Non-enzymatic		rxn09794		
CITRt2r	Citrulline reversible transport via proton symport	citr__L[e] + h[e] <=> citr__L[c] + h[c]	L_RS09460	BZO99_RS03545	-1000	1000	0	Membrane Transport: Organic Acids			rxn05674		
CITt4_1	Citrate transport via sodium symport	cit[e] + na1[e] -> cit[c] + na1[c]	L_RS04735	BZO99_RS04980	0	1000	0	Membrane Transport: Organic Acids					
GLCNt2r	D-gluconate transport via proton symport, reversible	glcn[e] + h[e] <=> glcn[c] + h[c]			-1000	1000	0	Membrane Transport: Organic Acids			rxn05571	META:TRANS-RXN0-209	
MALt4	Namalate symporter	mal__L[e] + na1[e] <=> mal__L[c] + na1[c]	L_RS04735	BZO99_RS04980	-1000	1000	0	Membrane Transport: Organic Acids			rxn05207		
MNLpts	Mannitol transport via PEP:Pyr PTS	mnl[e] + pep[c] -> pyr[c] + mnl1p[c]	L_RS00165 and L_RS00660 and L_RS00665	BZO99_RS09030 and BZO99_RS08560 and BZO99_RS08555	0	1000	0	Membrane Transport: Organic Acids	2.7.1.197; 4.A.2	R02704	rxn05617; rxn08949; rxn13934; rxn13944	META:TRANS-RXN-156	
PTRCabc	Putrescine transport via ABC system	atp[c] + ptrc[e] + h2o[c] -> adp[c] + pi[c] + ptrc[c] + h[c]	L_RS06095 and L_RS06100 and L_RS06105 and L_RS06110	BZO99_RS01235 and BZO99_RS01240 and BZO99_RS01245 and BZO99_RS01250	0	1000	0	Membrane Transport: Organic Acids	7.6.2.11; 3.A.1.11		rxn05163; rxn09213; rxn11263	META:ABC-25-RXN	
SBTpts	D-sorbitol transport via PEP:Pyr PTS	sbt__D[e] + pep[c] -> pyr[c] + sbt6p[c]	L_RS00660 and L_RS00665	BZO99_RS08560 and BZO99_RS08555	0	1000	0	Membrane Transport: Organic Acids	2.7.1.198	R05820	rxn09242	META:TRANS-RXN-169	
SPMDabc	Spermidine transport via ABC system	atp[c] + h2o[c] + spmd[e] -> adp[c] + pi[c] + h[c] + spmd[c]	L_RS06095 and L_RS06100 and L_RS06105 and L_RS06110	BZO99_RS01235 and BZO99_RS01240 and BZO99_RS01245 and BZO99_RS01250	0	1000	0	Membrane Transport: Organic Acids	7.6.2.11; 3.A.1.11		rxn05175; rxn09263; rxn11262	META:ABC-24-RXN	
FRDO5r	Ferredoxin	fdxr_42[c] + h[c] +	L_RS08590	BZO99_RS01940	-1000	1000	0	Miscellaneous: Others					

	oxidoreductase	nadp[c] <=> fdxo_42[c] + nadph[c]										
HCO3E	HCO3 equilibration reaction	co2[c] + h2o[c] <=> h[c] + hco3[c]			-1000	1000	0	Miscellaneous: Others	4.2.1.1	R10092; R00132	rxn00102	META:CARBODEHYDRAT-RXN; META:RXN0-5224
SPODM	Superoxide dismutase	2 h[c] + 2 o2s[c] -> h2o2[c] + o2[c]	L_RS02130	BZO99_RS04640	0	1000	0	Miscellaneous: Others	1.15.1.1	R00275	rxn00206	META:SUPEROX-DISMUT-RXN
THIORDXi	Hydrogen peroxide reductase (thioredoxin)	h2o2[c] + trdrd[c] -> 2 h2o[c] + trdox[c]	L_RS08575	BZO99_RS01925	0	1000	0	Miscellaneous: Others	1.11.1.24; 1.11.1.15; 1.11.1.16		rxn09296	META:RXN0-267
ADA	Adenosine deaminase	adn[c] + h2o[c] + h[c] -> ins[c] + nh4[c]	L_RS03840 or L_RS01530	BZO99_RS10900 or BZO99_RS02440	0	1000	0	Nucleotide Metabolism: Nucleotide Salvage Pathway	3.5.4.4	R01560	rxn01137	META:ADENODEAMIN-RXN
ADADir	Deoxycytidine kinase	dcyt[c] + atp[c] <=> dcmp[c] + adp[c] + h[c]	L_RS08655	BZO99_RS02005	-1000	1000	0	Nucleotide Metabolism: Nucleotide Salvage Pathway	2.7.1.145; 2.7.1.213; 2.7.1.74	R01666	rxn01220	META:RXN-14093
ADK3	Adentylate kinase (GTP)	gtp[c] + amp[c] <=> adp[c] + gdp[c]	L_RS10900	BZO99_RS06915	-1000	1000	0	Nucleotide Metabolism: Nucleotide Salvage Pathway	2.7.4.10; 2.7.4.4			
ADK4	Adentylate kinase (ITP)	itp[c] + amp[c] <=> adp[c] + idp[c]	L_RS10900	BZO99_RS06915	-1000	1000	0	Nucleotide Metabolism: Nucleotide Salvage Pathway				
ADKd	Adenylate kinase (d form)	damp[c] + datp[c] <=> 2 dadp[c]	L_RS10900	BZO99_RS06915	-1000	1000	0	Nucleotide Metabolism: Nucleotide Salvage Pathway			rxn10427	
ADNK1	Adenosine kinase	atp[c] + adn[c] -> h[c] + adp[c] + amp[c]	L_RS10900	BZO99_RS06915	0	1000	0	Nucleotide Metabolism: Nucleotide Salvage Pathway	2.7.1.74; 2.7.1.20	R00185	rxn00134	META:ADENOSINE-KINASE-RXN
CSND	Cytosine deaminase	csn[c] + h2o[c] + h[c] -> nh4[c] + ura[c]	L_RS03840	BZO99_RS10900	0	1000	0	Nucleotide Metabolism: Nucleotide Salvage Pathway	3.5.4.1	R00974	rxn00717	META:CYTDEAM-RXN
DADA	Deoxyadenosine deaminase	dad_2[c] + h2o[c] + h[c] -> din[c] + nh4[c]	L_RS01530	BZO99_RS02440	0	1000	0	Nucleotide Metabolism: Nucleotide Salvage Pathway	3.5.4.4	R02556	rxn01858	META:ADDALT-RXN
DADNK	Deoxyadenosine kinase	dad_2[c] + atp[c] -> damp[c] + adp[c] + h[c]	L_RS06070 or L_RS02615	BZO99_RS01210 or BZO99_RS04425	0	1000	0	Nucleotide Metabolism: Nucleotide Salvage Pathway	2.7.1.145; 2.7.1.74; 2.7.1.76	R02089	rxn01508	META:DEOXYADENOSINE-KINASE-RXN
DCMPDA	DCMP deaminase	dcmp[c] + h[c] + h2o[c] -> dump[c] + nh4[c]	L_RS05985	BZO99_RS01120	0	1000	0	Nucleotide Metabolism: Nucleotide Salvage Pathway	3.5.4.12	R01663	rxn01217	META:DCMP-DEAMINASE-RXN
DGNSK	Deoxyguanosine kinase	dgsn[c] + atp[c] -> adp[c] + dgmp[c] + h[c]	L_RS02615 or L_RS06070	BZO99_RS04425 or BZO99_RS01210	0	1000	0	Nucleotide Metabolism: Nucleotide Salvage Pathway	2.7.1.113; 2.7.1.145; 2.7.1.74	R01967	rxn01444	META:DEOXYGUANOSINE-KINASE-RXN
DURIK1	Deoxyuridine kinase (ATP:Deoxyuridine)	duri[c] + atp[c] -> adp[c] + dump[c] + h[c]	L_RS03195	BZO99_RS06090	0	1000	0	Nucleotide Metabolism: Nucleotide Salvage Pathway	2.7.1.145; 2.7.1.21	R02099	rxn01518	META:DURIDKI-RXN
GK1	Guanylate kinase (GMP:ATP)	atp[c] + gmp[c] <=> adp[c] + gdp[c]	L_RS09890	BZO99_RS10625	-1000	1000	0	Nucleotide Metabolism: Nucleotide Salvage Pathway	2.7.4.8	R00332	rxn00239	META:GUANYL-KIN-RXN
GK2	Guanylate kinase GMPdATP	datp[c] + gmp[c] <=> dadp[c] + gdp[c]	L_RS09890	BZO99_RS10625	-1000	1000	0	Nucleotide Metabolism: Nucleotide Salvage Pathway	2.7.4.8		rxn09562	
HXPRT	Hypoxanthine phosphoribosyltransferase (Hypoxanthine)	prpp[c] + hxan[c] -> ppi[c] + imp[c]	L_RS07925 or L_RS00105	BZO99_RS10325 or BZO99_RS08970	0	1000	0	Nucleotide Metabolism: Nucleotide Salvage Pathway	2.4.2.8	R01132	rxn00836	META:HYPOXANPRIBOSYLTRAN-RXN
NDPK1	Nucleoside-diphosphate kinase (ATP:GDP)	atp[c] + gdp[c] <=> adp[c] + gtp[c]	L_RS06980 or L_RS10900	BZO99_RS08300 or BZO99_RS06915	-1000	1000	0	Nucleotide Metabolism: Nucleotide Salvage Pathway	2.7.4.6	R00330	rxn00237	META:GDPKIN-RXN
NDPK2	Nucleoside-diphosphate kinase (ATP:UDP)	atp[c] + udp[c] <=> adp[c] + utp[c]	L_RS10900	BZO99_RS06915	-1000	1000	0	Nucleotide Metabolism: Nucleotide Salvage Pathway	2.7.4.6	R00156	rxn00117	META:UDPKIN-RXN
NDPK3	Nucleoside-diphosphate kinase (ATP:CDP)	atp[c] + cdp[c] <=> ctp[c] + adp[c]	L_RS06980 or L_RS10900	BZO99_RS08300 or BZO99_RS06915	-1000	1000	0	Nucleotide Metabolism: Nucleotide Salvage Pathway	2.7.4.6	R00570	rxn00409	META:CDPKIN-RXN
NDPK4	Nucleoside-diphosphate kinase (ATP:dTDP)	dtdp[c] + atp[c] <=> adp[c] + dttp[c]	L_RS10900	BZO99_RS06915	-1000	1000	0	Nucleotide Metabolism: Nucleotide Salvage Pathway	2.7.4.6	R02093	rxn01512	META:DTDPKIN-RXN
NDPK5	Nucleoside-diphosphate kinase (ATP:dGDP)	dgdp[c] + atp[c] <=> adp[c] + dgtp[c]	L_RS10900	BZO99_RS06915	-1000	1000	0	Nucleotide Metabolism: Nucleotide Salvage Pathway	2.7.4.6	R01857	rxn01353	META:DGDPKIN-RXN
NDPK6	Nucleoside-	dudp[c] + atp[c] <=>	L_RS10900	BZO99_RS06915	-1000	1000	0	Nucleotide Metabolism: Nucleotide	2.7.4.6	R02331	rxn01678	META:DUDPKIN-

	diphosphate kinase (ATP:dUDP)	adp[c] + dutp[c]						Salvage Pathway				RXN
NDPK7	Nucleoside-diphosphate kinase (ATP:dCDP)	dcdp[c] + atp[c] <=> dctp[c] + adp[c]	L_RS10900	BZO99_RS06915	-1000	1000	0	Nucleotide Metabolism: Nucleotide Salvage Pathway	2.7.4.6	R02326	rxn01673	META:DCDPKIN-RXN
NDPK8	Nucleoside-diphosphate kinase (ATP:dADP)	dadp[c] + atp[c] <=> datp[c] + adp[c]	L_RS10900	BZO99_RS06915	-1000	1000	0	Nucleotide Metabolism: Nucleotide Salvage Pathway	2.7.4.6	R01137	rxn00839	META:DADPKIN-RXN
NTD1	5'-nucleotidase (dUMP)	h2o[c] + dump[c] -> duri[c] + pi[c]	L_RS07915	BZO99_RS10335	0	1000	0	Nucleotide Metabolism: Nucleotide Salvage Pathway	3.1.3.5; 3.1.3.89	R02102	rxn01521	META:RXN-14143
NTD5	5'-nucleotidase (dTMP)	dtmp[c] + h2o[c] -> pi[c] + thymd[c]	L_RS07915	BZO99_RS10335	0	1000	0	Nucleotide Metabolism: Nucleotide Salvage Pathway	3.1.3.35; 3.1.3.89; 3.1.3.5	R01569	rxn01145	META:THYMIDYLATE-5-PHOSPHATASE-RXN
NTP10	Nucleoside-triphosphatase (ITP)	h2o[c] + itp[c] -> h[c] + pi[c] + idp[c]	L_RS10100	BZO99_RS10440	0	1000	0	Nucleotide Metabolism: Nucleotide Salvage Pathway	3.6.1; 3.6.1.5	R00719	rxn00513	META:RXN0-5073
NTP5	Nucleoside-triphosphatase (CTP)	ctp[c] + h2o[c] -> h[c] + pi[c] + cdp[c]	L_RS10100	BZO99_RS10440	0	1000	0	Nucleotide Metabolism: Nucleotide Salvage Pathway	3.6.1.5; 3.6.1.15	R00569	rxn00408	META:RXN-12195
PUNP1	Purine-nucleoside phosphorylase (Adenosine)	adn[c] + pi[c] <=> ade[c] + r1p[c]	L_RS04890	BZO99_RS04825	-1000	1000	0	Nucleotide Metabolism: Nucleotide Salvage Pathway	2.4.2.1	R01561	rxn01138	META:ADENPHOSPHOR-RXN
PUNP2	Purine-nucleoside phosphorylase (Deoxyadenosine)	dad_2[c] + pi[c] <=> 2dr1p[c] + ade[c]	L_RS04890	BZO99_RS04825	-1000	1000	0	Nucleotide Metabolism: Nucleotide Salvage Pathway	2.4.2.1	R02557	rxn01859	META:DEOXYADENPHOSPHOR-RXN
PUNP3	Purine-nucleoside phosphorylase (Guanosine)	pi[c] + gsn[c] <=> r1p[c] + gua[c]	L_RS04890	BZO99_RS04825	-1000	1000	0	Nucleotide Metabolism: Nucleotide Salvage Pathway	2.4.2.1; 2.4.2.15	R02147	rxn01548	META:RXN0-5199
PUNP4	Purine-nucleoside phosphorylase (Deoxyguanosine)	dgsn[c] + pi[c] <=> 2dr1p[c] + gua[c]	L_RS04890	BZO99_RS04825	-1000	1000	0	Nucleotide Metabolism: Nucleotide Salvage Pathway	2.4.2.1; 2.4.2.4	R01969	rxn01446	META:DEOXYGUANPHOSPHOR-RXN
PUNP5	Purine-nucleoside phosphorylase (Inosine)	ins[c] + pi[c] <=> r1p[c] + hxan[c]	L_RS04890	BZO99_RS04825	-1000	1000	0	Nucleotide Metabolism: Nucleotide Salvage Pathway	2.4.2.1; 2.4.2.15	R01863	rxn01358	META:INOPHOSPHOR-RXN
PUNP6	Purine-nucleoside phosphorylase (Deoxyinosine)	din[c] + pi[c] <=> 2dr1p[c] + hxan[c]	L_RS04890	BZO99_RS04825	-1000	1000	0	Nucleotide Metabolism: Nucleotide Salvage Pathway	2.4.2.1; 2.4.2.4	R02748	rxn01985	META:DEOXYINOPHOSPHOR-RXN
PUNP7	Purine-nucleoside phosphorylase (Xanthosine)	pi[c] + xtsn[c] <=> r1p[c] + xan[c]	L_RS04890	BZO99_RS04825	-1000	1000	0	Nucleotide Metabolism: Nucleotide Salvage Pathway	2.4.2.-; 2.4.2.1	R02297	rxn01649	META:XANTHOSINEPHOSPHORY-RXN
RNDR1	Ribonucleoside-diphosphate reductase (ADP)	adp[c] + trdrd[c] -> dadp[c] + h2o[c] + trdox[c]	L_RS05115 and L_RS05110 and L_RS05120	BZO99_RS00225 and BZO99_RS00220 and BZO99_RS00230	0	1000	0	Nucleotide Metabolism: Nucleotide Salvage Pathway	1.17.4.1	R02017	rxn05231	META:ADPREDUCT-RXN
RNDR2	Ribonucleoside-diphosphate reductase (GDP)	gdp[c] + trdrd[c] -> dgdp[c] + h2o[c] + trdox[c]	L_RS05115 and L_RS05110 and L_RS05120	BZO99_RS00225 and BZO99_RS00220 and BZO99_RS00230	0	1000	0	Nucleotide Metabolism: Nucleotide Salvage Pathway	1.17.4.1	R02019	rxn05233	META:GDPREDUCT-RXN
RNDR3	Ribonucleoside-diphosphate reductase (CDP)	cdp[c] + trdrd[c] -> dcdp[c] + h2o[c] + trdox[c]	L_RS05115 and L_RS05110 and L_RS05120	BZO99_RS00225 and BZO99_RS00220 and BZO99_RS00230	0	1000	0	Nucleotide Metabolism: Nucleotide Salvage Pathway	1.17.4.1	R02024	rxn06076	META:CDPREDUCT-RXN
RNDR4	Ribonucleoside-diphosphate reductase (UDP)	trdrd[c] + udp[c] -> dudp[c] + h2o[c] + trdox[c]	L_RS05115 and L_RS05110 and L_RS05120	BZO99_RS00225 and BZO99_RS00220 and BZO99_RS00230	0	1000	0	Nucleotide Metabolism: Nucleotide Salvage Pathway	1.17.4.1	R02018	rxn06075	META:UDPREDUCT-RXN
RNTR1	Ribonucleoside triphosphate reductase ATP	atp[c] + trdrd[c] -> datp[c] + h2o[c] + trdox[c]	L_RS01450 or L_RS01445	BZO99_RS02520 or BZO99_RS02525	0	1000	0	Nucleotide Metabolism: Nucleotide Salvage Pathway	1.17.4.2	R02014	rxn05232	META:1.17.4.2-RXN
RNTR2	Ribonucleoside triphosphate reductase GTP	gtp[c] + trdrd[c] -> dgtp[c] + h2o[c] + trdox[c]	L_RS01450 or L_RS01445	BZO99_RS02520 or BZO99_RS02525	0	1000	0	Nucleotide Metabolism: Nucleotide Salvage Pathway	1.17.4.2	R02020	rxn05234	META:1.17.4.2-RXN
RNTR3	Ribonucleoside triphosphate reductase CTP	ctp[c] + trdrd[c] -> dctp[c] + h2o[c] + trdox[c]	L_RS01450 or L_RS01445	BZO99_RS02520 or BZO99_RS02525	0	1000	0	Nucleotide Metabolism: Nucleotide Salvage Pathway	1.17.4.2	R02022	rxn05235	META:1.17.4.2-RXN
RNTR4	Ribonucleoside triphosphate reductase UTP	trdrd[c] + utp[c] -> dutp[c] + h2o[c] + trdox[c]	L_RS01450 or L_RS01445	BZO99_RS02520 or BZO99_RS02525	0	1000	0	Nucleotide Metabolism: Nucleotide Salvage Pathway	1.17.4.2	R02023	rxn05236	META:1.17.4.2-RXN
TMDK1	Thymidine kinase	atp[c] + thymd[c] ->	L_RS03195	BZO99_RS06090	0	1000	0	Nucleotide Metabolism: Nucleotide	2.7.1.145; 2.7.1.21	R01567	rxn01143	META:THYKI-RXN

	(ATP:thymidine)	adp[c] + dtmp[c] + h[c]						Salvage Pathway				
TMDK2	Thymidine kinase GTPThymidine	gtp[c] + thymd[c] -> dtmp[c] + gdp[c] + h[c]	L_RS03195	BZO99_RS06090	0	1000	0	Nucleotide Metabolism: Nucleotide Salvage Pathway	2.7.1.145; 2.7.1.21			
TMDS	Thymidylate synthase	dump[c] + mlthf[c] -> dhf[c] + dtmp[c]	L_RS08035	BZO99_RS10215	0	1000	0	Nucleotide Metabolism: Nucleotide Salvage Pathway	2.1.1.45	R02101	rxn01520	META:HYMIDYLATESYN-RXN
TRDR	Thioredoxin reductase (NADPH)	h[c] + nadph[c] + trdox[c] -> nadp[c] + trdrd[c]	(L_RS04940 and L_RS08575) or L_RS08590	(BZO99_RS00045 and BZO99_RS01925) or BZO99_RS01940	0	1000	0	Nucleotide Metabolism: Nucleotide Salvage Pathway	1.6.4.5; 1.8.1.9	R02016	rxn05289	META:THIOREDOXIN-REDUCT-NADPH-RXN
XPPT	Xanthine phosphoribosyltransferase	prpp[c] + xan[c] -> ppi[c] + xmp[c]	L_RS06010	BZO99_RS01145	0	1000	0	Nucleotide Metabolism: Nucleotide Salvage Pathway	2.4.2.22; 2.4.2.8	R02142	rxn01544	META:XANPRIBOSYLTRAN-RXN
G1PTT	Glucose-1-phosphate thymidylyltransferase	dttp[c] + g1p[c] + h[c] -> dtdpglu[c] + ppi[c]	L_RS01050	BZO99_RS02920	0	1000	0	Nucleotide Metabolism: Nucleotide Sugars Metabolism	2.7.7.24	R02328	rxn01675	META:DTDPGLUCOSEPP-RXN
TDPDRE	DTDP-4-dehydrorhamnose 3,5-epimerase	dtdp4d6dg[c] -> dtdp4d6dm[c]	L_RS01060	BZO99_RS02910	-1000	1000	0	Nucleotide Metabolism: Nucleotide Sugars Metabolism	5.1.3.13	R06514	rxn02000	META:DTDPDEHYDRHAMEPIM-RXN
TDPDRR	DTDP-4-dehydrorhamnose reductase	dtdp4d6dm[c] + h[c] + nadph[c] <=> dtdprmn[c] + nadp[c]	L_RS01075	BZO99_RS02895	-1000	1000	0	Nucleotide Metabolism: Nucleotide Sugars Metabolism	1.1.1.133	R02777	rxn02003	META:DTDPDEHYRHAMREDUCT-RXN
TDPGDH	DTDPglucose 4,6-dehydratase	dtdpglu[c] -> dtdp4d6dg[c] + h2o[c]	L_RS01070	BZO99_RS02900	0	1000	0	Nucleotide Metabolism: Nucleotide Sugars Metabolism	4.2.1.46	R06513	rxn01997	META:DTDPGLUCDEHYDRAT-RXN
NTPTP1	Nucleoside triphosphate tripolyhydrolase	dgtp[c] + h2o[c] -> dgsn[c] + pppi[c]	L_RS05665	BZO99_RS00795	0	1000	0	Nucleotide Metabolism: Purine and Pyrimidine Biosynthesis	3.1.5.1	R01856	rxn01352	META:DGTPTRIPHYDRO-RXN
YUMPS	YUMP synthetase	r5p[c] + ura[c] <=> psd5p[c] + h2o[c]	L_RS02560 or L_RS05910 or L_RS11755 or L_RS01920 or L_RS05225 or L_RS11075 or L_RS06685	BZO99_RS04480 or BZO99_RS01045 or BZO99_RS09830 or BZO99_RS02045 or BZO99_RS00340 or BZO99_RS06740 or BZO99_RS08035	-1000	1000	0	Nucleotide Metabolism: Purine and Pyrimidine Biosynthesis	4.2.1.70	R01055	rxn15113	META:RXN0-5398
ADK1	Adenylate kinase	amp[c] + atp[c] <=> 2 adp[c]	L_RS10900	BZO99_RS06915	-1000	1000	0	Nucleotide Metabolism: Purine Biosynthesis	2.7.4.3	R00127	rxn00097	META:ADENYL-KIN-RXN
ADK2	Adenylate kinase (Inorganic triphosphate)	amp[c] + pppi[c] <=> adp[c] + ppi[c]	L_RS10900	BZO99_RS06915	-1000	1000	0	Nucleotide Metabolism: Purine Biosynthesis	2.7.4.3		rxn10052	
ADPRDP	ADPribose diphosphatase	adprib[c] + h2o[c] -> amp[c] + r5p[c] + 2 h[c]	L_RS09800 or L_RS09870 or L_RS05705 or L_RS08450	BZO99_RS03205 or BZO99_RS10645 or BZO99_RS00835 or BZO99_RS01805	0	1000	0	Nucleotide Metabolism: Purine Biosynthesis	3.6.1.13	R01054	rxn00775	META:RXN-9925; META:RXN0-1441
ADPT	Adenine phosphoribosyltransferase	ade[c] + prpp[c] -> amp[c] + ppi[c]	L_RS00105 or L_RS03405	BZO99_RS08970 or BZO99_RS05880	0	1000	0	Nucleotide Metabolism: Purine Biosynthesis	2.4.2.7; 2.4.2.8	R00190	rxn00139	META:ADENPRIBOSYLTRAN-RXN
ADSL1r	Adenylsuccinate lyase	dcamp[c] -> amp[c] + fum[c]	L_RS08555	BZO99_RS01905	0	1000	0	Nucleotide Metabolism: Purine Biosynthesis	4.3.2.2	R01083	rxn00800	META:AMPSYN-RXN
ADSL2r	Adenylosuccinate lyase	25aics[c] -> aicar[c] + fum[c]	L_RS08555	BZO99_RS01905	0	1000	0	Nucleotide Metabolism: Purine Biosynthesis	4.3.2.2	R04559	rxn03136	META:AICARSYN-RXN
ADSS	Adenylosuccinate synthase	asp__L[c] + gtp[c] + imp[c] -> dcamp[c] + pi[c] + gdp[c] + 2 h[c]	L_RS10255	BZO99_RS07340	0	1000	0	Nucleotide Metabolism: Purine Biosynthesis	6.3.4.4	R01135	rxn00838	META:ADENYLOSUCCINATE-SYNTHASE-RXN
AGPOP	DGTP:pyruvate 2-O-phosphotransferase, cytosol	dgdp[c] + h[c] + pep[c] -> dgtp[c] + pyr[c]	L_RS06980	BZO99_RS08300	0	1000	0	Nucleotide Metabolism: Purine Biosynthesis	2.7.1.40	R01858	rxn01354	META:RXN-14207
AICART	Phosphoribosylamino imidazolecarboxamide formyltransferase	10fthf[c] + aicar[c] <=> fprica[c] + thf[c]	L_RS07920	BZO99_RS10330	-1000	1000	0	Nucleotide Metabolism: Purine Biosynthesis	2.1.2.3	R04560	rxn03137	META:AICARTRANSFORM-RXN
AIRC2	Phosphoribosylamino imidazole carboxylase	air[c] + atp[c] + hco3[c] -> 5caiz[c] +	L_RS07885	BZO99_RS05845	0	1000	0	Nucleotide Metabolism: Purine Biosynthesis	6.3.4.18	R07404	rxn05114	META:RXN0-742

	(bicarbonate)	adp[c] + h[c] + pi[c]										
AIRC3	Phosphoribosylamino imidazole carboxylase (mutase rxn)	5aizc[c] <=> 5caiz[c]	L_RS07890	BZO99_RS05850	-1000	1000	0	Nucleotide Metabolism: Purine Biosynthesis	5.4.99.18	R07405	rxn05115	META:RXN0-743
AIRCr	Phosphoribosylamino imidazole carboxylase	co2[c] + air[c] -> 5aizc[c] + h[c]	L_RS07890 and L_RS07885	BZO99_RS05850 and BZO99_RS05845	0	1000	0	Nucleotide Metabolism: Purine Biosynthesis	4.1.1.21	R04209	rxn02938	META:AIRCARBOXY-RXN
DADK	Deoxyadenylate kinase	damp[c] + atp[c] <=> dadp[c] + adp[c]	L_RS10900	BZO99_RS06915	-1000	1000	0	Nucleotide Metabolism: Purine Biosynthesis	2.7.4.11; 2.7.4.13; 2.7.4.3	R01547	rxn01127	META:DEOXYADENYLATE-KINASE-RXN
DGK1	Deoxyguanylate kinase (dGMP:ATP)	atp[c] + dgmp[c] <=> adp[c] + dgdp[c]	L_RS09890	BZO99_RS10625	-1000	1000	0	Nucleotide Metabolism: Purine Biosynthesis	2.7.4.8	R02090	rxn01509	META:GMKALT-RXN
GARFT	Phosphoribosylglycinamide formyltransferase	10fthf[c] + gar[c] <=> fgam[c] + h[c] + thf[c]	L_RS07945	BZO99_RS10305	-1000	1000	0	Nucleotide Metabolism: Purine Biosynthesis	2.1.2.2	R04325	rxn03004	META:GART-RXN
GDPDPK	GDP diphosphokinase	atp[c] + gdp[c] -> h[c] + ppgpp[c] + amp[c]	L_RS00605	BZO99_RS08615	0	1000	0	Nucleotide Metabolism: Purine Biosynthesis	2.7.6.5			
GDPTPDP	Guanosine 3'-diphosphate 5'-triphosphate 3'-diphosphatase	gdptp[c] + h2o[c] -> ppi[c] + gtp[c]	L_RS00605	BZO99_RS08615	0	1000	0	Nucleotide Metabolism: Purine Biosynthesis	3.1.7.2		rxn26396	META:RXN0-6427
GMPR	GMP reductase	gmp[c] + 2 h[c] + nadph[c] -> nadp[c] + nh4[c] + imp[c]	L_RS06005	BZO99_RS01140	0	1000	0	Nucleotide Metabolism: Purine Biosynthesis	1.7.1.7	R01134	rxn00837	META:GMP-REDUCT-RXN
GMPS	GMP synthase (ammonium)	nh4[c] + atp[c] + xmp[c] -> 2 h[c] + ppi[c] + gmp[c] + amp[c]	L_RS07765	BZO99_RS05725	0	1000	0	Nucleotide Metabolism: Purine Biosynthesis	6.3.5.2	R01230	rxn00916	META:GMP-SYN-NH3-RXN
GMPS2	GMP synthase (glutamine)	atp[c] + gln__L[c] + h2o[c] + xmp[c] -> amp[c] + ppi[c] + glu__L[c] + gmp[c] + 2 h[c]	L_RS07765	BZO99_RS05725	0	1000	0	Nucleotide Metabolism: Purine Biosynthesis	6.3.5.2	R01231	rxn00917	META:GMP-SYN-GLUT-RXN
GTPDPDP	Guanosine-5'-triphosphate,3'-diphosphate diphosphatase	gdptp[c] + h2o[c] -> h[c] + pi[c] + ppgpp[c]	L_RS09445	BZO99_RS03560	0	1000	0	Nucleotide Metabolism: Purine Biosynthesis	3.6.1.11; 3.6.1.40	R03409	rxn02449	META:PPPGPPHYDRO-RXN
GTPDPK	GTP diphosphokinase	atp[c] + gtp[c] -> amp[c] + gdptp[c] + h[c]	L_RS01910 or L_RS00605	BZO99_RS02055 or BZO99_RS08615	0	1000	0	Nucleotide Metabolism: Purine Biosynthesis	2.7.6.5	R00429	rxn00303	META:GTPPYPHOSKIN-RXN
GUAPRT	Guanine phosphoribosyltransferase	prpp[c] + gua[c] -> ppi[c] + gmp[c]	L_RS07925 or L_RS00105	BZO99_RS10325 or BZO99_RS08970	0	1000	0	Nucleotide Metabolism: Purine Biosynthesis	2.4.2.22; 2.4.2.7; 2.4.2.8	R01229	rxn00915	META:GUANPRIBOSYLTRAN-RXN
IMPC	IMP cyclohydrolase	h2o[c] + imp[c] <=> fprica[c]	L_RS07920	BZO99_RS10330	-1000	1000	0	Nucleotide Metabolism: Purine Biosynthesis	2.1.2.3; 3.5.4.10	R01127	rxn00832	META:IMPCYCLOHYDROLASE-RXN
IMPD	IMP dehydrogenase	h2o[c] + nad[c] + imp[c] -> h[c] + nadh[c] + xmp[c]	L_RS01180	BZO99_RS02790	0	1000	0	Nucleotide Metabolism: Purine Biosynthesis	1.1.1.205	R01130	rxn00834	META:IMP-DEHYDROG-RXN
NTD10	5'-nucleotidase (XMP)	h2o[c] + xmp[c] -> pi[c] + xtsn[c]	L_RS00975	BZO99_RS02995	0	1000	0	Nucleotide Metabolism: Purine Biosynthesis	3.1.3.5	R02719	rxn01961	META:XMPXAN-RXN
NTD11	5'-nucleotidase (IMP)	h2o[c] + imp[c] -> ins[c] + pi[c]	L_RS00975	BZO99_RS02995	0	1000	0	Nucleotide Metabolism: Purine Biosynthesis	3.1.3.5; 3.1.3.99	R01126	rxn00831	META:RXN-7607
NTD7	5'-nucleotidase (AMP)	amp[c] + h2o[c] -> adn[c] + pi[c]	L_RS00975	BZO99_RS02995	0	1000	0	Nucleotide Metabolism: Purine Biosynthesis	3.1.3.5	R00183	rxn00132	META:AMP-DEPHOSPHORYLATION-RXN
NTD9	5'-nucleotidase (GMP)	gmp[c] + h2o[c] -> gsn[c] + pi[c]	L_RS00975	BZO99_RS02995	0	1000	0	Nucleotide Metabolism: Purine Biosynthesis	3.1.3.5	R01227	rxn00913	META:RXN-7609
NTP3	Nucleoside-triphosphatase (GTP)	gtp[c] + h2o[c] -> gdp[c] + h[c] + pi[c]	L_RS08280 or L_RS01855 or L_RS01395 or L_RS10100 or L_RS01195 or L_RS09690	BZO99_RS01630 or BZO99_RS02115 or BZO99_RS02570 or BZO99_RS10440 or BZO99_RS02775 or BZO99_RS03315	0	1000	0	Nucleotide Metabolism: Purine Biosynthesis	3.6.1.15; 3.6.1.5; 3.6.5.1; 3.6.5.2; 3.6.5.3; 3.6.5.4; 3.6.5.5; 3.6.5.6	R00335	rxn00241	META:RXN0-5462
PPGPPDP	Guanosine-3',5'-	h2o[c] + ppgpp[c] ->	L_RS00605	BZO99_RS08615	0	1000	0	Nucleotide Metabolism: Purine	3.1.7.2	R00336	rxn00242	META:PPGPPSYN-

	bis(diphosphate) 3'-diphosphatase	gdp[c] + ppi[c]						Biosynthesis				RXN
PPM	Phosphopentomutase	r1p[c] <=> r5p[c]	L_RS04880	BZO99_RS04835	-1000	1000	0	Nucleotide Metabolism: Purine Biosynthesis	5.4.2; 5.4.2.2; 5.4.2.7	R01057	rxn15115; rxn00778	META:PPENTOMUT-RXN
PRAGSr	Phosphoribosylglycinamide synthase	atp[c] + pram[c] + gly[c] -> adp[c] + pi[c] + gar[c] + h[c]	L_RS07895	BZO99_RS05855	0	1000	0	Nucleotide Metabolism: Purine Biosynthesis	6.3.4.13	R04144	rxn02895	META:GLYRIBONUCSYN-RXN
PRAIS_1	Phosphoribosylaminoimidazole synthetase	atp[c] + fpram[c] -> adp[c] + air[c] + pi[c] + h[c]	L_RS07950	BZO99_RS10300	0	1000	0	Nucleotide Metabolism: Purine Biosynthesis	6.3.3.1	R04208	rxn02937	META:AIRS-RXN
PRASCSi	Phosphoribosylaminoimidazolesuccinocarboxamide synthase	5aizc[c] + asp__L[c] + atp[c] <=> 25aics[c] + adp[c] + pi[c] + h[c]	L_RS07995	BZO99_RS10255	-1000	1000	0	Nucleotide Metabolism: Purine Biosynthesis	6.3.2.6	R04591	rxn03147	META:SAICARSYN-RXN
PRFGS_1	Phosphoribosylformylglycinamidine synthase	atp[c] + fgam[c] + gln__L[c] + h2o[c] -> adp[c] + fpram[c] + pi[c] + glu__L[c] + 2 h[c]	L_RS07990 and L_RS07985 and L_RS07980	BZO99_RS10260 and BZO99_RS10265 and BZO99_RS10270	0	1000	0	Nucleotide Metabolism: Purine Biosynthesis	6.3.5.3	R04463	rxn03084	META:FGAMSYN-RXN
r0280	DATP:pyruvate O2-phosphotransferase Purine metabolism EC:2.7.1.40	dadp[c] + h[c] + pep[c] -> datp[c] + pyr[c]	L_RS06980	BZO99_RS08300	0	1000	0	Nucleotide Metabolism: Purine Biosynthesis	2.7.1.40	R01138	rxn00840	META:RXN-14192
ASPCT	Aspartate carbamoyltransferase	asp__L[c] + cbp[c] -> cbasp[c] + pi[c] + h[c]	L_RS08355	BZO99_RS01710	0	1000	0	Nucleotide Metabolism: Pyrimidine Biosynthesis	2.1.3.2	R01397	rxn01018	META:ASPCARBTRANS-RXN
CTPS1	CTP synthase NH3	atp[c] + nh4[c] + utp[c] -> ctp[c] + adp[c] + pi[c] + 2 h[c]	L_RS02585	BZO99_RS04455	0	1000	0	Nucleotide Metabolism: Pyrimidine Biosynthesis	6.3.4.2	R00571	rxn00410	META:RXN-14325
CTPS2	CTP synthase (glutamine)	atp[c] + gln__L[c] + h2o[c] + utp[c] -> ctp[c] + adp[c] + pi[c] + glu__L[c] + 2 h[c]	L_RS02585	BZO99_RS04455	0	1000	0	Nucleotide Metabolism: Pyrimidine Biosynthesis	6.3.4.2	R00573	rxn00412; rxn11276	META:CTPSYN-RXN
CYTD	Cytidine deaminase	cytd[c] + h2o[c] + h[c] -> nh4[c] + uri[c]	L_RS07525 or L_RS03840	BZO99_RS05485 or BZO99_RS10900	0	1000	0	Nucleotide Metabolism: Pyrimidine Biosynthesis	3.5.4.5	R01878	rxn01368	META:CYTIDEAM2-RXN
CYTDK1	ATP:cytidine 5'-phosphotransferase	cytd[c] + atp[c] -> cmp[c] + adp[c] + h[c]	L_RS08655	BZO99_RS02005	0	1000	0	Nucleotide Metabolism: Pyrimidine Biosynthesis	2.7.1.213; 2.7.1.48	R00513	rxn00365	META:CYTIKIN-RXN
CYTDK2	Cytidine kinase (GTP)	cytd[c] + gtp[c] -> cmp[c] + gdp[c] + h[c]	L_RS08655	BZO99_RS02005	0	1000	0	Nucleotide Metabolism: Pyrimidine Biosynthesis	2.7.1.48; 2.7.1.213	R00517	rxn00369	META:CYTIDINEKIN-RXN
CYTK1	Cytidylate kinase (CMP)	cmp[c] + atp[c] <=> adp[c] + cdp[c]	L_RS08885	BZO99_RS04115	-1000	1000	0	Nucleotide Metabolism: Pyrimidine Biosynthesis	2.7.4.14; 2.7.4.25	R00512	rxn00364	META:RXN-11832
CYTK2	Cytidylate kinase (dCMP)	dcmp[c] + atp[c] <=> dcdp[c] + adp[c]	L_RS08885	BZO99_RS04115	-1000	1000	0	Nucleotide Metabolism: Pyrimidine Biosynthesis	2.7.4.13; 2.7.4.14; 2.7.4.25	R01665	rxn01219	META:RXN-7913
DATCY	DATP:cytidine 5'-phosphotransferase	cytd[c] + datp[c] -> cmp[c] + dadp[c] + h[c]	L_RS08655	BZO99_RS02005	0	1000	0	Nucleotide Metabolism: Pyrimidine Biosynthesis	2.7.1.48	R01548	rxn01128	
DATUP	DATP:uridine 5'-phosphotransferase	datp[c] + uri[c] -> dadp[c] + h[c] + ump[c]	L_RS08655	BZO99_RS02005	0	1000	0	Nucleotide Metabolism: Pyrimidine Biosynthesis	2.7.1.48	R01549	rxn01129	
DCTCP	DCTP:cytidine 5'-phosphotransferase	cytd[c] + dctp[c] -> cmp[c] + dcdp[c] + h[c]	L_RS08655	BZO99_RS02005	0	1000	0	Nucleotide Metabolism: Pyrimidine Biosynthesis	2.7.1.48	R02371	rxn01705	
DCTUP	DCTP:uridine 5'-phosphotransferase	dctp[c] + uri[c] -> dcdp[c] + h[c] + ump[c]	L_RS08655	BZO99_RS02005	0	1000	0	Nucleotide Metabolism: Pyrimidine Biosynthesis	2.7.1.48	R02327	rxn01674	
DCYTD	Deoxycytidine deaminase	dcyt[c] + h2o[c] + h[c] -> duri[c] + nh4[c]	L_RS07525	BZO99_RS05485	0	1000	0	Nucleotide Metabolism: Pyrimidine Biosynthesis	3.5.4.5	R02485	rxn01800	META:CYTIDEAM-RXN
DGTCY	DGTP:cytidine 5'-phosphotransferase	cytd[c] + dgtp[c] <=> cmp[c] + dgdp[c] + h[c]	L_RS08655	BZO99_RS02005	-1000	1000	0	Nucleotide Metabolism: Pyrimidine Biosynthesis	2.7.1.48	R02091	rxn01510	
DGTUP	DGTP:uridine 5'-	dgtp[c] + uri[c] ->	L_RS08655	BZO99_RS02005	0	1000	0	Nucleotide Metabolism: Pyrimidine	2.7.1.48	R01880	rxn01370	

	phosphotransferase	dgdp[c] + h[c] + ump[c]						Biosynthesis				
DHORD6	Dihydoorotic acid dehydrogenase NAD	dhor__S[c] + nad[c] -> h[c] + nadh[c] + orot[c]	L_RS07050 and L_RS07045	BZO99_RS08225 and BZO99_RS08230	0	1000	0	Nucleotide Metabolism: Pyrimidine Biosynthesis	1.3.1.14	R01869	rxn01361	META:OROTATE-REDUCTASE-NADH-RXN
DHORDfum	Fumarate dependent DHORD	dhor__S[c] + fum[c] -> orot[c] + succ[c]	(L_RS08100 or L_RS07045) and L_RS07050	(BZO99_RS01445 or BZO99_RS08230) and BZO99_RS08225	0	1000	0	Nucleotide Metabolism: Pyrimidine Biosynthesis	1.3.98.1	R01867	rxn13251	META:RXN-9929
DHORDi	Dihydoorotic acid dehydrogenase irreversible	dhor__S[c] + o2[c] <=> h2o2[c] + orot[c]	(L_RS07050 and L_RS07045) or L_RS08100	(BZO99_RS08225 and BZO99_RS08230) or BZO99_RS01445	-1000	1000	0	Nucleotide Metabolism: Pyrimidine Biosynthesis	1.3.99.11; 1.3.5.2		rxn01360	
DHORTS	Dihydroorotase	dhor__S[c] + h2o[c] <=> cbasp[c] + h[c]	L_RS05630	BZO99_RS00760	-1000	1000	0	Nucleotide Metabolism: Pyrimidine Biosynthesis	3.5.2.3	R01993	rxn01465	META:DIHYDROOROT-RXN
DTMPK	DTMP kinase	dtmp[c] + atp[c] <=> adp[c] + dtdp[c]	L_RS02080	BZO99_RS04690	-1000	1000	0	Nucleotide Metabolism: Pyrimidine Biosynthesis	2.7.4.12; 2.7.4.13; 2.7.4.9	R02094	rxn01513	META:DTMPKI-RXN
DTTGY	DTTP:cytidine 5'-phosphotransferase	cytd[c] + dttp[c] <=> cmp[c] + dtdp[c] + h[c]	L_RS08655	BZO99_RS02005	-1000	1000	0	Nucleotide Metabolism: Pyrimidine Biosynthesis	2.7.1.48	R02096	rxn01515	
DTTUP	DTTP:uridine 5'-phosphotransferase	dttp[c] + uri[c] -> dtdp[c] + h[c] + ump[c]	L_RS08655	BZO99_RS02005	0	1000	0	Nucleotide Metabolism: Pyrimidine Biosynthesis	2.7.1.48	R02097	rxn01516	
DURIPP	Deoxyuridine phosphorylase	duri[c] + pi[c] <=> 2dr1p[c] + ura[c]	L_RS04420 or L_RS07540 or L_RS04890	BZO99_RS05290 or BZO99_RS05500 or BZO99_RS04825	-1000	1000	0	Nucleotide Metabolism: Pyrimidine Biosynthesis	2.4.2.1; 2.4.2.2; 2.4.2.3; 2.4.2.4	R02484	rxn01799	META:URA-PHOSPH-RXN
DUTCP	DUTP:cytidine 5'-phosphotransferase	cytd[c] + dutp[c] -> cmp[c] + dudp[c] + h[c]	L_RS08655	BZO99_RS02005	0	1000	0	Nucleotide Metabolism: Pyrimidine Biosynthesis	2.7.1.48	R02372	rxn01706	
DUTPDP	DUTP diphosphatase	dutp[c] + h2o[c] -> dump[c] + ppi[c] + h[c]	L_RS02395 or L_RS05400 or L_RS07355 or L_RS00970	BZO99_RS00510 or BZO99_RS06535 or BZO99_RS03000	0	1000	0	Nucleotide Metabolism: Pyrimidine Biosynthesis	3.6.1.-; 3.6.1.23; 3.6.1.9	R02100	rxn01519	META:DUTP-PYROP-RXN
DUTUP	DUTP:uridine 5'-phosphotransferase	dutp[c] + uri[c] -> dudp[c] + h[c] + ump[c]	L_RS08655	BZO99_RS02005	0	1000	0	Nucleotide Metabolism: Pyrimidine Biosynthesis	2.7.1.48	R02332	rxn01679	
ITCY	ITP:cytidine 5'-phosphotransferase	cytd[c] + itp[c] -> cmp[c] + h[c] + idp[c]	L_RS08655	BZO99_RS02005	0	1000	0	Nucleotide Metabolism: Pyrimidine Biosynthesis	2.7.1.48	R00962	rxn00707	
NTD2	5'-nucleotidase (UMP)	h2o[c] + ump[c] -> pi[c] + uri[c]	L_RS00975	BZO99_RS02995	0	1000	0	Nucleotide Metabolism: Pyrimidine Biosynthesis	3.1.3.5	R00963	rxn00708	META:RXN-14025
NTD4	5'-nucleotidase (CMP)	cmp[c] + h2o[c] -> cytd[c] + pi[c]	L_RS00975	BZO99_RS02995	0	1000	0	Nucleotide Metabolism: Pyrimidine Biosynthesis	3.1.3.5; 3.1.3.91	R00511	rxn00363	META:RXN-14026
OMPDC	Orotidine-5'-phosphate decarboxylase	h[c] + orot5p[c] -> co2[c] + ump[c]	L_RS07040	BZO99_RS08235	0	1000	0	Nucleotide Metabolism: Pyrimidine Biosynthesis	4.1.1.23	R00965	rxn00710	META:OROTPDECARB-RXN
ORPT	Orotate phosphoribosyltransferase	ppi[c] + orot5p[c] <=> prpp[c] + orot[c]	L_RS05625	BZO99_RS00755	-1000	1000	0	Nucleotide Metabolism: Pyrimidine Biosynthesis	2.4.2.10	R01870	rxn01362	META:OROPRIBTRANS-RXN
PYNP1	Pyrimidine-nucleoside phosphorylase (cytosine)	csn[c] + r1p[c] <=> cytd[c] + pi[c]	L_RS07540	BZO99_RS05500	-1000	1000	0	Nucleotide Metabolism: Pyrimidine Biosynthesis	2.4.2.2	R02296	rxn01648	
PYNP2r	Pyrimidine-nucleoside phosphorylase (uracil)	pi[c] + uri[c] <=> r1p[c] + ura[c]	L_RS04420 or L_RS07540	BZO99_RS05290 or BZO99_RS05500	-1000	1000	0	Nucleotide Metabolism: Pyrimidine Biosynthesis	2.4.2.2; 2.4.2.3	R01876	rxn01366	META:URPHOS-RXN
TMDPP	Thymidine phosphorylase	pi[c] + thymd[c] <=> 2dr1p[c] + thym[c]	L_RS07540	BZO99_RS05500	-1000	1000	0	Nucleotide Metabolism: Pyrimidine Biosynthesis	2.4.2.2; 2.4.2.4	R01570	rxn01146	META:THYM-PHOSPH-RXN
UMPK	UMP kinase	atp[c] + ump[c] -> adp[c] + udp[c]	L_RS10565	BZO99_RS07875	0	1000	0	Nucleotide Metabolism: Pyrimidine Biosynthesis	2.7.4.14; 2.7.4.22; 2.7.4.4	R00158	rxn00119	META:RXN-12002
UPPRT	Uracil phosphoribosyltransferase	prpp[c] + ura[c] -> ppi[c] + ump[c]	L_RS10030 or L_RS08365	BZO99_RS10370 or BZO99_RS01720	0	1000	0	Nucleotide Metabolism: Pyrimidine Biosynthesis	2.4.2.9	R00966	rxn00711	META:URACIL-PRIBOSYLTRANS-RXN
URIDK2r	Uridylate kinase (dUMP)	dump[c] + atp[c] -> adp[c] + dudp[c]	L_RS10565	BZO99_RS07875	0	1000	0	Nucleotide Metabolism: Pyrimidine Biosynthesis	2.7.4.13; 2.7.4.4; 2.7.4.9	R02098	rxn01517	META:RXN-14122
URIK1	Uridine kinase	atp[c] + uri[c] ->	L_RS08655	BZO99_RS02005	0	1000	0	Nucleotide Metabolism: Pyrimidine	2.7.1.213; 2.7.1.48	R00964	rxn00709	META:URIDINEKIN

	ATPUridine	adp[c] + h[c] + ump[c]						Biosynthesis				-RXN
URIK2	Uridine kinase (GTP:Uridine)	gtp[c] + uri[c] -> gdp[c] + h[c] + ump[c]	L_RS08655	BZO99_RS02005	0	1000	0	Nucleotide Metabolism: Pyrimidine Biosynthesis	2.7.1.48	R00968	rxn00713	META:URKI-RXN
URIK3	Uridine kinase (ITP:Uridine)	itp[c] + uri[c] -> h[c] + idp[c] + ump[c]	L_RS08655	BZO99_RS02005	0	1000	0	Nucleotide Metabolism: Pyrimidine Biosynthesis	2.7.1.48	R00970	rxn00715	
UTCY	UTP:cytidine 5'-phosphotransferase	cytd[c] + utp[c] -> cmp[c] + h[c] + udp[c]	L_RS08655	BZO99_RS02005	0	1000	0	Nucleotide Metabolism: Pyrimidine Biosynthesis	2.7.1.48	R00516	rxn00368	
UTUP	UTP:uridine 5'-phosphotransferase	uri[c] + utp[c] -> h[c] + udp[c] + ump[c]	L_RS08655	BZO99_RS02005	0	1000	0	Nucleotide Metabolism: Pyrimidine Biosynthesis	2.7.1.48	R00967	rxn00712	
LYSTRS	Lysyl-tRNA synthetase	atp[c] + lys__L[c] + trnalys[c] -> amp[c] + h[c] + lystrna[c] + ppi[c]	L_RS01955	BZO99_RS04815	0	1000	0	Nucleotide Metabolism: tRNA Charging	6.1.1.6	R03658	rxn06442; rxn08857	META:LYSINE--TRNA-LIGASE-RXN
DM_4hba_c	4-Hydroxy-benzyl alcohol demand	4hba[c] ->			0	1000	0	Pseudo-Reaction: Demand				
DM_acmalt_c	Acetyl-maltose demand	acmalt[c] ->			0	1000	0	Pseudo-Reaction: Demand				
DM_btamp_c	Biotinyl 5 AMP demand	btamp[c] ->			0	1000	0	Pseudo-Reaction: Demand				
DM_id3acald_c	Indole 3 acetaldehyde demand	id3acald[c] ->			0	1000	0	Pseudo-Reaction: Demand				
DM_lipopb_c	Lipoate (protein bound) demand	lipopb[c] ->			0	1000	0	Pseudo-Reaction: Demand				
DM_mqn8_c	Menaquinone 8 demand	mqn8[c] ->			0	1000	0	Pseudo-Reaction: Demand				
DM_mththf_c	(2R,4S)-2-methyl-2,3,3,4-tetrahydroxytetrahydrofuran demand	mththf[c] ->			0	1000	0	Pseudo-Reaction: Demand				
DM_thfglu_c	Tetrahydrofolyl Glu 2 demand	thfglu[c] ->			0	1000	0	Pseudo-Reaction: Demand				
EX_2h3mv_e	Exchange of 2-Hydroxy-3-Methyl-Valerate	2h3mv[e] <=>			0	1000	0	Pseudo-Reaction: Exchange				
EX_2hiv_e	Exchange of 2-Hydroxy-Isovalerate	2hiv[e] <=>			0	1000	0	Pseudo-Reaction: Exchange				
EX_2hxic__L_e	L-2-hydroxyisocaproate exchange	2hxic__L[e] <=>			0	1000	0	Pseudo-Reaction: Exchange				
EX_2mbald_e	2 methylbutyraldehyde exchange	2mbald[e] <=>			0	1000	0	Pseudo-Reaction: Exchange				
EX_3mb_e	3-Methylbutanoic acid exchange	3mb[e] <=>			0	1000	0	Pseudo-Reaction: Exchange				
EX_4abut_e	4-Aminobutanoate exchange	4abut[e] <=>			0	1000	0	Pseudo-Reaction: Exchange				
EX_4abz_e	4 Aminobenzoate exchange	4abz[e] <=>			0	1000	0	Pseudo-Reaction: Exchange				
EX_ac_e	Acetate exchange	ac[e] <=>			0	1.3725	0	Pseudo-Reaction: Exchange				
EX_acald_e	Acetaldehyde exchange	acald[e] <=>			0	1000	0	Pseudo-Reaction: Exchange				
EX_acgam_e	N-Acetyl-D-glucosamine exchange	acgam[e] <=>			0	1000	0	Pseudo-Reaction: Exchange				
EX_acmana_e	N-Acetyl-D-mannosamine exchange	acmana[e] <=>			0	1000	0	Pseudo-Reaction: Exchange				
EX_actn__R_e	EX actn R LPAREN RPAREN	actn__R[e] <=>			0	1000	0	Pseudo-Reaction: Exchange				
EX_ade_e	Adenine exchange	ade[e] <=>			0	1000	0	Pseudo-Reaction: Exchange				
EX_akg_e	2-Oxoglutarate	akg[e] <=>			0	1000	0	Pseudo-Reaction: Exchange				

	exchange					
EX_ala__D_e	D-Alanine exchange	ala__D[e] <=>	0	1000	0	Pseudo-Reaction: Exchange
EX_ala__L_e	L-Alanine exchange	ala__L[e] <=>	-0.2385	0	0	Pseudo-Reaction: Exchange
EX_allul_e	Allulose exchange	allul[e] <=>	0	1000	0	Pseudo-Reaction: Exchange
EX_arg__L_e	L-Arginine exchange	arg__L[e] <=>	-0.2205	0	0	Pseudo-Reaction: Exchange
EX_asn__L_e	L-Asparagine exchange	asn__L[e] <=>	-0.4635	0	0	Pseudo-Reaction: Exchange
EX_asp__L_e	L-Aspartate exchange	asp__L[e] <=>	-0.018	0	0	Pseudo-Reaction: Exchange
EX_btd_RR_e	R R 2 3 Butanediol exchange	btd_RR[e] <=>	0	1000	0	Pseudo-Reaction: Exchange
EX_btn_e	Biotin exchange	btn[e] <=>	-1000	1000	0	Pseudo-Reaction: Exchange
EX_ca2_e	Calcium exchange	ca2[e] <=>	-1000	1000	0	Pseudo-Reaction: Exchange
EX_cellb_e	Cellobiose exchange	cellb[e] <=>	0	1000	0	Pseudo-Reaction: Exchange
EX_ch4s_e	EX ch4s LPAREN e RPAREN	ch4s[e] <=>	0	1000	0	Pseudo-Reaction: Exchange
EX_chol_e	Choline exchange	chol[e] <=>	-1000	1000	0	Pseudo-Reaction: Exchange
EX_cit_e	Citrate exchange	cit[e] <=>	0	1000	0	Pseudo-Reaction: Exchange
EX_citr__L_e	L-Citrulline exchange	citr__L[e] <=>	0	1000	0	Pseudo-Reaction: Exchange
EX_cl_e	Chloride exchange	cl[e] <=>	-1000	1000	0	Pseudo-Reaction: Exchange
EX_co2_e	CO2 exchange	co2[e] <=>	0	1000	0	Pseudo-Reaction: Exchange
EX_cobalt2_e	Co2+ exchange	cobalt2[e] <=>	0	1000	0	Pseudo-Reaction: Exchange
EX_cu2_e	Cu2+ exchange	cu2[e] <=>	-1000	1000	0	Pseudo-Reaction: Exchange
EX_cys__L_e	L-Cysteine exchange	cys__L[e] <=>	-0.081	0	0	Pseudo-Reaction: Exchange
EX_dha_e	Dihydroxyacetone exchange	dha[e] <=>	0	1000	0	Pseudo-Reaction: Exchange
EX_diact_e	Diacetyl exchange	diact[e] <=>	0	1000	0	Pseudo-Reaction: Exchange
EX_drib_e	Deoxy D Ribose exchange	drib[e] <=>	0	1000	0	Pseudo-Reaction: Exchange
EX_etoh_e	Ethanol exchange	etoh[e] <=>	0	0.4995	0	Pseudo-Reaction: Exchange
EX_fe2_e	Fe2+ exchange	fe2[e] <=>	-1000	1000	0	Pseudo-Reaction: Exchange
EX_fe3_e	Fe3+ exchange	fe3[e] <=>	0	1000	0	Pseudo-Reaction: Exchange
EX_fe3dcit_e	Fe(III)dicitrate exchange	fe3dcit[e] <=>	0	1000	0	Pseudo-Reaction: Exchange
EX_fol_e	EX fol LPAREN e RPAREN	fol[e] <=>	-1000	1000	0	Pseudo-Reaction: Exchange
EX_for_e	Formate exchange	for[e] <=>	0	2.4165	0	Pseudo-Reaction: Exchange
EX_fru_e	D-Fructose exchange	fru[e] <=>	0	1000	0	Pseudo-Reaction: Exchange
EX_gal_e	D-Galactose exchange	gal[e] <=>	0	1000	0	Pseudo-Reaction: Exchange
EX_gam_e	D-Glucosamine exchange	gam[e] <=>	0	1000	0	Pseudo-Reaction: Exchange
EX_gcald_e	Glycolaldehyde exchange	gcald[e] <=>	0	1000	0	Pseudo-Reaction: Exchange
EX_glc__D_e	D-Glucose exchange	glc__D[e] <=>	-16.362	0	0	Pseudo-Reaction: Exchange
EX_glcn_e	D-Gluconate exchange	glcn[e] <=>	0	1000	0	Pseudo-Reaction: Exchange
EX_gln__L_e	L-Glutamine exchange	gln__L[e] <=>	-1.4805	0	0	Pseudo-Reaction: Exchange
EX_glu__L_e	L-Glutamate exchange	glu__L[e] <=>	0	0.054	0	Pseudo-Reaction: Exchange
EX_gly_e	Glycine exchange	gly[e] <=>	-0.207	0	0	Pseudo-Reaction: Exchange
EX_glyb_e	Glycine betaine exchange	glyb[e] <=>	0	1000	0	Pseudo-Reaction: Exchange
EX_glyc_e	Glycerol exchange	glyc[e] <=>	0	1000	0	Pseudo-Reaction: Exchange
EX_glyc3p_e	Glycerol 3-phosphate exchange	glyc3p[e] <=>	0	1000	0	Pseudo-Reaction: Exchange
EX_gua_e	Guanine exchange	gua[e] <=>	0	1000	0	Pseudo-Reaction: Exchange
EX_h_e	H+ exchange	h[e] <=>	-1000	1000	0	Pseudo-Reaction: Exchange
EX_h2o_e	H2O exchange	h2o[e] <=>	-1000	1000	0	Pseudo-Reaction: Exchange
EX_h2s_e	Hydrogen sulfide exchange	h2s[e] <=>	0	1000	0	Pseudo-Reaction: Exchange
EX_his__L_e	L-Histidine exchange	his__L[e] <=>	-0.030591	0	0	Pseudo-Reaction: Exchange
EX_hxan_e	Hypoxanthine exchange	hxan[e] <=>	-1000	1000	0	Pseudo-Reaction: Exchange

EX_ile__L_e	L-Isoleucine exchange	ile__L[e] <=>	-0.126	0	0	Pseudo-Reaction: Exchange
EX_inost_e	Myo-Inositol exchange	inost[e] <=>	-1000	1000	0	Pseudo-Reaction: Exchange
EX_ins_e	Inosine exchange	ins[e] <=>	0	1000	0	Pseudo-Reaction: Exchange
EX_isobuta_e	Isobutyric acid exchange	isobuta[e] <=>	0	1000	0	Pseudo-Reaction: Exchange
EX_k_e	K+ exchange	k[e] <=>	0	1000	0	Pseudo-Reaction: Exchange
EX_lac__D_e	D-lactate exchange	lac__D[e] <=>	0	1000	0	Pseudo-Reaction: Exchange
EX_lac__L_e	L-Lactate exchange	lac__L[e] <=>	0	29.1735	0	Pseudo-Reaction: Exchange
EX_lcts_e	Lactose exchange	lcts[e] <=>	0	1000	0	Pseudo-Reaction: Exchange
EX_leu__L_e	L-Leucine exchange	leu__L[e] <=>	-0.153	0	0	Pseudo-Reaction: Exchange
EX_lipoate_e	Lipoate exchange	lipoate[e] <=>	-1000	1000	0	Pseudo-Reaction: Exchange
EX_lys__L_e	L-Lysine exchange	lys__L[e] <=>	-0.1575	0	0	Pseudo-Reaction: Exchange
EX_m2but_e	2-Methylbutyric acid exchange	m2but[e] <=>	0	1000	0	Pseudo-Reaction: Exchange
EX_mal__L_e	L-Malate exchange	mal__L[e] <=>	0	1000	0	Pseudo-Reaction: Exchange
EX_malt_e	Maltose exchange	malt[e] <=>	0	1000	0	Pseudo-Reaction: Exchange
EX_malthp_e	Maltoheptaose exchange	malthp[e] <=>	0	1000	0	Pseudo-Reaction: Exchange
EX_malthx_e	Maltohexaose exchange	malthx[e] <=>	0	1000	0	Pseudo-Reaction: Exchange
EX_maltpt_e	Maltopentaose exchange	maltpt[e] <=>	0	1000	0	Pseudo-Reaction: Exchange
EX_malttr_e	Maltotriose exchange	malttr[e] <=>	0	1000	0	Pseudo-Reaction: Exchange
EX_maltttr_e	Maltotetraose exchange	maltttr[e] <=>	0	1000	0	Pseudo-Reaction: Exchange
EX_man_e	D-Mannose exchange	man[e] <=>	0	1000	0	Pseudo-Reaction: Exchange
EX_met__L_e	L-Methionine exchange	met__L[e] <=>	-0.0405	0	0	Pseudo-Reaction: Exchange
EX_mg2_e	Mg exchange	mg2[e] <=>	-1000	1000	0	Pseudo-Reaction: Exchange
EX_mn2_e	Mn2+ exchange	mn2[e] <=>	0	1000	0	Pseudo-Reaction: Exchange
EX_mnl_e	D-Mannitol exchange	mnl[e] <=>	0	1000	0	Pseudo-Reaction: Exchange
EX_na1_e	Sodium exchange	na1[e] <=>	-1000	1000	0	Pseudo-Reaction: Exchange
EX_nac_e	Nicotinate exchange	nac[e] <=>	0	1000	0	Pseudo-Reaction: Exchange
EX_ncam_e	Nicotinamide exchange	ncam[e] <=>	-1000	1000	0	Pseudo-Reaction: Exchange
EX_nh4_e	Ammonia exchange	nh4[e] <=>	0	1000	0	Pseudo-Reaction: Exchange
EX_o2_e	O2 exchange	o2[e] <=>	0	1000	0	Pseudo-Reaction: Exchange
EX_orn__L_e	Ornithine exchange	orn__L[e] <=>	0	0.018	0	Pseudo-Reaction: Exchange
EX_orot_e	Orotate exchange	orot[e] <=>	0	1000	0	Pseudo-Reaction: Exchange
EX_pacald_e	Phenylacetaldehyde exchange	pacald[e] <=>	0	1000	0	Pseudo-Reaction: Exchange
EX_pea_e	Phenylethyl alcohol exchange	pea[e] <=>	0	1000	0	Pseudo-Reaction: Exchange
EX_phe__L_e	L-Phenylalanine exchange	phe__L[e] <=>	-0.0765	0	0	Pseudo-Reaction: Exchange
EX_pi_e	Phosphate exchange	pi[e] <=>	-1000	1000	0	Pseudo-Reaction: Exchange
EX_pnto__R_e	(R)-Pantothenate exchange	pnto__R[e] <=>	-1000	1000	0	Pseudo-Reaction: Exchange
EX_ppi_e	Diphosphate exchange	ppi[e] <=>	0	1000	0	Pseudo-Reaction: Exchange
EX_pro__L_e	L-Proline exchange	pro__L[e] <=>	-0.0495	0	0	Pseudo-Reaction: Exchange
EX_ptrc_e	Putrescine exchange	ptrc[e] <=>	-1000	1000	0	Pseudo-Reaction: Exchange
EX_pydam_e	Pyridoxamine exchange	pydam[e] <=>	0	1000	0	Pseudo-Reaction: Exchange
EX_pydx_e	Pyridoxal exchange	pydx[e] <=>	0	1000	0	Pseudo-Reaction: Exchange
EX_pydxn_e	Pyridoxine exchange	pydxn[e] <=>	-1000	1000	0	Pseudo-Reaction: Exchange
EX_pyr_e	Pyruvate exchange	pyr[e] <=>	-1000	1000	0	Pseudo-Reaction: Exchange
EX_rib__D_e	D-Ribose exchange	rib__D[e] <=>	0	1000	0	Pseudo-Reaction: Exchange
EX_ribflv_e	Riboflavin exchange	ribflv[e] <=>	-1000	1000	0	Pseudo-Reaction: Exchange
EX_rnam_e	N-Ribosylnicotinamide exchange	rnam[e] <=>	0	1000	0	Pseudo-Reaction: Exchange

EX_sbt__D_e	D-Sorbitol exchange	sbt__D[e] <=>	0	1000	0	Pseudo-Reaction: Exchange
EX_ser__L_e	L-Serine exchange	ser__L[e] <=>	-0.4095	0	0	Pseudo-Reaction: Exchange
EX_so4_e	sulphate exchange	so4[e] <=>	-1000	1000	0	Pseudo-Reaction: Exchange
EX_spmd_e	Spermidine exchange	spmd[e] <=>	0	1000	0	Pseudo-Reaction: Exchange
EX_succ_e	Succinate exchange	succ[e] <=>	0	1000	0	Pseudo-Reaction: Exchange
EX_thm_e	Thiamin exchange	thm[e] <=>	-1000	1000	0	Pseudo-Reaction: Exchange
EX_thr__L_e	L-Threonine exchange	thr__L[e] <=>	-0.2295	0	0	Pseudo-Reaction: Exchange
EX_thym_e	Thymine exchange	thym[e] <=>	0	1000	0	Pseudo-Reaction: Exchange
EX_thymd_e	Thymidine exchange	thymd[e] <=>	-1000	1000	0	Pseudo-Reaction: Exchange
EX_tre_e	Trehalose exchange	tre[e] <=>	0	1000	0	Pseudo-Reaction: Exchange
EX_trp__L_e	L-Tryptophan exchange	trp__L[e] <=>	-0.009	0	0	Pseudo-Reaction: Exchange
EX_tyr__L_e	L-Tyrosine exchange	tyr__L[e] <=>	-0.036	0	0	Pseudo-Reaction: Exchange
EX_ura_e	Uracil exchange	ura[e] <=>	0	1000	0	Pseudo-Reaction: Exchange
EX_val__L_e	L-Valine exchange	val__L[e] <=>	-0.1395	0	0	Pseudo-Reaction: Exchange
EX_xan_e	Xanthine exchange	xan[e] <=>	0	1000	0	Pseudo-Reaction: Exchange
EX_zn2_e	Zinc exchange	zn2[e] <=>	-1000	1000	0	Pseudo-Reaction: Exchange
BIOMASS_Llac_lumped_39p5GAM	L.lactis combined biomass objective function with 39.5 GAM estimate from Flahaut2013	0.54366 ala__L[c] + 0.19632 arg__L[c] + 0.19665 asp__L[c] + 0.19665 asn__L[c] + 0.01452 cys__L[c] + 0.166158 glu__L[c] + 0.166158 gln__L[c] + 0.39012 gly[c] + 0.06834 his__L[c] + 0.21804 ile__L[c] + 0.33684 leu__L[c] + 0.3693 lys__L[c] + 0.09006 met__L[c] + 0.15408 phe__L[c] + 0.14898 pro__L[c] + 0.23322 ser__L[c] + 0.24636 thr__L[c] + 0.06 trp__L[c] + 0.1173 tyr__L[c] + 0.2934 val__L[c] + 0.00663448387402426 datp[c] + 0.00663448387402426 dttp[c] + 0.00363561500217428 dctp[c] + 0.00363561500217428 dgtp[c] + 39.5277384864291 atp[c] + 0.0228683704911661 utp[c] + 0.0211744171214501 ctp[c] + 0.0340908115655347 gtp[c] + 0.000102952922335255 pg_LLA[c] + 0.000231507894140124 clpn_LLA[c] + 0.000023423151642412 6 lyspg_LLA[c] + 0.000165051510410489 d12dg_LLA[c] + 0.000021788978272011 7 m12dg_LLA[c] + 0.000148370687694057 LTAAlaGal_LLA[c] + 0.231971426915498 PG[c] + 0.153336996383803 CPS_LLA[c] + 0.00177763 nad[c] + 0.00043397 nadp[c] + 0.0002165 amet[c] + 0.0002165 fad[c] + 0.0002165 ribflv[c] + 0.0002165 pydx5p[c] + 0.00055921 coa[c] + 0.0002165 10fthf[c] + 0.0002165 thf[c] + 0.0002165 mlthf[c] + 0.0002165 thmpp[c] + 0.00842213 mg2[c] + 39.5 h2o[c] -> 39.5 adp[c] + 39.5 pi[c] + 39.5 h[c]	0	1000	1	Pseudo-Reaction: Macromolecular and Biomass Assembly
ATPM	ATP maintenance requirement	atp[c] + h2o[c] -> adp[c] + pi[c] + h[c]	0.92	1000	0	Pseudo-Reaction: Maintenance

Supplementary Table S2: List of metabolites present in the GEM here developed for *L. lactis* IL1403. Except for icit[c] (isocitrate), every remaining metabolite is also present in the GEM developed for *L. lactis* LMG 19460.

Abbreviation	Description	Formula	Charge	Compartment
10fthf[c]	10-Formyltetrahydrofolate	C20H21N7O7	-2	cytosol
12dgr_LLA[c]	1-2-diacylglycerol	C3720H6998O500	0	cytosol
13dpg[c]	3-Phospho-D-glyceroyl-phosphate	C3H4O10P2	-4	cytosol
14dhncoa[c]	1,4-dihydroxy-2-napthoyl-CoA	C32H38N7O19P3S	-4	cytosol
1pyr5c[c]	1-Pyrroline-5-carboxylate	C5H6NO2	-1	cytosol
23dhdp[c]	2,3-Dihydrodipicolinate	C7H5NO4	-2	cytosol
23dhmb[c]	(R)-2,3-Dihydroxy-3-methylbutanoate	C5H9O4	-1	cytosol
23dhmp[c]	(R)-2,3-Dihydroxy-3-methylpentanoate	C6H11O4	-1	cytosol
25aics[c]	(S)-2-[5-Amino-1-(5-phospho-D-ribosyl)imidazole-4-carboxamido]succinate	C13H15N4O12P	-4	cytosol
25drapp[c]	2,5-Diamino-6-(ribosylamino)-4-(3H)-pyrimidinone 5'-phosphate	C9H14N5O8P	-2	cytosol
26dap__M[c]	Meso-2,6-Diaminoheptanedioate	C7H14N2O4	0	cytosol
26dap_LL[c]	LL-2,6-Diaminoheptanedioate	C7H14N2O4	0	cytosol
2ahbut[c]	(S)-2-Aceto-2-hydroxybutanoate	C6H9O4	-1	cytosol
2cpr5p[c]	1-(2-Carboxyphenylamino)-1-deoxy-D-ribulose-5-phosphate	C12H13NO9P	-3	cytosol
2dda7p[c]	2-Dehydro-3-deoxy-D-arabino-heptonate-7-phosphate	C7H10O10P	-3	cytosol
2ddg6p[c]	2-Dehydro-3-deoxy-D-gluconate 6-phosphate	C6H8O9P	-3	cytosol
2ddglcn[c]	2-Dehydro-3-deoxy-D-gluconate	C6H9O6	-1	cytosol
2dhp[c]	2-Dehydropantoate	C6H9O4	-1	cytosol
2dmmq8[c]	2-Demethylmenaquinone-8	C50H70O2	0	cytosol
2dmmql8[c]	2-Demethylmenaquinol 8	C50H72O2	0	cytosol
2dr1p[c]	2-Deoxy-D-ribose-1-phosphate	C5H9O7P	-2	cytosol
2dr5p[c]	2-Deoxy-D-ribose-5-phosphate	C5H9O7P	-2	cytosol
2h3mv[c]	2-Hydroxy-3-Methyl-Valerate	C6H11O3	-1	cytosol
2h3mv[e]	2-Hydroxy-3-Methyl-Valerate	C6H11O3	-1	extracellular
2hiv[c]	2-Hydroxy-Isovalerate	C5H9O3	-1	cytosol
2hiv[e]	2-Hydroxy-Isovalerate	C5H9O3	-1	extracellular
2hxic__L[c]	L 2 hydroxyisocaproate	C6H11O3	-1	cytosol
2hxic__L[e]	L 2 hydroxyisocaproate	C6H11O3	-1	extracellular
2ins[c]	2-Inosose	C6H10O6	0	cytosol
2ippm[c]	2-Isopropylmaleate	C7H8O4	-2	cytosol
2mahmp[c]	2-Methyl-4-amino-5-hydroxymethylpyrimidine-diphosphate	C6H8N3O7P2	-3	cytosol
2mbald[c]	2 methylbutyraldehyde C5H10O	C5H10O	0	cytosol
2mbald[e]	2 methylbutyraldehyde C5H10O	C5H10O	0	extracellular
2mbcoa[c]	2-Methylbutanoyl-CoA	C26H40N7O17P3S	-4	cytosol
2obut[c]	2-Oxobutanoate	C4H5O3	-1	cytosol
2pg[c]	D-Glycerate-2-phosphate	C3H4O7P	-3	cytosol
2sephchc[c]	2-succinyl-5-enolpyruvyl-6-hydroxy-3-cyclohexene-1-carboxylate	C14H13O9	-3	cytosol
2shchc[c]	2-Succinyl-6-hydroxy-2,4-cyclohexadiene-1-carboxylate	C11H10O6	-2	cytosol
34hpp[c]	3-(4-Hydroxyphenyl)pyruvate	C9H7O4	-1	cytosol
3c2hmp[c]	3-Carboxy-2-hydroxy-4-methylpentanoate	C7H10O5	-2	cytosol
3c3hmp[c]	3-Carboxy-3-hydroxy-4-methylpentanoate	C7H10O5	-2	cytosol
3c4mop[c]	3-Carboxy-4-methyl-2-oxopentanoate	C7H8O5	-2	cytosol
3dhq[c]	3-Dehydroquinate	C7H9O6	-1	cytosol
3dhsk[c]	3-Dehydroshikimate	C7H7O5	-1	cytosol
3haACP[c]	(3R)-3-Hydroxyacyl-[acyl-carrier protein]	C15H27N2O9PRS	-1	cytosol
3hcddec5eACP[c]	(R)-3-hydroxy-cis-dodec-5-enoyl-[acyl-carrier protein]	C23H41N2O9PRS	-1	cytosol

3hcmrs7eACP[c]	(R)-3-hydroxy-cis-myristol-7-eoyl-[acyl-carrier protein]	C25H45N2O9PRS	-1	cytosol
3hcpalm9eACP[c]	(R)-3-hydroxy-cis-palm-9-eoyl-[acyl-carrier protein]	C27H49N2O9PRS	-1	cytosol
3hcvac11eACP[c]	(R)-3-hydroxy-cis-vacc-11-enoyl-[acyl-carrier protein]	C29H53N2O9PRS	-1	cytosol
3hddecACP[c]	(R)-3-Hydroxydodecanoyl-[acyl-carrier protein]	C23H43N2O9PRS	-1	cytosol
3hdecACP[c]	(R)-3-Hydroxydecanoyl-[acyl-carrier protein]	C21H39N2O9PRS	-1	cytosol
3hhexACP[c]	(R)-3-Hydroxyhexanoyl-[acyl-carrier protein]	C17H31N2O9PRS	-1	cytosol
3hmrsACP[c]	(R)-3-Hydroxytetradecanoyl-[acyl-carrier protein]	C25H47N2O9PRS	-1	cytosol
3hoctaACP[c]	(R)-3-Hydroxyoctadecanoyl-[acyl-carrier protein]	C29H55N2O9PRS	-1	cytosol
3hoctACP[c]	(R)-3-Hydroxyoctanoyl-[acyl-carrier protein]	C19H35N2O9PRS	-1	cytosol
3hpalmACP[c]	R-3-hydroxypalmitoyl-[acyl-carrier protein]	C27H51N2O9PRS	-1	cytosol
3ig3p[c]	C'-(3-Indolyl)-glycerol-3-phosphate	C11H12NO6P	-2	cytosol
3mb[c]	3-Methylbutanoic acid	C5H9O2	-1	cytosol
3mb[e]	3-Methylbutanoic acid	C5H9O2	-1	extracellular
3mob[c]	3-Methyl-2-oxobutanoate	C5H7O3	-1	cytosol
3mop[c]	(S)-3-Methyl-2-oxopentanoate	C6H9O3	-1	cytosol
3ocddec5eACP[c]	3-oxo-cis-dodec-5-enoyl-[acyl-carrier protein]	C23H39N2O9PRS	-1	cytosol
3ocmrs7eACP[c]	3-oxo-cis-myristol-7-eoyl-[acyl-carrier protein]	C25H43N2O9PRS	-1	cytosol
3ocpalm9eACP[c]	3-oxo-cis-palm-9-eoyl-[acyl-carrier protein]	C27H47N2O9PRS	-1	cytosol
3ocvac11eACP[c]	3-oxo-cis-vacc-11-enoyl-[acyl-carrier protein]	C29H51N2O9PRS	-1	cytosol
3oddecACP[c]	3-Oxododecanoyl-[acyl-carrier protein]	C23H41N2O9PRS	-1	cytosol
3odecACP[c]	3-Oxodecanoyl-[acyl-carrier protein]	C21H37N2O9PRS	-1	cytosol
3ohexACP[c]	3-Oxohexanoyl-[acyl-carrier protein]	C17H29N2O9PRS	-1	cytosol
3omrsACP[c]	3-Oxotetradecanoyl-[acyl-carrier protein]	C25H45N2O9PRS	-1	cytosol
3ooctACP[c]	3-Oxooctanoyl-[acyl-carrier protein]	C19H33N2O9PRS	-1	cytosol
3ooctdACP[c]	3-Oxooctadecanoyl-[acyl-carrier protein]	C29H53N2O9PRS	-1	cytosol
3opalmACP[c]	3-Oxohexadecanoyl-[acyl-carrier protein]	C27H49N2O9PRS	-1	cytosol
3pg[c]	3-Phospho-D-glycerate	C3H4O7P	-3	cytosol
3php[c]	3-Phosphohydroxypyruvate	C3H2O7P	-3	cytosol
3psme[c]	5-O-(1-Carboxyvinyl)-3-phosphoshikimate	C10H9O10P	-4	cytosol
4abut[c]	4-Aminobutanoate	C4H9NO2	0	cytosol
4abut[e]	4-Aminobutanoate	C4H9NO2	0	extracellular
4abz[c]	4-Aminobenzoate	C7H6NO2	-1	cytosol
4abz[e]	4-Aminobenzoate	C7H6NO2	-1	extracellular
4adcho[c]	4-amino-4-deoxychorismate	C10H10NO5	-1	cytosol
4ahmmp[c]	4-Amino-5-hydroxymethyl-2-methylpyrimidine	C6H9N3O	0	cytosol
4ampm[c]	4-Amino-2-methyl-5-phosphomethylpyrimidine	C6H8N3O4P	-2	cytosol
4hba[c]	4-Hydroxy-benzyl alcohol	C7H8O2	0	cytosol
4mhetz[c]	4-Methyl-5-(2-hydroxyethyl)-thiazole	C6H9NOS	0	cytosol
4mop[c]	4-Methyl-2-oxopentanoate	C6H9O3	-1	cytosol
4mpetz[c]	4-Methyl-5-(2-phosphoethyl)-thiazole	C6H8NO4PS	-2	cytosol
4pasp[c]	4-Phospho-L-aspartate	C4H6NO7P	-2	cytosol
4per[c]	4-Phospho-D-erythronate	C4H6O8P	-3	cytosol
4ppan[c]	D-4'-Phosphopantothenate	C9H15NO8P	-3	cytosol
4ppcys[c]	N-((R)-4-Phosphopantothenoyl)-L-cysteine	C12H20N2O9PS	-3	cytosol
4r5au[c]	4-(1-D-Ribitylamino)-5-aminouracil	C9H16N4O6	0	cytosol
5aizc[c]	5-amino-1-(5-phospho-D-ribosyl)imidazole-4-carboxylate	C9H11N3O9P	-3	cytosol
5aprbu[c]	5-Amino-6-(5'-phosphoribitylamino)uracil	C9H15N4O9P	-2	cytosol
5apru[c]	5-Amino-6-(5'-phosphoribosylamino)uracil	C9H13N4O9P	-2	cytosol
5caiz[c]	5-phosphoribosyl-5-carboxyaminoimidazole	C9H11N3O9P	-3	cytosol
5dpmev[c]	R-5-Diphosphomevalonate	C6H10O10P2	-4	cytosol

5fthf[c]	5-Formyltetrahydrofolate	C20H21N7O7	-2	cytosol
5mta[c]	5-Methylthioadenosine	C11H15N5O3S	0	cytosol
5mthf[c]	5-Methyltetrahydrofolate	C20H24N7O6	-1	cytosol
5mtr[c]	5-Methylthio-D-ribose	C6H12O4S	0	cytosol
5pmev[c]	R-5-Phosphomevalonate	C6H10O7P	-3	cytosol
6hmhpt[c]	6-hydroxymethyl dihydropterin	C7H9N5O2	0	cytosol
6hmhptpp[c]	6-hydroxymethyl-dihydropterin pyrophosphate	C7H8N5O8P2	-3	cytosol
6pgc[c]	6-Phospho-D-gluconate	C6H10O10P	-3	cytosol
6pgg[c]	6-Phospho-beta-D-glucosyl-(1,4)-D-glucose	C12H21O14P	-2	cytosol
6pgl[c]	6-phospho-D-glucono-1,5-lactone	C6H9O9P	-2	cytosol
a_gal__D[c]	Alpha-D-galactose	C6H12O6	0	cytosol
aacoa[c]	Acetoacetyl-CoA	C25H36N7O18P3S	-4	cytosol
ac[c]	Acetate	C2H3O2	-1	cytosol
ac[e]	Acetate	C2H3O2	-1	extracellular
acACP[c]	Acetyl-ACP	C13H23N2O8PRS	-1	cytosol
acald[c]	Acetaldehyde	C2H4O	0	cytosol
acald[e]	Acetaldehyde	C2H4O	0	extracellular
accoa[c]	Acetyl-CoA	C23H34N7O17P3S	-4	cytosol
acg5p[c]	N-Acetyl-L-glutamyl-5-phosphate	C7H9NO8P	-3	cytosol
acg5sa[c]	N-Acetyl-L-glutamate-5-semialdehyde	C7H10NO4	-1	cytosol
acgam[e]	N-Acetyl-D-glucosamine	C8H15NO6	0	extracellular
acgam1p[c]	N-Acetyl-D-glucosamine-1-phosphate	C8H14NO9P	-2	cytosol
acgam6p[c]	N-Acetyl-D-glucosamine-6-phosphate	C8H14NO9P	-2	cytosol
acglu[c]	N-Acetyl-L-glutamate	C7H9NO5	-2	cytosol
achms[c]	O-Acetyl-L-homoserine	C6H11NO4	0	cytosol
acmalt[c]	Acetyl-maltose	C14H24O12	0	cytosol
acmana[c]	N-Acetyl-D-mannosamine	C8H15NO6	0	cytosol
acmana[e]	N-Acetyl-D-mannosamine	C8H15NO6	0	extracellular
acmanap[c]	N-Acetyl-D-mannosamine 6-phosphate	C8H14NO9P	-2	cytosol
acmum6p[c]	N-acetylmuramate 6-phosphate	C11H17NO11P	-3	cytosol
acon_C[c]	Cis-Aconitate	C6H3O6	-3	cytosol
acorn[c]	N2-Acetyl-L-ornithine	C7H14N2O3	0	cytosol
ACP[c]	Acyl-carrier-protein	C11H21N2O7PRS	-1	cytosol
acser[c]	O-Acetyl-L-serine	C5H9NO4	0	cytosol
actACP[c]	Acetoacetyl-ACP	C15H25N2O9PRS	-1	cytosol
actn__R[c]	R-Acetoin	C4H8O2	0	cytosol
actn__R[e]	R-Acetoin	C4H8O2	0	extracellular
actp[c]	Acetyl-phosphate	C2H3O5P	-2	cytosol
ade[c]	Adenine	C5H5N5	0	cytosol
ade[e]	Adenine	C5H5N5	0	extracellular
adhlam[c]	S-Acetyldihydrolipoamide	C10H19NO2S2	0	cytosol
adn[c]	Adenosine	C10H13N5O4	0	cytosol
adp[c]	ADP	C10H12N5O10P2	-3	cytosol
adpglc[c]	ADPglucose C16H23N5O15P2	C16H23N5O15P2	-2	cytosol
adprib[c]	ADPribose C15H21N5O14P2	C15H21N5O14P2	-2	cytosol
agly3p_LLA[c]	1-Acyl-sn-glycerol-3-phosphate	C2010H3799O700P100	-200	cytosol
ahcys[c]	S-Adenosyl-L-homocysteine	C14H20N6O5S	0	cytosol
ahdt[c]	2-Amino-4-hydroxy-6-(erythro-1,2,3-trihydroxypropyl)dihydropteridine-triphosphate	C9H12N5O13P3	-4	cytosol
aicar[c]	5-Amino-1-(5-Phospho-D-ribosyl)imidazole-4-carboxamide	C9H13N4O8P	-2	cytosol

air[c]	5-amino-1-(5-phospho-D-ribosyl)imidazole	C8H12N3O7P	-2	cytosol
akg[c]	2-Oxoglutarate	C5H4O5	-2	cytosol
akg[e]	2-Oxoglutarate	C5H4O5	-2	extracellular
ala__D[c]	D-Alanine	C3H7NO2	0	cytosol
ala__D[e]	D-Alanine	C3H7NO2	0	extracellular
ala__L[c]	L-Alanine	C3H7NO2	0	cytosol
ala__L[e]	L-Alanine	C3H7NO2	0	extracellular
ala_B[c]	Beta-Alanine	C3H7NO2	0	cytosol
alaala[c]	D-Alanyl-D-alanine	C6H12N2O3	0	cytosol
alac__S[c]	(S)-2-Acetolactate	C5H7O4	-1	cytosol
allul[e]	Allulose	C6H12O6	0	extracellular
allul6p[c]	Allulose 6-phosphate	C6H11O9P	-2	cytosol
amet[c]	S-Adenosyl-L-methionine	C15H23N6O5S	1	cytosol
amp[c]	AMP	C10H12N5O7P	-2	cytosol
anth[c]	Anthranilate	C7H6NO2	-1	cytosol
apoACP[c]	Apoprotein-[acyl-carrier-protein]	RHO	0	cytosol
arbt6p[c]	Arbutin-6-phosphate	C12H15O10P	-2	cytosol
arg__L[c]	L-Arginine	C6H15N4O2	1	cytosol
arg__L[e]	L-Arginine	C6H15N4O2	1	extracellular
argsuc[c]	N(omega)-(L-Arginino)succinate	C10H17N4O6	-1	cytosol
asn__L[c]	L-Asparagine	C4H8N2O3	0	cytosol
asn__L[e]	L-Asparagine	C4H8N2O3	0	extracellular
asp__L[c]	L-Aspartate	C4H6NO4	-1	cytosol
asp__L[e]	L-Aspartate	C4H6NO4	-1	extracellular
aspsa[c]	L-Aspartate-4-semialdehyde	C4H7NO3	0	cytosol
atp[c]	ATP	C10H12N5O13P3	-4	cytosol
betald[c]	Betaine aldehyde	C5H12NO	1	cytosol
btamp[c]	Biotinyl 5 AMP C20H27N7O9PS	C20H27N7O9PS	-1	cytosol
btd_RR[c]	R-R-2-3-Butanediol	C4H10O2	0	cytosol
btd_RR[e]	R-R-2-3-Butanediol	C4H10O2	0	extracellular
btn[c]	Biotin	C10H15N2O3S	-1	cytosol
btn[e]	Biotin	C10H15N2O3S	-1	extracellular
but2eACP[c]	But-2-enoyl-[acyl-carrier protein]	C15H25N2O8PRS	-1	cytosol
butACP[c]	Butyryl-ACP (n-C4:0ACP)	C15H27N2O8PRS	-1	cytosol
c190cACP[c]	19 carbon cyclopropane-ACP	C30H55N2O8PRS	0	cytosol
ca2[c]	Calcium	Ca	2	cytosol
ca2[e]	Calcium	Ca	2	extracellular
cbasp[c]	N-Carbamoyl-L-aspartate	C5H6N2O5	-2	cytosol
cbp[c]	Carbamoyl-phosphate	CH2NO5P	-2	cytosol
cddec5eACP[c]	Cis-dodec-5-enoyl-[acyl-carrier protein] (n-C12:1)	C23H41N2O8PRS	-1	cytosol
cdec3eACP[c]	Cis-dec-3-enoyl-[acyl-carrier protein] (n-C10:1)	C21H37N2O8PRS	-1	cytosol
cdp[c]	CDP	C9H12N3O11P2	-3	cytosol
cdpdag_LLA[c]	CDPdiacylglycerol	C4620H8098N300O1500P200	-200	cytosol
cellb[e]	Cellobiose	C12H22O11	0	extracellular
ch4s[c]	Methanethiol	CH4S	0	cytosol
ch4s[e]	Methanethiol	CH4S	0	extracellular
chol[c]	Choline	C5H14NO	1	cytosol
chol[e]	Choline	C5H14NO	1	extracellular
chor[c]	Chorismate	C10H8O6	-2	cytosol
cit[c]	Citrate	C6H5O7	-3	cytosol

cit[e]	Citrate	C6H5O7	-3	extracellular
citr__L[c]	L-Citrulline	C6H13N3O3	0	cytosol
citr__L[e]	L-Citrulline	C6H13N3O3	0	extracellular
cl[c]	Chloride	Cl	-1	cytosol
cl[e]	Chloride	Cl	-1	extracellular
clpn_LLA[c]	Cardiolipin	C7740H14396O1700P200	-200	cytosol
cmp[c]	CMP	C9H12N3O8P	-2	cytosol
co2[c]	CO2	CO2	0	cytosol
co2[e]	CO2	CO2	0	extracellular
coa[c]	Coenzyme-A	C21H32N7O16P3S	-4	cytosol
cobalt2[c]	Co2+	Co	2	cytosol
cobalt2[e]	Co2+	Co	2	extracellular
CPS_LLA[c]	Polysaccharide units Lactis specific	C24H47O26P1	-2	cytosol
csn[c]	Cytosine	C4H5N3O	0	cytosol
ctp[c]	CTP	C9H12N3O14P3	-4	cytosol
cu2[c]	Cu2+	Cu	2	cytosol
cu2[e]	Cu2+	Cu	2	extracellular
cys__L[c]	L-Cysteine	C3H7NO2S	0	cytosol
cys__L[e]	L-Cysteine	C3H7NO2S	0	extracellular
cyst__L[c]	L-Cystathionine	C7H14N2O4S	0	cytosol
cytd[c]	Cytidine	C9H13N3O5	0	cytosol
d12dg_LLA[c]	Diglucosyl-1-2-diacylglycerol	C4920H8998O1500	0	cytosol
dad_2[c]	Deoxyadenosine	C10H13N5O3	0	cytosol
dadp[c]	DADP	C10H12N5O9P2	-3	cytosol
damp[c]	DAMP	C10H12N5O6P	-2	cytosol
datp[c]	DATP	C10H12N5O12P3	-4	cytosol
db4p[c]	3,4-dihydroxy-2-butanone-4-phosphate	C4H7O6P	-2	cytosol
dcaACP[c]	Decanoyl-ACP (n-C10:0ACP)	C21H39N2O8PRS	-1	cytosol
dcamp[c]	N6-(1,2-Dicarboxyethyl)-AMP	C14H14N5O11P	-4	cytosol
dcdp[c]	DCDP	C9H12N3O10P2	-3	cytosol
dcmp[c]	DCMP	C9H12N3O7P	-2	cytosol
dctp[c]	DCTP	C9H12N3O13P3	-4	cytosol
dcyt[c]	Deoxycytidine	C9H13N3O4	0	cytosol
ddcaACP[c]	Dodecanoyl-ACP (n-C12:0ACP)	C23H43N2O8PRS	-1	cytosol
dgdp[c]	DGDP	C10H12N5O10P2	-3	cytosol
dgmp[c]	DGMP	C10H12N5O7P	-2	cytosol
dgsn[c]	Deoxyguanosine	C10H13N5O4	0	cytosol
dgtp[c]	DGTP	C10H12N5O13P3	-4	cytosol
dha[c]	Dihydroxyacetone	C3H6O3	0	cytosol
dha[e]	Dihydroxyacetone	C3H6O3	0	extracellular
dhap[c]	Dihydroxyacetone-phosphate	C3H5O6P	-2	cytosol
dhf[c]	7,8-Dihydrofolate	C19H19N7O6	-2	cytosol
dhlam[c]	Dihydrolipoamide C8H17NOS2	C8H17NOS2	0	cytosol
dhna[c]	1,4-Dihydroxy-2-naphthoate	C11H7O4	-1	cytosol
dhnpt[c]	Dihydroneopterin	C9H13N5O4	0	cytosol
dhor__S[c]	(S)-Dihydroorotate	C5H5N2O4	-1	cytosol
dhpmp[c]	Dihydroneopterin monophosphate	C9H12N5O7P	-2	cytosol
dhpt[c]	Dihydropteroate	C14H13N6O3	-1	cytosol
dhptd[c]	4,5-dihydroxy-2,3-pentanedione	C5H8O4	0	cytosol
diact[c]	Diacetyl	C4H6O2	0	cytosol

diact[e]	Diacetyl	C4H6O2	0	extracellular
din[c]	Deoxyinosine	C10H12N4O4	0	cytosol
dmlz[c]	6,7-Dimethyl-8-(1-D-ribityl)lumazine	C13H18N4O6	0	cytosol
dmpp[c]	Dimethylallyl-diphosphate	C5H9O7P2	-3	cytosol
dnad[c]	Deamino-NAD+	C21H24N6O15P2	-2	cytosol
dpcoa[c]	Dephospho-CoA	C21H33N7O13P2S	-2	cytosol
drib[c]	Deoxyribose C5H10O4	C5H10O4	0	cytosol
drib[e]	Deoxyribose C5H10O4	C5H10O4	0	extracellular
dtdp[c]	DTDP	C10H13N2O11P2	-3	cytosol
dtdp4d6dg[c]	DTDP-4-dehydro-6-deoxy-D-glucose	C16H22N2O15P2	-2	cytosol
dtdp4d6dm[c]	DTDP-4-dehydro-6-deoxy-L-mannose	C16H22N2O15P2	-2	cytosol
dtdpglu[c]	DTDPglucose	C16H24N2O16P2	-2	cytosol
dtdprmn[c]	DTDP-L-rhamnose	C16H24N2O15P2	-2	cytosol
dtmp[c]	DTMP	C10H13N2O8P	-2	cytosol
dttp[c]	DTTP	C10H13N2O14P3	-4	cytosol
dudp[c]	DUDP	C9H11N2O11P2	-3	cytosol
dump[c]	DUMP	C9H11N2O8P	-2	cytosol
duri[c]	Deoxyuridine	C9H12N2O5	0	cytosol
dutp[c]	DUTP	C9H11N2O14P3	-4	cytosol
dxyl5p[c]	1-deoxy-D-xylulose 5-phosphate	C5H9O7P	-2	cytosol
e4p[c]	D-Erythrose-4-phosphate	C4H7O7P	-2	cytosol
etha[c]	Ethanolamine	C2H8NO	1	cytosol
etoh[c]	Ethanol	C2H6O	0	cytosol
etoh[e]	Ethanol	C2H6O	0	extracellular
f1p[c]	D-Fructose-1-phosphate	C6H11O9P	-2	cytosol
f6p[c]	D-Fructose-6-phosphate	C6H11O9P	-2	cytosol
fad[c]	Flavin-adenine-dinucleotide-oxidized	C27H31N9O15P2	-2	cytosol
fadh2[c]	Flavin adenine dinucleotide reduced	C27H33N9O15P2	-2	cytosol
fdp[c]	D-Fructose 1,6-bisphosphate	C6H10O12P2	-4	cytosol
fdxo_42[c]	Ferredoxin (oxidized form 4:2)	Fe12S12X	0	cytosol
fdxr_42[c]	Ferredoxin (reduced form 4:2)	Fe12S12X	-3	cytosol
fe2[c]	Fe2+ mitochondria	Fe	2	cytosol
fe2[e]	Fe2+ mitochondria	Fe	2	extracellular
fe3[c]	Iron (Fe3+)	Fe	3	cytosol
fe3[e]	Iron (Fe3+)	Fe	3	extracellular
fe3dcit[e]	Fe(III)dicitrate	C12H10FeO14	-3	extracellular
fgam[c]	N2-Formyl-N1-(5-phospho-D-ribosyl)glycinamide	C8H13N2O9P	-2	cytosol
fmn[c]	FMN	C17H19N4O9P	-2	cytosol
fol[c]	Folate	C19H18N7O6	-1	cytosol
fol[e]	Folate	C19H18N7O6	-1	extracellular
for[c]	Formate	CH1O2	-1	cytosol
for[e]	Formate	CH1O2	-1	extracellular
fpram[c]	2-(Formamido)-N1-(5-phospho-D-ribosyl)acetamidine	C8H14N3O8P	-2	cytosol
fprica[c]	5-Formamido-1-(5-phospho-D-ribosyl)imidazole-4-carboxamide	C10H13N4O9P	-2	cytosol
frdp[c]	Farnesyl-diphosphate	C15H25O7P2	-3	cytosol
fru[c]	D-Fructose	C6H12O6	0	cytosol
fru[e]	D-Fructose	C6H12O6	0	extracellular
fruur[c]	D-Fructuronate	C6H9O7	-1	cytosol
fum[c]	Fumarate	C4H2O4	-2	cytosol
g1p_B[c]	Beta-D-Glucose-1-phosphate	C6H11O9P	-2	cytosol

g1p[c]	D-Glucose-1-phosphate	C6H11O9P	-2	cytosol
g3p[c]	Glyceraldehyde-3-phosphate	C3H5O6P	-2	cytosol
g3pc[c]	Sn-Glycero-3-phosphocholine	C8H20NO6P	0	cytosol
g3pe[c]	Sn-Glycero-3-phosphoethanolamine	C5H14NO6P	0	cytosol
g3pg[c]	Glycerophosphoglycerol	C6H14O8P	-1	cytosol
g3pi[c]	Sn-Glycero-3-phospho-1-inositol	C9H18O11P	-1	cytosol
g3ps[c]	Glycerophosphoserine	C6H13NO8P	-1	cytosol
g6p_B[c]	Beta-D-glucose-6-phosphate	C6H11O9P	-2	cytosol
g6p[c]	D-Glucose-6-phosphate	C6H11O9P	-2	cytosol
gal[c]	D-Galactose	C6H12O6	0	cytosol
gal[e]	D-Galactose	C6H12O6	0	extracellular
gal1p[c]	Alpha-D-Galactose-1-phosphate	C6H11O9P	-2	cytosol
gam[e]	D-Glucosamine	C6H14NO5	1	extracellular
gam1p[c]	D-Glucosamine-1-phosphate	C6H13NO8P	-1	cytosol
gam6p[c]	D-Glucosamine-6-phosphate	C6H13NO8P	-1	cytosol
gar[c]	N1-(5-Phospho-D-ribosyl)glycinamide	C7H14N2O8P	-1	cytosol
gcald[c]	Glycolaldehyde	C2H4O2	0	cytosol
gcald[e]	Glycolaldehyde	C2H4O2	0	extracellular
gdp[c]	GDP	C10H12N5O11P2	-3	cytosol
gdptp[c]	Guanosine 3'-diphosphate 5'-triphosphate	C10H11N5O20P5	-7	cytosol
glc__D[c]	D-Glucose	C6H12O6	0	cytosol
glc__D[e]	D-Glucose	C6H12O6	0	extracellular
glcn[c]	D-Gluconate	C6H11O7	-1	cytosol
glcn[e]	D-Gluconate	C6H11O7	-1	extracellular
glcur[c]	D-Glucuronate	C6H9O7	-1	cytosol
gln__L[c]	L-Glutamine	C5H10N2O3	0	cytosol
gln__L[e]	L-Glutamine	C5H10N2O3	0	extracellular
glu__D[c]	D-Glutamate	C5H8NO4	-1	cytosol
glu__L[c]	L-Glutamate	C5H8NO4	-1	cytosol
glu__L[e]	L-Glutamate	C5H8NO4	-1	extracellular
glu5p[c]	L-Glutamate-5-phosphate	C5H8NO7P	-2	cytosol
glu5sa[c]	L-Glutamate-5-semialdehyde	C5H9NO3	0	cytosol
gly[c]	Glycine	C2H5NO2	0	cytosol
gly[e]	Glycine	C2H5NO2	0	extracellular
glyald[c]	D-Glyceraldehyde	C3H6O3	0	cytosol
glyb[c]	Glycine-betaine	C5H11NO2	0	cytosol
glyb[e]	Glycine-betaine	C5H11NO2	0	extracellular
glyc__R[c]	(R)-Glycerate	C3H5O4	-1	cytosol
glyc[c]	Glycerol	C3H8O3	0	cytosol
glyc[e]	Glycerol	C3H8O3	0	extracellular
glyc3p[c]	Glycerol-3-phosphate	C3H7O6P	-2	cytosol
glyc3p[e]	Glycerol-3-phosphate	C3H7O6P	-2	extracellular
glycogen[c]	Glycogen C6H10O5	C6H10O5	0	cytosol
gmp[c]	GMP	C10H12N5O8P	-2	cytosol
grdp[c]	Geranyl-diphosphate	C10H17O7P2	-3	cytosol
gsn[c]	Guanosine	C10H13N5O5	0	cytosol
gthox[c]	Oxidized-glutathione	C20H30N6O12S2	-2	cytosol
gthrd[c]	Reduced-glutathione	C10H16N3O6S	-1	cytosol
gtp[c]	GTP	C10H12N5O14P3	-4	cytosol
gua[c]	Guanine	C5H5N5O	0	cytosol

gua[e]	Guanine	C5H5N5O	0	extracellular
h[c]	H+	H	1	cytosol
h[e]	H+	H	1	extracellular
h2o[c]	H2O-H2O	H2O	0	cytosol
h2o[e]	H2O-H2O	H2O	0	extracellular
h2o2[c]	Hydrogen-peroxide	H2O2	0	cytosol
h2s[c]	Hydrogen-sulfide	H2S	0	cytosol
h2s[e]	Hydrogen sulfide	H2S	0	extracellular
hco3[c]	Bicarbonate	CHO3	-1	cytosol
hcys__L[c]	L-Homocysteine	C4H9NO2S	0	cytosol
hdeACP[c]	Cis-hexadec-9-enoyl-[acyl-carrier protein] (n-C16:1)	C27H49N2O8PRS	-1	cytosol
hexACP[c]	Hexanoyl-ACP (n-C6:0ACP)	C17H31N2O8PRS	-1	cytosol
his__L[c]	L-Histidine	C6H9N3O2	0	cytosol
his__L[e]	L-Histidine	C6H9N3O2	0	extracellular
hisp[c]	L-Histidinol-phosphate	C6H11N3O4P	-1	cytosol
histd[c]	L-Histidinol	C6H12N3O	1	cytosol
hmgcoa[c]	Hydroxymethylglutaryl-CoA	C27H39N7O20P3S	-5	cytosol
hom__L[c]	L-Homoserine	C4H9NO3	0	cytosol
hpglu[c]	Tetrahydropteroyltri L glutamate C24H34N8O12	C24H32N8O12	-2	cytosol
hpyr[c]	Hydroxypyruvate	C3H3O4	-1	cytosol
hqn[c]	Hydroquinone	C6H6O2	0	cytosol
hxan[c]	Hypoxanthine	C5H4N4O	0	cytosol
hxan[e]	Hypoxanthine	C5H4N4O	0	extracellular
iasp[c]	Iminoaspartate	C4H3NO4	-2	cytosol
ibcoa[c]	Isobutyryl-CoA	C25H38N7O17P3S	-4	cytosol
ichor[c]	Isochorismate	C10H8O6	-2	cytosol
icit[c]	Isocitrate	C6H5O7	-3	cytosol
id3acald[c]	Indole-3-acetaldehyde	C10H9NO	0	cytosol
idp[c]	IDP C10H11N4O11P2	C10H11N4O11P2	-3	cytosol
ile__L[c]	L-Isoleucine	C6H13NO2	0	cytosol
ile__L[e]	L-Isoleucine	C6H13NO2	0	extracellular
imp[c]	IMP	C10H11N4O8P	-2	cytosol
indole[c]	Indole	C8H7N	0	cytosol
indpyr[c]	Indolepyruvate	C11H8NO3	-1	cytosol
inost[c]	Myo-Inositol	C6H12O6	0	cytosol
inost[e]	Myo-Inositol	C6H12O6	0	extracellular
ins[c]	Inosine	C10H12N4O5	0	cytosol
ins[e]	Inosine	C10H12N4O5	0	extracellular
ipdp[c]	Isopentenyl-diphosphate	C5H9O7P2	-3	cytosol
isobuta[c]	Isobutyric acid	C4H8O2	0	cytosol
isobuta[e]	Isobutyric acid	C4H8O2	0	extracellular
isobutp[c]	Isobutanoylphosphate	C4H7O5P	0	cytosol
itp[c]	ITP C10H11N4O14P3	C10H11N4O14P3	-4	cytosol
ivcoa[c]	Isovaleryl-CoA	C26H40N7O17P3S	-4	cytosol
k[c]	Potassium	K	1	cytosol
k[e]	Potassium	K	1	extracellular
lac__D[c]	D-Lactate	C3H5O3	-1	cytosol
lac__D[e]	D-Lactate	C3H5O3	-1	extracellular
lac__L[c]	L-Lactate	C3H5O3	-1	cytosol
lac__L[e]	L-Lactate	C3H5O3	-1	extracellular

lcts[c]	Lactose	C12H22O11	0	cytosol
lcts[e]	Lactose	C12H22O11	0	extracellular
leu__L[c]	L-Leucine	C6H13NO2	0	cytosol
leu__L[e]	L-Leucine	C6H13NO2	0	extracellular
lipoamp[c]	Lipoyl-AMP	C18H25N5O8PS2	-1	cytosol
lipoate[c]	Lipoate	C8H14O2S2	0	cytosol
lipoate[e]	Lipoate	C8H14O2S2	0	extracellular
lipopb[c]	Lipoate (protein bound)	C8H13OS2	1	cytosol
lpam[c]	Lipoamide C8H15NOS2	C8H15NOS2	0	cytosol
LTA_LLA[c]	Lipoteichoic-acid-n16	C9720H18598O9500P1600	0	cytosol
LTAala_LLA[c]	Lipoteichoic acid n16 with 038 ala substitutions	C11520H22198N600O10100P1600	0	cytosol
LTAAlaGal_LLA[c]	Lipoteichoic acid n16 with 0 38 ala and 062 gal	C17400H31998N600O15000P1600	0	cytosol
lys__L[c]	L-Lysine	C6H15N2O2	1	cytosol
lys__L[e]	L-Lysine	C6H15N2O2	1	extracellular
lyspg_LLA[c]	1 lysyl phosphatidyl glycerol lactis specific	C4620H8898N200O1100P100	0	cytosol
lystrna[c]	L-Lysine-tRNA (Lys)	C21H36N2O17P2R3	-1	cytosol
m12dg_LLA[c]	Monoglucosyl-1-2-diacylglycerol	C4320H7998O1000	0	cytosol
m2but[c]	2-Methylbutyric acid	C5H10O2	0	cytosol
m2but[e]	2-Methylbutyric acid	C5H10O2	0	extracellular
m2butp[c]	2-methylbutanoyl-phosphate	C5H10O5P	0	cytosol
mal__L[c]	L-Malate	C4H4O5	-2	cytosol
mal__L[e]	L-Malate	C4H4O5	-2	extracellular
malACP[c]	Malonyl-[acyl-carrier protein]	C14H22N2O10PRS	-2	cytosol
malcoa[c]	Malonyl-CoA	C24H33N7O19P3S	-5	cytosol
malt[c]	Maltose	C12H22O11	0	cytosol
malt[e]	Maltose	C12H22O11	0	extracellular
malt6p[c]	Maltose 6'-phosphate	C12H21O14P	-2	cytosol
malthp[c]	Maltoheptaose	C42H72O36	0	cytosol
malthp[e]	Maltoheptaose	C42H72O36	0	extracellular
malthx[c]	Maltohexaose	C36H62O31	0	cytosol
malthx[e]	Maltohexaose	C36H62O31	0	extracellular
maltpt[c]	Maltopentaose	C30H52O26	0	cytosol
maltpt[e]	Maltopentaose	C30H52O26	0	extracellular
malttr[c]	Maltotriose C18H32O16	C18H32O16	0	cytosol
malttr[e]	Maltotriose	C18H32O16	0	extracellular
maltttr[c]	Maltotetraose	C24H42O21	0	cytosol
maltttr[e]	Maltotetraose	C24H42O21	0	extracellular
man[e]	D-Mannose	C6H12O6	0	extracellular
man6p[c]	D-Mannose-6-phosphate	C6H11O9P	-2	cytosol
mana[c]	D-Mannonate	C6H11O7	-1	cytosol
mdhdhf[c]	(2R,4S)-2-methyl-2,4-dihydroxydihydrofuran-3-one	C5H8O4	0	cytosol
met__L[c]	L-Methionine	C5H11NO2S	0	cytosol
met__L[e]	L-Methionine	C5H11NO2S	0	extracellular
methf[c]	5,10-Methenyltetrahydrofolate	C20H20N7O6	-1	cytosol
metsox_R__L[c]	L-methionine-R-sulfoxide	C5H11NO3S	0	cytosol
metsox_S__L[c]	L-Methionine Sulfoxide	C5H11NO3S	0	cytosol
mev__R[c]	R-Mevalonate	C6H11O4	-1	cytosol
mg2[c]	Magnesium	Mg	2	cytosol
mg2[e]	Magnesium	Mg	2	extracellular

mhpglu[c]	5 Methyltetrahydropteroyltri L glutamate C25H36N8O12	C25H34N8O12	-2	cytosol
mi1p__D[c]	1D-myo-Inositol 1-phosphate	C6H11O9P	-2	cytosol
mlthf[c]	5,10-Methylenetetrahydrofolate	C20H21N7O6	-2	cytosol
mn2[c]	Manganese	Mn	2	cytosol
mn2[e]	Manganese	Mn	2	extracellular
mnl[e]	D-Mannitol	C6H14O6	0	extracellular
mnl1p[c]	D-Mannitol-1-phosphate	C6H13O9P	-2	cytosol
mql8[c]	Menaquinol 8	C51H74O2	0	cytosol
mqn8[c]	Menaquinone-8	C51H72O2	0	cytosol
msa[c]	Malonate semialdehyde	C3H3O3	-1	cytosol
mththf[c]	(2R,4S)-2-methyl-2,3,3,4-tetrahydroxytetrahydrofuran	C5H10O5	0	cytosol
myrsACP[c]	Myristoyl-ACP (n-C14:0ACP)	C25H47N2O8PRS	-1	cytosol
N1aspmd[c]	N1-Acetylspermidine	C9H23N3O	2	cytosol
n6all26d[c]	N6-Acetyl-LL-2,6-diaminoheptanedioate	C9H15N2O5	0	cytosol
n8aspmd[c]	N8-Acetylspermidine	C9H23N3O	2	cytosol
na1[c]	Sodium	Na	1	cytosol
na1[e]	Sodium	Na	1	extracellular
nac[c]	Nicotinate	C6H4NO2	-1	cytosol
nac[e]	Nicotinate	C6H4NO2	-1	extracellular
nad[c]	Nicotinamide-adenine-dinucleotide	C21H26N7O14P2	-1	cytosol
nadh[c]	Nicotinamide-adenine-dinucleotide-reduced	C21H27N7O14P2	-2	cytosol
nadp[c]	Nicotinamide-adenine-dinucleotide-phosphate	C21H25N7O17P3	-3	cytosol
nadph[c]	Nicotinamide-adenine-dinucleotide-phosphate-reduced	C21H26N7O17P3	-4	cytosol
nal2a6o[c]	N-Acetyl-L-2-amino-6-oxopimelate	C9H11NO6	0	cytosol
ncam[c]	Nicotinamide	C6H6N2O	0	cytosol
ncam[e]	Nicotinamide	C6H6N2O	0	extracellular
nh4[c]	Ammonium	H4N	1	cytosol
nh4[e]	Ammonium	H4N	1	extracellular
nicrnt[c]	Nicotinate-D-ribonucleotide	C11H12NO9P	-2	cytosol
nmn[c]	NMN	C11H14N2O8P	-1	cytosol
o2[c]	O2-O2	O2	0	cytosol
o2[e]	O2-O2	O2	0	extracellular
o2s[c]	Superoxide-anion	O2	-1	cytosol
oaa[c]	Oxaloacetate	C4H2O5	-2	cytosol
ocACP[c]	Octanoyl-ACP (n-C8:0ACP)	C19H35N2O8PRS	-1	cytosol
ocdcaACP[c]	Octadecanoyl-ACP (n-C18:0ACP)	C29H55N2O8PRS	-1	cytosol
octdp[c]	All-trans-Octaprenyl-diphosphate	C40H65O7P2	-3	cytosol
octeACP[c]	Cis-octadec-11-enoyl-[acyl-carrier protein] (n-C18:1)	C29H53N2O8PRS	-1	cytosol
ohpb[c]	2-Oxo-3-hydroxy-4-phosphobutanoate	C4H4O8P	-3	cytosol
orn__L[c]	L-Ornithine	C5H13N2O2	1	cytosol
orn__L[e]	L-Ornithine	C5H13N2O2	1	extracellular
orot[c]	Orotate	C5H3N2O4	-1	cytosol
orot[e]	Orotate C5H3N2O4	C5H3N2O4	-1	extracellular
orot5p[c]	Orotidine-5'-phosphate	C10H10N2O11P	-3	cytosol
pa_LLA[c]	Phosphatidic-acid	C3720H6898O800P100	-200	cytosol
pacald[c]	Phenylacetaldehyde	C8H8O	0	cytosol
pacald[e]	Phenylacetaldehyde	C8H8O	0	extracellular
palmACP[c]	Palmitoyl-ACP (n-C16:0ACP)	C27H51N2O8PRS	-1	cytosol
pan4p[c]	Pantetheine-4'-phosphate	C11H21N2O7PS	-2	cytosol
pant__R[c]	(R)-Pantoate	C6H11O4	-1	cytosol

pap[c]	Adenosine-3',5'-bisphosphate	C10H11N5O10P2	-4	cytosol
pdx5p[c]	Pyridoxine 5'-phosphate	C8H10NO6P	-2	cytosol
pea[c]	Phenylethyl alcohol	C8H10O	0	cytosol
pea[e]	Phenylethyl alcohol	C8H10O	0	extracellular
pep[c]	Phosphoenolpyruvate	C3H2O6P	-3	cytosol
pg_LLA[c]	Phospatidylglycerol	C4020H7598O1000P100	-100	cytosol
PG[c]	Peptidoglycan	C39H64N8O19	0	cytosol
pgp_LLA[c]	Phosphatidylglycerophosphate	C4020H7498O1300P200	-300	cytosol
phe__L[c]	L-Phenylalanine	C9H11NO2	0	cytosol
phe__L[e]	L-Phenylalanine	C9H11NO2	0	extracellular
phom[c]	O-Phospho-L-homoserine	C4H8NO6P	-2	cytosol
phpyr[c]	Phenylpyruvate	C9H7O3	-1	cytosol
phthr[c]	O-Phospho-4-hydroxy-L-threonine	C4H8NO7P	-2	cytosol
pi[c]	Phosphate	HO4P	-2	cytosol
pi[e]	Phosphate	HO4P	-2	extracellular
pnto__R[c]	(R)-Pantothenate	C9H16NO5	-1	cytosol
pnto__R[e]	(R)-Pantothenate	C9H16NO5	-1	extracellular
ppap[c]	Propanoyl phosphate	C3H5O5P	-2	cytosol
ppcoa[c]	Propanoyl-CoA	C24H36N7O17P3S	-4	cytosol
ppgpp[c]	Guanosine 3',5'-bis(diphosphate)	C10H11N5O17P4	-6	cytosol
pphn[c]	Prephenate	C10H8O6	-2	cytosol
ppi[c]	Diphosphate	HO7P2	-3	cytosol
ppi[e]	Diphosphate	HO7P2	-3	extracellular
pppi[c]	Inorganic-triphosphate	HO10P3	-4	cytosol
pram[c]	5-Phospho-beta-D-ribosylamine	C5H11NO7P	-1	cytosol
pran[c]	N-(5-Phospho-D-ribosyl)anthranilate	C12H13NO9P	-3	cytosol
prbamp[c]	1-(5-Phosphoribosyl)-AMP	C15H19N5O14P2	-4	cytosol
prbatp[c]	1-(5-Phosphoribosyl)-ATP	C15H19N5O20P4	-6	cytosol
prfp[c]	1-(5-Phosphoribosyl)-5-[(5-phosphoribosylamino)methylideneamino]imidazole-4-carboxamide	C15H22N5O15P2	-3	cytosol
pro__L[c]	L-Proline	C5H9NO2	0	cytosol
pro__L[e]	L-Proline	C5H9NO2	0	extracellular
prpp[c]	5-Phospho-alpha-D-ribose-1-diphosphate	C5H8O14P3	-5	cytosol
psd5p[c]	Pseudouridine 5 phosphate C9H11N2O9P	C9H11N2O9P	-2	cytosol
pser__L[c]	O-Phospho-L-serine	C3H6NO6P	-2	cytosol
ptrc[c]	Putrescine	C4H14N2	2	cytosol
ptrc[e]	Putrescine	C4H14N2	2	extracellular
pyam5p[c]	Pyridoxamine 5'-phosphate	C8H12N2O5P	-1	cytosol
pydam[c]	Pyridoxamine	C8H13N2O2	1	cytosol
pydam[e]	Pyridoxamine	C8H13N2O2	1	extracellular
pydx[c]	Pyridoxal	C8H9NO3	0	cytosol
pydx[e]	Pyridoxal	C8H9NO3	0	extracellular
pydx5p[c]	Pyridoxal 5'-phosphate	C8H8NO6P	-2	cytosol
pydxn[c]	Pyridoxine	C8H11NO3	0	cytosol
pydxn[e]	Pyridoxine	C8H11NO3	0	extracellular
pyr[c]	Pyruvate	C3H3O3	-1	cytosol
pyr[e]	Pyruvate	C3H3O3	-1	extracellular
quln[c]	Quinolinate	C7H3NO4	-2	cytosol
r1p[c]	Alpha-D-Ribose-1-phosphate	C5H9O8P	-2	cytosol
r5p[c]	Alpha-D-Ribose-5-phosphate	C5H9O8P	-2	cytosol

rhcys[c]	S-Ribosyl-L-homocysteine	C9H17NO6S	0	cytosol
rib__D[c]	D-Ribose	C5H10O5	0	cytosol
rib__D[e]	D-Ribose	C5H10O5	0	extracellular
ribflv[c]	Riboflavin	C17H20N4O6	0	cytosol
ribflv[e]	Riboflavin	C17H20N4O6	0	extracellular
rnam[c]	N Ribosylnicotinamide	C11H15N2O5	1	cytosol
rnam[e]	N Ribosylnicotinamide C11H15N2O5	C11H15N2O5	1	extracellular
ru5p__D[c]	D-Ribulose-5-phosphate	C5H9O8P	-2	cytosol
s17bp[c]	Sedoheptulose 1,7-bisphosphate	C7H12O13P2	-4	cytosol
s7p[c]	Sedoheptulose-7-phosphate	C7H13O10P	-2	cytosol
sbt__D[e]	D-Sorbitol	C6H14O6	0	extracellular
sbt6p[c]	D-Sorbitol 6-phosphate	C6H13O9P	-2	cytosol
sbzcoa[c]	O-Succinylbenzoyl-CoA	C32H39N7O20P3S	-5	cytosol
ser__L[c]	L-Serine	C3H7NO3	0	cytosol
ser__L[e]	L-Serine	C3H7NO3	0	extracellular
skm[c]	Shikimate	C7H9O5	-1	cytosol
skm5p[c]	Shikimate-5-phosphate	C7H8O8P	-3	cytosol
sl26da[c]	N-Succinyl-LL-2,6-diaminoheptanedioate	C11H16N2O7	-2	cytosol
sl2a6o[c]	N-Succinyl-2-L-amino-6-oxoheptanedioate	C11H12NO8	-3	cytosol
so4[c]	Sulfate	O4S	-2	cytosol
so4[e]	Sulfate	O4S	-2	extracellular
spmd[c]	Spermidine	C7H22N3	3	cytosol
spmd[e]	Spermidine	C7H22N3	3	extracellular
sucbz[c]	O-Succinylbenzoate	C11H8O5	-2	cytosol
succ[c]	Succinate	C4H4O4	-2	cytosol
succ[e]	Succinate	C4H4O4	-2	extracellular
succoa[c]	Succinyl-CoA	C25H35N7O19P3S	-5	cytosol
suchms[c]	O-Succinyl-L-homoserine	C8H12NO6	-1	cytosol
t3c11vaceACP[c]	Trans-3-cis-11-vacceoyl-[acyl-carrier protein]	C29H51N2O8PRS	-1	cytosol
t3c5ddeceACP[c]	Trans-3-cis-5-dodecenoyl-[acyl-carrier protein]	C23H39N2O8PRS	-1	cytosol
t3c7mrseACP[c]	Trans-3-cis-7-myristoleoyl-[acyl-carrier protein]	C25H43N2O8PRS	-1	cytosol
t3c9palmeACP[c]	Trans-3-cis-9-palmitoleoyl-[acyl-carrier protein]	C27H47N2O8PRS	-1	cytosol
tag6p__D[c]	D-Tagatose-6-phosphate	C6H11O9P	-2	cytosol
tagdp__D[c]	D-Tagatose-1,6-biphosphate	C6H10O12P2	-4	cytosol
tddec2eACP[c]	Trans-Dodec-2-enoyl-[acyl-carrier protein]	C23H41N2O8PRS	-1	cytosol
tdeACP[c]	Cis-tetradec-7-enoyl-[acyl-carrier protein] (n-C14:1)	C25H45N2O8PRS	-1	cytosol
tdec2eACP[c]	Trans-Dec-2-enoyl-[acyl-carrier protein]	C21H37N2O8PRS	-1	cytosol
thdp[c]	2,3,4,5-Tetrahydrodipicolinate	C7H7NO4	-2	cytosol
thex2eACP[c]	Trans-Hex-2-enoyl-[acyl-carrier protein]	C17H29N2O8PRS	-1	cytosol
thf[c]	5,6,7,8-Tetrahydrofolate	C19H21N7O6	-2	cytosol
thfglu[c]	Tetrahydrofolyl Glu 2	C24H27N8O9	-3	cytosol
thm[c]	Thiamin	C12H17N4OS	1	cytosol
thm[e]	Thiamin	C12H17N4OS	1	extracellular
thmmp[c]	Thiamin-monophosphate	C12H16N4O4PS	-1	cytosol
thmpp[c]	Thiamine diphosphate	C12H16N4O7P2S	-2	cytosol
thr__L[c]	L-Threonine	C4H9NO3	0	cytosol
thr__L[e]	L-Threonine	C4H9NO3	0	extracellular
thym[c]	Thymine	C5H6N2O2	0	cytosol
thym[e]	Thymine	C5H6N2O2	0	extracellular
thymd[c]	Thymidine	C10H14N2O5	0	cytosol

thymd[e]	Thymidine C10H14N2O5	C10H14N2O5	0	extracellular
tmrs2eACP[c]	Trans-Tetradec-2-enoyl-[acyl-carrier protein]	C25H45N2O8PRS	-1	cytosol
toct2eACP[c]	Trans-Oct-2-enoyl-[acyl-carrier protein]	C19H33N2O8PRS	-1	cytosol
toctd2eACP[c]	Trans-octadec-2-enoyl-[acyl-carrier protein]	C29H53N2O8PRS	-1	cytosol
tpalm2eACP[c]	Trans-Hexadec-2-enoyl-[acyl-carrier protein]	C27H49N2O8PRS	-1	cytosol
trdox[c]	Oxidized-thioredoxin	X	0	cytosol
trdrd[c]	Reduced-thioredoxin	XH2	0	cytosol
tre[e]	Trehalose	C12H22O11	0	extracellular
tre6p[c]	Alpha,alpha'-Trehalose-6-phosphate	C12H21O14P	-2	cytosol
trnalys[c]	TRNA(Lys)	C15H23O16P2R3	-2	cytosol
trp__L[c]	L-Tryptophan	C11H12N2O2	0	cytosol
trp__L[e]	L-Tryptophan	C11H12N2O2	0	extracellular
tyr__L[c]	L-Tyrosine	C9H11NO3	0	cytosol
tyr__L[e]	L-Tyrosine	C9H11NO3	0	extracellular
uaaAgla[c]	Undecaprenyl-diphospho-N-acetylmuramoyl-(N-acetylglucosamine)-L-alanyl-D-glutamyl-L-lysyl-D-alanyl-D-alanine	C94H153N8O26P2	-3	cytosol
uaAgla[c]	Undecaprenyl-diphospho-N-acetylmuramoyl-L-alanyl-D-glutamyl-L-lysyl-D-alanyl-D-alanine	C86H140N7O21P2	-3	cytosol
uaccg[c]	UDP-N-acetyl-3-O-(1-carboxyvinyl)-D-glucosamine	C20H26N3O19P2	-3	cytosol
uacgam[c]	UDP-N-acetyl-D-glucosamine	C17H25N3O17P2	-2	cytosol
uAgl[c]	UDP-N-acetylmuramoyl-L-alanyl-D-glutamyl-L-lysine	C34H51N7O24P2	-4	cytosol
uAgla[c]	UDP-N-acetylmuramoyl-L-alanyl-D-glutamyl-L-lysyl-D-alanyl-D-alanine	C40H62N9O26P2	-3	cytosol
uama[c]	UDP-N-acetylmuramoyl-L-alanine	C23H33N4O20P2	-3	cytosol
uamag[c]	UDP-N-acetylmuramoyl-L-alanyl-D-glutamate	C28H39N5O23P2	-4	cytosol
uamr[c]	UDP-N-acetylmuramate	C20H28N3O19P2	-3	cytosol
udcp[c]	Undecaprenol	C55H90O	0	cytosol
udcpdp[c]	Undecaprenyl-diphosphate	C55H89O7P2	-3	cytosol
udcpp[c]	Undecaprenyl-phosphate	C55H89O4P	-2	cytosol
udp[c]	UDP	C9H11N2O12P2	-3	cytosol
udpacgal[c]	UDP-N-acetyl-D-galactosamine	C17H25N3O17P2	-2	cytosol
udpg[c]	UDPglucose	C15H22N2O17P2	-2	cytosol
udpgal[c]	UDPgalactose	C15H22N2O17P2	-2	cytosol
ump[c]	UMP	C9H11N2O9P	-2	cytosol
ura[c]	Uracil	C4H4N2O2	0	cytosol
ura[e]	Uracil	C4H4N2O2	0	extracellular
uri[c]	Uridine	C9H12N2O6	0	cytosol
utp[c]	UTP	C9H11N2O15P3	-4	cytosol
val__L[c]	L-Valine	C5H11NO2	0	cytosol
val__L[e]	L-Valine	C5H11NO2	0	extracellular
xan[c]	Xanthine	C5H4N4O2	0	cytosol
xan[e]	Xanthine	C5H4N4O2	0	extracellular
xmp[c]	Xanthosine-5'-phosphate	C10H11N4O9P	-2	cytosol
xtsn[c]	Xanthosine	C10H12N4O6	0	cytosol
xu5p__D[c]	D-Xylulose-5-phosphate	C5H9O8P	-2	cytosol
xyl__D[c]	D-Xylose	C5H10O5	0	cytosol
xylu__D[c]	D-Xylulose	C5H10O5	0	cytosol
zn2[c]	Zinc	Zn	2	cytosol
zn2[e]	Zinc	Zn	2	extracellular

Supplementary Table S3: Metabolite composition of the assembled BOF, contained in both GEMs.

Group	Metabolite ID	Metabolite	Stoichiometry	Formula	Charge	Reference
Amino acid	ala__L[c]	L-Alanine	-0.54366	C3H7NO2	0	100
Amino acid	arg__L[c]	L-Arginine	-0.19632	C6H15N4O2	1	100
Amino acid	asp__L[c]	L-Aspartate	-0.19665	C4H6NO4	-1	100
Amino acid	asn__L[c]	L-Asparagine	-0.19665	C4H8N2O3	0	100
Amino acid	cys__L[c]	L-Cysteine	-0.01452	C3H7NO2S	0	100
Amino acid	glu__L[c]	L-Glutamate	-0.166158	C5H8NO4	-1	
Amino acid	gln__L[c]	L-Glutamine	-0.166158	C5H10N2O3	0	100
Amino acid	gly[c]	Glycine	-0.39012	C2H5NO2	0	100
Amino acid	his__L[c]	L-Histidine	-0.06834	C6H9N3O2	0	100
Amino acid	ile__L[c]	L-Isoleucine	-0.21804	C6H13NO2	0	100
Amino acid	leu__L[c]	L-Leucine	-0.33684	C6H13NO2	0	100
Amino acid	lys__L[c]	L-Lysine	-0.3693	C6H15N2O2	1	
Amino acid	met__L[c]	L-Methionine	-0.09006	C5H11NO2S	0	100
Amino acid	phe__L[c]	L-Phenylalanine	-0.15408	C9H11NO2	0	100
Amino acid	pro__L[c]	L-Proline	-0.14898	C5H9NO2	0	100
Amino acid	ser__L[c]	L-Serine	-0.23322	C3H7NO3	0	100
Amino acid	thr__L[c]	L-Threonine	-0.24636	C4H9NO3	0	100
Amino acid	trp__L[c]	L-Tryptophan	-0.06	C11H12N2O2	0	
Amino acid	tyr__L[c]	L-Tyrosine	-0.1173	C9H11NO3	0	100
Amino acid	val__L[c]	L-Valine	-0.2934	C5H11NO2	0	100
Nucleotide	datp[c]	DATP	-0.006634483874024	C10H12N5O12P3	-4	100
Nucleotide	dttp[c]	DTTP	-0.006634483874024	C10H13N2O14P3	-4	100
Nucleotide	dctp[c]	DCTP	-0.003635615002174	C9H12N3O13P3	-4	100
Nucleotide	dgtp[c]	DGTP	-0.003635615002174	C10H12N5O13P3	-4	100
Nucleotide and GAM	atp[c]	ATP	-39.5277384864291	C10H12N5O13P3	-4	100, 73
Nucleotide	utp[c]	UTP	-0.022868370491166	C9H11N2O15P3	-4	100
Nucleotide	ctp[c]	CTP	-0.02117441712145	C9H12N3O14P3	-4	100
Nucleotide	gtp[c]	GTP	-0.034090811565535	C10H12N5O14P3	-4	100
Lipid	pg_LLA[c]	Phospatidylglycerol	-0.000102952922335	C4020H7598O1000P100	-100	71, 73
Lipid	clpn_LLA[c]	Cardiolipin	-0.00023150789414	C7740H14396O1700P200	-200	71, 73
Lipid	lyspg_LLA[c]	1 lysyl phosphatidyl glycerol lactis specific	-2.34231516424126E-05	C4620H8898N200O1100P100	0	71, 73
Lipid	d12dg_LLA[c]	Diglucosyl-1-2-diacylglycerol	-0.00016505151041	C4920H8998O1500	0	71, 73
Lipid	m12dg_LLA[c]	Monoglucosyl-1-2-diacylglycerol	-2.17889782720117E-05	C4320H7998O1000	0	71, 73
Lipoteichoic acid	LTAAlaGal_LLA[c]	Lipoteichoic acid n16 with 0 38 ala and 062 gal	-0.000148370687694	C17400H31998N600O15000P1600	0	71, 73
Peptidoglycan	PG[c]	Peptidoglycan	-0.231971426915498	C39H64N8O19	0	71, 73
Cell wall polysaccharide	CPS_LLA[c]	Polysaccharide units Lactis specific	-0.153336996383803	C24H47O26P1	-2	71, 73
Essential cofactor	nad[c]	Nicotinamide-adenine-dinucleotide	-0.00177763	C21H26N7O14P2	-1	101
Essential cofactor	nadp[c]	Nicotinamide-adenine-dinucleotide-phosphate	-0.00043397	C21H25N7O17P3	-3	101
Essential cofactor	amet[c]	S-Adenosyl-L-methionine	-0.0002165	C15H23N6O5S	1	101
Essential cofactor	fad[c]	Flavin-adenine-dinucleotide-oxidized	-0.0002165	C27H31N9O15P2	-2	101
Essential cofactor	ribflv[c]	Riboflavin	-0.0002165	C17H20N4O6	0	101
Essential cofactor	pydx5p[c]	Pyridoxal 5'-phosphate	-0.0002165	C8H8NO6P	-2	101
Essential cofactor	coa[c]	Coenzyme-A	-0.00055921	C21H32N7O16P3S	-4	101
Essential cofactor	10fthf[c]	10-Formyltetrahydrofolate	-0.0002165	C20H21N7O7	-2	101
Essential cofactor	thf[c]	5,6,7,8-Tetrahydrofolate	-0.0002165	C19H21N7O6	-2	101
Essential cofactor	mlthf[c]	5,10-Methylenetetrahydrofolate	-0.0002165	C20H21N7O6	-2	101
Essential cofactor	thmpp[c]	Thiamine diphosphate	-0.0002165	C12H16N4O7P2S	-2	101
Essential ion	mg2[c]	Magnesium	-0.00842213	Mg	2	95, 96, 97
GAM	h2o[c]	H2O	-39.5	H2O	0	73
GAM	adp[c]	ADP	39.5	C10H12N5O10P2	-3	73
GAM	pi[c]	Phosphate	39.5	HO4P	-2	73
GAM	h[c]	H+	39.5	H	1	73

Supplementary Table S4: Dead-end metabolites present in the final version of the GEM for *L. lactis* IL1403.

Metabolite ID	Metabolite
3c2hmp[c]	3-Carboxy-2-hydroxy-4-methylpentanoate
3c3hmp[c]	3-Carboxy-3-hydroxy-4-methylpentanoate
3c4mop[c]	3-Carboxy-4-methyl-2-oxopentanoate
5mta[c]	5-Methylthioadenosine
5mtr[c]	5-Methylthio-D-ribose
N1aspmd[c]	N1-Acetylspermidine
acmum6p[c]	N-acetylmuramate 6-phosphate
arbt6p[c]	Arbutin-6-phosphate
hqn[c]	Hydroquinone
ca2[c]	Calcium
cl[c]	Chloride
etha[c]	Ethanolamine
g3pe[c]	Sn-Glycero-3-phosphoethanolamine
fe2[c]	Fe2+ mitochondria
fe3[c]	Iron (Fe3+)
g3pc[c]	Sn-Glycero-3-phosphocholine
g3pg[c]	Glycerophosphoglycerol
g3pi[c]	Sn-Glycero-3-phospho-1-inositol
g3ps[c]	Glycerophosphoserine
glcur[c]	D-Glucuronate
hisp[c]	L-Histidinol-phosphate
histd[c]	L-Histidinol
k[c]	Potassium
mn2[c]	Manganese
n8aspmd[c]	N8-Acetylspermidine
o2s[c]	Superoxide-anion
prbatp[c]	1-(5-Phosphoribosyl)-ATP
prfp[c]	1-(5-Phosphoribosyl)-5-[(5-phosphoribosylamino)methylideneamino]imidazole-4-carboxamide
psd5p[c]	Pseudouridine 5 phosphate C9H11N2O9P
ptrc[c]	Putrescine
so4[c]	sulphate
tag6p__D[c]	D-Tagatose-6-phosphate
tagdp__D[c]	D-Tagatose-1,6-biphosphate
udcp[c]	Undecaprenol
xyl__D[c]	D-Xylose

Supplementary Table S5: Reactions leading to dead-end metabolites, present in the final version of the GEM for *L. lactis* IL4103.

Reaction ID	Reaction name	Reaction formula
IPPMIa	3-isopropylmalate dehydratase	3c2hmp[c] <=> 2ippm[c] + h2o[c]
IPPMIb	2-isopropylmalate hydratase	2ippm[c] + h2o[c] <=> 3c3hmp[c]
OMCDC	2-Oxo-4-methyl-3-carboxypentanoate decarboxylation	3c4mop[c] + h[c] -> 4mop[c] + co2[c]
MTAN	Methylthioadenosine nucleosidase	5mta[c] + h2o[c] -> 5mtr[c] + ade[c]
SPMDAT1	Spermidine acetyltransferase	accoa[c] + spmd[c] -> N1aspmd[c] + coa[c] + h[c]
ACM6PH	N-acetylmuramate 6-phosphate hydrolase	acmum6p[c] + h2o[c] -> acgam6p[c] + lac__D[c]
AB6PGH	Arbutin 6-phosphate glucohydrolase	arbt6p[c] + h2o[c] -> g6p[c] + hqn[c]
CA2abc	Calcium transport via ABC system	atp[c] + ca2[e] + h2o[c] -> adp[c] + ca2[c] + h[c] + pi[c]
Clt	Major Facilitator(MFS) TCDB:2.A.1.14.6	cl[e] <=> cl[c]
GPDDA2	Glycerophosphodiester phosphodiesterase (Glycerophosphoethanolamine)	g3pe[c] + h2o[c] -> etha[c] + glyc3p[c] + h[c]
FE2abc	Iron (II) transport via ABC system	atp[c] + fe2[e] + h2o[c] -> adp[c] + fe2[c] + h[c] + pi[c]
FE3abc	Iron (III) transport via ABC system	atp[c] + fe3[e] + h2o[c] -> adp[c] + fe3[c] + h[c] + pi[c]
GPDDA1	Glycerophosphodiester phosphodiesterase (Glycerophosphocholine)	g3pc[c] + h2o[c] -> chol[c] + glyc3p[c] + h[c]
GPDDA4	Glycerophosphodiester phosphodiesterase (Glycerophosphoglycerol)	g3pg[c] + h2o[c] -> glyc3p[c] + glyc[c] + h[c]
GPDDA5	Glycerophosphodiester phosphodiesterase (Glycerophosphoinositol)	g3pi[c] + h2o[c] -> glyc3p[c] + h[c] + inost[c]
GPDDA3	Glycerophosphodiester phosphodiesterase (Glycerophosphoserine)	g3ps[c] + h2o[c] -> glyc3p[c] + h[c] + ser__L[c]
GUI1	Glucuronate isomerase (D-glucuronate)	glcur[c] <=> fruur[c]
HISTP	Histidinol-phosphatase	h2o[c] + hisp[c] -> histd[c] + pi[c]
Kt1	Potassium transport via uniport (facilitated diffusion)	k[e] -> k[c]
Kt2r	Potassium reversible transport via proton symport	h[e] + k[e] -> h[c] + k[c]
ZN2t4	Zinc transport out via antiport	h[e] + k[e] + zn2[c] -> h[c] + k[c] + zn2[e]
MNabc	Manganese transport via ABC system	atp[c] + h2o[c] + mn2[e] -> adp[c] + h[c] + mn2[c] + pi[c]
SPMDAT2	Spermidine acetyltransferase (N8)	accoa[c] + spmd[c] -> coa[c] + h[c] + n8aspmd[c]
SPODM	Superoxide dismutase	2 h[c] + 2 o2s[c] -> h2o2[c] + o2[c]
PRATPP	Phosphoribosyl-ATP pyrophosphatase	h2o[c] + prbatp[c] -> h[c] + ppi[c] + prbamp[c]
PRAMPC_1	Phosphoribosyl AMP cyclohydrolase	h2o[c] + h[c] + prbamp[c] -> prfp[c]
YUMPS	YUMP synthetase	r5p[c] + ura[c] <=> h2o[c] + psd5p[c]
PTRCabc	Putrescine transport via ABC system	atp[c] + h2o[c] + ptrc[e] -> adp[c] + h[c] + pi[c] + ptrc[c]
SO4t2	sulphate transport in via proton symport	h[e] + so4[e] -> h[c] + so4[c]
PFK_2	Phosphofructokinase (D-tagatose 6-phosphate)	atp[c] + tag6p__D[c] -> adp[c] + h[c] + tagdp__D[c]
UDCPKr	Undecaprenol kinase (reversible)	atp[c] + udcp[c] -> adp[c] + h[c] + udcpp[c]
XYLI1	Xylose isomerase	xyl__D[c] <=> xylu__D[c]

Supplementary Table S6: Blocked reactions (reactions unable to carry flux) present in the final version of the model for *L. lactis* IL1403.

Reaction ID	Reaction formula	Reaction subsystem
MTAN	5mta[c] + h2o[c] -> 5mtr[c] + ade[c]	Amino Acid Metabolism: Arginine and Proline Metabolism
SPMDAT1	accoa[c] + spmd[c] -> N1aspmd[c] + coa[c] + h[c]	Amino Acid Metabolism: Arginine and Proline Metabolism
SPMDAT2	accoa[c] + spmd[c] -> coa[c] + h[c] + n8aspmd[c]	Amino Acid Metabolism: Arginine and Proline Metabolism
HISTP	h2o[c] + hisp[c] -> histd[c] + pi[c]	Amino Acid Metabolism: Histidine Metabolism
PRAMPC_1	h2o[c] + h[c] + prbamp[c] -> prfp[c]	Amino Acid Metabolism: Histidine Metabolism
PRATPP	h2o[c] + prbatp[c] -> h[c] + ppi[c] + prbamp[c]	Amino Acid Metabolism: Histidine Metabolism
IPPMIa	3c2hmp[c] <=> 2ippm[c] + h2o[c]	Amino Acid Metabolism: Valine, Leucine and Isoleucine Metabolism
IPPMIb	2ippm[c] + h2o[c] <=> 3c3hmp[c]	Amino Acid Metabolism: Valine, Leucine and Isoleucine Metabolism
OMCDC	3c4mop[c] + h[c] -> 4mop[c] + co2[c]	Amino Acid Metabolism: Valine, Leucine and Isoleucine Metabolism
AB6PGH	arbt6p[c] + h2o[c] -> g6p[c] + hqn[c]	Carbohydrate Metabolism: Alternative Carbon Metabolism
GUI1	glcur[c] <=> fruur[c]	Carbohydrate Metabolism: Alternative Carbon Metabolism
MANAO	mana[c] + nad[c] <=> fruur[c] + h[c] + nadh[c]	Carbohydrate Metabolism: Alternative Carbon Metabolism
MNNH	mana[c] -> 2ddglcn[c] + h2o[c]	Carbohydrate Metabolism: Alternative Carbon Metabolism
XYLI1	xyl__D[c] <=> xylu__D[c]	Carbohydrate Metabolism: Alternative Carbon Metabolism
XYLK	atp[c] + xylu__D[c] -> adp[c] + h[c] + xu5p__D[c]	Carbohydrate Metabolism: Alternative Carbon Metabolism
ACM6PH	acmum6p[c] + h2o[c] -> acgam6p[c] + lac__D[c]	Carbohydrate Metabolism: Aminosugars Metabolism
PFK_2	atp[c] + tag6p__D[c] -> adp[c] + h[c] + tagdp__D[c]	Carbohydrate Metabolism: Galactose Metabolism
UDCPKr	atp[c] + udcp[c] -> adp[c] + h[c] + udcpp[c]	Cell Envelope Biosynthesis: Peptidoglycan Biosynthesis
UDCPDPS	frdp[c] + 8 ipdp[c] -> 8 ppi[c] + udcpdp[c]	Cofactor and Prosthetic Group Biosynthesis: Isoprenoid Biosynthesis
DDGLK	2ddglcn[c] + atp[c] <=> 2ddg6p[c] + adp[c] + h[c]	Energy Production and Conversion: Pentose Phosphate Pathway
EDA	2ddg6p[c] -> g3p[c] + pyr[c]	Energy Production and Conversion: Pentose Phosphate Pathway
GPDDA1	g3pc[c] + h2o[c] -> chol[c] + glyc3p[c] + h[c]	Lipid Metabolism: Glycerophospholipids
GPDDA2	g3pe[c] + h2o[c] -> etha[c] + glyc3p[c] + h[c]	Lipid Metabolism: Glycerophospholipids
GPDDA3	g3ps[c] + h2o[c] -> glyc3p[c] + h[c] + ser__L[c]	Lipid Metabolism: Glycerophospholipids
GPDDA4	g3pg[c] + h2o[c] -> glyc3p[c] + glyc[c] + h[c]	Lipid Metabolism: Glycerophospholipids
GPDDA5	g3pi[c] + h2o[c] -> glyc3p[c] + h[c] + inost[c]	Lipid Metabolism: Glycerophospholipids
CA2abc	atp[c] + ca2[e] + h2o[c] -> adp[c] + ca2[c] + h[c] + pi[c]	Membrane Transport: Ions and Gases
Clt	cl[e] <=> cl[c]	Membrane Transport: Ions and Gases
FE2abc	atp[c] + fe2[e] + h2o[c] -> adp[c] + fe2[c] + h[c] + pi[c]	Membrane Transport: Ions and Gases
FE3abc	atp[c] + fe3[e] + h2o[c] -> adp[c] + fe3[c] + h[c] + pi[c]	Membrane Transport: Ions and Gases
Kt1	k[e] -> k[c]	Membrane Transport: Ions and Gases
Kt2r	h[e] + k[e] -> h[c] + k[c]	Membrane Transport: Ions and Gases
MNabc	atp[c] + h2o[c] + mn2[e] -> adp[c] + h[c] + mn2[c] + pi[c]	Membrane Transport: Ions and Gases
SO4t2	h[e] + so4[e] -> h[c] + so4[c]	Membrane Transport: Ions and Gases
ZN2t4	h[e] + k[e] + zn2[c] -> h[c] + k[c] + zn2[e]	Membrane Transport: Ions and Gases
ZNabc	atp[c] + h2o[c] + zn2[e] -> adp[c] + h[c] + pi[c] + zn2[c]	Membrane Transport: Ions and Gases
PTRCabc	atp[c] + h2o[c] + ptrc[e] -> adp[c] + h[c] + pi[c] + ptrc[c]	Membrane Transport: Organic Acids
SPMDabc	atp[c] + h2o[c] + spmd[e] -> adp[c] + h[c] + pi[c] + spmd[c]	Membrane Transport: Organic Acids
SPODM	2 h[c] + 2 o2s[c] -> h2o2[c] + o2[c]	Miscellaneous: Others
YUMPS	r5p[c] + ura[c] <=> h2o[c] + psd5p[c]	Nucleotide Metabolism: Purine and Pyrimidine Biosynthesis
EX_ca2_e	ca2[e] <=>	Pseudo-Reaction: Exchange
EX_cl_e	cl[e] <=>	Pseudo-Reaction: Exchange
EX_cobalt2_e	cobalt2[e] <=>	Pseudo-Reaction: Exchange
EX_cu2_e	cu2[e] <=>	Pseudo-Reaction: Exchange
EX_fe2_e	fe2[e] <=>	Pseudo-Reaction: Exchange
EX_k_e	k[e] <=>	Pseudo-Reaction: Exchange
EX_mn2_e	mn2[e] <=>	Pseudo-Reaction: Exchange
EX_na1_e	na1[e] <=>	Pseudo-Reaction: Exchange
EX_ptrc_e	ptrc[e] <=>	Pseudo-Reaction: Exchange
EX_so4_e	so4[e] <=>	Pseudo-Reaction: Exchange
EX_spmd_e	spmd[e] <=>	Pseudo-Reaction: Exchange
EX_zn2_e	zn2[e] <=>	Pseudo-Reaction: Exchange

Supplementary Table S7: Identified stoichiometric balanced cycles involving ATP and their respective reactions.

SBC	Reaction abbreviation	Reaction name	Reaction formula	Reaction flux (mmol g_{DW}^{-1} h^{-1})	Estimated $\Delta_r G'^{m}$ [kJ/mol]
				-1000	
Cycle A	HSERTA	Homoserine O trans acetylase	accoa[c] + hom__L[c] <=> achms[c] + coa[c]		-20.6 (± 9.3)
	SHSL4r	O succinylhomoserine lyase elimination (reversible)	h2o[c] + suchms[c] <=> 2obut[c] + h[c] + nh4[c] + succ[c]	-1000	-92.3 (± 9.2)
	HSDA	Homoserine deaminase	hom__L[c] -> 2obut[c] + nh4[c]	1000	-74.8 (± 10.8)
	AHSERL	O acetylhomoserine thiol lyase	achms[c] + ch4s[c] <=> ac[c] + h[c] + met__L[c]	-1000	-57.0 (± 8.7)
	SHSL3	O succinylhomoserine lyase (methanethiol)	ch4s[c] + suchms[c] -> h[c] + met__L[c] + succ[c]	1000	-48.0 (± 9.5)
	ACKr	Acetate kinase	ac[c] + atp[c] <=> actp[c] + adp[c]	-1000	13.4 (± 1.1)
	PTAr	Phosphotransacetylase	accoa[c] + pi[c] <=> actp[c] + coa[c]	1000	9.8 (± 1.2)
	ATPM	ATP maintenance requirement	atp[c] + h2o[c] -> adp[c] + h[c] + pi[c]	1000	-43.5 (± 0.6)
Cycle B	ATPS4r	ATP synthase (four protons for one ATP)	adp[c] + 4 h[e] + pi[c] <=> atp[c] + h2o[c] + 3 h[c]	750	N/A
	CITt3	Citrate transport out via proton antiport	cit[c] + h[e] <=> cit[e] + h[c]	-1000	N/A
	FORt2	Formate transport in via proton symport	for[e] + h[e] <=> for[c] + h[c]	-1000	N/A
	CITt2r	Citrate reversible transport via symport	cit[e] + h[e] <=> cit[c] + h[c]	-1000	N/A
	FORt	Formate transport via diffusion	for[e] <=> for[c]	1000	N/A
	ATPM	ATP maintenance requirement	atp[c] + h2o[c] -> adp[c] + h[c] + pi[c]	750	-43.5 (± 0.6)